Antenna Selection and Channel Estimation for Hybrid Relay Systems

by

Shivali Goel Bansal (B. Tech., M.E.)

Submitted in fulfilment of the requirements for the degree of

Doctor of Philosophy

Deakin University

April, 2012

DEAKIN UNIVERSITY

ACCESS TO THESIS – A

I am the author of the thesis entitled "Antenna Selection and Channel Estimation for Hybrid Relay Systems" submitted for the degree of "Doctor of Philosophy"

This thesis may be made available for consultation, loan and limited copying in accordance with the Copyright Act 1968.

'I certify that I am the student named below and that the information provided in the form is correct'

Full Name .....SHIVALI GOEL BANSAL.....

Signed .....Signature Redacted by Library.....

Date .....4th April, 2012.....

DEAKIN UNIVERSITY

CANDIDATE DECLARATION

I certify that the thesis entitled "Antenna Selection and Channel Estimation for Hybrid Relay Systems" submitted for the degree of "Doctor of Philosophy" is the result of my own work and that where reference is made to the work of others, due acknowledgment is given.

I also certify that any material in the thesis which has been accepted for a degree or diploma by any university or institution is identified in the text.

Full Name .....SHIVALI GOEL BANSAL.....

Signed .....Signature Redacted by Library.....

Date .....4th April, 2012.....

Acknowledgments

First and foremost, I would like to express my sincere gratitude to my supervisor Associate Professor Jemal Abawajy for his constant guidance, support and encouragement throughout my PhD studies. Working with him has been a true privilege and a great experience for me. I would also like to thank my supervisor for his constant belief in me throughout the working period. I would also like to thank Dr Robin Doss and Dr. Ming Li for their helpful suggestions and lively discussions. I would like to pay my sincere gratitude to the examiners for reading through my thesis and providing comments.

I am also grateful to Ms Janine Truter, HDR Candidature Manager, and Dr. Margaret Kumar from the Division of Student Life for providing me with the much needed support. I would also like to acknowledge Mr Dominic Sgro, Systems Administrator, for helping with the basic necessities needed for the research. My special thanks go to my ex-supervisor Dr. Van Khanh Nyugen for helping me to obtain the Deakin University International Research Scholarship. I would also like to thanks ISSNIP for providing financial support for my travel to India for attending the "International Conference on Signal Processing, Communications and Networking (ICSCN – 2008)" Madras Institute of Technology, Anna University, Chennai, India, in 2008.

Finally, I would like to thank my family and friends for their continual support and encouragement. In particular, my heartiest thanks to my co-PhD candidates for their involvement in timely discussions and relaxing moments which helped keep the pressure off, my parents in India for their never-ending faith in me, my respects to my mum-in-law for visiting me all the way from India to Australia to look after my home and family during the tougher times, to my daughter for being patient with her grandmother while I was away and busy with my work. Most importantly my heart-felt thanks to my dear husband for his

constant encouragement throughout all these years, for his moral and emotional support at times when I used to be out of patience, his patience for looking after my daughter's activities when I couldn't and for giving the motivation for finishing this thesis successfully.

Abstract

Multiple-input multiple-output (MIMO) systems help in improving transmission reliability by transmitting multiple copies of data. A MIMO system can effectively combat the effects of fading. Another approach of improving transmission reliability is to make use of relays. Wireless relay systems have successfully helped to overcome the problems associated with conventional wireless systems and have enabled cost-effective augmentation of coverage, throughput and system capacity with minimal increment in capital expenditures. Some other notable characteristics of relay-based systems are higher QoS, robustness, swift and flexible on demand build out alternate multiple routes.

The aim of this thesis is to incorporate more diverse paths within the wireless communication system in order to increase the number of information carrying multiple paths to increase transmission reliability. To achieve this, a dual hop decode-amplify and forward (DAF) relay system with single-antenna relay is presented in this thesis. The diversity in this system is achieved in two ways: firstly by the use of relay which is placed in between the transmitter and the receiver; and secondly by the use of multiple antennas at both the transmitter and the receiver. The DAF relay system is a hybrid of Decode-and-Forward (DF) and Amplify-and-Forward (AF) relay systems that shows the benefits of both DF and AF relay systems and is also called hybrid relay system or hybrid DAF (HDAF) relay system. Dual hop relaying gives better trunking efficiency and with single antenna at the relay site acquisition and antenna structures are much less expensive. The Nakagami-*m* distribution has been considered for modelling the channel paths between the transmitter and the receiver and also for the channel paths available via the relay. This is because of the fact that a wide range of fading channels, from severe to moderate, can be modelled by using Nakagami-*m* distribution. Since multiple antennas are used at the transmitter, Space Time Block Codes are

used for encoding the data. The multiple receive antennas used at the receiver make use of Maximal Ratio Combining Technique to combine all the information arriving from the multiple paths. The Performance of the two-hop DAF relay system with maximal ratio combining (MRC) at the receiver and space-time block codes (STBC) at the transmitter over Nakagami-*m* fading channels for various system models has been analysed in terms of bit error rates (BER). The variations in the performance levels when the relay is moved to different locations within the line-of-sight (LOS) of the transmitter and the receiver have also been analysed. Furthermore, Antenna Selection (AS) has been used to deal with the cost associated with the deployment of multiple antennas at the source and the destination. The AS process in this thesis is based on the maximum channel power gains associated with the channel links between the transmitter and the relay, and the relay and the receiver. At first place, AS is performed only at the transmitter. The work is further expanded by performing joint AS at both the transmitter and the receiver. The performance of the system with AS has also been analysed for various system models and in different fading conditions. The benefits of channel estimation have also been analysed by developing two feedback based channel estimation algorithms. The efficiency of the overall system is further enhanced by performing joint channel estimation and antenna selection.

Thus, simulations demonstrate that the relay based wireless system has a significant improvement in the signal-to-noise ratio (SNR), subsequently leading to a lower bit error rate as compared to the conventional wireless MIMO systems. Simulations also reveal that by using Antennas Selection techniques and further performing channel estimation, transmission reliability of the relay based systems can be significantly enhanced. All analyses were performed under ideal identical independent fading conditions and MPSK modulation has been used for modulating the incoming input sequence.

Publications

(During the course of PhD)

Journals

1. Goel, Shivali; Abawajy, Jemal and Kim, Tai-hoon. Performance analysis of receive diversity in wireless sensor networks over GBSBE models, Sensors, vol. 10, no. 12, pp. 11021-11037, Dec. 2010.

Conference Papers

2. Shivali Goel and Jemal Abawajy. Performance of a Two-Hop Hybrid Relayed MIMO Systems in different Fading Conditions. International Postgraduate Conference on Engineering (IPCE 2011), Perlis, Malaysia, 22 – 23 October 2011.
3. Goel, S.; Abawajy, J.H. Performance of Smart Antennas with Receive Diversity in Wireless Sensor Networks. In Proceedings of ICSCN 2008: International Conference on Signal Processing Communications and Networking, Los Alamitos, CA, USA, 4–6 January 2008; pp. 272-278.

Book Chapter

4. Shivali G. Bansal and Jemal Abawajy. Multi-Input-Multi-Output Antennas for Radio Frequency Identification Systems. Accepted for Publication, IGI Global.

Technical Reports

5. Shivali Goel and Jemal Abawajy. Performance of a Simplified Two-Hop Decode-Amplify-Forward Relayed System in different Fading Conditions, Computing Series, School of Engg. and IT, Deakin University, Geelong.
6. Shivali Goel and Jemal Abawajy. Transmit Antenna Selection for Hybrid Relay Systems, Computing Series, School of Engg. and IT, Deakin University, Geelong.
7. Shivali Goel and Jemal H. Abawajy, "Performance of Smart Antennas with Receive Diversity in Wireless Sensor Networks" (Tech. Rep. TR C09/23), Computing Series, School of Engg. and IT, Deakin University, Geelong.

Table of Contents

List of Figures

List of Tables

List of Acronyms

2G	Second Generation
3G	Third Generation
3GPP	3rd Generation Partnership Project
3GPP2	3rd Generation Partnership Project 2
4G	Fourth Generation
ADF	Adaptive Decode-and-Forward
AF	Amplify-and-Forward
AM	Amplitude Modulation
AR	Auto-Regressive
ARA	Auto-Regressive Algorithm
ARMA	Auto-Regressive Moving Averages
AS	Antenna Selection
AWGN	Additive White Gaussian Noise
B3G	Beyond 3G
BER	Bit Error Rates
BLAST	Bell Labs Layered Space-Time
BPSK	Binary Phase Shift Keying
BS	Base Station
CDF	Cumulative Density Function
CDMA	Code Division Multiple Access
CIR	Channel Impulse Response
CSI	Channel State Information
CSIT	Channel State Information at the Transmitter
DAF	Decode-Amplify-and-Forward
dB	Decibels
DF	Decode-and-Forward
DSCM	Differential Space Code Modulation
D-STBC	Differential Space-Time Block Codes
DTV	Digital television
EGC	Equal Gain Combining

EM	Expectation Maximization
FDF	Fixed Decode-and-Forward
FM	Frequency Modulation
GSC	Generalized Selection Combining
HDAF	Hybrid Decode-Amplify-Forward
i.i.d.	Independent and identically distributed
ISI	Inter-symbol Interference
J-TR-AS	Joint Transit-Receive Antenna Selection
KHz	Kilo Hertz
LMS	Least Mean Square
LOS	Line of Sight
LS	Least Square
LS-ARA	Least square Auto-regressive Algorithm
MAN	Metropolitan Area Networks
MAP	Maximum a-posteriori Probability
MATLAB	Mathematics Laboratory
MEA	Multi-element Antennas
MGF	Moment Generating Function
MHz	Mega Hertz
MIMO	Multiple Input Multiple Output
MISO	Multiple Input Single Output
ML	Maximum Likelihood
MMSE	Minimum Mean Square Error
MPSK	Multiple Phase Shift Keying
MRC	Maximal Ratio Combining
MRT	Maximal Ratio Transmission
MUI	Multi-user Interference
OFDM	Orthogonal Frequency Domain Modulation
OSTBC	Orthogonal Space-Time Block Codes
PDA	Personal Digital Assistant
PDF	Probability Density Function
PM	Phase Modulation
PSAM	Pilot Symbol Aided Modulation

PSK	Phase Shift Keying
PSP	Per-survivor Processor
QAM	Quadrature Amplitude Modulation
QoS	Quality-of-Service
QPSK	Quadrature Phase Shift Keying
RAS	Receive Antenna Selection
RF	Radio Frequency
SC	Selection Combining
SC-FDE	Single Carrier Frequency Domain Equalization
SE	Spectral Efficiency
SER	Symbol Error Rates
SIMO	Single Input Multiple Output
SISO	Single Input Single Output
SNR	Signal to Noise Ratio
ST	Space-Time
STBC	Space-Time Block Codes
STC	Space-Time codes
STTC	Space-Time Trellis Codes
TAS	Transmit Antenna Selection
TR	Transceiver
WINNER	Wireless World Initiative New Radio
WLAN	Wireless Local Area Network

Notation and Symbols

$x(t)$	Input signal at time t
$h(t)$	Fading channel coefficient at time t
$n(t)$	AWGN at time t
$y(t)$	Output signal at time t
H	Channel matrix
N_t	Number of transmit antennas
N_r	Number of receive antennas
$h_{i,j}(t)$	Channel coefficients from i^{th} transmit antenna to j^{th} receive antenna
$n_{N_r}(t)$	AWGN at channel path to ${N_r}^{th}$ receive antenna
$y_{N_r}(t)$	Output at ${N_r}^{th}$ receive antenna
r	Code Rate of STBC
k	Input block length
p	Symbol period
l	Frame length
G_{N_t}	Encoder (or transmission) matrix for real signal constellations with $r = 1/2$
${G_{N_t}}^*$	Encoder (or transmission) matrix for complex signal constellations with $r = 1/2$
H_{N_t}	Encoder (or transmission) matrix for complex signal constellations with $r = 3/4$
$(.)^*$	Complex conjugate of $(.)$
$(.)^H$	Hermitian transpose of $(.)$
$(.)^{\#}$	Pseudo-inverse of $(.)$
$(.)^{-1}$	inverse of $(.)$
I	Identity matrix
$\mathcal{N}(0,1)$	Gaussian density with zero mean and unity variance
$'m'$	Nakagami fading parameter
$J_0(.)$	Zeroth order Bessel function of the first kind
f_d	Maximum Doppler Frequency

f_s	Symbol frequency
L_t	Number of selected transmit antennas
L_r	Number of selected receive antennas
E_s or E_b	Symbol energy or bit energy
$\mathcal{A}$	MPSK Constellation alphabet
$\|\|.\|\|$	Norm of sequence $(.)$
$\|\|.\|\|_F$	Frobenius Norm of sequence $(.)$
Λ	Moment generating function
γ	Signal-to-noise Ratio
Γ	Gamma Function
Σ	Summation
$\int$	Integral
$\sqrt{}$	Square root
e or exp	Exponential function
$>$	Greater than
$<$	Less than
$\otimes$	Product
$\oplus$	Summation
$\sin(.)$	Sine function
π	pi function
$argmax(.)$	argument of the maximum (returns the set of points of the given argument for which the value of $(.)$ attains its maximum value)
$argmin(.)$	argument of the minimum (returns the set of points of the given argument for which the value of $(.)$ attains its minimum value)

Chapter 1 – Introduction

1.1 Wireless Communication

Wireless communication is the fastest growing segments of the communications industry and also the most active areas of technological development. It has been a topic of study for over half a century now. But the past decade has been the most exhaustive period and this research thrust in the past decade has led to a much richer set of perspectives and tools on how to communicate over wireless channels. The high rise in demand for new wireless capacities, low-powered sophisticated signal processing algorithms and coding techniques, the successful second-generation (2G) and third-generation (3G) digital wireless standards surge towards the demands for continued research activities in this area and the picture is still very much evolving. The conventional single-input single-output (SISO) systems failed to meet the growing demands for supporting transmission of images, voice, data and video related services, new wireless multimedia services such as Internet access, and multimedia data transfer, hence, wireless systems with multiple element antennas (MEAs) were proposed. The fundamental theoretic research using multiple antennas was initiated by Winters [1], Telatar [2], Gans [3], and Foschini [4]. Since then there has been exploring interests in multiple input multiple output (MIMO) systems and it has been proved that these systems greatly enhance the data rates and channel capacity.

Despite the significant physical layer performance enhancements provided by multiple-input multiple-output (MIMO) systems, a major problem in the deployment of these systems is obtaining adequate coverage. To aid the endless growing demand for a higher spectrum and power efficiency arising from the next generation mobile communication system, relay-aided communication came into existing. The concept of relaying signals has been shown to be the most practical improvement under high rate and coverage in a power-efficient manner along with operation cost and transmission capacity. In addition, simple relaying systems have been shown to increase diversity through node collaboration.

The basic idea behind radio relaying [5-7] is to employ relay nodes, reprocess the base station (BS) signals and resend them out towards the destination. By employing multi-hop relaying, the cell coverage can be expanded to reduce dead spots during communications. Additionally, it can transfer traffic in hot spots to reach load balance. Further, radio relaying saves the transmitting power of terminals, which may prolong battery life. As a result, relay-based architecture and its cooperation diversity and cooperative multipath technologies have attracted much attention worldwide and have recently been adopted into recent standards [8]. All the standards for future mobile communications systems (3GPP, 3GPP2, B3G and 4G), Wireless Local Area Network (WLAN) and broadband wireless networks (802.16j) introduce the concept of relaying, and take the problems of relay-assisted communications into account. Moreover, the Wireless World Initiative New Radio (WINNER) project has a detailed planning for ubiquitous broadband mobile radio relaying system [9].

According to signal processing models, relaying can be divided into the Amplify and Forward (AF), and Decode and Forward (DF) Relaying models [10]. According to the signal transmitted and received, relaying models can have either analogue mode or digital mode. The analogue relaying is also called non-regenerative relaying, in which signals are not required to be digitalized before forwarded by the relays. AF is a kind of analogue relaying.

On the contrary, digital relaying model decodes and encodes signals before sending them out. Therefore, digital relaying is also called regenerative relaying and DF belongs to this mode. An end-to-end performance of two-hop relay systems was studied and presented in [11][12][13], which included outage probability and average bit error rate (BER) calculations in different fading environments. However, in [11][12][13] all assumed single antenna at both end. Recently, a two-hop AF relay system in which both ends are equipped with multiple antennas appeared in [14][15] with a single antenna at the relay. In [14], orthogonal space-time block codes (OSTBCs) were employed at the source, and end-to-end average bit error rate (BER) was investigated. However, the method in [14] is only suitable for systems with equal numbers of antennas at both ends. In [16], system performance including outage probability and average symbol error rates (SER) was determined with multiple antennas at the source and a single antenna at the destination. Although the method used in [16] has been often used in the literature, it cannot be easily generalized to the case of multiple antennas at the destination. For arbitrary number of DF relays an exact outage and error analysis over Rayleigh fading channels was conducted in [17] and [18], respectively.

Recently, the performance analysis of relay communication over Nakagami-m fading channels has gained a lot of interest. BER performance for a three-node model based on AF relaying was presented and investigated in [19] and the SER for AF relaying for cooperative networks was investigated in [20], both over Nakagami-m fading channels. Similar work was presented in [21]. Performance analysis of DF cooperative diversity using differential equal gain combining (EGC) was presented in [22] and closed form expression for outage probability of DF relaying and selection DF relaying was derived in [23] and [24] over Nakagami-m fading channel, respectively. Recently, a hybrid scheme combining AF and DF was noticed in [25]. It showed that the relay performed soft decision decoding and forwarded the reliability information at the output of its decoder to the destination. This hybrid scheme

showed the benefits of both AF and DF mode and was named as decode-amplify-forward (DAF) protocol or the Hybrid relay system. This DAF relay system provided the basis for this thesis. The communication model is based on the three-node relay model. It can also be called as a two-hop model as the relay transmits to the destination only. To maintain the simplicity of the whole system, we have used a one-antenna relay. Also unlike other DF or DAF relay systems, which forward the data only if it is error free and remains inactive if the signal from the source is inactive, the relay considered in this thesis performs decoding and uses maximum likelihood (ML) algorithm to retrieve back the signal. The relay then forwards the signal to the destination irrespective of wether the signal has any errors or not. However, it keeps a watch on the number of errors received in the frame.

1.2 Technical Issues and Motivation

In this thesis, we aim to develop an adaptive and simplified dual-hop Hybrid Decode-Amplify-Forward (HDAF) Relay System capable of providing improved performance as compared to the conventional MIMO system in terms of improved Bit-Error-Rates (BER). The system is called adaptive as it is capable of working with any number of transmit or receive antennas at either end and simplified as the computational complexity and number of antennas at the relay is kept to minimal. Also, the system is capable of working in different fading conditions. The system is further expanded by performing the tasks of antenna selection and channel estimation on the developed system. We focus on the following while designing the system

- Reliable data communication
- Efficient modulation, coding, and diversity techniques
- Bandwidth and Mobility requirements
- Improved Performance
- Wireless trends

These are explained in detail in the following sections along with the implementation aspects.

1.2.1 The adverse multipath, fading mobile channel

A wirelessly transmitted signal usually propagates through several different paths before it finally reaches the receiver and this is referred to as multipath propagation. These multiple paths have randomly distributed amplitudes, phases, and angle of arrivals, which causes fluctuations in the received signal strength, hence causing multipath fading. In addition, the wireless communication systems suffer from various design challenges due to the mobility of users and the channel characteristics. Due to changing reflections and

attenuation, the channel characteristics tend to change rapidly with time thus making it difficult to design a reliable communication system.

Since radio-wave propagation through wireless channels is a complicated phenomenon, it is characterized by various other effects as well such as fading, inter-symbol interference (ISI), multi-user interference (MUI), multi-path, shadowing etc. Among these challenges, the most troublesome and frustrating problem in receiving radio signals is variations in signal strength, most commonly known as FADING. Channel fading significantly degrades the performance of wireless transmission. A signal transmitted may reach the access point directly through line-of-sight or through multiple reflections from the scatterers at slightly different times. These multiple delayed echoes of the signal, called multipath waves, combine at the receiver antenna to give a resultant signal, which can vary widely in amplitude and phase, depending on the distribution of the intensity and relative propagation time of the waves and the bandwidth of the transmitted signal.

Need for Diversity

Diversity can be explained as the technique to provide the receiver with one or more copies of the same information bearing signals transmitted over independently faded channels. It is an effective approach to reduce the effects of multipath fading. The common diversity techniques used are the time diversity and frequency diversity where the same information is transmitted at different time instants of in different frequency bands. The other most commonly used diversity technique in recent years is the spatial diversity which uses multiple antennas for transmission and reception and is based on the assumption that the fading is independent between the different points in space. Due to the statistical behaviour of the wireless channel, the channel gains can sometimes become small enough such that

reliable transmission may not be possible. However, if by any means the diversity can be increased; there is lesser possibility of getting lower channel gains.

Since diversity means provision of more channel paths, it is a direct expansion of the single-input single-output (SISO) system. Space diversity can be applied at the transmitter or the receiver hence it is categorized as transmit diversity or receive diversity. In receive diversity, the receiver is equipped with multiple antennas. This system improvement with receive diversity is also referred to as single-input multiple-output (SIMO) system. These systems are capable of achieving considerable gains in performance in terms of better link budget, and in effectively combating with co-channel interference. The coherent phases of the signals are combined at the receiver, the signals are combined resulting in diversity gain obtained from independent fading of the signal paths corresponding to the different antennas.

System improvements and performance gains in terms of diversity are not limited to the receiver side. The transmitter can also be equipped with multiple antennas and the diversity technique is known as transmit diversity. These system enhancements can be either multiple-input single-output (MISO) or MIMO case.

1.2.2 Spectral Bandwidth

Systems communicating over a SISO wireless channel have limited capacity and also sometimes, communication over such a channel is not reliable due to multipath fading. Though capacity can be increased directly by allocating more bandwidth in the electromagnetic spectrum, but since bandwidth is scarce resource, it may not be feasible to do so. Thus, to increase the capacity, we may need to utilize the existing spectrum allocation more efficiently and come up with a wireless communication system capable of sending more bits faster within a given bandwidth. One major technological breakthrough possibly making its way in increasing the data rates and hence the capacity is the use of multiple antennas at the transmitters and the receivers in the communication system referred to as multiple-input-

multiple-output (MIMO) systems. The multiple antennas in MIMO systems can be used to increase both the data rates and performance: data rates can be increased through multiplexing whereas performance can be improved through diversity where both the transmitter and the receiver can be used for diversity gains. The increase in the capacity of the MIMO systems was first shown by Winters [1] followed by Telatar [2] and Foschini [4] in proving the fundamental results on the capacity of flat-fading MIMO channels but the focus of study in this thesis is performance improvement through diversity.

Need for MIMO systems

One of the goals of third and fourth-generation cellular systems is to provide broadband data access to highly mobile users. Real-time multimedia services, such as video-conferencing, can require data rates on the order of 2-20 Mb/s. In order to meet this goal, it is important to develop new wireless communication methods that achieve a higher spectral efficiency for a given power expenditure. On multi-path radio channels, the trade-off between spectral efficiency and power consumption can be dramatically improved by deploying multiple antennas at the transmitter/receiver. As the broadband wireless industry struggles to find the right technology to give operators what they need to provide service cost-effectively, MIMO systems have entered the perspective of many as a very promising solution. These systems have attracted significant attention over the past few years as they bring excellent performance enhancements in terms of data transmission rate and interference reduction. For example, MIMO systems help to increase the spectral efficiency (SE) of the overall communication system by exploiting channel diversity and by providing the ability to separate multiple users on one hand and can reduce the effect of channel interferences and achieve high-rate reliable signal transmission on the other hand. Multiple antennas at the transmitter/receiver are becoming very common in wireless systems because of their diversity

and capacity benefits. MIMO systems can increase network capacity without additional bandwidth and energy consumption.

1.2.3 System Complexity

The wireless communication systems combine MIMO technology with different signalling schemes to increase throughput, link quality, stability, and range. But the introduction of MIMO has also lead to a significant increase in the hardware and system complexity of the baseband signal processing and has multiplied the number of modes of operation. Also multiple expensive radio frequency (RF) chains are required to be implemented for multiple antennas in MIMO systems. Antenna selection (AS) techniques has been proposed to deal with this problem. The AS techniques are capable of selecting a subset out of the total available transmit and/or receive antennas based on some selection criteria like maximization of the received signal-to-noise ratio (SNR), channel capacity, or maximum channel power gains.

Need for Antenna Selection Techniques

Antenna Selection (AS) process successfully addresses alleviating the hardware cost of MIMO systems involved in the implementation of multiple expensive RF chains. The number of required RF chains is reduced to the number of selected antennas and thus the cost of the system decreases significantly while exploiting the advantages of the full-complexity MIMO system. AS can be performed at the transmitter, receiver or at both ends. In this thesis, we focus on the AS process based on the maximum channel power gains at the destination. Also, we discuss in details the transmit antenna selection (TAS) process and the joint transmit-receive antenna selection (J-TR-AS) process.

1.2.4 Energy

The traditional resources that have been used to add capacity to wireless systems are radio bandwidth and transmission power. Unfortunately, these two resources are among the most severely limited in the deployment of modern wireless networks: radio bandwidth because of the very tight situation with regard to useful radio spectrum, and transmission power because mobile and other portable services require the use of battery power, which is limited. For example, the battery weight dominates the weight of handheld devices, talk-time of portable telephones is very limited, other handheld devices like laptops and PDAs operate only a few hours without external power supply

These two resources are simply not growing or improving at rates that can support anticipated demands for wireless capacity. Given these circumstances, there has been considerable research effort in recent years aimed at developing new wireless capacity through the deployment of greater intelligence in wireless networks. In particular, to access wireless and multimedia applications, an increase in the information throughput is required with orders of magnitude compared to the data rates provided by today's technologies. However, high network throughput usually implies more energy consumption, which is sometimes unaffordable for energy-aware networks or energy-limited devices. Recently, energy-efficient devices have attracted a lot of attention. A survey on the basic concepts of energy-efficient communications and the advanced techniques for energy efficiency (EE) are summarized in [26] for orthogonal frequency division multiple access (OFDMA) networks, multiple-input multiple-output (MIMO) techniques, and relay transmission systems.

Relay Transmission

Although MIMO techniques have proved quite effective in increased spectral efficiency and capacity but due to additional circuitry and more number of antenna elements at the

source and destination, the energy consumption also increases. If we calculate the ratio of the extra capacity improved and the extra energy consumed, in some case the energy efficiency of a wireless system with multiple antennas might be even lower than the single antenna systems. Antenna Selection is one effective way for reducing energy consumption of multiple antenna systems. Another effective approach to energy efficient system is the use of relays. By positioning relay nodes between the source and the destination, additional channel paths are provided for the data delivery through the multiple RF links. Due to independent fading among different fading channels/links, diversity gain can be obtained and SE can be consequently improved [27]. Therefore, the time to transmit a fixed amount of data reduces and so does the consumed energy. With additional advanced resource allocation schemes, energy can be further saved.

Need for Channel Estimation Techniques

The quality of service offered by any wireless communication system strongly depends on the channel conditions after being affected by channel impairments. Also the performance of MIMO communication systems is known to crucially depend on the amount of channel state information (CSI) available at the transmitter. When no CSI is known, channel estimation plays an important role. Channel estimation is based on transmission of known sequence of bits, which is unique for a certain transmitter and which is repeated depending on the system requirement. In this way, the channel estimator is able to estimate the channel impulse response (CIR) by exploiting the known transmitted bits and the corresponding received samples and better performances are achieved.

Although many techniques have been developed to deal with the issues associated with wireless transmission, it is still quite difficult to overcome the obstacles associated with the wireless environments. Interference from other users causes signal distortion and ISI from

multiple path of one's own signal effectively causes the frequency-selective properties of the channel to occur. There are yet other problems associated like path-loss, channel fading, co-channel interference and above all stringent power limitations on both the mobile unit and the base station which needs attention. Hence to deliver optimal Quality-of-Service (QoS) for different applications over different communication environments, flexibility and adaptivity should be the key features of the future generation wireless systems. So while designing a wireless system it is very important to choose the best scheme that best matches with the desirable constraint. In doing so, it is usually advantageous to rely on the exact quantitative evaluation such as Bit Error Rates (BER) or Symbol Error Rates (SER) to get an insight into the performance limits and evaluate the performance of the wireless systems. The performances based on BER and SER basically relies on the amount of channel fading and thus affects the performance of the whole system.

1.3 Research Problems and Major Contributions

This thesis aims at dealing with various research challenges in relation to improving the performance of relay based systems. In particular the research is based on two-hop hybrid relay systems performing under different fading conditions. The major contributions of the thesis are summarized as follows:

1. How to improve the performance of a two-hop hybrid decode-amplify-forward (HDAF) relay system?

   Various relaying protocols were investigated and based on the information and theoretic analysis, we provide a framework for an adaptive and simplified two-hop hybrid decode-amplify-forward (HDAF) relay system capable of performing in different fading conditions with any number of transmit and receive antenna elements. The focus of the framework is to help increase the diversity. The use of relay and the use of multiple antennas at both the transmitter and the receiver help to achieve diversity in two ways which in turn aids in enhanced performance of the overall system in terms of BERs.

2. How to execute the task of antenna selection (AS) on the two-hop HDAF relay system?

   Here the focus is to investigate various antenna selection strategies and to show that it is possible to have energy efficient transmission using hybrid scheme under different propagation conditions for improved performance. The antenna selection is based on the selection criteria that the transmit antennas associated with the channel paths with maximum channel power gains are selected. It helps in improving the performance of the system, is energy efficient and cost effective. The following antenna selection processes were used

a. Transmit antenna selection (TAS-TR) based on the feedback path from the relay to the transmitter which helps in improving the performance of the system. It proved to be energy efficient and cost effective based on simulations.

b. Joint transmit-receive antenna selection (J-TR-AS) based on the feedback path from the relay to the transmitter for TAS and from the receiver to the relay and the transmitter for receive antenna selection (RAS).

3. Feedback based channel estimation method that provides the fading channel estimates and its approximate auto-regressive (AR) parameters.

    a. The channel estimation algorithm to suit a wireless communication system with lower bandwidth availability where the pilot sequence is used only once, and we refer to this as Auto-Regressive Channel Approximation (ARA) algorithm

    b. The channel approximation and estimation algorithm for the communication systems with the availability of extra bandwidth where the pilot sequence can be inserted before every frame transmission and we refer this as Joint LS Estimation and AR Channel Approximation (LS-ARA)

4. Joint Transmit-Receive Antenna Selection and Channel Estimation where the relay path is used for antenna selection and the direct path is used for channel estimation by using the developed channel estimation algorithms.

1.4 Significance of Contributions

The research carried out in this thesis provides the following significance:

The developed hybrid relay system provides increased diverse paths. The diversity is achieved in two ways: firstly from the use of relay and secondly from the use of multiple antennas at either end. This increased diversity provides reliable Communication and aid in minimizing the error probability. The system is adaptive, thus, even if the TR node fails, the communication can still take place. Nakagami-m fading channel model provides an excellent fit when dealing with various fading conditions. It was shown in chapter – 3 based on the simulation results that if we move the TR node towards the source or the destination, the performance of the system was affected. Nakagami-m distribution helped pick up those small changes in fading conditions arising due to the varying distance between the source and the relay, and the relay and the destination. Use of OSTBC at the transmitter for encoding keeps the complexity of coding the signals to a low and the use of maximum likelihood decision decoding keeps the complexity of decoding the received bits to low at the receiver. Use of MRC gives the best possible results in terms of BER. At the TR node, use of simplified relay with single-antenna keeps the complexity at the relay to minimal thus controlled expenses. No encoding of symbols again at the TR node is required. This proves in lower energy consumption at the relay due to less computational complexity and also makes it easier to keep the relay node mobile and adaptive in different fading conditions.

With the use of Antenna Selection (AS) process, the system is more cost-effective as it uses a subset from all the available antenna elements, and still providing the diversity order similar to using all the available antenna elements. Further AS provides improved performance as compared to the conventional approach with same number of antennas elements. For antenna selection in a conventional MIMO wireless system, antennas can be selected based on the capacity or the SNRs associated. In this thesis, the process of antenna

selection is based on the highest channel power gains associated with the signal. Unlike antenna selection in conventional MIMO systems, where the feedback path from the destination to the source is provided to carry information about the antennas to be selected, in this thesis, we have provided the feedback path from the relay to the source. This reduced the computational complexity of calculating the subsets from each transmit to each receive antenna thus reducing the processing power. Antennas can be selected at the transmitter, receiver or at both ends. We have focused on transmit antennas selection (TAS) and joint transmit-receive antenna selection (J-TR-AS) in this thesis.

The Channel Estimation Algorithms minimize complexity and cost of implementation. However, a trade-off between efficient Bandwidth Usage and performance needs to be maintained. It further helps minimize error probability, thus giving better quality.

The Joint Antenna Selection and Channel Estimation process provides optimum utilization of available bandwidth by making efficient usage of the feedback path available. It further enhances the performance in terms of BER as compared to system with AS alone.

1.5 Research Methodology

Most of the work on the AF and DF relaying focused on flat Rayleigh fading channels. In recent years, the performance of relay transmission over Nakagami-*m* fading channels has been identified. The Nakagami-*m* distribution is widely used as a useful model for physical fading channels. A wide range of fading channels from severe to moderate can be modeled by using Nakagami-*m* distribution depending on the value of the fading parameter m in the range $m \geq 0.5$. The practical importance of Nakagami-*m* fading channels has motivated researchers to investigate the performance of digital communication systems over these channels. For the same reasons, Nakagami-*m* fading channels has been the basis and focus of work presented in this thesis. The use of such channel gave us the freedom of analyzing the performance of the system under study in different fading environments. We have tried to maintain the simplicity and the complexity of the system to minimum. The whole task has been divided into various smaller tasks.

Task – 1 System Modelling

To start with, we first need to model the wireless system which best suits our requirement. We have focused on a two-hop DAF (or Hybrid) relay systems. The background of work performed in the field of relay transmission as presented in Section 1.1 have focused on various system models separately but none of them have presented with the system that can be generalized. For example in [11][12] single antenna at both end was assumed, in [16], multiple antennas at the source and a single antenna at the destination was used, in [15] both ends were equipped with multiple antennas appeared with a single antenna at the relay bt it only amplified the signal at the relay. So far, no system has been successfully modeled that can be easily generalized to the case of single or multiple antennas at the source and/or the destination. DF relays were used to decode the signal at the relays but they were highly

dependent on reliability of the relay to successfully receive the signal without any errors. This is practically not possible. Hybrid system used the benefits of both AF and DF but they were confined to a specific fading environment only and to some extent were again dependent on the reliability of the relay to successfully decode the data.

In this thesis, a two-hop hybrid relay system with single-antenna relay communicating over Nakagami-m fading channel has been developed. Multiple phase shift keying (MPSK) modulation scheme has been focused on for modulation. The system is totally adaptive to any number of antennas at the source and the destination.

At the source, if there is a single antenna, it will transmit an uncoded but modulated data to the relay and the destination. This forms a SISO or a SIMO system model depending on if the receiver has single or multiple antennas. If there are multiple antennas, the signal is coded using OSTBC, thus a modulated and coded version of the original signal is sent to the relay and the destination. This forms a MISO or a MIMO system model depending on the number of antennas elements at the receiver. The reason for using OSTBC is that these have emerged as a key component of MIMO systems that has attracted tremendous attention. First, OSTBC does not require complicated feedback links to provide channel state information at the transmitter (CSIT). Second, OSTBC methods enable maximum likelihood detection to be performed with low computational complexity [28]. Thus, it maintains the simplicity of the system. The system is less complex as no complicated feedback path is required and less computational complex decoding algorithms are required at the destination, thus, keeping the cost low.

At the relay, the single antenna element receives the signal. If the signal is coming from a single antenna source, it is simply demodulated and maximum likelihood operation takes place. The received signal is checked for errors to ensure that the signal is not highly corrupted. We have assumed that the signal never undergoes deep fading and the signal

received at the relay has tolerable errors. The signal received at the relay is normalized, modulated, amplified and then forwarded towards the destination. If the signal is coming from a multi antenna source, then the received signal at relay is first decoded and then modulated. The processes as in single-antenna case are repeated. When forwarding the amplified signal to the destination, the signals are only modulated and they are not encoded again at the relay due to single antenna relay. This helps keep the complexity lower at the relay node. The reason behind this is depending on the requirement of the system, the relay node can be moved at different locations within the distance between the source and the destination. As explained later in chapter – 3 and onwards, the location of the relay affects the performance of the system because of varying fading conditions between source and relay and relay and destination.

At the destination, the receiver receives the signal from the relay as well as from the source directly. So a combining mechanism is needed at the receiver at all times. Out of the many combining techniques available in the literature, we have opted for maximal ratio combining (MRC) in this thesis. When the signal is received over single antennas at the receiver, the signals from the relay and the source are summed after normalizing them separately which is then demodulated to recover the original signal. When the signal is received over multiple antennas at the receiver, the signals from the relay and the source are combined using MRC and then demodulated to recover the original signal. In all cases, the signals from the relay and the source are normalized separately. When the signal is transmitted using multiple transmit antennas, the signals are first decoded and then combined with the signal received from the relay.

Task – 2 Antenna Selection

MIMO systems require multiple expensive RF chains for transmission. Antenna selection has come up as a promising solution which is capable of selecting only a subset of the available antennas to transmit or receive antenna [29]. Antenna selection over conventional MIMO systems has attracted lot of attention due to its lower complexity and cost. In this thesis, we perform antennas selection for MPSK over Nakagami-m fading channels for a two-hop DAF relay system. Firstly, we develop the system model only for transmit antenna selection (TAS) and then we extend it to joint transmit-receive antenna selection (J-TR-AS).

In Transmit Antennas Selection for the two-hop DAF relay system, feedback from the relay and the destination can be used for TAS. This involves a feedback path from the relay as well as from the receiver. This will increase the cost of the system due to the requirement of the two feedback paths and when selecting multiple antennas, more feedback is required. Also, the subsets of selected antennas from the relay and the receiver may not be same each time TAS is performed due to different fading conditions between the source and the relay, and source and the destination. To simplify the system, the TAS process discussed in this thesis is based on the feedback from the relay node only. Pilot symbols are transmitted from the multiple transmit antennas to the relay. At the relay, the channel power gains are calculated and fed back to the transmitter where the transmit antennas corresponding to the highest channel power gains are selected for transmission. Once the antennas are selected, data transmission takes place through the selected antennas.

In Joint Transmit-Receive Antennas Selection for the two-hop DAF relay system, again the feedback from both the relay and the receiver can be used for used for antennas selection. In J-TR-AS, antennas selection involving multiple antennas at both ends become more complex due to the subset formation from each transmit antenna to every receive

antenna. But by using the relay for antenna selection, the complexity of the system is highly reduced. Pilot symbols are transmitted from the source to the relay, where based on the channel power gains, transmit antennas are selected, the pilot symbols are further transmitted from the relay to the receiver where again based on the maximum channel power gains, receive antennas are selected. The source now knows which antennas to be used for transmission and at the receiver; it knows which antennas are to be used for reception. During the TAS, it is similar to selecting antennas from a MISO system and for receive antenna selection (RAS), it is similar to selecting antennas from a SIMO system, which is much simpler than selecting antennas from a MIMO system.

Task – 3 Channel Estimation Algorithms

Since there is a feedback involved is sending the information for the antennas selected at both ends, we decided to utilize these feedback paths for estimating the channel and providing CSI. For this, we proposed two feedback-based algorithms based on first-order auto-regressive process which is discussed in Chapter – 6.

Task – 4 Joint Channel Estimation and Antenna Selection

The developed channel estimation algorithm has been employed to the two-hop DAF relay system under study and performs the task of joint channel estimation and antenna selection. When the source-relay-destination path is busy in antenna selection, the direct source-destination path is inactive. Also, the CSI between the source-relay and relay-destination is known due to the process of antenna selection but the CSI of the direct path is still not known. So based on the channel estimation algorithms proposed, we use the direct source-destination path for channel estimation and the source-relay-destination path for antenna selection.

Thus, the following system models have been developed in this thesis.

- Two-hop DAF relay system no AS at either end.
- Two-hop DAF relay system with TAS.
- Two-hop DAF relay system with J-TR-AS.
- Two-hop DAF relay system with channel estimation using Least Square (LS) Algorithm.
- Two-hop DAF relay system with channel estimation using Least Square Auto-Regressive Algorithm (LS-ARA).

To track the improvement in performance, the developed systems have been compared with the following systems.

- Conventional wireless systems with no AS at either end.
- Conventional wireless systems with TAS.

Also the relay has been defined as the transceiver (TR) node, therefore, TR node and relay has been alternatively used throughout the thesis.

1.6 Thesis Organization

The thesis consists of seven chapters and four Appendices in total. The framework of this thesis report is as follows:

Chapter – 1 presents a brief introduction of the wireless communication scenario, MIMO systems, Relay Systems, Antenna Selection Techniques, diversity techniques and channel estimation algorithms followed by the motivation for carrying this research, discussion of the research problem and methodology.

Chapter 2 explains the basic concepts and principles of the wireless relay systems. It also provides a brief literature review on their advancements.

Chapter 3 introduces some fundamental concepts related to this thesis. This includes a general description of the wireless communication system and its components, digital modulation techniques, wireless channel impairments, various system channel models, transmit and receive diversity, diversity due to relaying, antenna selection and channel estimation algorithms.

Chapter – 4 primarily focuses on the Hybrid relay system over Nakagami-*m* fading channels. The chapter starts with system modelling of a two-hop decode-amplify-forward (DAF) relay systems where the signal processing has been described in detail. Then we derive the equivalent end-to-end SNR for various system models under study followed by the derivation of the symbol error probability (SEP) for MPSK modulations. It has been revealed that with the use of a TR node at the relay, the system performance improves due to increase in the diverse paths. We show this by performing the simulations using MATLAB.

Chapter – 5 focuses on the concept of antenna selection (AS) where we focus on the process of transmit antenna selection (TAS-TR) in the first half of the chapter followed by joint transmit-receive antenna selection (J-TR-AS) in the later half. Firstly we present a brief introduction of using antennas selection and its benefits in MIMO systems. Then we discuss

the system and channel model for transmit antennas selection and joint transmit-receive antenna selection for the two-hop DAF system. We also derive the SEP for the overall system. We then present the simulations results using Monte Carlo simulation for the system under study and compare their performances based on the BERs. It is revealed that the equivalent system models formed after antenna selection performs better than the system models without antenna selection with same number of transmit and receive antennas.

Chapter – 6 focuses on the channel estimation algorithms. In this chapter we have developed two feedback based channel estimation algorithms that follow first order auto-regressive process. Based on how the pilot symbols are inserted within the frame, the performance of the two algorithms were analysed by simulations. The algorithm that showed better performance was then used by the two-hop DAF system that also performs joint transmit-receive antenna selection. Thus, we form a system model capable of performing the joint task of antenna selection and channel estimation rather than using all the available channel paths for antenna selection alone. This results in a system model which is less complex that the existing system of joint antenna selection.

Chapter – 7 summarizes the major findings and contributions of the thesis and provides some suggestions for further study.

Chapter 2 – Literature Review

Future wireless communication systems need to support very high data rates in order to fulfil increasing customer demands. The vision is not feasible with the conventional wireless communication architecture as it demands a radical increase in the number of base stations. Introduction of wireless relays is one possible solution to the problem to increase the capacity as well as radio coverage area with minimal increment in the capital expenditures. The purpose of this chapter is to provide an overview of the recent developments, issues and future trends in wireless relay networks. Firstly, brief overview on the context of wireless relay networks is presented including the importance and literature review on wireless relays. The following sections discuss various relaying modes and topologies.

2.1 Introduction

The increasing popularity of mobile and handheld devices and the urge to provide communication anywhere and anytime has motivated the growth of wireless networks in the last decades. The need for continuous access to wireless information has led to more demands on system designers to provide higher throughput and enhanced battery longevity. To achieve this, the designed wireless networks should be able to reveal a high spectral efficiency and be able to combat channel impairments including multipath fading, shadowing and path loss for an improved consistent coverage.

In recent advances, radio transceiver techniques such as multiple input multiple output (MIMO) system designs have shown an improvement in the capacity of the current systems by dealing with the channel multipath fading. This is possible by adding multiple antennas at the transmitter and/or the receiver. Fig. 2.1 shows a standard MIMO architecture.

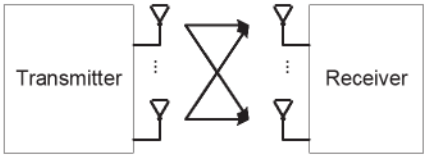

Fig. 2.1 Multiple Input Multiple Output (MIMO) architecture

The MIMO architecture exploits the random fading effects in wireless system, thus increasing the diversity of the transmission. Space-time codes are used to provide diversity and coding gains in multiple antenna systems over fading channels. Space-time coding (STC) has received a significant amount of attention in the last few years as a way to increase data rates and/or reduce the transmitted power necessary to achieve targeted bit error rates (BERs) using multiple antenna transceivers. Diversity gains are possible when an information sequence is passed through multiple, independent paths of the channel. Spatial diversity gains can be achieved by using multiple antennas. Performance is improved due to the increased likelihood of one of the data streams experiencing a good channel condition. Despite the

promise shown by multiple antennas in mitigating the effects of fading, in ad-hoc or distributed large scale wireless networks, constrains due to hardware complexity and size makes multiple antenna systems impractical for certain applications. To meet the demands of increased reliability, and spectral and power efficiency without increasing the size of mobile devices, fundamentally new paradigms are needed to improve performance. Cooperative diversity schemes have been introduced in an effort to overcome these limitations and meet the growing demands. Cooperative communications [30–34] exploit the spatial diversity inherent in multiuser systems by allowing users with diverse channel qualities to cooperate and relay each other's messages to the destination. Each transmitted message is passed through multiple independent relay paths, and thus, the probability that the message fails to reach the destination is significantly reduced. Even if the user is equipped with only one antenna, their relays form a distributed antenna array to achieve the diversity gain of a Multiple-Input-Multiple-Output (MIMO) system which combat multipath fading in wireless channels. This makes cooperative techniques attractive for deployment in cellular mobile devices as well as in ad-hoc mobile networks. The simplest example of a cooperative network is the Relay-assisted communication which has recently gained a lot of attention. In contrast to conventional MIMO systems, the relay-assisted transmission is able to combat not only the small scale but also large scale effects like shadowing and path-loss.

In the following sections, we first present a brief overview on the context of wireless relay networks, followed by relaying protocols, various network topologies and performance measures for wireless relay networks.

2.2 Wireless Relays Networks and the Advancements

Relay based communication was first introduced in [5] and was further studied in [35]. The work was further extended by deriving upper and lower capacity bounds in [6] which provided an information-theoretic analysis for a one-way full-duplex relay channel under additive white Gaussian channels. The basic principle for relay based communications is that a new element called the relay terminal comes up in the communication. Figure 2.2 shows a standard three node wireless relay network architecture. When the source (S) transmits the message to the destination (D), obstacles degrade the source-destination link quality. With the relay terminal (R) in place that message is also received by the relay terminal, which re-transmits that message to destination. The destination combines the transmissions received by the source and relay in order to decode the message.

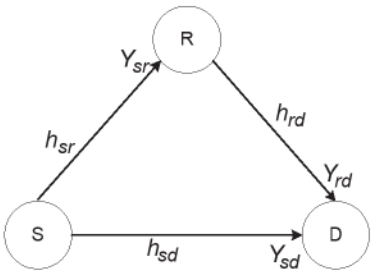

Fig. 2.2 A one-way three-node relay network architecture

In [7], a low-complexity cooperative diversity protocols were developed and analysed that can combat fading induced by multipath propagation in wireless networks. It was shown that the underlying techniques exploit space diversity available through cooperating terminals' relaying signals for one another. Several strategies employed by the cooperating radios, including fixed relaying schemes such as amplify-and-forward and decode-and-forward, selection relaying schemes that adapt based upon channel measurements between the cooperating terminals, and incremental relaying schemes that adapt based upon limited feedback from the destination terminal were outlined. Performance characterizations in terms

of outage events and associated outage probabilities, which measure robustness of the transmissions to fading, focusing on the high signal-to-noise ratio (SNR) regime were also developed. It was also shown that by using distributed antennas, powerful benefits of space diversity without need for physical arrays can be provided, though at a loss of spectral efficiency due to half-duplex operation and possibly at the cost of additional receive hardware. An amplify-and-forward cooperative diversity system was considered in [36] and two power allocation schemes were presented to minimize the system outage probability. A selection scheme to select the best relay node was also proposed. In [37], it was shown that an optimal selection and transmission of a single relay among a set of multiple amplify-and-forward (AF) candidates minimizes the outage probability (i.e., outage-optimal) and outperform any other strategy that involves simultaneous transmissions from more than one AF relay under an aggregate power constraint. In contrast, a novel scheme that selects the best relay between source and destination based on instantaneous channel measurements was proposed in [38] which required no knowledge of the topology or its estimation. Further, a distributed power allocation algorithm was developed in [39] to maximize the network throughput of DF relay networks.

The concept of single-relay diversity was extended in [40], and a distributed version of the well-known switch and stay combining (SSC) technique was proposed. The performance analysis of cooperative diversity with MRC and EGC has been extensively studied over Rayleigh and Nakagami-m fading channel in [21], [41] and the effect of the imperfect channel estimates on the performance of SSC and SEC in Rayleigh, Ricean and Nakagami fading was studied in [42], [43]. The tight bounds for the outage and error probability of a distributed spatial diversity wireless system in the presence of Rayleigh fading was presented in [44]. An end-to-end performance of a dual hop fixed gain relaying system when the source-relay and the relay-destination channels experience Rayleigh/Rician

and Rician/Rayleigh fading scenarios, respectively, were presented in [45]. In [46], tight upper bounds for the end-to-end SNR and error probability of dual-hop wireless communications systems with non-regenerative relays over Nakagami-m fading channels were presented while in [47] the end-to-end SNR for multi-hop wireless communications systems with non-regenerative fixed-gain relays and upper bound using the harmonic and geometric mean of positive RVs were presented. Using this bound, simple closed-form expressions are also derived for the moments of the end-to-end SNR in Rayleigh, Nakagami-*m*, and Rician fading. Moreover, the outage probability and the average error probability are derived for several coherent and non-coherent modulation schemes using the MGF approach. The closed form expressions of outage probability and bit error rate for BPSK for the case when communication between source and destination is supported by multi-antenna relay were derived in [48]. Outage probability of two-hop multi-antenna relay based system for the case when relay performs SC of signals and destination performs MRC of signals and the closed form expressions for outage probability and BER for multi-antenna cooperative relay network have been derived in [49] and [50], respectively, where source and relay are communicating with multi-antenna destination over correlated Nakagami-m fading channel. In [50], both the relay and destination perform MRC combining of signals.

The above-mentioned relay schemes, however, were only considered for one-way relay networks where the source and the relay transmit information to the destination in successive time slots in which the relay does not actively help the source, but rather, facilitates the source transmission by inducing as little interference as possible; as shown in Fig. 2.2. Recently, there has been increasing attention paid to the two-way/bidirectional relay channel (e.g., [51]–[55]), where two senders exchange information via one assisting relay. Fig. 2.3 shows architecture for a two-way relay channel where for bidirectional traffic, the destination node *d* is also a source node, and node *s* is also a destination node.

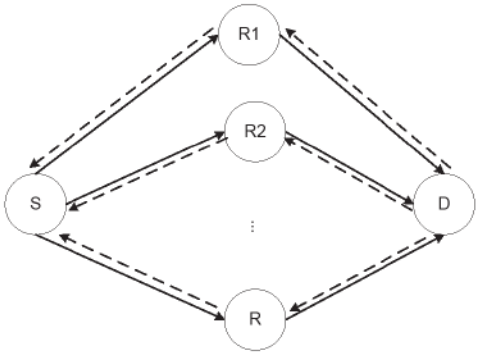

Fig. 2.3 A two-way wireless relay network

The two-way communication channel was first studied by Shannon [56] in 1961, when the inner and outer bounds of the capacity region were derived. Achievable rate regions for some two-way channels and two-way relay channels were later derived in [57] and [58], respectively. In comparison with the traditional one-way relaying that forwards messages from one of the two source nodes to the other in an alternate manner, the two-way relaying provides an improved spectral efficiency for information exchange between two source nodes by allowing the relay to receive/forward from/to two source nodes at the same time. Therefore, combining the two-way relaying with other transmission technologies, such as multicarrier [59] and/or multi-antenna [60], creates promising designs for the future generation of wireless systems.

The conventional relay selection methods proposed for one-way relaying may also be applied to the bidirectional communication scenario after some modifications. In [61], a bidirectional relay selection criterion is proposed, wherein the relay is chosen to maximize the weighted sum of the bidirectional rate pair on the boundary of the achievable rate region. Similar to one-way relaying, there are also DF and AF modes for two-way relay networks, in which the AF relay strategy is similar to that in one-way relay network, while the DF applies the concept of network coding. Though studies of the two-way relay channel [62], [63] indicate the possibility of no interference even if there is more than one source, in this thesis

we focus on one-way relaying for the sake of simplicity. In the following section we discuss some of the relaying protocols.

2.3 Relaying Protocols in Wireless Networks

In this section, we outline several relaying protocols and exhibit their robustness to fairly general channel conditions. The most common relaying protocols are the ones in which either the relay amplifies what it receives, or it fully decodes, re-encodes, and retransmits the source message. These two relay signalling methods are now reviewed.

2.3.1 Amplify-and-Forward

The amplify-and-forward relaying mode allows the relay station to amplify the received signal from the source and forward it to the destination. In this method each relay node receives the signals transmitted by the source but do not decode them. These signals in their noisy form are amplified to compensate for the attenuation suffered between the source-to-relay links and retransmitted. The AF method was proposed and analysed in [7, 64] where has been shown that for the two-user case, AF relay method achieves diversity order of two, which is the best possible outcome at high SNR. In [65], a wireless network with fading and a single source-destination pair is considered where the information reaches the destination via multiple hops through a sequence of layers of single-antenna relays. It has been shown that the performance of this amplify-and-forward strategy degrades with increasing network size. This phenomenon is analysed by finding the tradeoffs between network size, rate, and diversity. A lower bound on the diversity-multiplexing trade-off for concatenation of multiple random Gaussian matrices is also obtained. A framework to compute the maximum achievable rate with AF schemes for a class of general wireless relay networks, namely Gaussian relay networks has been provided in [66]. This framework casts the problem of computing the maximum rate achievable with AF relay networks as an optimization problem.

In A&F, it is assumed that the destination requires knowledge of the channel state between source-to-relay links to correctly decode the symbols sent from the source. This requires transmission of pilots over the relays resulting in overhead in terms of additional

bandwidth. Another potential challenge is that sampling, amplifying, and retransmitting analogue values are technologically nontrivial. Nevertheless, AF is a simple method that lends itself to analysis and thus has been very useful in furthering our understanding of cooperative communication systems.

2.3.2 Decode-and-Forward (DF)

The decode-and-forward relaying strategy allows the relay node to decode the received signal from the source, re-encode it and forward it to the destination. The receiver at the destination uses information retransmitted from multiple relays and the source (when available) to make decisions. During decoding, it is possible for a relay node to decode symbols in error resulting in error propagation making it unsuitable for delay limited networks. Perfect regeneration of symbols at the relays may not be possible. However, retransmission of symbols or use of forward error correction (FEC) depending on the quality of the channel between the source and the relays may help in regeneration of symbols with least errors. In [67], end-to-end bit error, outage probabilities and the diversity performance of wireless relay networks with multiple parallel relays communicating with the destination over orthogonal channels has been investigated with a focus on the decode-and-forward (DF) relaying protocol. In [68], an ideal case using DF protocol is studied where the relay is able to know exactly whether each decoded symbol is correct. A framework of non-coherent cooperative relaying for the DF protocol employing FSK has been studied in [69]. A maximum likelihood (ML) demodulation was developed to detect the signals at the destination. Due to the nonlinearity form and high complexity of the ML scheme, a suboptimal piecewise-linear (PL) scheme was also proposed in [69] and was shown to perform very close to the ML scheme. Selection combining scheme has been widely investigated for coherent DF relay systems in which a perfect knowledge of channel state information (CSI) is available at the relays and destination [70-73]. In [74], a new decode-

and-forward relaying scheme for a cooperative wireless network composed of one source, K relays, and one destination and with binary frequency-shift keying modulation has been studied. The paper claims through analytical and simulation results that the obtained optimal threshold scheme or jointly optimal threshold and power-allocation scheme can significantly improve the BER performance compared to the previously proposed schemes.

DF relay can be further classified as Fixed DF and Adaptive DF scheme. For the fixed DF scheme, the relay always detects and forwards the original data by maximum likelihood (ML) detection. Although this scheme is simple, the cooperation can be detrimental to the eventual detection of symbols at the destination due to error propagation if the detection at relay is unsuccessful. In Adaptive DF Scheme, relay evaluates the quality of the received signal and check whether it satisfies the preset requirement. The relay detects and forwards the data to the destination. Otherwise, it keeps silent in the second phase. Therefore, the problem of erroneous retransmission and error propagation induced by the relay in fixed DF scheme can be mitigated.

2.3.3 Hybrid amplify-decode-and-forward

Recently, a new class of forwarding strategy, named as decode-amplify-forward (DAF), was proposed for relay channels. The proposed DAF strategy cleverly combined the merits of both decode-forward (DF) and amplify-forward (AF) by exploiting the coding gain on the inter-user channel and maximizing the data reliability. Since this new scheme hybrid the merits of both AF and DF relay schemes, it is also known as Hybrid DAF (HDAF) scheme. The HDAF scheme combining AF and FDF with soft-decision, namely decode-amplify-forward protocol, has recently been reported in [25]. The relay performed soft decoding and forwarded the reliability information at the output of its decoder to the destination, hence combining both AF and DF mode. Another hybrid scheme of ADF and AF for orthogonal frequency division multiplexing (OFDM) systems was proposed in [75].

Depending on the channel condition of the source-to-relay link on each subcarrier, the better protocol between ADF and AF is selected. Simulation results verified the advantages of the proposed hybrid scheme. In [76], a cooperative communication scheme with hybrid decode-amplify-forward (HDAF) protocol combining the AF mode and ADF mode with hard decision was focussed on. It was shown that instead of remaining silent during the second-hop transmission if the signal is corrupted as in the ADF protocol, the HDAF scheme can increase the performance by having the relay perform in the AF mode. When the relay has full knowledge about the instantaneous fading channel of the source-to-relay link, it can operate in channel state information (CSI)-assisted AF relay mode. The performance gain of hybrid decode-amplify-forward (HDAF) relay protocol over the ADF and AF in dual-hop multiple-relay networks were also investigated in [77]. The performance gain in terms of the symbol error probability (SEP) in the high signal-to-noise ratio (SNR) regime were analysed. It was also shown that in contrast to the single-relay case in which the HDAF scheme has no benefit compared to ADF and AF as the relay is located close to the source, HDAF still achieves a small gain with multiple relays.

2.4 Various Relay Network Topologies

2.4.1 Two-hop relays

The two-hop relaying systems typically operate over two phases or hops. In the first hop, signal transmission from source is received by single/multiple relays and the destination. In the second phase, relays forward the information to the destination as shown in Fig. 2.2. The destination combines the relayed signals and the direct signal received in the first hop to improve the SNR. This process creates multiple fading channels from the source to the destination.

Past works concerning the performance of dual-hop systems over fading channels can be found in [45], [46], [49], [50], [76]. In [78], an end-to-end performance of dual-hop transmission systems with regenerative and non-regenerative relays over Rayleigh fading channels was studied. In [79], the performance of dual-hop wireless communication systems with fixed-gain relays over Nakagami-m fading channels was investigated. In [80], the end-to-end performance of one of branch dual-hop relaying systems operating in Rayleigh fading channels is analysed. The Dual hop relay systems can employ single or multiple relays at the relay node. However, due to the use of only one relay, the diversity of these systems remains limited. The performance of the dual-hop relay systems can be enhanced by utilizing multi relays. The end-to-end performance of multi branch dual-hop wireless communication systems with non-regenerative relays and equal gain combiner (EGC) at the destination over independent Nakagami-m fading channels was studied in [81] and new closed form expressions for probability distribution function (PDF) and cumulative distribution function (CDF) of end-to-end signal to noise ratio (SNR) per branch in terms of Meijer's G function were presented. In [44], the error performance of a multi branch dual-hop relay system in Rayleigh fading channels is studied. The main aim of the next-generation cellular wireless networks is to support high data rates and maintain the required quality of service (QoS) for

multimedia applications with increased network capacity. Dual hop cellular networks possess the potential of enhanced coverage, data rates, QoS performance, as well as bit error rates. However, in-depth analysis and careful system designs are required to exploit these potential advantages. Furthermore, dual hop relaying gives better trunking efficiency at aggregation points, along with the fact that site acquisition and antenna structures are much less expensive.

2.4.2 Multi-hop relays

In multi hop relays, the information transmitted from the source reaches the destination is successive multiple hops via multiple relays installed between the source and the destination as shown in Fig. 2.4

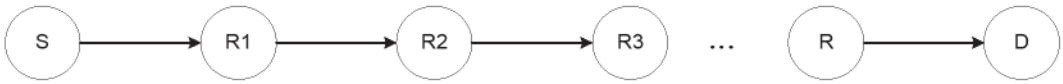

Fig. 2.4 A multi-hop wireless relay network

The source, destination and relays nodes can be equipped with single or multiple antennas. Recently, multi-hop relaying for wireless communication has attracted considerable attention in both industry and academia. It has been shown in the literature that by using multi-hop relaying, problems like coverage, capacity and cost can be easily solved in wireless communication systems. Several analyses have been proposed for more general multi-hop relay networks [33], [47], [65], [82]–[84]. The tradeoffs between rate, diversity, and network size for multi-hop MIMO AF networks were analysed in [65], and the diversity-multiplexing trade-off was derived in [82]. In [83], the asymptotic capacity of multi-hop MIMO AF relay systems was obtained when all channel links experience i.i.d. Rayleigh fading while the number of transmit and receive antennas, as well as the number of relays at each hop grow large with the same rate. In [84] hierarchical multi-hop MIMO networks were studied, the scaling laws of capacity were derived when the network density increases.

A multi-hop relaying system where data is sent by a multi-antenna source and is relayed by successive multi-antenna relays until it reaches a multi-antenna destination is analysed in [85]. In [86], the general model and the bit error rate (BER) of multi-hop WRNs employing distributed STBC at the relay nodes were analysed. The pair wise error probability was also derived and the impact of several parameters, such as distributed STBC at the relays, the number of relays, the distances between the nodes, and the channel state information available at the receivers, on the BER performance of the multi-hop WRN were also examined.

It is very obvious that the dual hop wireless channels can be extended into multi-hop wireless channels by merely inserting few more relay stations (RS) in order to meet the coverage and throughput when the demand grows further. However, as RSs close to source have to carry traffic originated from and destined to multiple RS and destination stations (DSs), traffic accumulation occurs and tends to grow larger with more number of hops. The congestion with multi-hop forwarding will be at its peak at the RS nearest to source. Because of unnecessary congestion and rise in media access time, the overall end-to-end packet delay would also increase. Along with, due to node mobility and fluctuations in radio signal strength, the routing path from the source to the destination could easily become invalid. Frequent route changes and the resulting route discovery procedures could cause high signalling overheads. As a consequence of all these limitations, IEEE 802.11 has been reported not to perform well in multi-hop relay environments.

Though relay-assisted multi-hop networks are expected to play a significant role in 4G wireless communication systems, because of its great potential to cost-effectively extend the coverage and/or increase the spectral efficiency, and driving the cost of deploying 3G+ and 4G systems lower, considering the limitations which include packet delay, signalling overhead, and system complexity, simple dual-hop relay implementation may appear better in

contrast to the multi-hop relay systems. Thus, throughout thesis our discussions are limited to dual hop relay links only.

Chapter 3 – Theory of Wireless Communications

Signal transmission through a wireless medium tends to deteriorate the signal due to multipath, fading and inter-symbol interference (ISI). These attenuations can be dealt with up to some level by using multiple antennas at the transmitter and the receiver to improve the performance. Also by estimating the channel state information of the channel paths through which transmission takes place, performance of the wireless system can be further increased. There are a few more ways that may help in improving the performance of the wireless systems. These include Diversity methods, Antenna Selection Schemes, Relayed Transmissions, channel estimation and data detection algorithms. This chapter gives a brief introduction about the channel impairments, fading channels involved in data transmission and some of the solutions to deal with the problem of multipath and fading.

3.1 Introduction

The field of wireless communication has been known since the first humans began to communicate using fire smoke and sounds as signals for transmitting messages over short distances. But communication over long distances wasn't made easy until late 1800's, when Marconi and his associate successfully established a 14.5 miles fixed wireless link over the sea [87]. His invention was even used by the Italian Navy for sea-to-shore communication. These were the first digital communications that took place at a rate of 12 words per minute and operated at wavelengths of up to 10,000 meters with corresponding frequencies of 3-30 kHz. It was at this time when many great communications companies came into existence. The number of developments in the field of digital communication grew rapidly over the late 20th century. Since then there has been a widespread increase in developing new wireless communication techniques capable of transmitting information over high data rates and providing low bit error rates (BER). [88] focused on some of the wireless technologies that emerged in the past and also provided an insight into the future wireless technologies.

Currently this has led to growing use of cellular phones, cordless phones, and digital satellite systems capable of communicating at many different frequencies ranging from tens or hundreds of Hertz for underwater communication to infrared range of 10^{14} Hertz. As people are becoming more accustomed to immediate access to any available information like news, sports or even their own location, the area of wireless communication will continue to grow and the next generation wireless communication systems will continue to provide variety of services to everyone and everywhere.

3.2 Digital Communication System

Any efficient wireless communication system requires proper characterization of its components to deal with the harsh environment. Irrespective of the purpose for which a wireless system has been designed, it necessarily has three major components: a transmitter, a channel, and a receiver. Fig. 3.1 shows a basic block diagram of a wireless communication system [89].

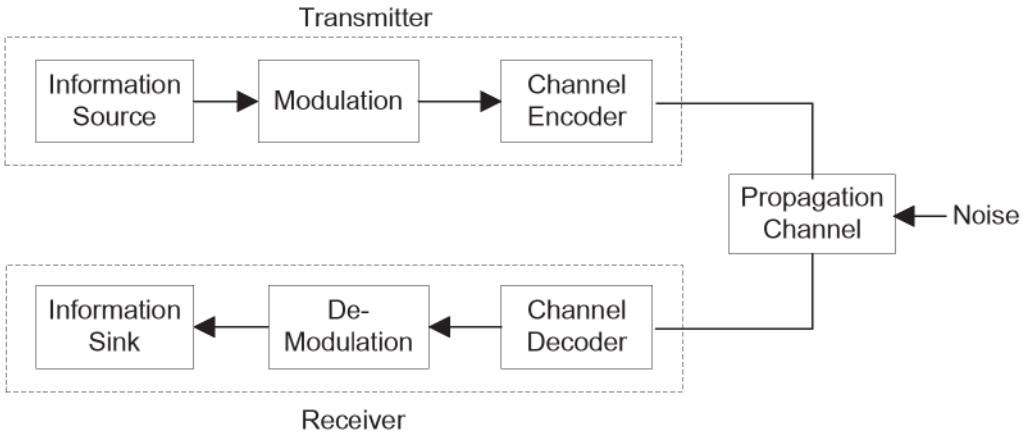

Fig. 3.1 A general wireless communication system

The information source is the actual data that needs to be transmitted. The data can be in analog form like voice, video and pictures, or in digital form like text or multi-media. The transmitter accepts the data in form of signal from this information source and processes it into an appropriate format to be transmitted over the channel. If the data is in analog format, the source encoder converts it into digital (binary) form. The binary data is then subjected to channel encoder for reliable transmission. The channel encoder adds controlled redundancy to the binary sequence for error detection and correction. The encoded data sequence is then modulated to generate waveforms for transmission over the channel.

The channel is a physical medium between the transmitter and the receiver in the form of a telephone line, a high frequency radio link, a storage device, vacuum etc. and usually contains disturbances like noise and obstacles like buildings, terrestrial features.

At the receiver, the signal is captured and processed in a form appropriate to trace back the transmitted information. During this whole sequence of data transmission, the signal gets corrupted, degraded and attenuated due to noise and channel impairments. By carefully compensating these channel impairments and system designing, the data rates can be maximized and the signal degradation can be improved.

3.3 Digital Modulation Techniques

The process of modulation is to modify a signal so as to carry data over the communication channel. Successful simulation of any wireless communication system depends on the modulation techniques used which is capable enough of capturing all the significant deviations from the ideal behaviour. While designing any wireless communication system, the use of any particular modulation scheme is based on the application as well as on the channel characteristics such as available bandwidth and its susceptibility to fading. When data transmission takes place through a channel, the signal amplitude tends to vary with time due to the variability in the transmission medium. In such situation we need a modulator and demodulator at the transmit and the receive side, respectively, in order to recover the signal.

During transmission if a binary waveform is superimposed on the carrier then amplitude modulation (AM), phase modulation (PM) or frequency modulation (FM) may be used. However, in some cases a combination of AM-PM can be employed such as Quadrature amplitude modulation (QAM). FM shows more resistant to channel impairments and performs better in terms of power efficiency whereas AM and PM outperforms in terms of spectral efficiency. In this thesis we mainly focus on AM, MPSK.

3.3.1 MPSK Modulation/De-Modulation

If we group together N bits over the time $T_s = NT_b$, where T_b is the bit duration and T_s is the symbol duration, then there are $2^N = M$ possible symbols. MPSK modulation uses these M possible symbols to represent the digital data where each possible symbol encodes $log_2 M$ binary bits to represent a particular symbol [90]. The phase of the carrier signal is shifted by the modulation signal with the phase measured relative to the previous bit interval. The transmitted signals can be identified as

$$x(t) = \sqrt{\frac{2E_b}{T}}\cos(2\pi f_c t + \theta_m) \tag{3.1}$$

where E_b is the energy contained per bit

T is the bit duration

f_c is the carrier frequency

θ_m is the phase of the un-modulated carrier given by $(2m+1)\pi/M$ where $m = 0,1,\ldots,M-1$

Depending on the number of bits being transmitted in a symbol, M can take different values of 2,4,8,16. When $M = 2$, each bit is transmitted individually to control the phase of the carrier and is called as binary phase shift keying (BPSK) modulation [91]. During each bit interval, the modulator shifts the carrier to one of the two possible phases which are π radians apart. Thus with two phases $0\ and\ \pi$, the binary data is communicated with the following signals:

For binary '0'

$$x_0(t) = \sqrt{\frac{2E_b}{T}}\cos(2\pi f_c t + \pi), \qquad when\ \theta = \pi, \text{ and} \tag{3.2}$$

For binary '1'

$$x_1(t) = \sqrt{\frac{2E_b}{T}}\cos(2\pi f_c t), \qquad when\ \theta = 0, \tag{3.3}$$

In the complex form, the modulated signal can be expressed as

$$x(t) = I(t) + jQ(t) \tag{3.4}$$

where $I(t) = R(t)cos\theta$, $Q(t) = R(t)sin\theta$, and $R(t) = \sqrt{\frac{2E_b}{T}}$ is the bipolar baseband signal.

When $M = 4$, two bits are grouped together to form a symbol and is called quadrature phase shift keying (QPSK) modulation. QPSK modulation uses four constellation points which are equi-spaced around a circle and it is more resilient to noise. With four phases

present, QPSK encodes two bits per symbol and there are four possible combinations for each symbol:$00, 01, 10, or\ 11$. Unlike BPSK where the modulator shifts the carrier to $0\ or\ \pi$, in QPSK the modulator shifts the carrier to one of the four possible phases corresponding to the four possible input symbols [92]. Thus, a QPSK signal can be defined as

$$x(t) = \sqrt{\frac{2E_b}{T}}\cos(2\pi f_c t + \theta) \tag{3.5}$$

where θ can take four possible phases of $\frac{\pi}{4}, \frac{3\pi}{4}, \frac{5\pi}{4}, or \frac{7\pi}{4}$ as needed. The BPSK and QPSK constellations [93] are shown in Fig. 3.2. At the receiver the demodulator removes the data from the carrier and the data bits are recovered.

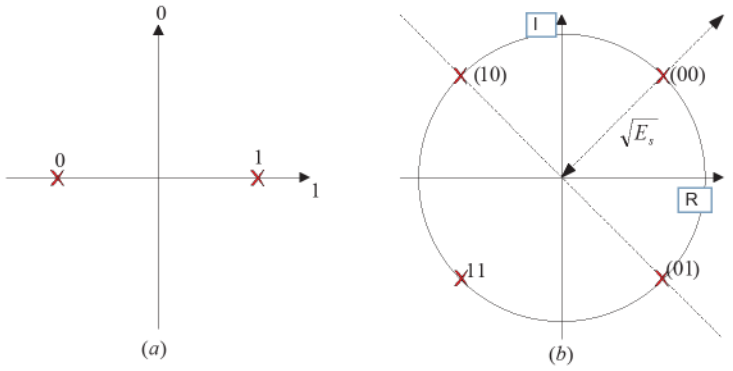

Fig. 3.2 (a) BPSK constellation, (b) QPSK constellation

In terms of handling noise and distortion, BPSK modulation is the strongest of all the PSKs as it takes the highest noise or distortion level aiding demodulator to reach to a correct decision. But since it is capable of handling only one bit per symbols it is not suitable for band-limited high data-rate applications. Another advantage of using QPSK over BPSK is that in BPSK the data stream is transmitted with T_b bit duration with channel bandwidth of $2f_b$, where $f_b = 1/T_b$, whereas in QPSK the data stream is transmitted with $2T_b$ bit duration using channel bandwidth of f_b, thus using half the available bandwidth.

3.4 Wireless Fading Channels

3.4.1 Fading channel impairments

Wireless communication takes place over radio waves for transmitting information, where the carrier frequency of these radio waves can vary from a few hundred megahertz to several gigahertz depending on the system. The wireless channel can be described as a function of time and space. The signal received at the receiver is the combination of the many replicas of the same transmitted signal arriving at the receiver from several directions. Therefore, signaling over a wireless channel is severely affected by the environmental radio propagation effects as the channel state may change within a very short time span and hence suffers from many channel impairments.

3.4.1.1 Attenuation

When the wireless transmission takes place over a large distance of several kilometres, there occurs a steady decrease in the power of the transmitted signal at the receiver. This refers to attenuation. The attenuation caused by wireless propagation causes path loss, shadowing loss, and fading loss. Path loss refers to signal attenuation due to distance between the communication nodes, shadowing loss occurs due to absorption of signals in local structures like buildings, and fading loss occurs due to the constructive and destructive interference of the multiple reflected radio wave paths.

3.4.1.2 Noise

Noise is present in every communication system in various forms. It can be in a form of thermal noise which occurs due to agitation of electrons, a function of temperature, and is present in all electronic devices and transmission media. Hence it is impossible to eliminate. It can be in terms of Inter-modulation noise which occurs when the signals having different

frequencies travel through the same medium. Noise can also occur due to irregular pulses or noise spikes caused by external electro-magnetic disturbances, or faults in the communication system and is known as Impulsive noise. These spikes are of short duration but relatively high amplitude.

3.4.1.3 Multipath fading

Multipath refers to the situation where the transmitted signal is reflected by various physical obstacles like buildings, tree and similar structures, thus creating multiple signal paths between the base station and the mobile/user terminal. The scenario is shown in Fig. 3.3. These multiple paths have randomly distributed amplitudes, phases, and angle of arrivals, which causes fluctuations in the received signal strength causing fading, hence called multipath fading. It also increase the time period required for the transmitted signal to reach the receiver hence causing delay spread. The relative attenuation between the antennas becomes an important issue when dealing with multiple antennas. Channel fading significantly degrades the performance of wireless transmissions.

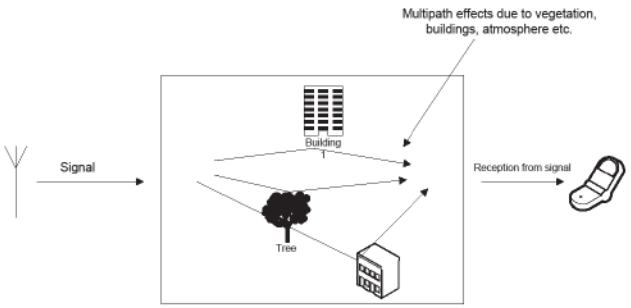

Fig. 3.3 Multipath Propagation

3.4.1.3.1 Slow Fading and Fast Fading

Based on the Doppler spread, multipath fading can be classified as slow-fading or fast-fading. In a slow fading channel, the channel impulse response changes at a much slower rate than the transmitted baseband signal. The channel may be assumed to be static over one

or several reciprocal bandwidth intervals [94]. In the frequency domain, this implies that the Doppler spread of the channel is much less than the bandwidth of the baseband signals.

In a fast fading channel, the channel impulse response changes rapidly within the symbol duration. That is, the coherence time of the channel is smaller than the symbol period of the transmitted signal. This causes frequency dispersion due to Doppler spreading, which leads to signal distortion. Fast fading channel only deals with the rate of change of the channel due to motion. In practice, fast fading only occurs for very low data rates.

3.4.1.3.2 Flat Fading and Frequency-Selective Fading

Depending on the relative magnitude between the delay spread and symbol period, multipath fading can be identified as frequency-flat fading or frequency-selective fading. A channel exhibits flat fading when $T_m < T_s$. In this case, all the received multipath components arrive within the symbol time duration [95]. There does not occur any channel-induced ISI as the neighbouring received signals do not overlap, therefore, the frequency components arriving at the receiver have either little or no distortion, hence flat fading.

Frequency selectivity occurs whenever the received multipath components of the symbol extend beyond the symbol time duration i.e. $T_m > T_s$ where T_m is the maximum excess delay time and T_s is the symbol time. Different frequency components are subject to dispersive behaviour introducing ISI, hence frequency-selective fading.

3.4.1.4 Inter Symbol Interference (ISI)

ISI is one of the most severe limitations encountered in high-speed data transmission systems. Using any practical channel, the effects of filter are unavoidable which causes spreading of individual data symbols passing through the channel and for consecutive symbols this spreading causes part of the symbol energy to overlap with the neighbouring

symbols. This phenomenon causes ISI as shown in Fig. 3.4 and it significantly degrades the system performance.

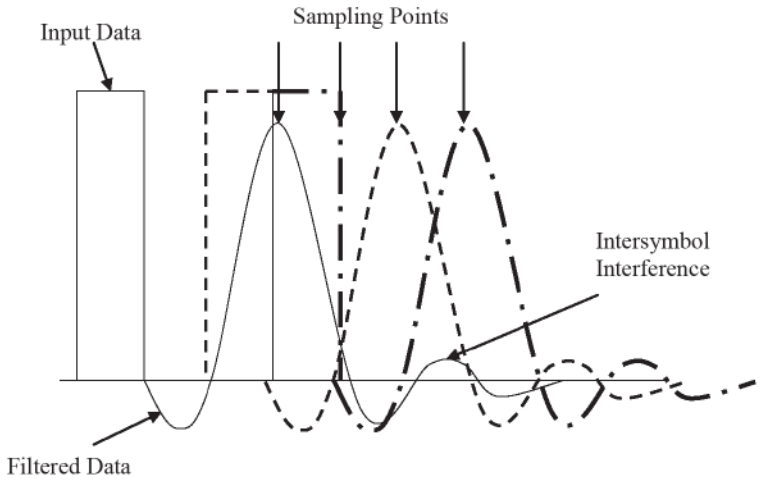

Fig. 3.4 Inter-symbol Interference

3.4.2 Statistical Fading channel Models

The statistical models are based on measurements made specifically for an intended communication system or spectrum allocation. A significant advantage of the wireless channel models is their flexibility, which means by changing the statistical parameters; the same model can be used to simulate the channel under different conditions. Depending on the nature of the radio propagation environment, there are different models describing the statistical behaviour of the multipath-fading envelope. The Rayleigh, Ricean and Nakagami are the most commonly used statistical models to represent small-scale fading phenomenon [92], [94] – [99]. In this section, we present different types of fading channels and the mathematical models to describe these channels over which transmission of information takes place or in which information can be stored. These channels can be classified by the environments to which they apply.

3.4.2.1 Additive White Gaussian Noise (AWGN)

The AWGN is one of the most frequently assumed transmission channel model and is generally used to model an environment which has a large number of additive noise sources. These additive sources can be modelled as Gaussian random process. The statistical model for the AWGN channel with zero mean and variance (σ^2) is given by its probability density function (PDF) [92] as

$$p(x) = \frac{1}{\sqrt{2\pi\sigma^2}} exp\left(-\frac{1}{2\sigma^2}x^2\right) \tag{3.6}$$

where $\sigma^2 = \frac{N_0}{2RE_b}$, R is the coding rate given by the ratio of the number of information bits to the number of transmitted bits, and $\frac{E_b}{N_0}$ is the ratio of the bit energy to noise power spectral density. As the name suggests the AWGN channel is defined as the addition of white Gaussian noise to the transmitted signal as shown in Fig. 3.5.

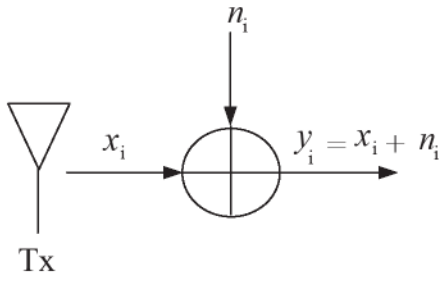

Fig.3.5 the AWGN System Model

The signals are transmitted with energy E_b using one transmit antenna. The received signal *y* after modulation at any time instant *t* is given by

$$y_t = x_t + n_t \tag{3.7}$$

where x_t and n_t are the information bits and the white noise added by the channel, respectively, at time *t*.

3.4.2.2 Rayleigh Fading Channel

AWGN is a hypothetical situation where the transmitter is assumed to be ideal and noiseless. It is merely noise generation at the receiver side assumed to have a constant power spectral density over the entire channel bandwidth and the amplitude following Gaussian distribution.

In real-time scenario, when a signal is transmitted it is received as a superposition of many pulses arriving at the receiver due to multi-path fading. Rayleigh fading model is one such model motivated by the fading effects arising due to long distance transmission. In Rayleigh flat fading channel model, it is assumed that the channel induces amplitude, which varies in time according to the Rayleigh distribution. If there is no line-of-sight component and the multiple reflective paths are large in number (as in the case of dense urban environments) then small-scale fading is also termed as Rayleigh fading as the Gaussian distribution has a zero mean and the envelope of the received signal is statistically described by a Rayleigh PDF [95][100].

When the channel impulse response is modelled as a zero-mean complex-valued Gaussian process, the envelope at any instant is Rayleigh-distributed [94] [101]. The Rayleigh PDF of a received complex envelope of a signal $r(t)$ at any time t is given as

$$p(r) = \frac{r}{\sigma^2} e^{\left(\frac{-r^2}{2\sigma^2}\right)} \quad (r \geq 0) \tag{3.8}$$

where σ is the root mean square value of the received voltage signal before envelope detection, and σ^2 is the time-average power of the received signal before envelope detection. It is well known that the envelope of the sum of two quadrature Gaussian noise signals obeys a Rayleigh distribution. This fading distribution could be applied to any scenario where there is no LOS path between transmitter and receiver antennas [98], [99].

The Rayleigh Channel model is forced by the fading effects added into the system while transmitting over a distance and is defined as the product of transmitted signal with a complex fading coefficient. AWGN is also part of the model and is added after fading as shown in Fig.3.6.

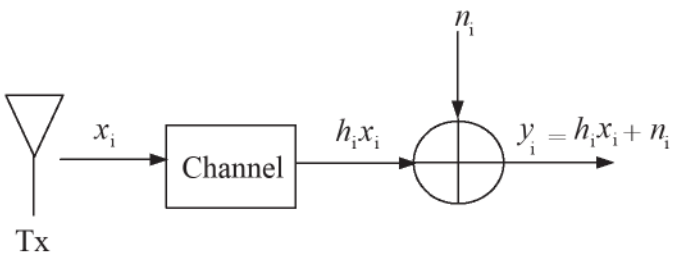

Fig.3.6 Fading Channel Model

Then the received signal y after modulation at any time instant t is given by

$$y_t = h_t x_t + n_t \tag{3.9}$$

where x_t is the transmitted sequence, n_t is the white noise added and h_t is the complex fading coefficient added as a result of fading.

3.4.2.3 Nakagami-*m* Fading Channel

The Nakagami distribution is selected to fit empirical data and is known to provide a close match to some experimental data than the Rayleigh distributions. The Nakagami distribution is often used to model multipath fading as it can model fading conditions that are either more or less severe than Rayleigh fading. When $m = 1$, Nakagami distribution becomes the Rayleigh distribution, when $m = 1/2$ it becomes a one-sided Gaussian distribution and when $m = \infty$ the distribution becomes an impulse (no fading). Even Rice distribution can be closely approximated using Nakagami parameter m via the relationship $m = (K + 1)^2/(2K + 1)$ [96].

K-Factor — The fading signal magnitude follows a Rice distribution, which can be characterized by two parameters: the power P_c of constant channel components and the power

P_s from scatter channel components. The ratio of these two $\left(P_c/P_s\right)$ is called the Ricean K-factor. The worst-case fading occurs when $P_c = 0$ and the distribution is regarded as Rayleigh distribution ($K = 0$). The K-factor is an important parameter in system design since it relates to the probability of a fade of certain depth. Both fixed and mobile communications systems have to be designed for the most severe fading conditions for reliable operation (i.e., Rayleigh fading).

Considering a receiver with M diversity branches, let the received instantaneous signal A_k at the k^{th} branch be characterized by the Nakagami distribution. The Nakagami distribution describes the received envelope $z(t) = r(t)$ by a central chi-square distribution with m degrees of freedom, i.e. [102] [103],

$$p(A_k) = \frac{2}{\Gamma m_k}\left(\frac{m_k}{\Omega_k}\right)^{m_k} r^{2m_k-1} e^{\left(-\frac{m_k}{\Omega_k}\right)r^2}, \quad k = 1,2, \dots M \tag{3.10}$$

where $\Gamma(.)$is the Gamma function, $\Omega_k = \overline{A_k^2}$ is the average power on k^{th} branch, m_k is the fading parameter.

For the Rayleigh PDF given by (3.8) and r denoting the amplitude of the Rayleigh fading, the cumulative distribution function (CDF) of the Rayleigh fading can be written as

$$F_R(r) = 1 - e^{-r^2/2\sigma^2} \tag{3.11}$$

For the Nakagami-*m* PDF given by (3.10), the Nakagami-*m* CDF can be written as

$$F_N(r) = \int_0^r \frac{2}{\Gamma(m_k)}\left(\frac{m_k}{\Omega_k}\right)^{m_k} r^{2m_k-1} e^{\left(-\frac{m_k}{\Omega_k}\right)r^2} dr \tag{3.12}$$

Then the complex Nakagami-*m* amplitudes can be calculated as

$$A = F_N^{-1}(u) \tag{3.13}$$

where F_N^{-1} is the inverse function of Nakagami-m CDF, and u is the uniformly distributed variable generated by Rayleigh fading coefficients, $u = F_R(r) = 1 - e^{-r^2/2\sigma^2}$. A is Nakagami-*m* distributed can be further expressed as

$$A = F_N^{-1}\left(F_R(r)\right) \tag{3.14}$$

A general form of the inverse Nakagami-*m* CDF is obtained as

$$F_N^{-1}(u) = v + \frac{a_1 v + a_2 v^2 + a_3 v^3}{1 + b_1 v + b_2 v^2} \tag{3.15}$$

where $v = \left(\sqrt{ln\frac{1}{1-u}}\right)^{\frac{1}{m}}$, and *m* is the Nakagami-*m* fading parameter, and $0.65 \leq m \leq 10$.

Each $'m'$ has a different set of parameters and is listed in Table 3.1 [104].

Table 3.1 Set of parameters corresponding to different values of $'m'$

$\boldsymbol{m}$	$\boldsymbol{a_1}$	$\boldsymbol{a_2}$	$\boldsymbol{a_3}$	$\boldsymbol{b_1}$	$\boldsymbol{b_2}$
0.65	-0.0828	-4.5634	-15.8819	63.1955	23.2981
0.75	-0.0547	-0.3679	-1.0336	6.2107	1.8533
0.85	-0.0336	-0.1543	-0.4733	4.9250	1.2082
1.00	0.0000	0.0000	0.0000	1.0000	1.0000
1.50	0.0993	0.0560	0.2565	0.5276	0.0770
2.00	0.1890	-0.0128	0.2808	-0.0809	0.0638
3.00	0.3472	-0.2145	0.2626	-0.6779	0.1690
4.00	0.4846	-0.4231	0.2642	-0.9729	0.2727
5.00	0.6023	-0.6238	0.2789	-1.1798	0.3732
6.00	0.7139	-0.8305	0.3223	-1.3232	0.4558
7.00	0.8167	-1.0244	0.3761	-1.4233	0.5192
8.00	0.9260	-1.2350	0.4557	-1.4872	0.5628
10.0	1.1088	-1.6095	0.6015	-1.6046	0.6488

3.5 Wireless System Models

In conventional wireless communications, a single antenna is used at the source, and another single antenna is used at the destination. These systems are one of the simplest in the antenna technology but in some environments these systems are vulnerable to problems caused by multipath effects. In order to minimize or eliminate problems caused by multipath wave propagation, multiple antennas can be employed at the transmitter and/or the receiver. Depending on the number of transmit and/or receive antennas deployed at either end there are four possible system models:

1. Single Input Single Output (SISO) Systems
2. Multiple Input Single Output (MISO) Systems
3. Single Input Multiple Output (SIMO) Systems
4. Multiple Input Multiple Output (MIMO) Systems

We will be discussing each them in brief in the next few sections and these four different types of system models will be the focus of the entire thesis.

3.5.1 Single Input Single Output (SISO) Systems

A Single Input Single Output (SISO) system refers to a wireless communications system in which a single antenna is used both at the transmitter and the receiver as shown in Fig. 3.7. In a digital communications system, such systems cause a reduction in data speed and an increase in the number of errors.

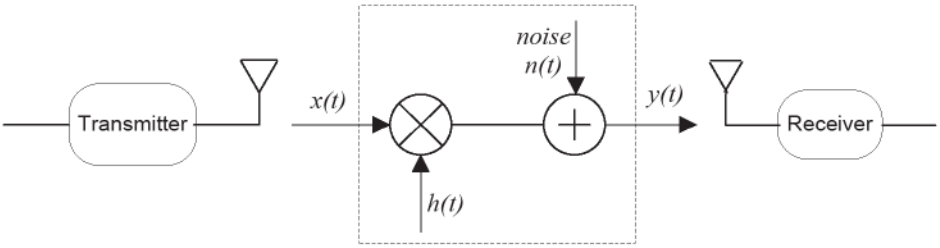

Fig.3.7 SISO Communication Model

3.5.2 Multiple Input Single Output (MISO) Systems

A Multiple Input Single Output (MISO) is an antenna technology for wireless communications in which two or more antennas are used at the transmitter and a single antenna at the receiver as shown in Fig. 3.8. The data stream is converted from serial to parallel at the transmitter side and vice-versa at the receiver to minimize errors and optimize data speed.

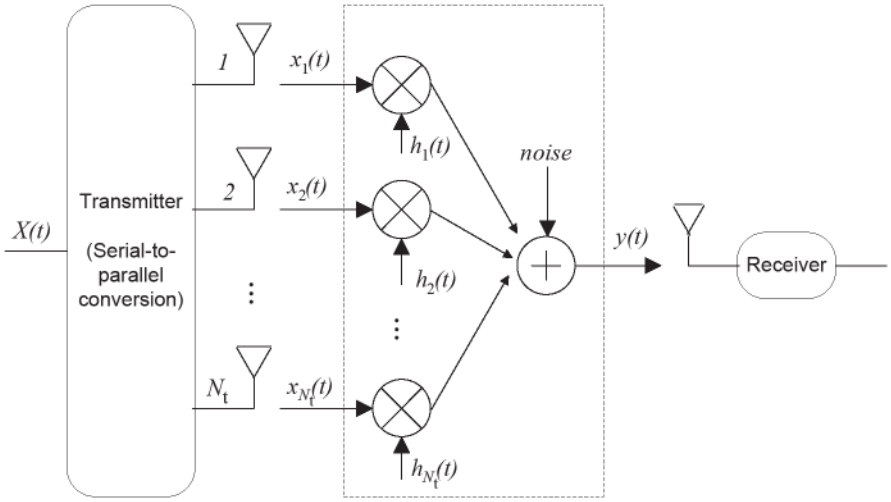

Fig.3.8 MISO Communication Model

3.5.3 Single Input Multiple Output (SIMO) Systems

A Single Input Multiple Output (SIMO) is an antenna technology for wireless communications in which two or more antennas are used at the receiver and a single antenna at the transmitter as shown in Fig. 3.9. The signals arriving from different directions are combined in various ways at the receiver to minimize errors and optimize data speed. An early form of SIMO, known as diversity reception, has been used by military, commercial, amateur, and shortwave radio operators at frequencies below 30 MHz since the First World War.

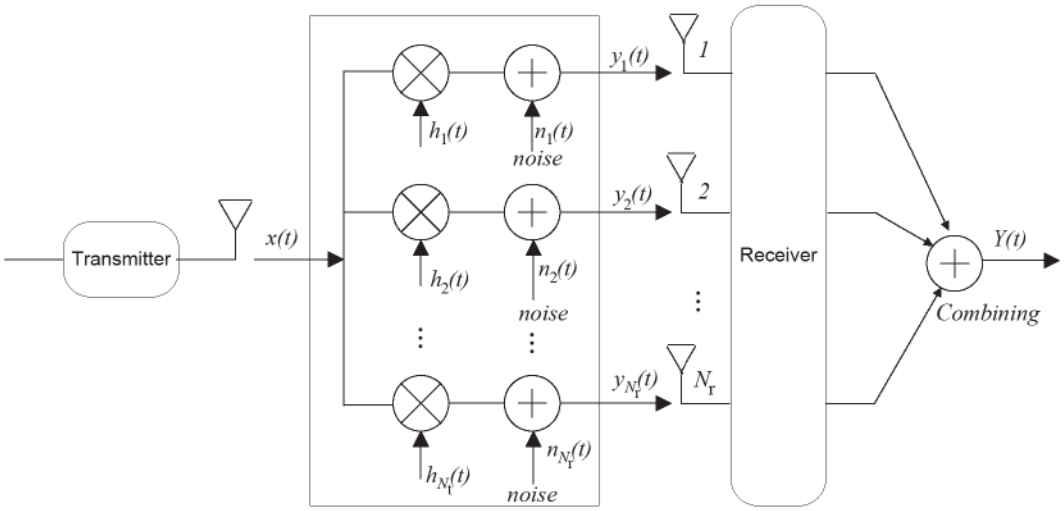

Fig.3.9 SIMO Communication Model

3.5.4 Multiple Input Multiple Output (MIMO) Systems

A Multiple Input Multiple Output (MIMO) is a wireless communications system in which multiple antennas are used at both the transmitter and the receiver as shown in Fig. 3.10. The antennas at each end of the communications circuit are combined to minimize errors and optimize data speed.

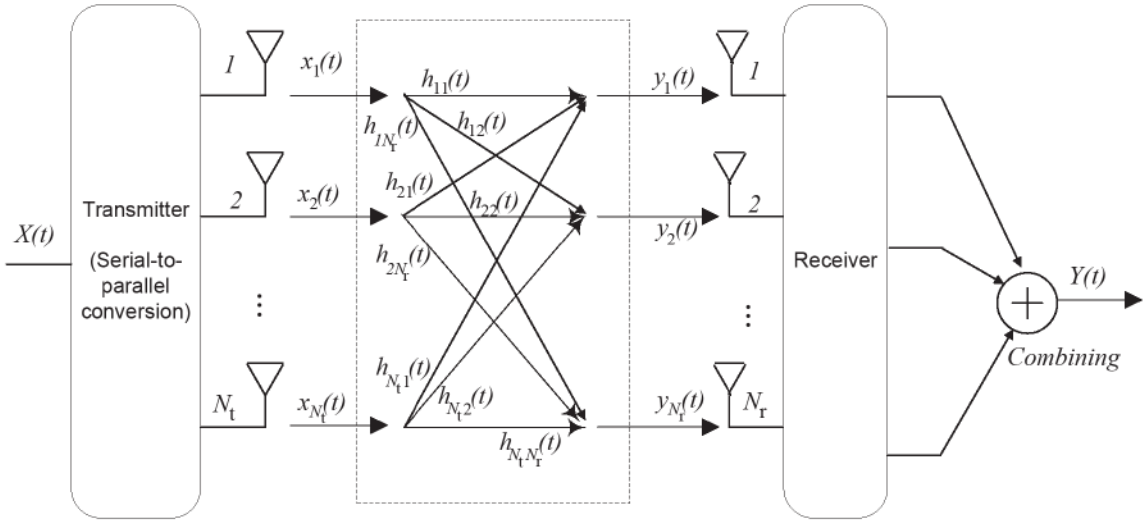

Fig.3.10 MIMO Communication Model

MISO, SIMO, MIMO technologies all have possible widespread applications in digital television (DTV), wireless local area networks (WLANs), metropolitan area networks (MANs), and mobile communications.

3.6 Diversity

Diversity is an important way to help mitigate the multipath-induced fading that results from users' mobility. It is a method that is used to develop information from several signals transmitted over independent fading paths. This means that the diversity method requires that a number of transmission paths be available, all carrying the same message but having independent fading statistics. The mean signal strengths of the paths should also be approximately the same. The basic requirement of independent fading is that the received signals are uncorrelated. Therefore, the success of diversity schemes depends on the degree to which the signals on the different diversity branches are uncorrelated. To meet the stringent requirements for quality service requirements and spectrally efficient multilevel constellations, antenna diversity is needed to offset penalty on the SNR due to fading and denser signal constellation. By proper combining of the multiple signals severity of fading can be greatly reduced and reliability of transmission can be improved. The use of diversity permits a direct comparison of improvement offered by multiple antenna compared to a single one [105]. The effectiveness of diversity and adaptive combining schemes has been proven in [106].

There are several diversity schemes available to choose from which includes time diversity, frequency diversity, space diversity, receive diversity [107]. The information bearing signal copies are transmitted at different time instants or different frequencies, while using time or frequency diversity respectively [108]. Time diversity is usually effective for fast-fading channel as the coherence time of this channel is small. In frequency diversity, the frequencies have to be separated enough to make sure that the fading coefficients are independent and uncorrelated. In space diversity, multiple antennas separated by a few wavelengths are used at the receiver/transmitter to create independent fading channels. This

is the most popular technique used in wireless communication. Unlike in frequency diversity, no bandwidth efficiency loss occurs in space-diversity. By placing the antennas sufficiently apart, independent channel fading coefficients can be obtained between different antenna pairs and thus independent signal paths can be created [109].

3.6.1 Transmit Diversity – Space-Time Codes

Transmit diversity schemes have increasingly grown popular over the last decade as they promise high data rate transmission over wireless fading channels in both the uplink and downlink while putting the diversity burden on the base station. Also it helps to improve the quality and the data rates of the multiple antenna systems in order to obtain diversity orders.

An effective approach to maintain a trade-off between diversity and bit-rate and to increase data rates over wireless channels is to employ coding techniques appropriately to multiple transmit antennas. The effect of spatial diversity on the throughput and reliability of the wireless channels is clearly examined in [56]. The information-theoretic results in single-user multiple antenna channels, which guides the way to recent developments in reliable high data-rate wireless networks, has been reviewed using the concept of capacity introduced by Shannon in 1948 [110]. The concept given by Shannon stimulated the scientific community to seek for better channel coding method to improve the reliability of transmission and it was soon realized that the performance gains achieved by receive diversity can be reproduced by employing multi-antennas at the transmitters to achieve transmit diversity. The capacity of antenna systems far exceeded by using Multiple Input Multiple Output (MIMO) channels as compared to single-antenna system. Use of multiple transmit antennas provided diversity in the space domain i.e. space diversity and the channel coding designed for wireless communications system with multiple transmit antennas provided both space and time diversity and came to be known as space-time codes.

Space-time codes (STCs) were first introduced by Tarokh [111] in 1998 as a novel means of providing transmit diversity for multiple-antenna fading channel. Since then, space-time codes have attracted considerable attention because of their ability to exploit the capacity increase of MIMO antenna systems capable of maintaining the best trade-off between the fundamental quantities of rate gain, diversity, and receiver complexity [107], [109], [112], [113]. Today, space-time coding has gained enough consideration for implementation over third (and beyond) generation wireless systems.

The performance criteria for designing these codes is under the assumption that the fading is slow and frequency non-selective and is determined by diversity gain quantified by ranks and coding gain quantified by determinants of certain matrices that are constructed using the code sequences. The codes are such designed so as to improve the data and/or reliability of communication over fading channels using MIMO systems [114]. While in [111], it is shown that Space-time codes provides the best trade-off between diversity gain, transmission rate, constellation size, signal space dimension and trellis complexity when CSI is available at the receiver, [115] presents a theoretical study of effects of channel estimation errors, frequency selectivity and speed of the change of channel i.e. Doppler effect on the diversity advantage in the absence of CSI. When the channel statistics are not known, a channel estimator is used to estimate the CSI when all points in the constellation have equal energy. The space-time codes thus constructed will continue to work even when CSI is known at the receiver but the sensitivity of the system to channel estimation error increases with the increase in the number of transmit antennas. It is also well shown that the presence of multipath rays does not affect the diversity advantage as offered by the original space-time codes' design criteria. Since Space-Time coding is a bandwidth and power efficient method, therefore, one should have a fundamental understanding of the limits of bandwidth efficient

delivery of higher bit-rates. Band-limited channels do not accumulate rapid flow of data but by exploiting multiple antennas at the transmitter, higher bit-rates can be achieved [116].

There are mainly two types of STC- Space time block codes (STBC) and Space-time trellis codes (STTC). While STBC operate on a block of input symbols, producing a matrix output whose column represents time and rows represent antennas, STTC operate on one input symbol at a time, producing a vector symbols whose length represents antennas [117]. Also, STBC do not provide coding gain unless concatenated with some outer code whereas the key advantage of using STTC is that they provide coding gain. However, both types of codes provide full diversity gain. STTC have a disadvantage that they are extremely hard to design and generally require high complexity encoders and decoders while STBC require simple encoding and decoding at low computational cost. Marked comparisons between these two types of transmit diversity schemes in terms of frame error rate are clearly mentioned in [118]. The main theories of the Space-Time Trellis Code (STTC) [111] and the Space-Time Block Code (STBC) [28] have been mentioned in the two key papers for flat independent Rayleigh fading channels. A number of other schemes employing multiple antenna arrays were also developed at about the same time, e.g., the simple and popular Alamouti STBC [119], a transmit diversity scheme using pilot symbol-assisted modulation [120] and the Bell Labs layered Space-Time (BLAST) multiplexing framework [121]. Several design criteria are available in the literature depending on the channel characteristics [122] – [124]. Considering the computational simplicity of the encoding and decoding process of the STBCs, we focus on these codes in this thesis.

3.6.1.1 Space-Time Block Codes (STBC)

In hope of reducing the exponential decoder complexity of STTC, Alamouti proposed a simple transmit diversity scheme [28], which was later expanded by Tarokh et al. [119] for an arbitrary number of array elements to form the class of Space-Time Block Codes (STBC).

It presented a simple two-branch transmit diversity scheme which referred to a full-rate orthogonal design. The orthogonality spread across sequence of symbols transmitted simultaneously from two antennas was exploited at the receiver by the combining rule.

STBC can be achieved by a complex orthogonal designed matrix called the encoder (or the transmission) matrix G_{N_t}, where N_t represents the number of transmit antennas, p represents the number of time periods for transmission of one block of symbols. The elements of the encoder matrix are the indeterminants $[\pm x_1, \pm x_2, \ldots\ldots, \pm x_n]$, their conjugates $[\pm x_1^*, \pm x_2^*, \ldots\ldots, \pm x_k^*]$ and the superposition of those. The encoder matrix maps k input $m-ary$ symbols into N_t orthogonal sequence of length p. Thus the rate of $r = k/p$ is achieved.

To construct space-time block codes, the classical mathematical framework of orthogonal designs can be applied [119]. An orthogonal design exists if and only if $N_t = 2,4\ or\ 8$. That means the STBCs constructed using this method exists only for a few sporadic values of n. These codes have a simple maximum likelihood decoding algorithm based on linear processing and also they exploit full diversity given by transmit and receive antennas and achieve maximum possible transmission rate. However, a generalization of orthogonal designs can provide STBC for both real and complex constellations for any number of transmit antennas but the maximum possible transmission rate achieved is half for any number N_t of the transmit antennas.

STBC can be classified into STBC with real signals and STBC with complex signals. It is worthwhile to note that full rate orthogonal design exists for arbitrary real signal constellations for N_t number of antenna elements; it does not exist for complex signal constellations like PSK or QAM for more than two antenna elements. For $N_t \geq 2$, the code design aims at constructing high data rate complex transmission matrices G_{N_t} whilst keeping

the decoding complexity low and achieving full diversity order. Also the value of p must be minimized to minimize the decoding delay. Alamouti scheme can be regarded as a STBC with complex signal constellations for $N_t = 2$. Also it is the only STBC with $N_t \times N_t$ complex encoder matrix that achieves a full rate $r = 1$.

In [125], a complete classification of STBC based on the principle of linearity and unitarity is given for complex symbol constellation. STBC offer the advantage that no bandwidth expansion is needed. Also as STBC have decreased sensitivity to fading it can be used for higher levels of modulation to increase the effective data rate and can be used to increase the coverage area of the wireless systems. Quasi-Orthogonal STBC (QO-STBC) were developed in [126] based on the unifying algebraic structure. Based on the graph theory it was proved that these codes provided higher data rates that orthogonal STBCs (OSTBC). A new algebraic construction for STBC with 2, 3, 4 and 6 antennas were presented in [127]. These codes provided full rate and full diversity and had a constant minimum determinant as the spectral efficiency increased

So far, most of the research has been done assuming that the channel estimates are available at the receiver. In some situations we want to forego the requirement for channel estimation at the receiver, just to reduce the cost and complexity of the handset, or, sometimes fading conditions change so rapidly that channel estimation becomes difficult, to deal with such situations a differential space-time block coding (D-STBC) scheme was proposed [128]. The performance of D-STBC is inferior to the performance of coherent STBC (C-STBC) by 3 dB under ideal conditions but is much more robust to frequency and phase errors and does not rely on instantaneous tracking of channel state information [129].

There are a few complex orthogonal designs proposed in [28] for 2, 3 and 4 transmit antennas which accommodates rates as close to one as possible. For example, complex

encoder matrices G_3^* and G_4^* for three and four transmit antennas are orthogonal designs and have the rate $r = 1/2$.

$$G_3^* = \begin{bmatrix} x_1 & -x_2 & -x_3 & -x_4 & x_1^* & -x_2^* & -x_3^* & -x_4^* \\ x_2 & x_1 & x_4 & -x_3 & x_2^* & x_1^* & x_4^* & -x_3^* \\ x_3 & -x_4 & x_1 & x_2 & x_3^* & -x_4^* & x_1^* & x_2^* \end{bmatrix} \tag{3.16}$$

$$G_4^* = \begin{bmatrix} x_1 & -x_2 & -x_3 & -x_4 & x_1^* & -x_2^* & -x_3^* & -x_4^* \\ x_2 & x_1 & x_4 & -x_3 & x_2^* & x_1^* & x_4^* & -x_3^* \\ x_3 & -x_4 & x_1 & x_2 & x_3^* & -x_4^* & x_1^* & x_2^* \\ x_4 & x_3 & -x_2 & x_1 & x_4^* & x_3^* & -x_2^* & x_1^* \end{bmatrix} \tag{3.17}$$

It can be seen that the inner product of any two rows of these matrices is zero which proves the orthogonality of these schemes. Considering the encoder matrix G_3^*, four complex symbols are taken at a time and transmitted by three transmit antennas in eight symbol periods, hence giving the transmission rate $r = 1/2$.

The encoder matrices H_3 and H_4 are complex generalized orthogonal designs for STBC and achieves the transmission rate of $r = 3/4$.

$$H_3 = \begin{bmatrix} x_1 & -x_2^* & \frac{x_3^*}{\sqrt{2}} & \frac{x_3^*}{\sqrt{2}} \\ x_2 & x_1^* & \frac{x_3^*}{\sqrt{2}} & -\frac{x_3^*}{\sqrt{2}} \\ \frac{x_3}{\sqrt{2}} & \frac{x_3}{\sqrt{2}} & \frac{(-x_1 - x_1^* + x_2 - x_2^*)}{2} & \frac{(+x_1 - x_1^* + x_2 + x_2^*)}{2} \end{bmatrix} \tag{3.18}$$

$$H_4 = \begin{bmatrix} x_1 & -x_2^* & \frac{x_3^*}{\sqrt{2}} & \frac{x_3^*}{\sqrt{2}} \\ x_2 & x_1^* & \frac{x_3^*}{\sqrt{2}} & -\frac{x_3^*}{\sqrt{2}} \\ \frac{x_3}{\sqrt{2}} & \frac{x_3}{\sqrt{2}} & \frac{(-x_1 - x_1^* + x_2 - x_2^*)}{2} & \frac{(x_1 - x_1^* + x_2 + x_2^*)}{2} \\ \frac{x_3}{\sqrt{2}} & -\frac{x_3}{\sqrt{2}} & \frac{(x_1 - x_1^* - x_2 - x_2^*)}{2} & -\frac{(x_1 + x_1^* + x_2 - x_2^*)}{2} \end{bmatrix} \tag{3.19}$$

The orthogonality of these matrices can be proved since the columns of these matrices fulfil the orthogonality requirements. Discussions on STBC for real signal constellations are available in [109]. The orthogonal transmission matrices for different number of antenna elements and input block length for both real and complex signal constellations are summarized in Table 3.2.

Table 3.2 Orthogonal Encoder Matrices and Transmission rates for STBC for different number of antenna elements at the transmitter

Orthogonal Design (G_{N_t})	**N_t**	**k (input block length)**	**p (symbol periods)**	**Rate $r = k/p$**
FOR COMPLEX SIGNAL CONSTELLATIONS				
G_2^*	2	2	2	1
G_3^*	3	4	8	1/2
G_4^*	4	4	8	1/2
H_3	3	3	4	3/4
H_4	4	3	4	3/4
FOR REAL SIGNAL CONSTELLATIONS				
G_2	2	2	2	1
G_4	4	4	4	1
G_8	8	8	8	1
G_3	3	4	4	1
G_5	5	8	8	1
G_6	6	8	8	1
G_7	7	8	8	1

3.6.2 Receive Diversity – Combining Techniques

Motivated by the aim to mitigate signal degradation caused by multipath propagation, applying spatial diversity techniques focused on using multiple antennas at the receiver. It led to considerable performance gain in terms of tolerance to co-channel interference [106], [130]. Assuming that the paths taken by each of the copies result in statistically independent

fading effects, it can be concluded that the signals are unlikely to be in deep fade i.e. highly distorted. Thus an improved signal can be obtained by forming a weighted combination of the received copies. The combining of the received copies can be performed using several different methods in different environments based on the applications. The three most commonly used receive diversity techniques when signalling over various statistical fading channels are [94]

1. Selection Combining (SC)
2. Maximal Ratio Combining (MRC), and
3. Equal Gain Combining (EGC).

3.6.2.1 Selection Combining (SC)

Selection Diversity is the simplest diversity technique where gains of M pre-detection diversity branches are adjusted to provide the same SNR ratio for each branch [104]. The receiver branch having the highest instantaneous SNR will be fed to detector circuit. Selection combining can be used with coherent as well as non-coherent modulations schemes as it does not require the signal phase knowledge of each diversity branch. The conventional selection combining techniques can be extended to generalized selection combining (GSC) [131], based on different statistical channel models [132], [133].

3.6.2.2 Maximal Ratio Combining (MRC)

In MRC, the signal in each branch is first co-phased and once the phase distortions are cancelled out, the signal in each branch is weighted by a weighting factor proportional to the ratio of the carrier amplitude to the noise power for the i^{th} branch [134], [135]. MRC provides full diversity and also yields the highest SNR but due to channel estimation the complexity is high. MRC has been actively used for calculating the capacities and error probabilities over fading channels with different channel effects [136] – [138].

3.6.2.3 Equal Gain Combining (EGC)

In an EGC receiver, the received signal carriers are first co-phased as in the case of MRC and are then equally weighted by their amplitudes. In other words, the branch weights are all set to unity. The possibility of producing an acceptable signal from a number of unacceptable inputs is still retained [139]. EGC has performance close to that of MRC but with lower implementation complexity [140]. The exact outage performance for EGC is presented in [141] for mobile cellular radio systems for Rayleigh fading with limited co-channel interference.

3.6.3 Relaying

In the last few sections, we exhaustively discussed about the undesirable multipath induced propagation impairments. The solution was to generate multiple replicas of the information bearing signals to be propagated over individual paths. We learned that by using multiple numbers of transmit antennas higher diversity gains can be achieved and then the classic diversity combining techniques can be invoked at the receiver for recovering the original signal, thereby, improving the performance.

In the meantime, an alternative technique capable of providing multiple independently faded replicas of the information signal was developed known as Relaying. Relays and co-operative systems were proposed which helped in improving the performance of the wireless systems.

Cooperative Relaying in communications has now been a centre of research in dealing with channel fading for quite some time now [13], [142], [7]. The basic idea behind cooperative diversity is that the receiver combines the information received from both the transmitter and the relay [21], thus exploiting spatial diversity. Cooperative relaying schemes can be categorized as amplify-forward (AF) [80], where the relay terminal simply amplifies

the received signal and transmits it to the receiver; and decode-and-forward (DF) where the relay terminal decodes and then forwards the signal to the receiver [143]. DF can be further sub-categorized as fixed DF (FDF) and adaptive DF (ADF).

A cooperative relay based network with a large number of relay nodes transmitting over independent non-identical Nakagami-*m* fading channels with AF has been discussed in [80]. The performances of FDF and ADF schemes over Nakagami-*m* fading channels have been analysed and compared in [143] where the results were obtained considering that the *m* parameter of the fading channel is always an integer. In wireless communication, MIMO technology has provided significant performance improvements. Similar to multiple antenna systems, use of MIMO technology to relay systems has proved to be very promising and has attracted lot of research interest in the past few years [144], [145]. Performance analysis of OSTBCs in two-hop relay systems with multiple antennas at the source and destination, and a single antenna at the relay has been studied in [14] over Rayleigh fading channels.

Convinced by the benefits of using AF and DF, a hybrid scheme combining AF and FDF with soft-decision, namely, decode-amplify-forward protocol, was presented in [25] and [146] over Rayleigh Fading Channels. This hybrid scheme cleverly combined the merits of both AF and FDF mode. In [146], it was mentioned that during the second-hop transmission, if the signal gets corrupted as in the ADF protocol, in the HDAF scheme the relay starts to perform in the AF mode.

3.7 Channel Estimation and the Algorithms

Most of the work on space-time coding and modulation schemes assumed that perfect channel state information (CSI) is available at the receiver [111], [115], [119]. However, under fast fading channels, channel estimation becomes very challenging. In such cases, the coherence time can be too small to estimate the channel accurately or alternately it may

require quite a large number of pilot symbols to achieve the desired accuracy. While dealing with space-time modulation, this problem increase as the number of transmit antenna increases as now the receiver has to estimate the path gain from each transmit antenna to each receive antenna. The problem can be solved by using either of the two ways

- A non-coherent or differential space-time (ST) modulation techniques [128], [129], [147] (though it shows a performance degradation by 3dB as compared to coherent modulation technique)
- Joint channel estimation and data detection methods that can approach the coherent performance by using a minimum number of pilot symbols.

3.7.1 Differential ST Modulation techniques

Non-coherent or differential space-time modulation techniques do not require any channel estimates at the receiver. Many differential modulation schemes are available in the literature [128], [129], [148] – [152]. While [128] presented a differential detection scheme for exploiting diversity given by two transmit antennas, [129] proposed a general approach to differential modulation for multiple transmit antennas based on group codes. Another differential modulation framework was presented in [148] for a continuously fading channel, where a class of diagonal signals was introduced and only one antenna being active at a time. These schemes were sensitive to interference due to the assumption of spatially and temporally WGN in the receiver antenna array outputs. As a result, their performance degraded significantly in the presence of even mild interference and was therefore more likely to deteriorate or even break down completely in the presence of strong interference. A new coding and modulation scheme referred to as Differential Space-Code Modulation (DSCM) was introduced in [149]. This scheme exploited the merits offered by MIMO system as well as spread spectrum technology for interference suppression. Though all the above mentioned differential modulation schemes typically assumed constant channels of arbitrary

length undergoing random variations between frames, [152] described a new model in which the channel was kept constant over each space-time symbol period but varying between the symbols according to the first order auto-regressive (AR) model. With no knowledge of channel at either end, differential modulation schemes suffer from significant performance loss in terms of SNR as compared to coherent transmission especially in fast fading environment.

3.7.2 Joint channel estimation and data detection methods

Another approach for estimating the channel is to use joint estimation and detection methods. It is well known that in a multipath scenario ISI takes place when the sampling period gets smaller than the delay spread of the channel. At this point ISI needs to be combated at the receiver in order to restore the transmitted information and hence increase data rates. This is usually done using serial or block equalization where CSI is required at the receiver for designing the equalizer. This results in ISI suppression in an efficient manner. Several algorithms are available in the literature [120], [153] – [157] to refine the CSI through iterations. This includes the classical hard-decision directed methods and the new soft-decision directed variants [158] of the known techniques such as the Least Squares [159] or the Kalman Estimators [154], [160].

An iterative receiver based on Kalman filtering was proposed in [155] for decoding Alamouti's STBC. It was based on the time-varying channels modelled as AR processes and used a Kalman filtering process for channel tracking. A per-survivor processor (PSP) based receiver for decoding STTC was proposed in [157] which used an accelerated self-tuned least mean square (LMS) algorithm for tracking the fading channels and provided good performance both for slowly and moderately varying channels. Another PSP based receiver similar to [157] was proposed in [154] which combined the Viterbi algorithm with data-aided channel estimation.

Soft iterative equalization has come up as a powerful solution that can be adopted at the receiver where the data protected by an error correction code is transmitted over a channel causing ISI. These techniques were proposed to improve the CSI accuracy and to refine the channel estimates using the soft information provided by the channel decoder. Soft-decision feedback is preferred over hard-decision directed estimation as it allows to properly weight reliable and unreliable symbols. In this the propagation error effects are avoided that usually arise in the latter. Recently several soft iterative channel estimation methods have been developed for single user [161], [162] and multi-user [163] – [166] such as code division multiple access (CDMA) systems with either single or multiple antennas [164], [166] transceivers over frequency-flat [167] or frequency-selective channels [158], [164], [166].

Since the estimator at the receiver has practically no access to the transmitted signal that enters the channel due to considerably large distances between the transmitter and the receiver, the CSI can be obtained through the use of channel estimation algorithms. These identification algorithms can be categorized as

- Blind Algorithms, and
- Training-based Algorithms.

Blind algorithms do not rely on the knowledge of the transmitted signal rather they depend on the demodulated and detected sequence at the receiver to reconstruct the transmitted signal [168]. This reconstructed signal is then used as if it was the actual transmitted signal. Decision-directed or decision feedback algorithms are amongst the popular class of Blind algorithms. However, this method has an obvious drawback that the decision or the bit error rate at the receiver will result in the construction of an incorrect transmitted signal. This decision error will introduce a bias while estimating the channel thus making it less accurate.

In training-based method [169], [170], the receiver uses the training sequence known and sent by the transmitter to reconstruct the transmitted waveform irrespective of the fact that the receiver might not have direct access to the transmitted signal. The channel is identified at the receiver by exploiting this known training sequence. In comparison to blind techniques where the channel is continually updated, training-based techniques produces the most accurate estimates of the channel during the training interval but the estimates become out of control between these intervals. The channel estimates are obtained using different criteria:

- The Least Square (LS) Criteria [161], [163], [164], [171], [172],
- The Minimum Mean Square Estimation (MMSE) Method [162], [164] – [166], [173],
- Expectation-Minimization (EM) based Algorithms [153], [174] – [178], and
- Adaptive Methods for estimating the time-varying channels like Modified MMSE [179], [180].

In this thesis we focus on the family of training based channel identification algorithms considering a wireless transmission scheme where a constant and known training sequence is repeatedly inserted between blocks of data symbols. Considering quasi-static channels, the channel stays constant during the transmission of several blocks of data.

3.7.3 Least Square (LS) Estimation Algorithm

The LS channel coefficients can be represented by

$$\hat{h}_{LS} = arg\max_h (y - xh)^H (y - xh) \tag{3.20}$$

Differentiating (3.20) with respect to the channel coefficients and equating to zero, the LS channel estimate can be represented as

$$\hat{h}_{LS} = x^{\#} y \tag{3.21}$$

where $x^{\#} = (x^H x)^{-1} x^H$ denotes the pseudo-inverse of x. Substituting (3.9) in (3.21), the following expression can be obtained for the LS channel estimate

$$\hat{h}_{LS} = h + (x^H x)^{-1} x^H n \tag{3.22}$$

3.7.4 Minimum Mean Square Estimation (MMSE) Algorithm

An MMSE estimator treats the channel coefficients as random variables. Also this approach is independent of the channel coefficients; however, it depends on the moments of the channel coefficients [121]. The MMSE channel estimator is defined as

$$\hat{h}_{MMSE} = arg\min_h \left[E\left\{ \left(h - \hat{h}\right)^H \left(h - \hat{h}\right) \right\} \right] \tag{3.23}$$

Solving for (3.23), the MMSE solution can be expressed as

$$\hat{h}_{MMSE} = R_{hh} \times c_p^* \times G_{mmse} \times y_p \tag{3.24}$$

where $G_{mmse} = \left(c_p R_{hh} c_p^* + \sigma_n^2 I \right)^{-1}$, R_{hh} is the auto-covariance matrix of h and is assumed to be known, and σ_n^2 is the noise variance. Similar to Maximum a-posteriori Probability (MAP) algorithm, MMSE also requires prior information of the channel coefficients. Also MMSE is similar to MAP under the assumption that the channel coefficients are Gaussian. Hence, MMSE estimates the channel $\hat{h}_{MMSE}$ for the Gaussian channel $h(k)$.

3.7.5 Auto-Regressive (AR) Model

AR process can be used for modelling time-varying channels [181]. A joint detection and channel estimation algorithm has been presented in [182] for Rayleigh faded channels using Monte-Carlo simulations together with classical identification methods and the channel has been modelled as AR process. In [183], the fading process has been modelled as AR moving average (ARMA) but in this case the coefficients are found based on MMSE of the estimated channel under the assumption that perfect CSI of the transmitted sequence is known.

In our case the channel is not fast-fading but varies only from one frame to another, it can be very well described by a hidden Markov Model and can be modelled by a multi-channel auto-regressive (AR) process of order P, generally defined as

$$h(t) = \sum_{l=0}^{L-1} \mathbb{h}_l(t)\delta(t - \tau_l(t)) \tag{3.25}$$

where $\tau_l(t)$is the delay, and $\mathbb{h}_l(t)$is the complex amplitude of the l^{th} multipath tap. In order to keep the complexity of the receiver at a reasonable level, we have preferred to use only the first order AR process to model the time-varying channel. The performance of this time-varying nature of the fading channel can be analysed by assuming that the channel matrix varies according to the following first-order auto-regressive model

$$H_t = \sqrt{\alpha}H_{t-1} + \sqrt{1-\alpha^2}w_t \tag{3.26}$$

where H_t is the time-varying channel, w_t is the $N_t \times N_r$ matrix containing independent zero-mean Gaussian noise processes with variance ½. The coefficient α is related to the doppler spread f_d according to the first order approximation of Jakes channel model as $\alpha = J_0(2\pi f_d T_s)$ where $f_d T_s$ is used as the measure for fading rate. Typically its value falls in the range of (0.01-0.1).

3.8 Antenna Selection Techniques

Communication systems exploiting multiple antennas at the transmitter and/or the receiver are able to provide both data rates (capacity) and performance (BER). These two main advantages of the MIMO systems can be achieved in two different ways namely diversity methods and spatial multiplexing. Apart from the benefits achieved from using MIMO systems, they impose a few drawbacks as well. These include poor link reliability, little advantage of antenna diversity, and the need of sub-optimum detection interfaces at the receiver when large number of antennas is used. Another major problem that arises while using MIMO systems is the increased complexity, leading to increased cost, due to the need of multiple $N_t(N_r)$ RF chains. While deploying multiple antennas at mobile stations such high degree of hardware complexity becomes totally detrimental. Also, the ever rising desire of owning smaller and lighter mobile sets without significant performance loss forces to devolve more processing burden on the transmit side. Therefore, considerable efforts have been put in exploring new MIMO systems that can significantly reduce this complexity but continue to provide similar capacity and performance improvements.

A promising technique to achieve this goal is based on selecting antennas at the transmitter and/or receiver. Antenna selection procedure may involve selecting a single antenna or multiple antennas and can be at the transmitter and/or receiver [184], [185]. The selection procedure involves selecting a subset of the transmit and/or receive antennas based on selection criteria including maximization of the received SNR [167], [184] – [190] and the channel capacity [180], [185], [186], [191] – [195], similar to MIMO systems. Achieving a certain diversity order may be opted as the system design criteria. On the other hand, processing power of the receiver can also be accounted for while determining the number of active antennas that a system can support.

3.8.1 Antenna Selection methods

3.8.1.1 Receive Antenna Selection

When selecting single antenna at the receiver, by keeping track of the received power periodically, the signal of the receive antenna observing the largest instantaneous SNR can be selected and fed to the RF chain for processing [184]. Selection combining (or Equal Gain Combining) can be applied for receive antenna selection. Due to availability of only one RF chain, the problem of knowing the entire branch SNR arises (which is required for optimal selection). This problem can be solved by using preamble at the start of every transmitted frame and known pilot symbols be sent with this preamble. The receiver can exploit this preamble while scanning the antennas, finds the antenna with the highest channel gain and selects it for receiving the next data burst.

For multiple antenna selection at the receiver where there are multiple RF chains available (but always less than the number of receive antennas) subset selection criteria can be followed where L_r branches with the highest SNR are chosen [185]. The signals of the selected subset are combined. This is known as generalized selection combining or hybrid selection/maximal ratio combining.

3.8.1.2 Transmit Antenna Selection

For transmit antenna selection, a feedback path is required from the receiver to the transmitter. Single antenna selection at the transmitter is approximately similar to the single receive antenna selection i.e. the antenna with highest equivalent receive SNR is selected [186], [196].

For selecting multiple antennas at the transmitter, the most suitable L_t antennas out of N_t transmit antennas are chosen assuming that there is only one receive antenna and that there are L_t RF chains and N_t transmit antennas, and $L_t < N_t$. The phase and amplitude of

the transmit signals have to be such that their superposition at the receiver provides the maximal receive SNR. In doing so, the L_t transmit antennas with highest channel gain are chosen. This is equivalent to beamforming over selected antennas and is known as hybrid maximal ratio transmission (MRT) [167]. Hybrid MRT requires that apart from knowing the L_t most suitable transmit antennas, the relative complex valued channel gains from each transmit antenna to the receiver should also be known, which in return requires more feedback as compared to selecting single transmit antenna

3.8.1.3 Joint Transmit and Receive Antenna Selection

Antenna selection can be performed at both transmit and receive end simultaneously also. In this case selection diversity is applied at both ends. Assuming that there are N_t transmit and N_r receiver antennas, the transmit and receive ends have L_t and L_r RF chains [187]. Thus space-time codes are used to provide diversity at the transmitter to transmit L_t parallel data streams. Joint transmit/receive antenna selection is a quite complex task as it requires to choose a subset of the rows and columns of H, where H is the $N_t \times N_r$ overall channel matrix, such as to maximize the sum of the squared magnitudes of transmit-receive channel gains [185]. The problem that occurs is selecting the best receivers and then best transmitters may not necessarily result in the overall best possible choice. Thus efficient joint transmit/receive antenna selection requires systematic solution apart from exhaustive search for antenna selection.

3.9 Chapter Summary

In this chapter, we provided an insight into the current state of technology in the field of wireless communication. We conclude that there are various ways adopting which the performance of any wireless system can be significantly improved. By combining various modulation and coding techniques, by efficient channel estimation and by considering the amount of diversity involved, new communication systems can be modelled. One efficient way of dealing with diversity is the relayed transmission where a relay is used to transfer data from the transmitter to the receiver. Most of the relay based systems are formed assuming single transmit and receive antennas. These systems were further elaborated by using multiple relays but this added to the system cost of employing relays and complexity of tasks at the relays as the number of relays grows. Relay-based systems were further enhanced by using relays in MIMO systems. Though such systems gave higher performance but fear of failure of a single or multiple relays highly affected the performance of the system. Relay based systems like amplify-and-forward (AF), decode-and-forward (DF), and decode-amplify-forward (DAF) further enhanced the performance of the system but with some limitations. In this thesis, we lay emphasis on a two-hop amplify-decode-forward relay based system with a difference that at the transceiver (TR) node i.e. the relay, the received bits are decoded, estimated, de-modulated, amplified, and then forwarded to the receiver. This system model maintains low complexity as the data bits are not encoded again at the TR node. Also the number of antennas at the TR node is kept low to one. However, the number of antennas at the transmitter and/or receiver can be varied, thus, capable of forming a system model with any number of antennas at either end as explained in Chapter-4. Also, the system proves to be dynamic that even if the TR node fails to perform due to any un-avoidable circumstances, the transmission will still take place as normal. Also the ability of the system to have variable

number of transmit and receive antennas, Antenna Selection (AS) can be easily applied at either end without any modifications at the TR node as explained in Chapter-5. The pilot symbols used for AS are further exploited for channel estimation as explained in Chapter-6.

Chapter 4 – System Modelling

In this chapter, we focus on a two-hop decode-amplify-forward (DAF) relay based system with a difference that at the transceiver (TR) node i.e. the relay, the received bits are decoded, estimated, de-modulated, amplified, and then forwarded to the receiver. This system model maintains low complexity as the data bits are not encoded again at the TR node as is done in almost all the present relay-based systems. Also the number of antennas at the TR node is kept low to one. However, the number of antennas at the transmitter and/or receiver can be varied, thus, capable of forming a system model with any number of antennas at either end. Also, the system proves to be dynamic that even if the TR node fails to perform due to any un-avoidable circumstances, the transmission will still take place as normal. The ability of the system to have variable number of transmit and receive antennas without modifying the functionality of the TR node makes it novel. This method provides increased diversity at the transmitter by sending more number of signal copies and at the receiver by receiving them over additional channel paths provided by the TR node in addition to the direct transmission paths.

4.1 Introduction

The performance of any wireless system can be improved if the number of information bearing signal copies transmitted or received can be increased i.e. by increasing the number of diverse paths. Thus, exploiting diversity is one of the many options available that promises significant improvements in terms of efficiency and link reliability. However, in order to increase the number of diverse paths, multiple antennas need to be installed at the source and the destination. This leads to significant increase in performance but it also adds the extra cost of antennas and its installation at either or both ends.

By using cooperative techniques, diversity gain can be obtained without increasing the number of antennas at the transmitter or the receiver side. The use of relay node in cooperative diversity helps in providing the additional information bearing paths. At the receiver, both the relay forwarded and directly received signals are combined. Single or multiple antennas can be used at the relay node along with single or multiple antennas at the source and the destination. Though multiple antennas at either ends along with MIMO relaying significantly improves the performance of the wireless systems, but for wireless systems with limited terminal sizes, increased complexity, extra cost including added RF elements and additional signal processing hinders the use of such heavy systems. Also, small handheld and mobile devices are not capable of handling large number of antennas. In order to deal with these factors, we have developed a simplified adaptive two-hop decode-amplify-forward (also called Hybrid relay system) relay system capable of achieving better BER as compared to the normal wireless system models with any number of antennas at either end and a single transceiver (TR) at the relay node. Also unlike in all the existing relaying schemes where the transmission from the relay to the receiver takes place only when the data received at the relay is error free [10], [22], [23], [25], [146], in the DAF scheme presented here, the TR node transmits information to the destination irrespective of the error

occurrences; thus, there is no restriction on the relay and it forwards the data towards the destination at all times. However, the bit errors are calculated at the node. If the number of errors at the node is more than a threshold value of the number of errors, which the system can withstand, such that further transmission will no longer be helpful, re-transmission of signal takes place.

We use Nakagami distribution to model the wireless fading channel as it provides a good fit to experimental results in exploiting a wide variety of different fading conditions. From the family of Nakagami fading channel models, we focus on using Nakagami-m fading channel as the path for data transmission. We describe the relay as the transceiver (TR) node capable of transmitting and receiving the information. Unlike in [143], we have presented the error performance where the fading parameters of the channel paths from the transmitter to the TR node and TR node to receiver can take any value from $0.65 \leq m \leq 10$. However, the sum of these two fading parameters is always an integer. Also the results in [143] were limited to BPSK modulation while the system model described in this chapter works for higher orders of PSK modulation as well. To maintain the simplicity of the system, we have considered that the TR node comprises of single antenna relay. Due to the use of single-antenna relay, an uncoded but modulated signal transmission takes place from the TR node to the receiver unlike MIMO relaying where the signal has to be re-encoded at the TR node for further transmission. Further, using larger number of relays may help in performance improvement but may also result in significant drop in the performance if the TR node fails by significantly reducing the order of diversity. Single-antenna relay makes the system dynamic as in case of any unlikely failure of the TR node, the communication can still take place by bypassing the TR node. Also the load of signal processing is reduced considerable at the relay. This is an important thing to consider and has been really focused for the system model developed here. Later in the chapter, the performance of the system model has been

analysed based on the relay position. Thus, simpler the relay computations, better it will be to relocate.

4.2 General System and Channel Model Description for a Two-hop DAF Relayed System

The data transmission in a two-hop DAF relayed system follows three different paths; transmitter to the TR node, TR node to receiver, and transmitter to receiver. For simplicity, the communication taking place between these three paths will be written as $(T-TR)$, $(TR-R)$, and $(T-R)$, respectively. Assuming that perfect channel state information (CSI) is available at the receiver and known partially at the transmitter via a feedback channel, the system is modelled based on the following assumptions:

- The channel is quasi-static and fading is frequency-flat.
- The path gains are modelled as independent complex Gaussian random variables with zero mean and variance 1 i.e. $h_{ij} \sim \mathcal{N}(0,1)$.
- The signal is MPSK modulated, specifically BPSK and QPSK modulation but can be easily extended to higher PSK schemes.
- The noise samples n_j are independent and identically distributed (i.i.d.) zero mean complex Gaussian with variance $\sigma^2 = \frac{1}{2E_s N_0} = \frac{1}{2SNR}$.
- The transmit antennas are assumed to have equal transmission power.
- The signals received between $(T-TR)$, $(TR-R)$, and $(T-R)$ experience independent fading and are normalized individually.

Considering the wireless communication system with N_t transmit and N_r receive antennas communicating over independent and identically distributed (i.i.d.) Nakagami-*m* fading channel, the baseline MIMO system model is as shown in Fig. 3.10. The channel matrix H for the MIMO system can be defined as an $N_t \times N_r$ channel matrix whose entries are the fading coefficients $h_{i,j}, i = 1, \dots, N_t,\ j = 1, \dots, N_r$ and can be expressed as

$$H = \begin{bmatrix} h_{11} & \cdots & h_{1,N_r} \\ \vdots & \ddots & \vdots \\ h_{N_t,1} & \cdots & h_{N_t,N_r} \end{bmatrix} \tag{4.1}$$

The amplitude of the channel fading coefficients follow Nakagami distribution with fading parameter $0.65 \leq m \leq 10$.

Considering another wireless communication system where the source and the destination has N_t transmit and N_r receive antennas, respectively, but the source and the destination does not communicate directly with each other but through a transceiver node. The communication model is shown in Fig. 4.1.

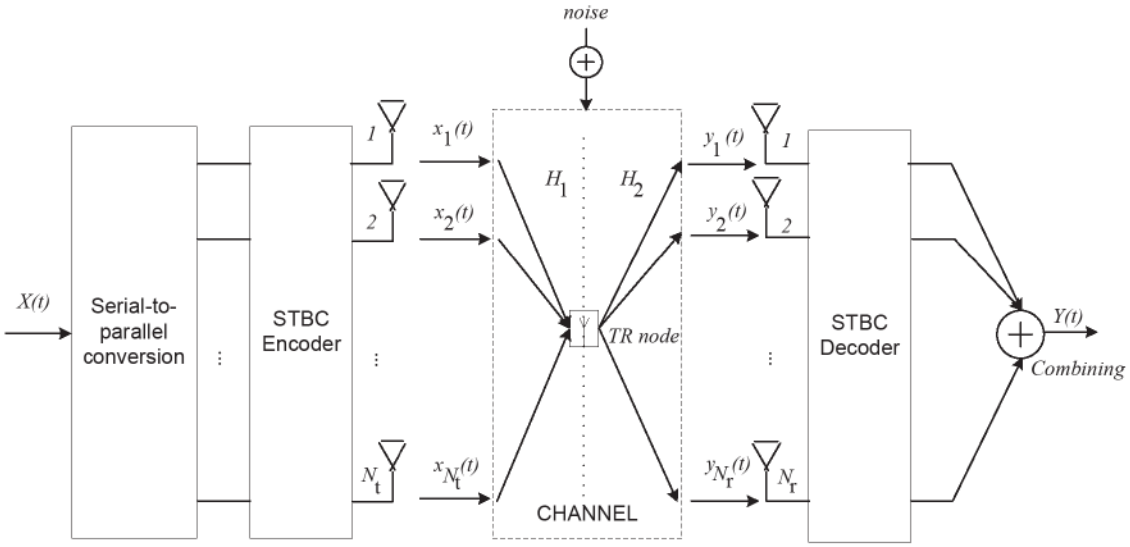

Fig. 4.1 MIMO system communicating via TR node

As can be seen from Fig. 4.1, the transmit antennas communicate with the receive antennas via the TR node. The channel matrix H for this system model can be defined as follows: from the source to the TR node, the communication takes place over channel H_1. Thus H_1 can be defined as a $N_t \times 1$ channel matrix whose entries are the fading coefficients $h_{i,1}, i = 1, \ldots, N_t$. From the TR node to the destination the communication takes place over H_2 which can be defined as a $1 \times N_r$ channel matrix whose entries are the fading coefficients $h_{1,j}, j = 1, \ldots, N_r$. The channel matrices H_1 and H_2 can be expressed as

$$H_1 = \begin{bmatrix} h_{11} \\ h_{21} \\ \vdots \\ h_{N_t,1} \end{bmatrix}, \text{ and} \tag{4.2}$$

$$H_2 = \begin{bmatrix} h_{11} & h_{12} \dots h_{1,N_r} \end{bmatrix}, \tag{4.3}$$

respectively. Each of these channel matrices consists of i.i.d. Nakagami-*m* channel coefficients. It is assumed that the two matrices are also independent of each other.

Theoretical analyses of the two MIMO systems from Fig. 4.1 and Fig.4.2 shows that though both the systems have equivalent number of transmit and receive antennas, the MIMO system with a TR node will perform poorer as compared to the conventional MIMO system of Fig. 3.10. The reasonable explanation is due to lesser number of channel paths carrying the information to the receiver, the MIMO system with TR node provides less diversity. It is well known that the performance of any wireless communication system can be improved by adding diversity. In this chapter we try to apply this fact and provide a novel MIMO communication system with added diversity in comparison to the conventional MIMO system. If we try to combine the two systems explained in Fig. 3.10 and Fig. 4.1 into one single equivalent system that acts as a two-hop DAF relayed system, it may perform better than either of the two systems. The two-hop DAF relayed with an additional TR node is shown in Fig. 4.2.

There is a direct transmission of information from transmitter to the receiver via a direct path over the channel H_3 and the information is also sent over another path via the TR node. The transmitters transmits the information to the TR node over H_1, the TR node receives the information, decodes, amplifies, and then forwards it to the receiving array over the channel path H_2.

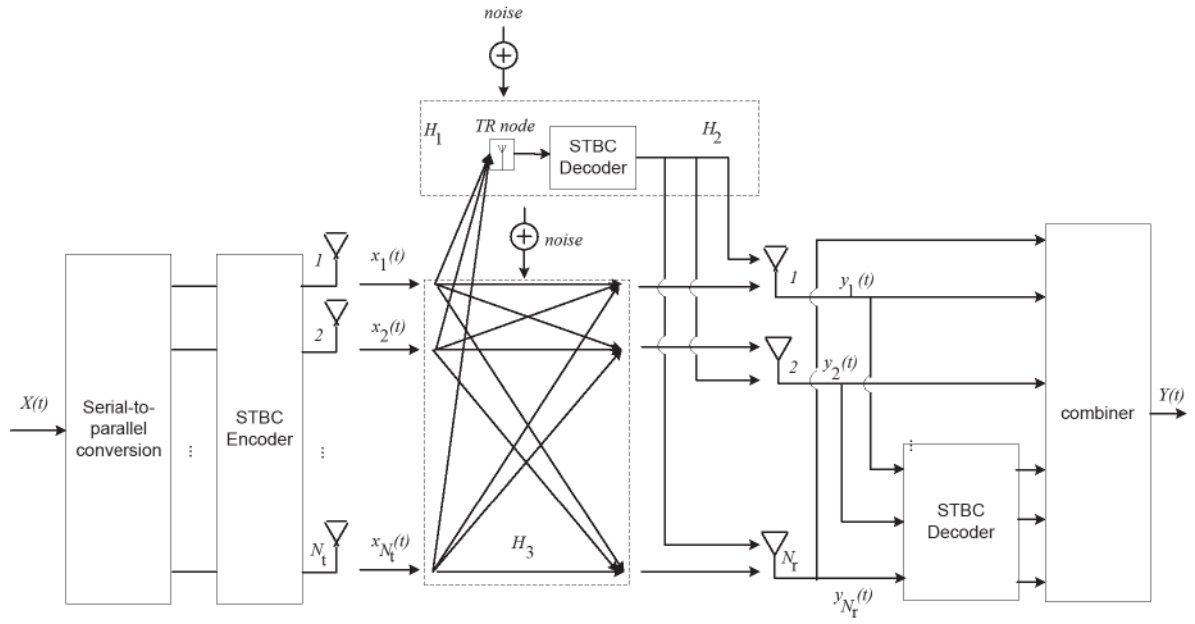

Fig. 4.2 Hybrid MIMO-TR communication system

Another interesting question that arises here is about the placement of the TR node. It is quite obvious that channels H_1 and H_2 experience independent fading conditions. However, if the TR node lies within such a range that the channel H_3 is dependent on H_1 and H_2 such that

$$H_3 = H_1 H_2 \tag{4.4}$$

The computational complexities may grow in an attempt to obtain H_3 from H_1 and H_2. On the other hand, considering H_1, H_2 and H_3 to be independent of each other will ease the data flow. Also, though the three channels are independent of each other, it is considered that the variations in the fading conditions are not fast and are not highly deviated. H_1, H_2 and H_3 are all Nakagami-m distributed channel models.

At the receiver, all the information bearing signals, both from direct transmission and from the TR node are received by the receiving arrays. The received signals are then sorted such that the signals received from direct transmission are sent to the decoder whereas the signals received after transmission from the TR node are fed directly to the combiner. The decoder output is also sent to the combiner and the signals received from two different

sources are then combined. The combined signals are then demodulated to retrieve the actual information sent and the number of error accounted for.

In the following sections, we present in detail, the data flow and the signal processing for the two-hop DAF relayed system for the various system models discussed in Section 3.5.1 based on different number of antennas at the source and the destination. We also explain the corresponding equivalent SNRs and the error probabilities for various system models.

4.2.1 SISO System and Channel Model for two-hop DAF Relayed System

Fig. 4.3 shows the SISO communication model with one transmitter (T) and one receiver (R)where the information is sent over a single data channel and also via a TR node.

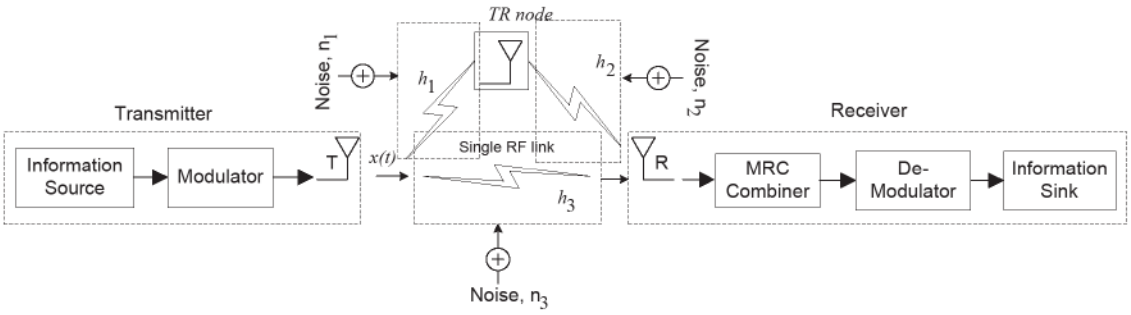

Fig. 4.3 A SISO Communication Model with additional TR node

Considering that x is the transmitted sequence, h_1, h_2, h_3 are the channel coefficients for the paths between the transmitter and the TR node $(T - TR)$, TR node and the receiver $(TR - R)$, and transmitter and the receiver $(T - R)$, respectively, and n_1, n_2, n_3 are the additive white noises with zero mean and variance equal to N_0 for $(T - TR)$, $(TR - R)$, and $(T - R)$, respectively, then the transmission takes place as follows:

Considering x is the MPSK modulated signal, during the first time-slot the transmitter sends the signal directly to the receiver over the direct channel path given by h_3 and to the TR node over another channel path given by h_1. During the second time slot, the TR node sends the received signal to the receiver over the channel path given by h_2. No coding is

performed here due to the use of single antenna at the transmitter. The signals are transmitted with energy $E_b$using single transmit antenna over single RF link which has Nakagami-*m* distribution. Then the signal received at the TR node from the transmitter is given by

$$y_{(T-TR)} = \sqrt{E_b}xh_1 + n_1 \tag{4.5}$$

Equalization is performed at the TR node by dividing the received signal $y_{(T-TR)}$ by the apriori known h_1

$$\hat{y}_{(T-TR)} = \frac{y_{(T-TR)}}{h_1} = \frac{xh_1+n_1}{h_1} = x + \dot{n} \tag{4.6}$$

where $\dot{n} = \frac{n_1}{h_1}$ is the additive noise scaled by the channel coefficient h_1. No decoding takes place at the TR node as the data sent was un-coded. Maximum Likelihood demodulation of the signal $\hat{y}_{(T-TR)}$ is performed as follows

$$\left(\hat{y}_{(T-TR)}\right)_{est} = (\hat{y}_{(T-TR)} - MPSK_{map_{set}})'.(\hat{y}_{(T-TR)} - MPSK_{map_{set}}) \tag{4.7}$$

where $MPSK_{map_{set}} \in \begin{cases} \{0,1\}\ when\ M = 2 \\ \{0,1,2,3\}\ when\ M = 4, \\ and\ so\ on\ for\ higher\ modulations \end{cases}$

The decision is made in favor of the symbol with minimum distance to retrieve the signal with minimum number of errors as

$$\hat{x} = min\left(\hat{y}_{(T-TR)}\right)_{est} \tag{4.8}$$

At this stage no error correction is performed at the TR node and the erroneous estimated signal $\hat{x}$ at the TR node is transmitted to the receiver over the channel path h_2. The signal received at the receiver from the TR node is then given by

$$y_{(TR-R)} = \sqrt{E_b}\hat{x}h_2 + n_2 \tag{4.9}$$

The received signal y_{TR-R} is equalized as per (4.6) given by

$$\hat{y}_{(TR-R)} = \frac{y_{(TR-R)}}{h_2} = \frac{\hat{x}h_2+n_2}{h_2} = \hat{x} + \ddot{n} \tag{4.10}$$

where $\ddot{n} = \frac{n_2}{h_2}$ is the additive noise scaled by the channel coefficient h_2.

The signal received at the receiver directly from the transmitter is given by

$$y_{(T-R)} = \sqrt{E_b} x h_3 + n_3 \tag{4.11}$$

which is again individually normalized as

$$\hat{y}_{(T-R)} = \frac{y_{T-R}}{h_3} = \frac{x h_3 + n_3}{h_3} = x + \ddot{n} \tag{4.12}$$

where $\ddot{n} = \frac{n_3}{h_3}$ is the additive noise scaled by the channel coefficient h_3. At the receiver, the received signals $\hat{y}_{(TR-R)}$ and $\hat{y}_{(T-R)}$ are summed. Since there is only one antenna at the receiver the two signals are combined as

$$Y = sum(\hat{y}_{(TR-R)}, \hat{y}_{(T-R)}) \tag{4.13}$$

Maximum Likelihood demodulation of the signal Y is performed as follows

$$(Y)_{est} = \left| Y - MPSK_{map_{set}} \right|^2 \tag{4.14}$$

The decision is again made in favor of the symbol with minimum distance to retrieve the signal with minimum number of errors as

$$X = arg \min_{MPSK_{map_{set}} \in \mathcal{A}} (Y_{est}) \tag{4.15}$$

where $\mathcal{A}$ is the constellation alphabet.

4.2.2 MISO System and Channel Model for two-hop DAF Relayed System

In this section, MISO system transmission using the TR node is presented. Fig. 4.4 shows such a communication model with N_t transmit and a single receive antenna passing information via a direct path and a TR node.

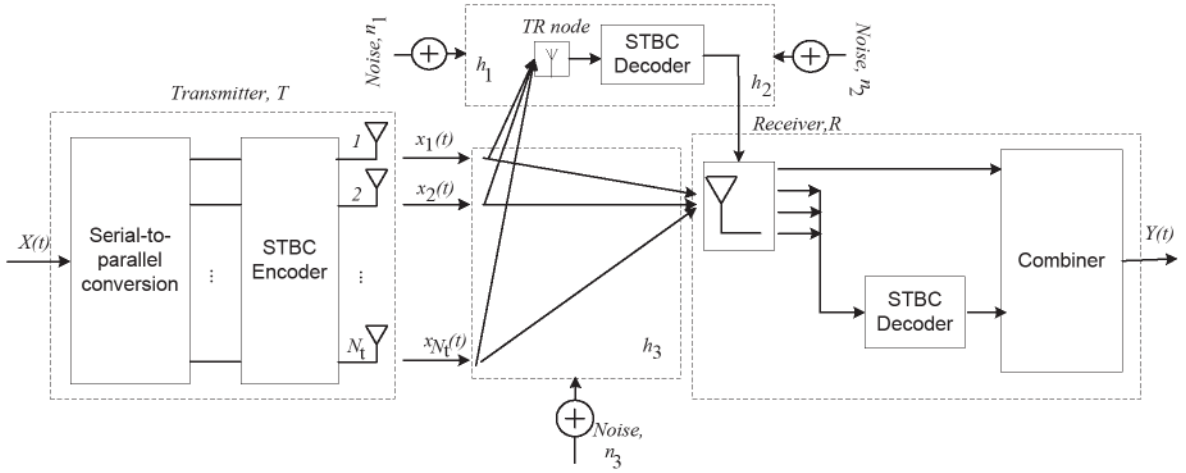

Fig. 4.4 A MISO Communication Model with additional TR node

Since there are multiple antennas at the transmitter, diversity is exploited by using STBC transmission where the datasets are encoded based on the criteria of block coding both in space and time. A generalized version of the STBC encoded MISO scheme is presented where the transmitted data is split into n sub-streams simultaneously transmitting over N_t antennas and received over a single receive antenna. Each time the encoding operation takes place a block of km information bits are mapped into the signal constellation to select k modulated signals $x_1, x_2, \dots, x_k$. The k modulated signals are then encoded by a ST block encoder to generate N_t parallel signal sequences of length p and mapped according to the encoder matrix G_{N_t} which are linear combinations of the k modulated signals and their complex conjugates $x_1^*, x_2^*, \dots, x_k^*$. These parallel sequences are then transmitted through N_t transmit antennas simultaneously in p time periods. The encoder matrix is based on the orthogonal design rule such that $G_{N_t}.G_{N_t}^H = (|x_1|^2 + |x_2|^2 + \cdots + |x_k|^2)I$ in order to achieve full transmit diversity of N_t. $G_{N_t}^H$ is the hermitian transpose of G_{N_t} and I is the $N_t \times N_t$ identity matrix. The i^{th} row of G_{N_t} represents the symbols transmitted from i^{th} transmit antenna consecutively in p transmission periods, and the j^{th} column of G_{N_t} represents the symbols transmitted simultaneously through N_t transmit antennas at time j. In other words, the elements $g_{i,j}$ of G_{N_t} in the i^{th} row and j^{th} column, where $i = 1,2, \dots N_t$ and $j = 1,2, \dots p$,

represents the signal transmitted from antenna i at time j. At the receiver the decoding is performed by using a simple ML detection rule i.e. symbol-by-symbol detection. The spectral efficiency of km/p bits/s/Hz is achieved.

Assume that the transmission at the baseband employs a signal constellation with 2^m elements. The whole data sequence is divided into a number of short symbol frames and that the data is transmitted in the frames of length l. Each frame of data passes through the STBC encoder and is encoded. The serially transmitted frame of encoded data is then converted into a parallel set of information depending on the number of transmit antennas available, i.e., divided into N_t streams of data, one data bit for each antenna. At each time slot t, the transmitted signal from the i-th is a signal c_t^i for $1 \leq i \leq N_t$.

We limit our discussion to two and three transmit antennas and discuss the transmission based on the proposed model, which obviously can be extended to any number of transmit antennas.

4.2.2.1 System and Channel Model when $N_t = 2$ and $N_r = 1$

4.2.2.1.1 Encoding Algorithm: coding and Modulation

For $N_t = 2$ and $N_r = 1$ when direct transmission between T and R takes place, information sent from the information source is coded using a ST Block encoder to be transmitted over the channel through two transmit antennas. Each set of m bits is mapped to form $m - ary$ PSK symbol. The STBC encoding algorithm is described by the encoder matrix G_2^* which maps a block of $k = 2$ bits into $N_t = 2$ sequences each of length $p = 2$. G_2^* is given by

$$G_2^* = \begin{pmatrix} x_1 & x_2 \\ -x_2^* & x_1^* \end{pmatrix} \tag{4.16}$$

where x_1 and x_2 are the set of symbols at the encoder input. The first and second rows of the encoder matrix are transmitted at times t and $t + T$ from the two antennas.

4.2.2.1.2 Combining

We define the channel paths H_1, H_2, H_3 for the $(T-TR)$, $(TR-R)$, and $(T-R)$ links, respectively, as

$$H_1 = \begin{bmatrix} h_{11} \\ h_{12} \end{bmatrix} \tag{4.17}$$

$$H_2 = [h_{21}] \tag{4.18}$$

$$H_3 = \begin{bmatrix} h_{31} \\ h_{32} \end{bmatrix} \tag{4.19}$$

Considering a quasi-static flat fading channel such that no channel induced ISI term is present, the MPSK modulated signal is transmitted from T to R over the channel path H_3 and to TR over the channel path H_1, where H_3 and H_1 are 2×1 channel matrices. The signal received at the TR node sees a complex weighted version of the $N_t = 2$ simultaneously transmitted signals weighted by fade coefficients and noisy superposition of the signals corrupted by Nakagami-*m* fading and is given by

$$y^1_{(T-TR)} = \sqrt{\frac{E_b}{2}} [x_1 \quad x_2] \begin{bmatrix} h_{11} \\ h_{12} \end{bmatrix} + n_{11} = \sqrt{\frac{E_b}{2}} (x_1 h_{11} + x_2 h_{12}) + n_{11} \tag{4.20}$$

during the first time slot and

$$y^2_{(T-TR)} = \sqrt{\frac{E_b}{2}} [-x_2^* \quad x_1^*] \begin{bmatrix} h_{11} \\ h_{12} \end{bmatrix} + n_{12} = \sqrt{\frac{E_b}{2}} (-x_2^* h_{11} + x_1^* h_{12}) + n_{12} \tag{4.21}$$

during the second time slot, or equivalently as

$$\begin{bmatrix} y^1_{(T-TR)} \\ y^2_{(T-TR)}{}^* \end{bmatrix} = \begin{bmatrix} h_{11} & h_{12} \\ h_{12}^* & -h_{11}^* \end{bmatrix} \begin{bmatrix} x_1 \\ x_2 \end{bmatrix} + \begin{bmatrix} n_{11} \\ n_{12}^* \end{bmatrix} \tag{4.22}$$

where $y^1_{(T-TR)}$ and $y^2_{(T-TR)}$ is the received symbol, h_{11} and h_{12} is the channel, x_1 and x_2 is the transmitted symbol, and, n_{11} and n_{12} is the noise during the first and second time slot, respectively. Defining $\widetilde{H}_1 = \begin{bmatrix} h_{11} & h_{12} \\ h_{12}^* & -h_{11}^* \end{bmatrix}$,

$$\begin{bmatrix} y^1_{(T-TR)} \\ y^2_{(T-TR)}{}^* \end{bmatrix} = \widetilde{H}_1 \begin{bmatrix} x_1 \\ x_2 \end{bmatrix} + \begin{bmatrix} n_{11} \\ n^*_{12} \end{bmatrix} \tag{4.23}$$

4.2.2.1.3 Decoding and estimating

The transmitted symbols can be estimated by following the LS estimation rule i.e.

$$\hat{y}_{(T-TR)} = \begin{bmatrix} y^1_{(T-TR)} \\ y^2_{(T-TR)}{}^* \end{bmatrix} . inv(\widetilde{H}_1) \tag{4.24}$$

Thus to calculate $inv(\widetilde{H}_1)$, we first calculate the pseudo inverse of $\widetilde{H}_1$ as

$$inv\left(\widetilde{H}_1\right) = \acute{H}_1 = (\widetilde{H}_1{}^H \widetilde{H}_1)^{-1} \widetilde{H}_1{}^H \tag{4.25}$$

Describing $(\widetilde{H}_1{}^H \widetilde{H}_1)$ and $(\widetilde{H}_1{}^H \widetilde{H}_1)^{-1}$ as

$$\widetilde{H}_1{}^H \widetilde{H}_1 = \begin{bmatrix} h_{11} & h_{12} \\ h^*_{12} & -h^*_{11} \end{bmatrix} \begin{bmatrix} h^*_{11} & h_{12} \\ h^*_{12} & -h_{11} \end{bmatrix} \tag{4.26}$$

$$= \begin{bmatrix} |h_{11}|^2 + |h_{12}|^2 & h^*_{11}h_{12} - h^*_{11}h_{12} \\ h_{11}h^*_{12} - h_{11}h^*_{12} & |h_{11}|^2 + |h_{12}|^2 \end{bmatrix} \tag{4.27}$$

$$= (|h_{11}|^2 + |h_{12}|^2)I \tag{4.28}$$

$$(\widetilde{H}_1{}^H \widetilde{H}_1)^{-1} = \left(\frac{1}{|h_{11}|^2 + |h_{12}|^2}\right) I \tag{4.29}$$

Thus, from (4.24) and (4.25)

$$\hat{y}_{(T-TR)} = (\widetilde{H}_1{}^H \widetilde{H}_1)^{-1} \widetilde{H}_1{}^H \begin{bmatrix} y^1_{(T-TR)} \\ y^2_{(T-TR)}{}^* \end{bmatrix} \tag{4.30}$$

$$= (\widetilde{H}_1{}^H \widetilde{H}_1)^{-1} \widetilde{H}_1{}^H \left(\widetilde{H}_1 \begin{bmatrix} x_1 \\ x_2 \end{bmatrix} + \begin{bmatrix} n_{11} \\ n^*_{12} \end{bmatrix}\right) \tag{4.31}$$

$$\hat{y}_{(T-TR)} = \begin{bmatrix} \hat{y}^1_{(T-TR)} \\ \hat{y}^2_{(T-TR)}{}^* \end{bmatrix} = \begin{bmatrix} x_1 \\ x_2 \end{bmatrix} + (\widetilde{H}_1{}^H \widetilde{H}_1)^{-1} \widetilde{H}_1{}^H \begin{bmatrix} n_{11} \\ n^*_{12} \end{bmatrix} \tag{4.32}$$

$$\hat{y}_{(T-TR)} = \begin{bmatrix} x_1 \\ x_2 \end{bmatrix} + \dot{n} \tag{4.33}$$

where $\dot{n} = (\widetilde{H}_1{}^H \widetilde{H}_1)^{-1} \widetilde{H}_1{}^H \begin{bmatrix} n_{11} \\ n^*_{12} \end{bmatrix}$.

As the signal is received at the receiver, the demodulator examines the received symbol corrupted by the channel or the receiver. During the maximum likelihood detection, the demodulator selects that point on the constellation diagram as its estimate of actually transmitted symbol which is closest to the received symbol in terms of the minimum Euclidean distance on the constellation diagram. At this point, if the corruption caused the received symbol to shift closer to any other constellation point than the one transmitted, it will incorrectly demodulate the symbol.

Assuming that the channel coefficients are constant over the p received symbols and starting with square transmission matrix, let ϵ_t denote the permutations of the first column to the t-th column and $\epsilon_t(i)$ denote the row position of x_i in the t-th column. Then the ML detection rule is to form the decision variables

$$\widetilde{x_i} = \sum_{t=1}^{N_t} \sum_{j=1}^{N_r} y_j^t \, h_{j,\epsilon_t(i)}^* \delta_t(i) \tag{4.34}$$

where $\delta_t(i)$ is the sign of x_i in the t-th column and $i = 1,2, \ldots N_t$ and then deciding on the constellation symbol x_i that satisfies

$$\hat{x}_i = arg \min_{c \in \mathcal{A}} \left(|\widetilde{x_i} - c|^2 + \left(-1 + \sum_{j=1}^{N_r} \sum_{i=1}^{N_t} \left| h_{i,j} \right|^2 \right) |c|^2 \right) \tag{4.35}$$

with $\mathcal{A}$ the constellation alphabet. For M-PSK signal constellation, $\left(-1 + \sum_{j=1}^{N_r} \sum_{i=1}^{N_t} \left| h_{i,j} \right|^2 \right) |c|^2, i = 1,2$ are constant for all signal points, given $h_{i,j}$. Therefore, the decision rule in (4.35) can be further simplified to

$$\hat{x}_i = arg \min_{c \in \mathcal{A}} (|\widetilde{x_i} - c|^2) \tag{4.36}$$

At this stage no error correction is performed at the TR node and the erroneous estimated signal $\hat{x}$ at the TR node is again modulated using MPSK and transmitted to the receiver over the channel path H_2. The signal received at the receiver from the TR node is then given by

$$y_{(TR-R)} = \sqrt{E_b} \hat{x} H_2 + n_2 \tag{4.37}$$

The received signal y_{TR-R} is equalized as per (4.6) given by

$$\hat{y}_{(TR-R)} = \frac{y_{(TR-R)}}{h_2} = \frac{\hat{x}h_{21}+n_2}{h_{21}} = \hat{x} + \ddot{n} \tag{4.38}$$

where $\ddot{n} = \frac{n_2}{h_2}$ is the additive noise scaled by the channel coefficient h_{21}.

The signal received at the receiver directly from the transmitter follows similar combining, demodulating and estimating process given by (4.20) – (4.33) such that the received signal in two time slots is given by

$$\begin{bmatrix} y^1_{(T-R)} \\ y^2_{(T-R)}{}^* \end{bmatrix} = \tilde{H}_3 \begin{bmatrix} x_1 \\ x_2 \end{bmatrix} + \begin{bmatrix} n_{31} \\ n^*_{32} \end{bmatrix} \tag{4.39}$$

where $y^1_{(T-R)}$ and $y^2_{(T-R)}$ are the received symbols, x_1 and x_2 are the transmitted symbols, and, n_{31} and n_{32} is the noise during the first and second time slot, respectively, from the $(T-R)$, and the estimate of the transmitted symbols is given by

$$\hat{y}_{(T-R)} = \begin{bmatrix} x_1 \\ x_2 \end{bmatrix} + \ddot{n} \tag{4.40}$$

where $\ddot{n} = (\tilde{H}_3{}^H \tilde{H}_3)^{-1} \tilde{H}_3{}^H \begin{bmatrix} n_{31} \\ n^*_{32} \end{bmatrix}$, $\tilde{H}_3 = \begin{bmatrix} h_{31} & h_{32} \\ h^*_{32} & -h^*_{31} \end{bmatrix}$, h_{31} and h_{32} is the $(T-R)$ channel. At the receiver, the received signals $\hat{y}_{(TR-R)}$ and $\hat{y}_{(T-R)}$ are combined as

$$Y = sum(\hat{y}_{(TR-R)}, \hat{y}_{(T-R)}) \tag{4.41}$$

Maximum Likelihood demodulation of the signal Y is performed to obtain X following (4.14) and the decision is made in favor of the symbol with minimum distance following (4.36).

$$X = arg\ \min_{MPSK_{map_{set}} \in \mathcal{A}} \left(\left| Y - MPSK_{map_{set}} \right|^2 \right) \tag{4.42}$$

4.2.3 SIMO System and Channel Model for two-hop DAF Relayed System

In this section we present the SIMO system transmission using the TR node as shown in Fig. 4.5.

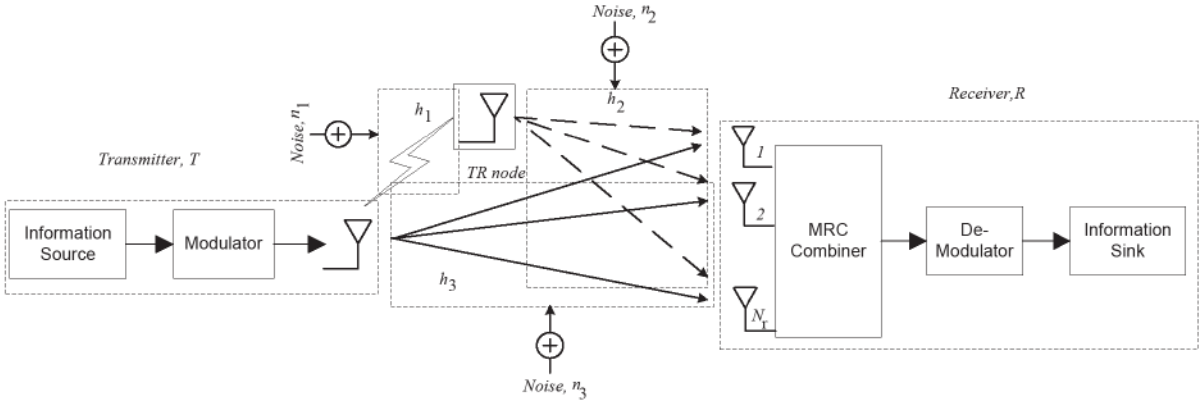

Fig. 4.5 A SIMO Communication Model with additional TR node

To show the efficacy of diversity techniques in combating multipath fading, consider a wireless system with one transmit and N_r receive antennas. Also consider that the system is uncoded MPSK system with receive diversity. This is equivalent to having N_r identical and independent Nakagami-*m* fading links between the transmitter and the receiver [90], [92]. With multiple antennas in the receiving array we exploit diversity by using Maximal Ratio Combining at the receiver. Assuming that perfect channel state information (CSI) is available at the receiver, if at any time t, $x(t)$ is the transmitted signal across all links, then the transmitted signals are received over N_r independent and identically distributed Nakagami-*m* fading channels corrupted by complex Gaussian noise. The received signal at receiver j is given by

$$y_j(t) = \sqrt{E_b}x(t)h_j(t) + n_j(t), \quad j = 1 \dots \dots \dots \dots . N_r \tag{4.43}$$

where $\sqrt{E_b}$ is the bit energy available for each diversity branch

$n_j(t)$ is the Gaussian complex noise variable with variance N_0.

$h_j(t)$ is the complex channel coefficient.

The noise on each diversity branch is assumed to be uncorrelated. The received signals are combined at the receiver using MRC to maximize the SNR and give the following expression

$$\tilde{y}(t) = \sum_{j=1}^{n_R} h_j^* y_j(t) = x(t) \sum_j^{n_R} \left|h_j\right|^2 + n'(t) \tag{4.44}$$

In terms of the weight vector w, where $w = h^H$, the output x at the receiver is given by

$$x=\sqrt{E_s}h^H hx + h^H n \tag{4.45}$$

where $h^H h = \sum_j^{n_R} |h_j|^2$ is the sum of the channel powers across all the receive antennas.

While designing a SIMO system, we prefer to place the TR node closer to the transmitter. The reason behind this is that firstly due to single transmitter, hence no transmit diversity, the signal is more prone to multipath and fading. Also due to larger distance to be covered while travelling from the transmitter to the TR node, the signal will suffer further deterioration. On the other hand, by placing the TR node closer to the transmitter, the signal is expected to suffer less from fading due to shorter distance to be travelled. Also, the amount of fading affecting the signal while travelling larger distance from the TR node to the receiver will be somehow compensated at the receiver as the received signal is combined using MRC. Thus, for the system under discussion the fading parameter m of the $(T - TR)$ link is always kept higher than the fading parameter of the $(TR - R)$ link, where the fading parameter for both the channel links is still integers.

4.2.3.1 System and Channel Model when $N_t = 1$ and $N_r = 2$

We first define the channel paths H_1, H_2, H_3 for the $(T - TR)$, $(TR - R)$, and $(T - R)$ links, respectively, as

$$H_1 = [h_{11}] \tag{4.46}$$

$$H_2 = \begin{bmatrix} h_{21} \\ h_{22} \end{bmatrix} \tag{4.47}$$

$$H_3 = \begin{bmatrix} h_{31} \\ h_{32} \end{bmatrix} \tag{4.48}$$

For an uncoded MPSK modulated signal, the transmission from $(T - TR)$ is similar to explained in Section 4.2.1 for SISO systems. Thus the signal transmitted by a single transmitter over H_1 and received at the TR node after demodulation, estimation, and re-

modulation is similar to as given by (4.8). The signal $\hat{x}$ is now transmitted by the TR node over the channel H_2 to the receiver. Representing $h_{21}$and h_{22} as the complex channels between the TR node and transmit antennas and receive antenna1 and between TR node and receive antenna2, respectively, the signals received at the receiver are given by

$$y_{(TR-R)1} = h_{21}\hat{x} + n_{21} \tag{4.49}$$

$$y_{(TR-R)2} = h_{22}\hat{x} + n_{22} \tag{4.50}$$

where n_{21} and n_{22} are the complex noise added at the two receivers. At the receiver, the two signals are combined using MRC and the matched filter output is given by

$$\tilde{y}_{(TR-R)}(t) = (|h_{21}^2| + |h_{22}^2|)\hat{x}(t) + \ddot{n}(t) \tag{4.51}$$

where $\ddot{n}(t) = [n_{21}(t) \quad n_{22}(t)]^{\mathrm{T}}$ is the complex noise vector.

The signal received at the receiver directly from the transmitter is given by

$$y_{(T-R)1} = h_{31}x + n_{31} \tag{4.52}$$

$$y_{(T-R)2} = h_{32}x + n_{32} \tag{4.53}$$

where n_{31} and n_{32} are the complex noise added at the two receivers. At the receiver, the two signals are combined using MRC and the matched filter output is given by

$$\tilde{y}_{(T-R)}(t) = (|h_{31}^2| + |h_{32}^2|)x(t) + \ddot{n}(t) \tag{4.54}$$

where $\ddot{n}(t) = [n_{31}(t) \quad n_{32}(t)]^{\mathrm{T}}$ is the complex noise vector. It is worthwhile to note here that the copies of the signals received at the receiver from the TR node and T are MR combined separately as is clear from (4.51) and (4.54). At the receiver, the received signals $\hat{y}_{(TR-R)}$ and $\hat{y}_{(T-R)}$ are summed as

$$Y = sum(\hat{y}_{(TR-R)}, \hat{y}_{(T-R)}) \tag{4.55}$$

Maximum Likelihood demodulation of the signal Y is performed as follows

$$(Y)_{est} = \left|Y - MPSK_{map_{set}}\right|^2 \tag{4.56}$$

The decision is again made in favour of the symbol with minimum distance to retrieve the signal with minimum number of errors as

$$X = arg\ \min_{MPSK_{map\ set} \in \mathcal{A}}(Y_{est}) \tag{4.57}$$

where $\mathcal{A}$ is the constellation alphabet.

4.2.4 MIMO System and Channel Model for two-hop DAF Relayed System

In this section we present the MIMO system transmission using the TR node as shown in Fig. 4.6.

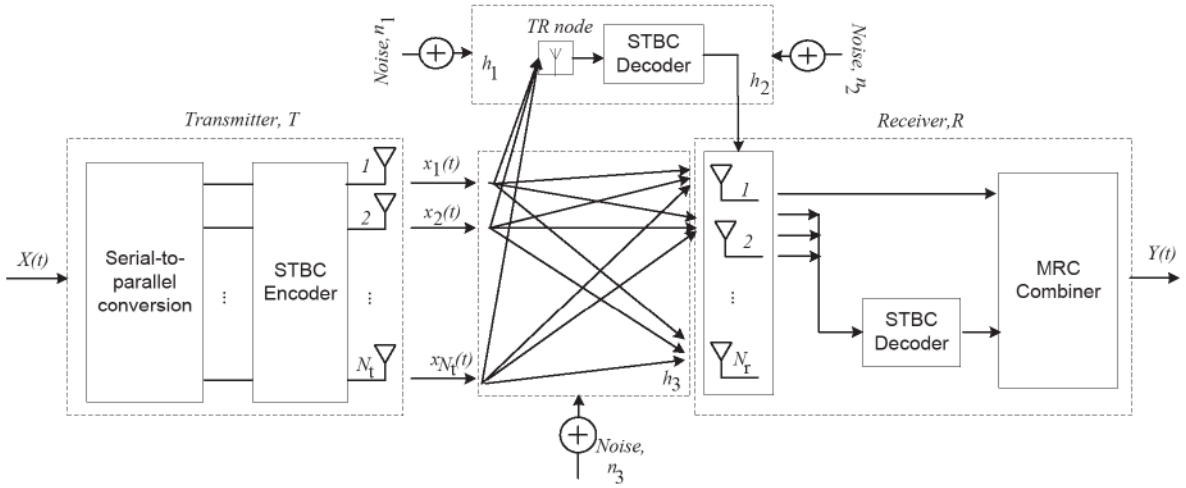

Fig. 4.6 A MIMO Communication Model with additional TR node

By using multiple antennas at the transmitter and the receiver, we exploit transmit diversity by using STBC and receive diversity by MRC. At the receiving side, by using the same channel every receive antennas receives the direct components intended for it as well as the indirect components which are meant for other receive antennas. Thus by using the direct and the cross channel components, the channel transmission matrix is given by (4.1).

The signal to be transmitted are encoded by using STBC and the signals received at the receiver are combined using MRC as explained in sections 4.2.2 and 4.2.3 respectively.

4.3 Equivalent SNR Description for Two-hop DAF Relayed System

The Signal-Noise-Ratio (SNR) of the $(T-R)$ link is given by

$$\gamma_{(T-R)} = \frac{E_b}{N_0}\|H\|_F^2 \tag{4.58}$$

where $\|H\|_F^2 = \sum_{i=1}^{N_t}\sum_{j=1}^{N_r}\left\|h_{i,j}\right\|^2$, F is the Frobenious norm of H, and $\frac{E_b}{N_0}$ is the average SNR of the $(T-R)$ channel represented by γ_3. The TR node forwards the received signal to R with errors. R then combines the two signals by applying MRC followed by ML demodulation. The $(T-TR)$ link and the $(TR-R)$ link undergoes independent Nakagami-m fading, thus, the received SNR $\gamma_{(T-TR)}$and $\gamma_{(TR-R)}$ for each link, respectively, is gamma distributed with parameters α and β. Under this system, we consider the following unified model for the received SNR of the $(T-TR-R)$ link

$$\gamma_{(TR)} = \frac{\gamma_{(T-TR)}\cdot\gamma_{(TR-R)}}{a\gamma_{(T-TR)}+\gamma_{(TR-R)}+b} \tag{4.59}$$

The parameters a and b are real and non-negative and chosen such as to reflect the configuration of the TR node [197]. For a channel assisted transmission this configuration can be represented as $(a,b) \in (0,1)$. Thus (4.59) can be re-written as

$$\gamma_{(TR)} = \frac{\gamma_{(T-TR)}\cdot\gamma_{(TR-R)}}{\gamma_{(T-TR)}+\gamma_{(TR-R)}} \tag{4.60}$$

where $\gamma_{(T-TR)}$ and $\gamma_{(TR-R)}$ are the equivalent instantaneous SNRs of the $(T-TR)$ and $(TR-R)$ channels, respectively. Thus, the equivalent end-to-end SNR at R is given by

$$\gamma_{eq} = \gamma_{(T-R)} + \gamma_{(TR)} \tag{4.61}$$

$$\gamma_{eq} = \gamma_{(T-R)} + \frac{\gamma_{(T-TR)}\cdot\gamma_{(TR-R)}}{\gamma_{(T-TR)}+\gamma_{(TR-R)}} \tag{4.62}$$

4.3.1 Equivalent SNR Description for SISO System

For $N_t = 1$, and $N_r = 1$, (4.58) can be written as

$$\gamma_{(T-R)} = \gamma_3 \|h_3\|^2 \tag{4.63}$$

Considering a perfect channel assisted SISO system with no coding performed at the transmitter, the system works as an amplify-and-forward network [198]. Following (4.16) and (4.63),

$$\gamma_{(T-TR)} = \gamma_1 \|h_1\|^2 \tag{4.64}$$

$$\gamma_{(TR-R)} = \gamma_2 \|h_2\|^2 \tag{4.65}$$

where $\gamma_{(T-TR)}$ and $\gamma_{(TR-R)}$ are the equivalent instantaneous SNRs, and, γ_1 and $\gamma_2$are the average SNRS of the $(T-TR)$ and $(TR-R)$ channels, respectively. Thus, using (4.62), the equivalent end-to-end SNR at R for $N_t = N_r = 1$ is given by

$$\gamma_{eq} = \gamma_3 \|h_3\|^2 + \frac{\gamma_1 \|h_1\|^2 . \gamma_2 \|h_2\|^2}{\gamma_1 \|h_1\|^2 + \gamma_2 \|h_2\|^2} \tag{4.66}$$

4.3.2 Equivalent SNR Description for MISO System

Following (4.60), we derive the expressions for the equivalent SNR of the $(T-R)$ link.

4.3.2.1 $N_t = 2$ and $N_r = 1$

For direct transmission between the transmitter and the receiver, the received signal energy $(E_{r,1})$ and the received noise energy $(N_{0,1})$for the first symbol estimate can be evaluated as

$$E_{r,1} = E\{(|h_{31}^2| + |h_{32}^2|)^2 x_1 x_1^*\} = (|h_{31}^2| + |h_{32}^2|)^2 E_{x1} \tag{4.67}$$

and

$$\begin{aligned} N_{0,1} &= E\{(h_{31}^* n_{31} + h_{32} n_{32})(h_{31} n_{31}^* + h_{32}^* n_{32}^*)\} \\ &= |h_{31}^2| \, E\{n_{31} n_{31}^*\} + |h_2^2| E\{n_{32} n_{32}^*\} \\ &= N_0(|h_{31}^2| + |h_{32}^2|) \end{aligned} \tag{4.68}$$

respectively, where $E\{n_{31} n_{32}\} = 0$ and $N_0 = \sigma_{n1}^2 = \sigma_{n2}^2$.

Similarly, the received signal energy $(E_{r,2})$ and the received noise energy $(N_{0,2})$for the second symbol estimate can be evaluated as

$$E_{r,2} = E\{(|h_{31}^2| + |h_{32}^2|)^2 x_2 x_2^*\} = (|h_{31}^2| + |h_{32}^2|)^2 E_{x2} \quad (4.69)$$

and

$$\begin{aligned} N_{0,2} &= E\{(h_{32}^* n_{31} - h_{31} n_{32})(h_{32} n_{31}^* - h_{31}^* n_{32}^*)\} \\ &= |h_{32}^2|\, E\{n_{31} n_{31}^*\} + |h_{31}^2| E\{n_{32} n_{32}^*\} \\ &= N_0(|h_{31}^2| + |h_{32}^2|) \end{aligned} \quad (4.70)$$

respectively. Assuming $E_b = E_{x1} = E_{x2}$, the received symbol SNR can be written as

$$\gamma_{(T-R)} = \frac{E_{r,1}}{N_{0,1}} = \frac{E_{r,2}}{N_{0,2}} = \frac{E_b}{N_0}(|h_{31}^2| + |h_{32}^2|) = \gamma_3(|h_{31}^2| + |h_{32}^2|) \quad (4.71)$$

where $\frac{E_b}{N_0}$ is the average SNR per receive antenna of the $(T-R)$ channel represented by γ_3. The received SNR $\gamma_{(T-TR)}$ and $\gamma_{(TR-R)}$ for $(T-TR)$ link and the $(TR-R)$ link can be written as

$$\gamma_{(T-TR)} = \gamma_1(|h_{11}^2| + |h_{12}^2|) \quad (4.72)$$

$$\gamma_{(TR-R)} = \gamma_2 \|h_2\|^2 \quad (4.73)$$

where $\gamma_{(T-TR)}$ and $\gamma_{(TR-R)}$ are the equivalent instantaneous SNRs, and, γ_1 and γ_2 are the average SNRS of the $(T-TR)$ and $(TR-R)$ channels, respectively. Thus, the equivalent end-to-end SNR at R is given by

$$\gamma_{eq} = \gamma_{(T-R)} + \gamma_{(TR)} \quad (4.74)$$

$$\gamma_{eq} = \gamma_{(T-R)} + \frac{\gamma_{(T-TR)} \cdot \gamma_{(TR-R)}}{\gamma_{(T-TR)} + \gamma_{(TR-R)}} \quad (4.75)$$

$$\gamma_{eq} = \gamma_3(|h_{31}^2| + |h_{32}^2|) + \frac{\gamma_1(|h_{11}^2| + |h_{12}^2|) \cdot \gamma_2 \|h_2\|^2}{\gamma_1(|h_{11}^2| + |h_{12}^2|) + \gamma_2 \|h_2\|^2} \quad (4.76)$$

4.3.2.2 $N_t = 3$ and $N_r = 1$

From (4.71), the received symbol SNR of the $(T-R)$, $(T-TR)$ and $(TR-R)$ transmissions can be written as

$$\gamma_{(T-R)} = \gamma_3(|h_{31}^2| + |h_{32}^2| + |h_{33}^2|) \quad (4.77)$$

$$\gamma_{(T-TR)} = \gamma_1(|h_{11}^2| + |h_{12}^2| + |h_{13}^2|) \tag{4.178}$$

$$\gamma_{(TR-R)} = \gamma_2\|h_2\|^2 \tag{4.79}$$

and the equivalent end-to-end SNR at R can be written as

$$\gamma_{eq} = \gamma_3(|h_{31}^2| + |h_{32}^2| + |h_{33}^2|) + \frac{\gamma_1(|h_{11}^2|+|h_{12}^2|+|h_{13}^2|).\gamma_2\|h_2\|^2}{\gamma_1(|h_{11}^2|+|h_{12}^2|+|h_{13}^2|)+\gamma_2\|h_2\|^2} \tag{4.80}$$

4.3.3 Equivalent SNR Description for SIMO System

Following (4.58), we derive the expressions for the equivalent SNR of the $(T-R)$ link. In the presence of channel h_j, the instantaneous SNR at j^{th} receive antenna is given by

$$\gamma_j = \frac{|h_j|^2 E_b}{N_0} \tag{4.81}$$

With N_r receive antennas, the effective SNR is given by

$$\gamma_{b_j} = \sum_{j=1}^{N_r}|h_j|^2 \frac{E_b}{N_0} \tag{4.82}$$

$$\gamma_{b_j} = N_r\gamma_j \tag{4.83}$$

4.3.3.1 $N_t = 1$ and $N_r = 2$

For direct transmission between the transmitter and the receiver, the received symbol SNR of the $(T-R)$link can be written as

$$\gamma_{(T-R)} = \gamma_3(\|h_{31}\|^2 + \|h_{32}\|^2) \tag{4.84}$$

The received SNR $\gamma_{(T-TR)}$ and $\gamma_{(TR-R)}$ for $(T-TR)$ link and the $(TR-R)$ link can be written as

$$\gamma_{(T-TR)} = \gamma_1\|h_{11}\|^2 \tag{4.85}$$

$$\gamma_{(TR-R)} = \gamma_2(\|h_{21}\|^2 + \|h_{22}\|^2) \tag{4.86}$$

where $\gamma_{(T-TR)}$ *and* $\gamma_{(TR-R)}$ are the equivalent instantaneous SNRs, and, γ_1 *and* γ_2 are the average SNRS of the $(T-TR)$ and $(TR-R)$ channels, respectively. Thus, the equivalent end-to-end SNR at R is given by

$$\gamma_{eq} = \gamma_{(T-R)} + \gamma_{(TR)} \tag{4.87}$$

$$\gamma_{eq} = \gamma_{(T-R)} + \frac{\gamma_{(T-TR)} \cdot \gamma_{(TR-R)}}{\gamma_{(T-TR)} + \gamma_{(TR-R)}} \tag{4.88}$$

$$\gamma_{eq} = \gamma_3(\|h_{31}\|^2 + \|h_{32}\|^2) + \frac{\gamma_1 \|h_{11}\|^2 . \gamma_2(\|h_{21}\|^2 + \|h_{22}\|^2)}{\gamma_1 \|h_{11}\|^2 + \gamma_2(\|h_{21}\|^2 + \|h_{22}\|^2)} \tag{4.89}$$

4.3.3.2 $N_t = 1$ and $N_r = 3$

The received symbol SNR of the $(T - R)$link can be written as

$$\gamma_{(T-R)} = \gamma_3(\|h_{31}\|^2 + \|h_{32}\|^2 + \|h_{33}\|^2) \tag{4.90}$$

and, the received symbol SNR of the $(T - TR)$ and $(TR - R)$ links can be written as

$$\gamma_{(T-TR)} = \gamma_1 \|h_{11}\|^2 \tag{4.91}$$

$$\gamma_{(TR-R)} = \gamma_2(\|h_{21}\|^2 + \|h_{22}\|^2 + \|h_{23}\|^2) \tag{4.92}$$

Hence, the equivalent end-to-end SNR at R can be written as

$$\gamma_{eq} = \gamma_3(\|h_{31}\|^2 + \|h_{32}\|^2 + \|h_{33}\|^2) + \frac{\gamma_1 \|h_{11}\|^2 . \gamma_2(\|h_{21}\|^2 + \|h_{22}\|^2 + \|h_{23}\|^2)}{\gamma_1 \|h_{11}\|^2 + \gamma_2(\|h_{21}\|^2 + \|h_{22}\|^2 + \|h_{23}\|^2)} \tag{4.93}$$

and so on for higher number of receive antennas in the receiving array.

4.3.4 Equivalent SNR Description for MIMO System

The equivalent SNR for a MIMO system using TR node can be described depending on the number of transmit and receive antennas used in the arrays. Thus, with N_t transmit and N_r receive antennas, the SNR of the $(T - R)$ link is given by

$$\gamma_{(T-R)} = \gamma_3 \sum_{i=1}^{N_t} \sum_{j=1}^{N_r} \left\| h_{3i}^{j} \right\|^2 \tag{4.94}$$

The SNR of the $(T - TR)$ link is given by

$$\gamma_{(T-TR)} = \gamma_1 \sum_{i=1}^{N_t} \|h_{1i}\|^2 \tag{4.95}$$

The SNR of the $(TR - R)$ link is given by

$$\gamma_{(TR-R)} = \gamma_2 \sum_{j=1}^{N_r} \left\| h_{2j} \right\|^2 \tag{4.96}$$

and the equivalent SNR can be written as

$$\gamma_{eq} = \gamma_3 \sum_{i=1}^{N_t} \sum_{j=1}^{N_r} \left\| h_{3i}^{j} \right\|^2 + \frac{\gamma_1 \sum_{i=1}^{N_t} \|h_{1i}\|^2 . \gamma_2 \sum_{j=1}^{N_r} \|h_{2j}\|^2}{\gamma_1 \sum_{i=1}^{N_t} \|h_{1i}\|^2 + \gamma_2 \sum_{j=1}^{N_r} \|h_{2j}\|^2} \quad (4.97)$$

For example, for $N_t = 2$ and $N_r = 2$, $i = j = 2$, thus γ_{eq} can be written as

$$\gamma_{eq} = \gamma_3 (|h_{31}^1|^2 + |h_{31}^2|^2 + |h_{32}^1|^2 + |h_{32}^2|^2) + \frac{\gamma_1 (\|h_{11}\|^2 + \|h_{12}\|^2) . \gamma_2 (\|h_{21}\|^2 + \|h_{22}\|^2)}{\gamma_1 (\|h_{11}\|^2 + \|h_{12}\|^2) + \gamma_2 (\|h_{21}\|^2 + \|h_{22}\|^2)} \quad (4.98)$$

4.4 Error Probabilities for Two-hop DAF Relayed System

In this section, we present the exact expressions for SEP for M-PSK modulation on the principle of amplify-and-forward relaying using the moment generating function (MGF) approach. We present the system model proposed in Fig. 4.2 in a simpler form as shown in Fig. 4.7. We divide the paths shown in Fig. 4.3 in two separate systems as shown in Fig. 4.7 (a) and (b), respectively.

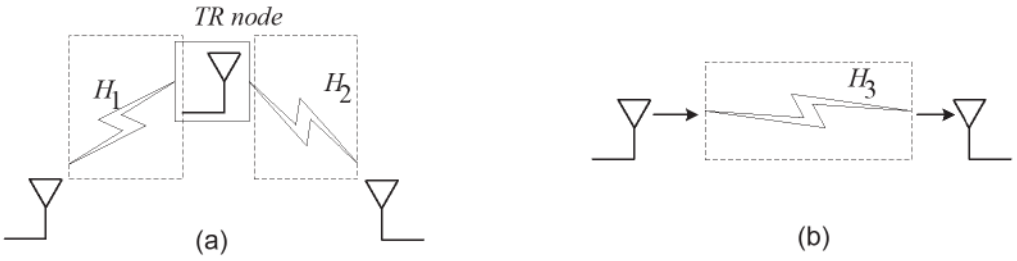

Fig. 4.7 (a) Individual $(T - TR - R)$ *link* *(b) Direct* $(T - R)$ *link*

We first present the PDFs for the SNRs of the two paths shown in Fig. 4.7 (a) and (b) and then present the complete end-to-end PDF of the two-hop DAF relay system following which we finally present the exact SEP of the overall system model. From Fig. 4.7 (b), the PDF $p_{\gamma_{(T-R)}}(\gamma)$ of $\gamma_{(T-R)}$ is given by

$$p_{\gamma_{(T-R)}}(\gamma) = \frac{1}{\Gamma(m)}\left(\frac{m}{\overline{\gamma}_{(T-R)}}\right)^m \gamma^{m-1} e^{-m\gamma_{(T-R)}/\overline{\gamma}_{(T-R)}} \tag{4.99}$$

and the MGF $(\Lambda_{(\gamma_{(T-R)})}))$ is given by

$$\Lambda_{(\gamma_{(T-R)})}\left(\frac{-g}{\sin^2(\theta)}\right) = \int_0^\infty p_{\gamma_{(T-R)}}(\gamma) e^{s\gamma_{(T-R)}} d\gamma \tag{4.100}$$

for a non-negative random variable $\gamma, \gamma \geq 0$ [199]. From Fig. 4.7 (a), we calculate the PDF for the $(T - TR - R)$ link. When the independently Nakagami-*m* faded $(T - TR)$ and $(TR - R)$ channels experience different fading, the PDF $p_{\gamma_{(TR)}}(\gamma)$ can be expressed as [200], (29)]

$$p_{\gamma_{(TR)}}(\gamma) = \int_0^\gamma \frac{r^2}{(r-\gamma)^2} \cdot p_{\gamma_{(T-TR)}}\left(\frac{r\gamma}{(r-\gamma)}\right) \cdot p_{\gamma_{(TR-R)}}(r) dr \tag{4.101}$$

By analyzing (4.101), we can see that it involves the pdf terms of $\gamma_{(T-TR)}$ and $\gamma_{(TR-R)}$, thus, following (4.99) the pdfs $p_{\gamma_{(T-TR)}}\left(\frac{r\gamma}{(r-\gamma)}\right)$ and $p_{\gamma_{(TR-R)}}(r)$ can be written as

$$p_{\gamma_{(T-TR)}}\left(\frac{r\gamma}{r-\gamma}\right) = \frac{1}{\Gamma(m_1)}\left(\frac{m_1}{\overline{\gamma}_{(T-TR)}}\right)^{m_1}\left(\frac{r\gamma}{r-\gamma}\right)^{m_1-1} exp\left(\frac{-m_1}{\overline{\gamma}_{(T-TR)}}.\left(\frac{r\gamma}{r-\gamma}\right)\right), \text{ and} \quad (4.102)$$

$$p_{\gamma_{(TR-R)}}(r) = \frac{1}{\Gamma(m_2)}\left(\frac{m_2}{\overline{\gamma}_{(TR-R)}}\right)^{m_2}(r)^{m_2-1} exp\left(\frac{-m_1}{\overline{\gamma}_{(TR-R)}}.r\right), \quad (4.103)$$

respectively. Substituting (4.102) and (4.103) in (4.101) and solving, $p_{\gamma_{(TR)}}(\gamma)$ can be expressed as

$$p_{\gamma_{(TR)}}(\gamma) = \frac{\gamma^{m_1-1}}{\Gamma(m_1)\Gamma(m_2)}\left(\frac{m_1}{\overline{\gamma}_{(T-TR)}}\right)^{m_1}\left(\frac{m_2}{\overline{\gamma}_{(TR-R)}}\right)^{m_2} \times exp\left[-\left(\frac{m_1}{\overline{\gamma}_{(T-TR)}}+\frac{m_2}{\overline{\gamma}_{(TR-R)}}\right)\gamma\right]\int_0^\infty r^{m_2-1} \times$$
$$\left(1+\frac{\gamma}{r}\right)^{m_1+m_2} exp\left[-\left(\frac{m_1\gamma^2}{\overline{\gamma}_{(T-TR)}r}+\frac{m_2 r}{\overline{\gamma}_{(TR-R)}}\right)\right]dr \quad (4.104)$$

Following (4.100) and substituting (4.104), the MGF of $\gamma_{(TR)}$ can be calculated as

$$\Lambda_{(\gamma_{(TR)})}\left(\frac{-g}{\sin^2(\theta)}\right) = \int_0^\infty p_{\gamma_{(TR)}}(\gamma) exp\left(\frac{-g\gamma_{(TR)}}{\sin^2(\theta)}\right)d\gamma_{(TR)} \quad (4.105)$$

If $(\Lambda_{(\gamma_{(TR)})})$ and $(\Lambda_{(\gamma_{(T-R)})})$ is the MGF of $\gamma_{(TR)}$ and $\gamma_{(T-R)}$, respectively, then the combined (MGF,$(\Lambda_{\gamma_{eq}})$) of γ_{eq} can be calculated as

$$\Lambda_{\gamma_{eq}}(x) = \Lambda_{(\gamma_{(TR)})}(x)\Lambda_{(\gamma_{(T-R)})}(x) \quad (4.106)$$

where γ_{eq} is the end-to-end SNR. By substituting (4.100) and (4.105) in (4.106), MGF,$(\Lambda_{\gamma_{eq}})$) of γ_{eq} can be calculated. The average error probability in fading for modulations is given by [90]

$$\bar{P}_s = \frac{\alpha}{\pi}\int_0^\infty P_s(\gamma)p_{\gamma_s}(\gamma)d\gamma \quad (4.107)$$

Here, we need to calculate the end-to-end SEP, thus

$$\bar{P}_s = \frac{\alpha}{\pi}\int_0^\infty P_s(\gamma)p_{\gamma_{eq}}(\gamma)d\gamma$$

$$\bar{P}_s = \frac{\alpha}{\pi}\int_0^\infty \int_0^{\pi/2} exp\left[\frac{-g\gamma}{\sin^2\theta}\right]d\theta p_{\gamma_{eq}}(\gamma)d\gamma$$

$$= \frac{\alpha}{\pi}\int_0^{\pi/2}\left[\int_0^{\infty} exp\left[\frac{-g\gamma}{\sin^2\theta}\right] p_{\gamma_{eq}}(\gamma)d\gamma\right]d\theta$$

$$\bar{P}_s = \frac{\alpha}{\pi}\int_0^{\pi/2}\Lambda_{\gamma_{eq}}\left(\frac{-g}{\sin^2\theta}\right)d\theta \tag{4.108}$$

where $\Lambda_{\gamma_{eq}}(\mathrm{s})$ is the MGF associated with pdf $p_{\gamma_{eq}}(\gamma)$ and $g = \sin^2(\pi/M)$. By substituting (4.106) in (4.108), the SEP can be calculated as

$$\bar{P}_s = \frac{1}{\pi}\int_0^{(M-1)\pi/M}\frac{2}{\Gamma(m_1)\Gamma(m_2)}\left(\frac{m_1}{\bar{\gamma}_{(T-TR)}}\right)^{m_1}\left(\frac{m_2}{\bar{\gamma}_{(TR-R)}}\right)^{m_2}\times\sum_{k=0}^{\mu}\binom{\mu}{k}\times\left(\frac{m_1\bar{\gamma}_{(TR-R)}}{m_2\bar{\gamma}_{(T-TR)}}\right)^{\frac{(m_2-k)}{2}}$$

$$\times\frac{\sqrt{\pi}(2\beta)^{\nu}}{\left(\mu+\frac{1}{2}\right)^{\mu+\nu}}\frac{\Gamma(\mu+\nu)\Gamma(\mu-\nu)}{\Gamma\left(\mu+\frac{1}{2}\right)}\,{}_2F_1\left(\mu+\nu;\nu+\frac{1}{2};\mu+\frac{1}{2};\frac{\alpha-\beta}{\alpha+\beta}\right)\times\left(\left(\frac{m\sin^2(\theta)}{g\bar{\gamma}_{(T-R)}+m\sin^2(\theta)}\right)^{m}\right)d\theta \tag{4.109}$$

Thus, the SEP of the two-hop DAF under consideration here for $N_t = N_r = 1$ is given by (4.109). For BPSK modulation $(i.e.M = 2)$,$g_{psk} = \sin^2(\pi/M) = 1$ [201], $\alpha = \left(\frac{m_1}{\bar{\gamma}_{(T-TR)}} + \frac{m_2}{\bar{\gamma}_{(TR-R)}} + \frac{1}{\sin^2(\theta)}\right)$, thus, the average probability of error can be achieved as

$$\bar{P}_s = \frac{1}{\pi}\int_0^{\pi/2}\frac{2}{\Gamma(m_1)\Gamma(m_2)}\left(\frac{m_1}{\bar{\gamma}_{(T-TR)}}\right)^{m_1}\left(\frac{m_2}{\bar{\gamma}_{(TR-R)}}\right)^{m_2}\times\sum_{k=0}^{\mu}\binom{\mu}{k}\times\left(\frac{m_1\bar{\gamma}_{(TR-R)}}{m_2\bar{\gamma}_{(T-TR)}}\right)^{\frac{(m_2-k)}{2}}$$

$$\times\frac{\sqrt{\pi}(2\beta)^{\nu}}{\left(\mu+\frac{1}{2}\right)^{\mu+\nu}}\frac{\Gamma(\mu+\nu)\Gamma(\mu-\nu)}{\Gamma\left(\mu+\frac{1}{2}\right)}\,{}_2F_1\left(\mu+\nu;\nu+\frac{1}{2};\mu+\frac{1}{2};\frac{\alpha-\beta}{\alpha+\beta}\right)\times\left(\frac{m\sin^2(\theta)}{\bar{\gamma}_{(T-R)}+m\sin^2(\theta)}\right)^{m}d\theta \tag{4.110}$$

The integration in (4.110) can be solved for different values of *m*.

For QPSK modulation $(i.e.M = 4)$, $g_{psk} = \sin^2(\pi/M) = \sin^2(\pi/4) = 1/2$, $\alpha = \left(\frac{m_1}{\bar{\gamma}_{(T-TR)}} + \frac{m_2}{\bar{\gamma}_{(TR-R)}} + \frac{1}{2\sin^2(\theta)}\right)$, thus, the average probability of error can be achieved as

$$\bar{P}_s = \frac{1}{\pi}\int_0^{3\pi/4}\frac{2}{\Gamma(m_1)\Gamma(m_2)}\left(\frac{m_1}{\bar{\gamma}_{(T-TR)}}\right)^{m_1}\left(\frac{m_2}{\bar{\gamma}_{(TR-R)}}\right)^{m_2}\times\sum_{k=0}^{\mu}\binom{\mu}{k}\times\left(\frac{m_1\bar{\gamma}_{(TR-R)}}{m_2\bar{\gamma}_{(T-TR)}}\right)^{\frac{(m_2-k)}{2}}$$

$$\times\frac{\sqrt{\pi}(2\beta)^{\nu}}{\left(\mu+\frac{1}{2}\right)^{\mu+\nu}}\frac{\Gamma(\mu+\nu)\Gamma(\mu-\nu)}{\Gamma\left(\mu+\frac{1}{2}\right)}\,{}_2F_1\left(\mu+\nu;\nu+\frac{1}{2};\mu+\frac{1}{2};\frac{\alpha-\beta}{\alpha+\beta}\right)\times\left(\frac{m\sin^2(\theta)}{\frac{1}{2}\bar{\gamma}_{(T-R)}+m\sin^2(\theta)}\right)^{m}d\theta \tag{4.111}$$

The detailed derivation for the Symbol error probability for the system defined here is given in Appendix C. The SEPs for the various system models with different number of N_t and N_r for the two-hop DAF relay system are also presented in Appendix C for convenience.

4.5 Performance Evaluation

In this section we present the simulation results for the models discussed in the previous sections.

4.5.1 Experimental Setup

We summarize the parametric values used for simulation in Table 4.1. Monte Carlo method has been used for simulating. We have limited our results to $M = 2, and\ 4$ and the extension to higher modulation orders of $M > 4$ is straight forward.

Table 4.1 Set of Simulation Parameters used

Parameters	**Types/Values**
Channel Type	Quasi-Static
Channel Statistics	Nakagami-*m*
Fading Parameter range	$0.65 \leq m \leq 10$
Number of frames	10^4
Frame Length	100
Modulation Type	MPSK *(for M = 2 and 4)*
Mathematical Software used	MATLAB

Before presenting the BERs for the two-hop DAF relay system developed, we have provide the some simulations results in Appendix D for some of the baseline wireless system models used for communication. It is known to the researchers that Nakagami-*m* distribution is widely used for modelling the fading channels due to its capabilities in exploiting a wide range of fading conditions based on its fading parameter. So our purpose of presenting these results here was to recall the effects of fading parameter *'m'* on the performance of the

wireless communication system. These results also helped us in validating our basic MATLAB code developed for various models in different fading conditions. We will be comparing the BERs for the system model developed here to the BERs for the baseline approaches shown in Appendix D.

The simulation results presented in Fig. D.1 – Fig. D.4 shows the effect of fading parameter *m* and it can be concluded that irrespective of the type of wireless communication system under consideration and the modulation scheme used, a low fading parameter results in poorer performance. In the next few figures, the bit error rates of each of the proposed wireless communication system are presented and their performances are analysed based on the fading parameter.

4.5.2 Results for Two-hop DAF Relay System for SISO System Models

Starting with a SISO system, Fig. 4.8 shows the BER of the proposed SISO system and compares it with the baseline approach. Fig. 4.8 (i) and (ii) shows the BER when the simulations were carried out for BPSK and QPSK modulated sequences, respectively. It was shown in [21] that the SER degrades with the increase in the number of relays at low values of SNR. Thus, we have assumed that the TR node consists of a single relay capable of receiving and forwarding the information. Following the SISO transmission model described in Fig. 4.3, we see that with the added diversity at the receiver side from the TR node, the performance of the system improves by approximately 1dB as compared to the conventional SISO transmission model as can be seen from Fig. 4.8 for both BPSK and QPSK modulation. The fading parameter was kept at one for all the available channel paths of both the SISO models to obtain the results mentioned in Fig. 4.8.

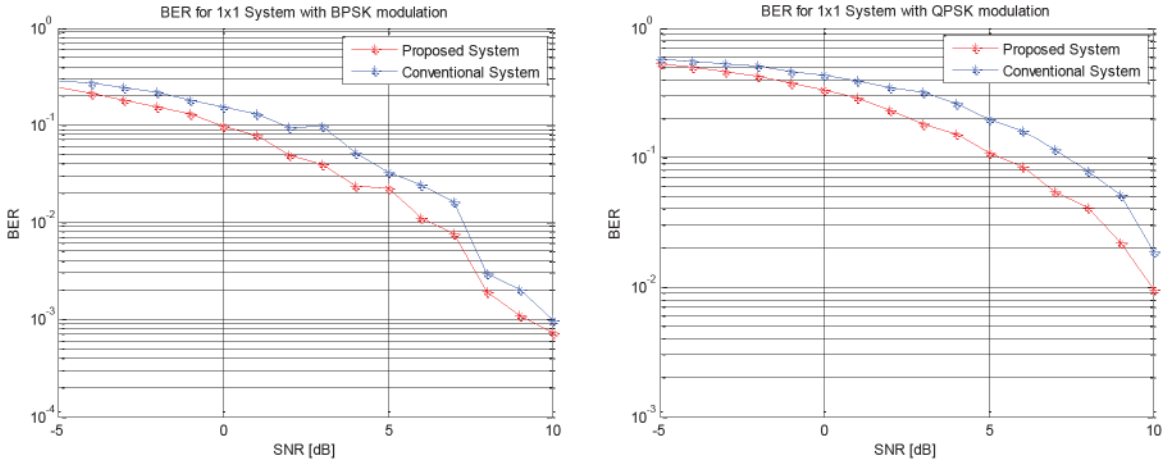

(i) *(ii)*

Fig.4.8 BER of the proposed SISO System with m=1 for BPSK and QPSK modulated Nakagami-m faded channel model and its comparison with the baseline model

Fig. 4.9 shows the performance of the proposed SISO system with different values of fading parameter.

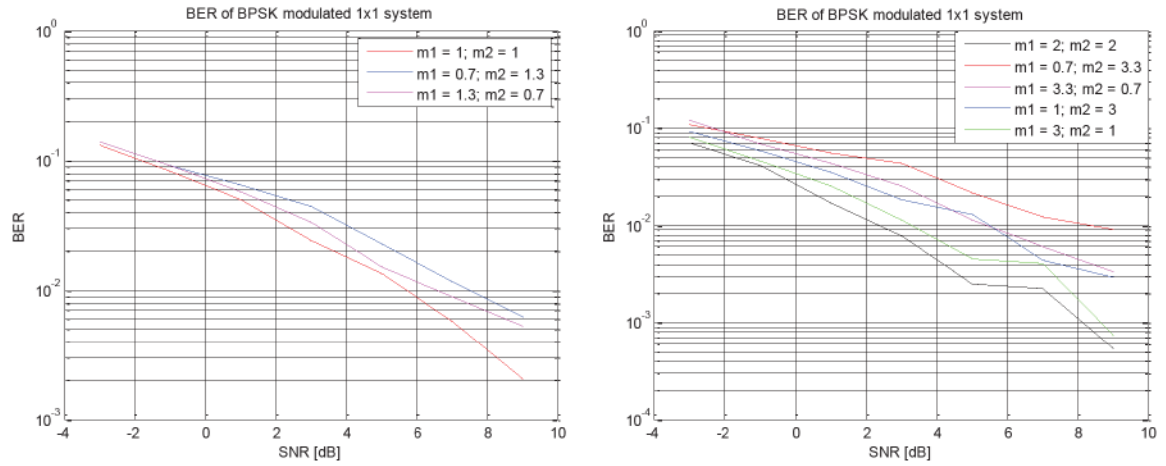

(i) *(ii)*

Fig.4.9 Performance Analysis of the proposed SISO System with different fading parameters

According to the path loss models, the performance of the system is improved as the distance between the transmitter and the receiver is decreased. In [199], the impact of variations in Nakagami-*m* fading parameter with distance has been investigated over Frequency Selective Nakagami fading channel and it was observed that the operations at

shorter distances gave better error rate performance. Also, the simulation results in Fig. D.1 – D.4 show an improved performance at higher values of fading parameter. Hence, we assume that a higher fading parametric value means a shorter distance between the transmitter and the receiver. Based on this assumption, the performance of the system is analysed with varying fading parameter. The fading parameters for different channel links are referred as follows:

Fading parameter for the direct $(T - R)$ link is m_0

Fading parameter for $(T - TR)$ link is m_1, and

Fading parameter for $(TR - R)$ link is m_2.

Also, m_1 and m_2 can take any value from $0.65 \leq m \leq 10$, but $m_1 + m_2$ is always an integer and also $(m_1 + m_2) > 1$, as m_1 and m_2 are always greater than 0.65. Fig 4.9 (i) shows the performance of the system when $m_0 = 1$, and $(m_1 + m_2) = 2$. With different values of fading parameter, it can be seen that the proposed SISO system gives the best performance when the fading conditions of both $(T - TR)$ and $(TR - R)$ link is Rayleigh i.e. $m_1 = m_2 = 1$. For the cases when the amount of fading on the two channel links is not same, the system gives better performance when $m_1 > m_2$. This can be explained based on the assumption that higher fading parameter means less distance between the two links, thus, with $m_1 = 1.3, and\ m_2 = 0.7$, means that the distance between $(T - TR)$ link is shorter than the $(TR - R)$ link. According to Fig. 4.3, the signals received directly from the transmitter and that from the TR node are combined at the receiver, thus when the TR node is placed at a farther distance from the transmitter, the fading effects of the $(T - TR)$ are stronger than the case when the TR node is placed closer to the transmitter. At the receiver, even if the TR node is placed farther from the receiver, the fading effects are reduced as the incoming signals from both the paths are combined. As can be seen from Fig. 4.9 (i), $m_1 = 0.7$ means higher fading effects and lower performance, and even though $m_2 = 0.7$, the system still shows a better performance as the fading effects are compensated by the signal combining at

the receiver. Fig. 4.9 (ii) shows the BER when the fading conditions of both $(T-TR)$ and $(TR-R)$ link is less severe than Rayleigh i.e. $m_1 = m_2 = 2$, and comparing it with the BER when $m_1 \neq m_2$. In all the case $m_1 + m_2 = 4$. The simulation results show that the system gives the best performance when $m_1 = m_2$. When comparing the BER when $m_1 \neq m_2$, it can be seen that a better performance is achieved when the fading conditions on the $(T-TR)$ link are less severe. For example, when $m_1 = 0.7$, the performance of the system degrades as compared to when $m_1 = 1$. It can also be noted that the performance of the system somehow depends on the fading conditions of the $(TR-R)$ link. With $m_2 = 0.7$, the performance degrades as compared to when $m_2 = 1, 2, 3$.

4.5.3 Results for Two-hop DAF Relay System for SIMO System Models

Fig. 4.10 shows the BER of the proposed SIMO systems and compares its performance with the baseline approach for BPSK and QPSK modulated sequences. With $m_0 = m_1 = m_2 = 1$, the simulations were done for $1, 2, 3, and\ 4$ receive antennas.

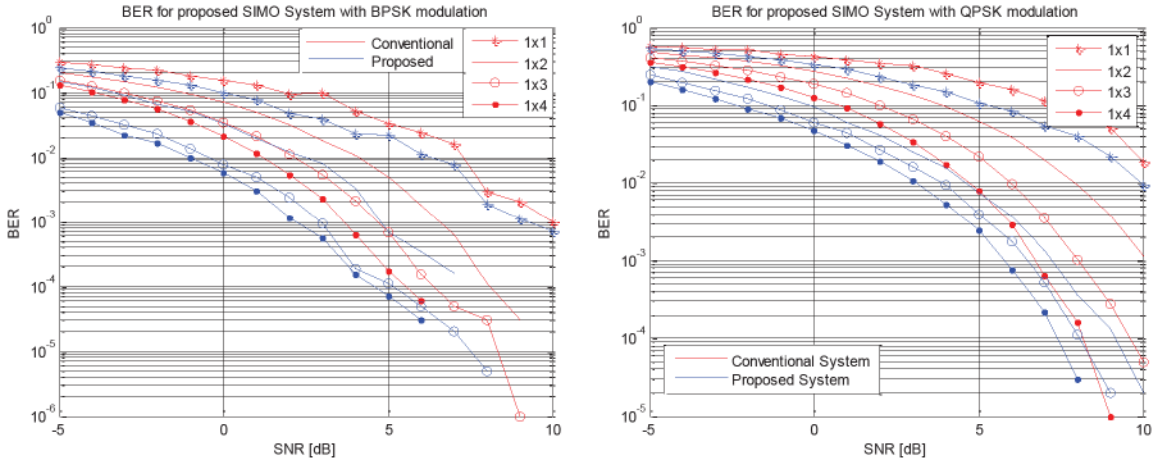

(i) *(ii)*

Fig.4.10 BER of the proposed SIMO System with m=1 for BPSK and QPSK modulated Nakagami-m faded channel model and its comparison with the baseline model

As can be seen from the figure, at lower SNRs the proposed system shows a performance improvement of approximately 2dB but at higher SNR values, the performance

slightly degrades but still shows an improvement of approximately 1dB when compared with the baseline SIMO system models, for both BPSK and QPSK modulation.

In Fig. 4.11 we analyze the performance of the proposed SIMO system in different fading environments with two and three receive antennas. We perform the simulations under different fading conditions.

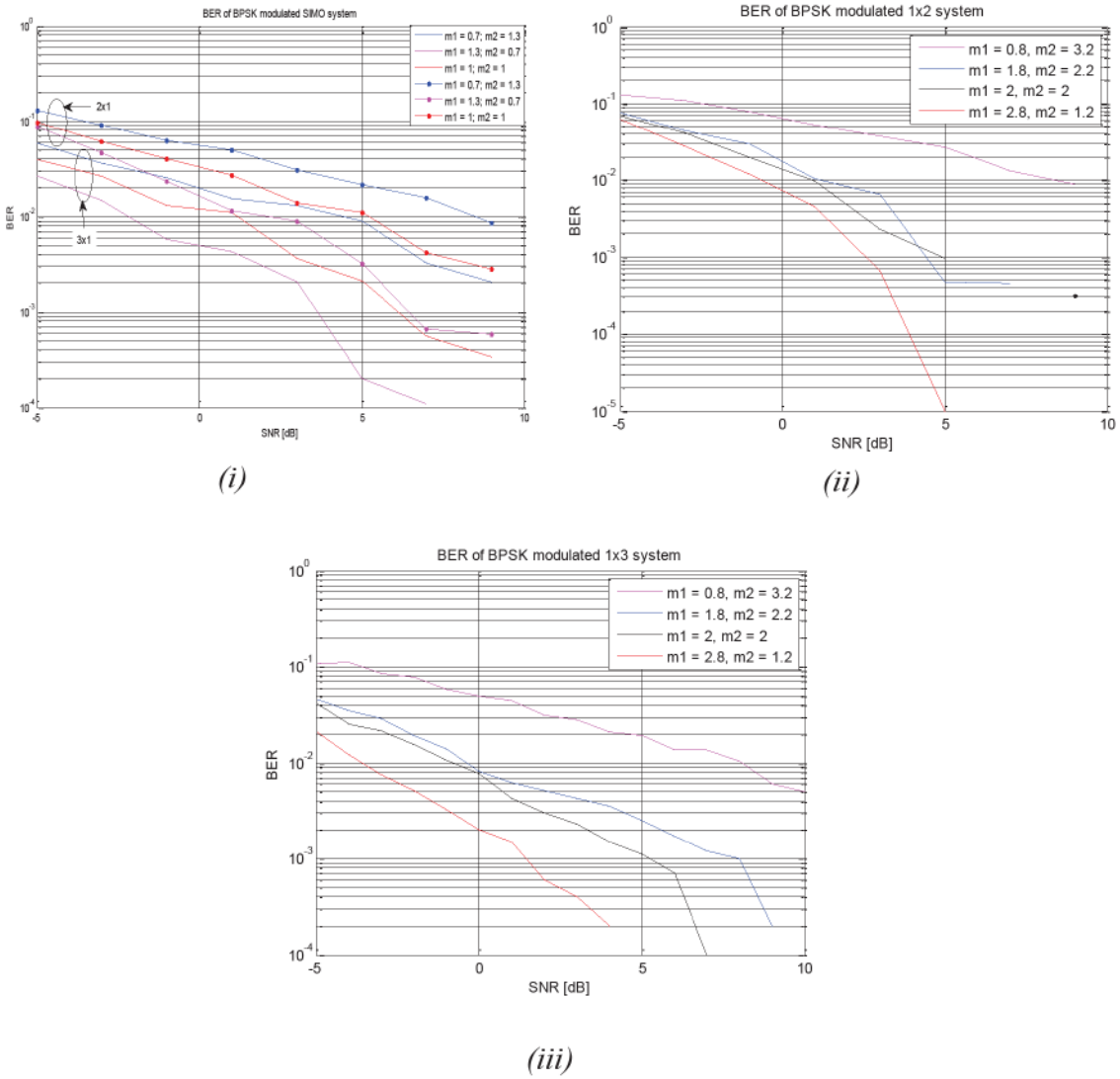

Fig.4.11 Effect of fading parameter on the performance of the proposed SIMO System

By varying m_1 and m_2 such that $m_1 + m_2 = 2$ in Fig.4.11 (i), it can be seen that the performance of the system is improved when $m_1 > m_2$. As mentioned earlier, one of the many reasons for better performance is shorter distance between the transmitter and the

receiver, thus when the TR node is placed closer to the transmitter (higher m_1), the fading conditions on the $(T-TR)$ link improves. At the receiver, though the distance between $(TR-R)$ gets larger (lower m_2), MRC combining compensates for the poor fading conditions of the $(TR-R)$ link. Fig. 4.11 (ii) and (iii), shows the BER for 2 and 3 receive antennas and shows similar pattern of results with m_1 and m_2 taking different values such that $m_1 + m_2 = 4$. It can be seen that the performance of the system is better when $m_1 > m_2$.

4.5.4 Results for Two-hop DAF Relay System for MISO System Models

Fig. 4.12 shows the BER for the proposed MISO system as shown in Fig. 4.4. The simulations were done for $1, 2, 3$ transmit antennas.

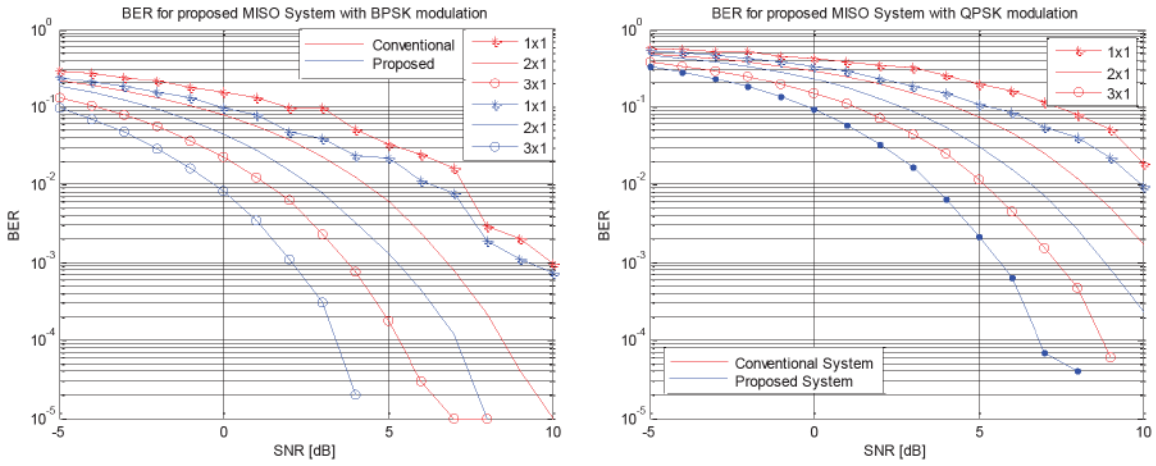

(i) *(ii)*

Fig.4.12 BER of the proposed MISO System with m=1 for BPSK and QPSK modulated Nakagami-m faded channel model and its comparison with the baseline model

The BERs were calculated for both BPSK and QPSK modulated data sequences as shown in Fig. 4.12 (i) and (ii), respectively. It can be seen that with added diversity, the performance of the system is increased by approximately 1.5dB as compared to the conventional MISO wireless system [182] for both BPSK and QPSK modulated systems.

Fig. 4.13 compares the BER of 2×1 system for different fading conditions. Fig. 4.13 (i) plots the BER for varying m_1 and m_2 with $m_1 + m_2 = 2$. It shows that in this case, the BER improves when $m_1 < m_2$ which is in contrast with the SIMO model where the performance improves when $m_1 > m_2$. It can be explained as follows: with multiple transmit antennas transmitting towards the TR node; the signals are MRC combined so even if the TR node is placed at a larger distance from the transmitter than from the receiver, the higher fading effects are tolerated due to the MRC taking place at the TR node. At the receiver, if the distance between $(TR - R)$ is larger than $(T - TR)$, the fading effects of the $(TR - R)$ are not efficiently compensated by the receiver. Thus, the proposed system shows degraded performance when $m_1 > m_2$ and the performance improves when $m_1 < m_2$. However, the best performance is achieved when $m_1 = m_2$.

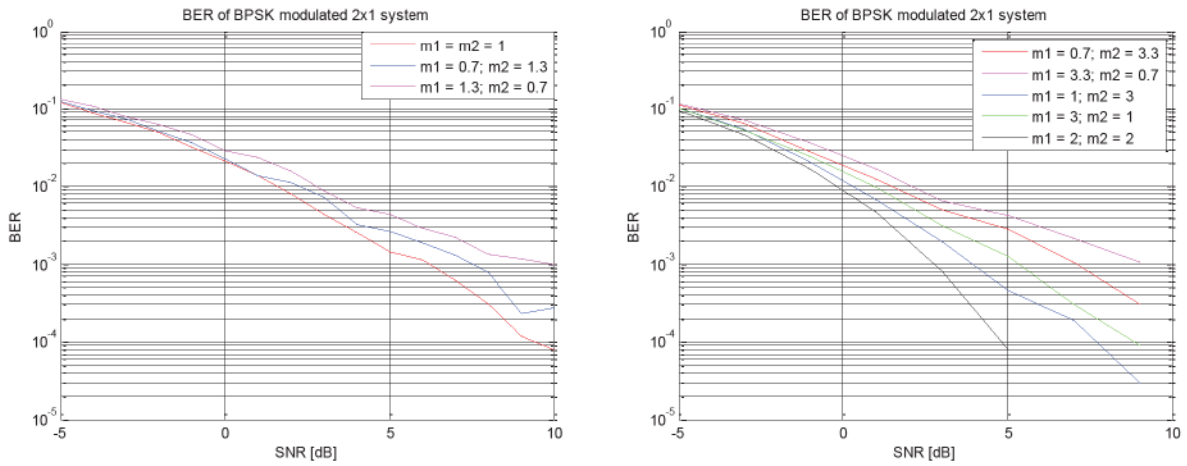

(i) *(ii)*

Fig.4.13 Effect of fading parameter on the performance of the proposed 2x1 System

Fig. 4.13 (ii) shows the BER for BPSK modulated system for varying m_1 and m_2 with $m_1 + m_2 = 4$. From the simulation plots we analyzed that the best performance is achieved when both $(T - TR)$ and $(TR - R)$ links experience similar fading conditions. For the case when $m_1 \neq m_2$, a better performance is achieved when $m_1 < m_2$. One interesting thing to note is that if either of m_1 *or* m_2 values is below one, i.e. if the fading conditions on

any of the channel link fall below Rayleigh fading, the performance degrades as compared to when either of m_1 *or* m_2 values is one or more than one, i.e. when the fading conditions on any of the channel link is Rayleigh or less severe than Rayleigh fading.

Fig. 4.14 shows the BER variations for a BPSK modulated 3×1 and 4×1 system for different fading conditions and it was analyzed that the BER improves when $m_1 < m_2$.

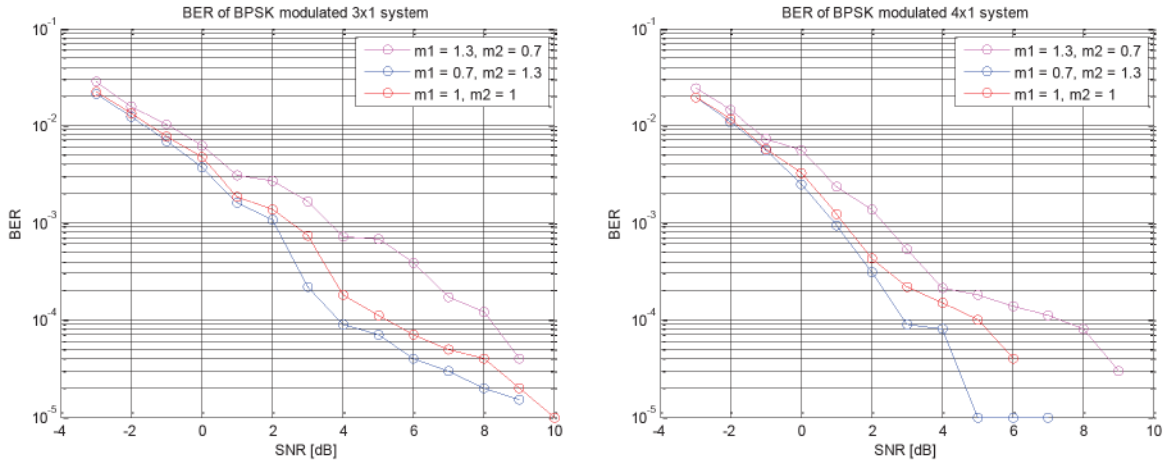

(i) *(ii)*

Fig.4.14 Effect of fading parameter on the performance of the proposed 3x1 System

No deviations from the results were seen even when $m_1 = m_2$, as in 3×1 and 4×1 system. This can be because of larger number for transmit antennas as compared to a single receive antenna. The MRC combining with larger number of transmit antennas compensated for the higher fading effects when $m_1 < m_2$ thus giving better performance compared to $m_1 = m_2$ as in 2×1 which gives the best performance when $m_1 = m_2$.

4.5.5 Results for Two-hop DAF Relay System for MIMO System Models

Fig. 4.15 shows the BERs for the proposed MIMO system and compares its performance with the conventional MIMO system model for both BPSK and QPSK modulation. The simulations were done for $2 \times 2, 2 \times 3, 3 \times 2, and\ 3 \times 3$ transmission

systems and it was seen that the added diversity improved the performance of the proposed system by approximately 1dB.

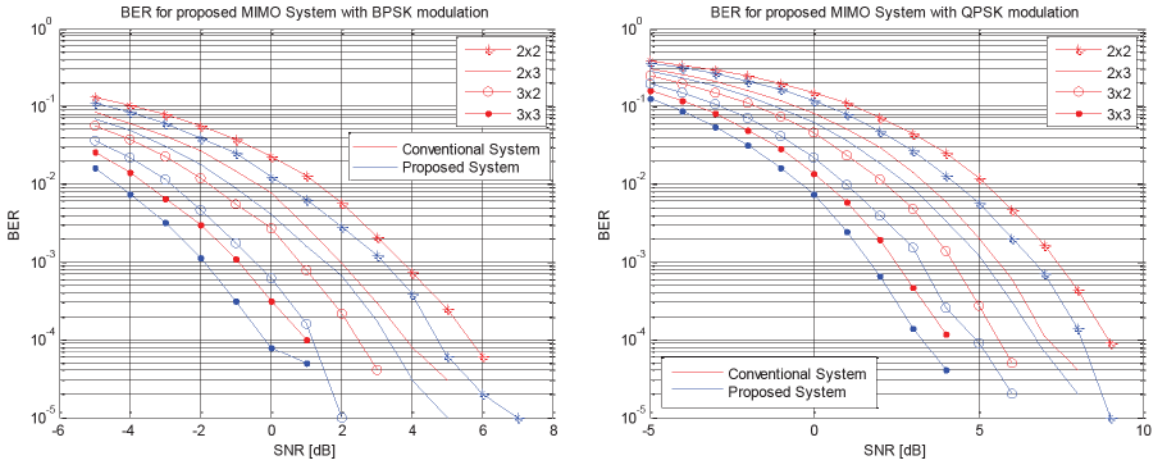

(i) *(ii)*

Fig.4.15 BER of the proposed MISO System with m=1 for BPSK and QPSK modulated Nakagami-m faded channel model and its comparison with the baseline model

Fig. 4.16 (i) and (ii) plots the variations in terms of BER with varying fading conditions on the $(T-TR)$ and $(TR-R)$ links for a 2×2 and 3×3 system model, i.e. $N_t = N_r$ respectively. It was analyzed that when $N_t = N_r$ and also N_t *and* N_r is not very high, for e.g. 2×2 system model, the BER improves as m_1 is increased, i.e. with $m_1 > m_2$, the performance is better and it improves with increasing value of m_1. In other words, the system performs better when the TR node is placed closer to the transmitter.

For higher N_t and N_r, for e.g. 3×3 system model, best performance is achieved when $m_1 = m_2$ and when $m_1 \neq m_2$, better performance is still achieved when $m_1 > m_2$. Thus a 3×3 model combined the effects of a MISO system model with higher number of transmit antennas and that of a MIMO system model with multiple transmit and receive antennas. Fig. 4.16 (iii) plots the BER when $N_t \neq N_r$ and we analyzed that the best performance is achieved when $m_1 = m_2$ and in case $m_1 \neq m_2$, $m_1 < m_2$ gives better

performance,. For e.g. with N_t greater than N_r by one, 3×2 and 2×1 system model gives similar performance variations.

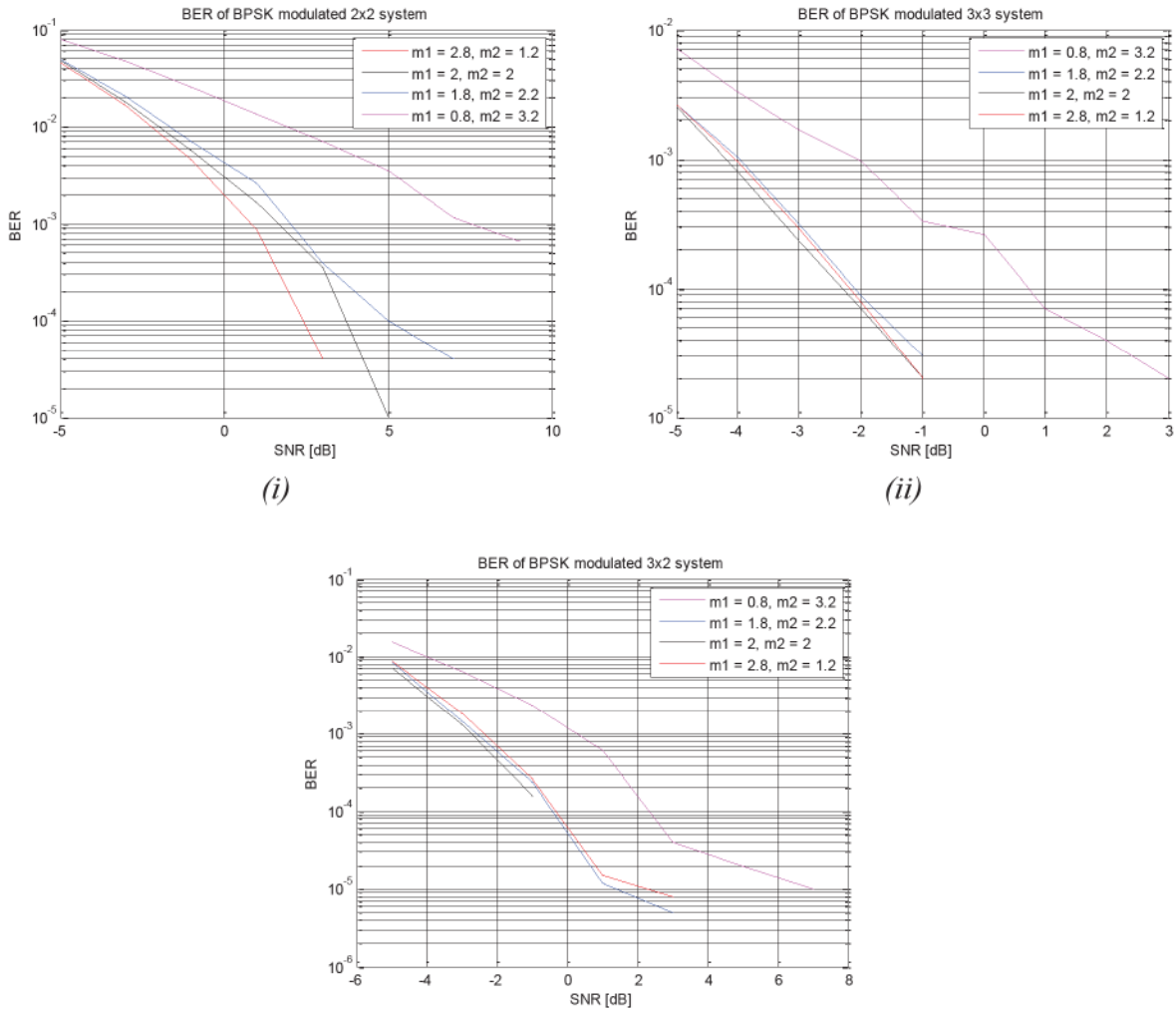

Fig.4.16 Effect of fading parameter on the performance of the proposed MIMO System

4.6 Summary and Conclusion

In this chapter we have presented the BER analysis of SISO, MISO, SIMO, and MIMO wireless system models. We have studied the importance of exploiting diversity and concluded that by increasing the number of diverse paths the performance of the overall system can be improved. For doing so we have used an additional TR node placed in between the transmitter and the receiver and the system behaves as a two-hop decode-amplify-forward (DAF) relay system. The channel paths between $(T-TR), (TR-R)$ and $(T-R)$ are independent of each other but they do not vary significantly in terms of their amplitudes and phases. The DAF relay system under study is dynamic as if the TR node fails to work due to any reason or if the system designing is cost effective, the TR node can be bypassed and the proposed system model can be used like an conventional wireless system model. Also by placing the TR node at varying distances from the transmitter and the receiver, the followings conclusions were derived for various system models:

- For SISO systems, the proposed model gave the best performance when both $(T-TR)$ and $(TR-R)$ links experienced similar fading conditions, i.e. when $m_1 = m_2$. However due to topological limitations when $m_1 = m_2$ may not be possible, the a better performance is achieved when $m_1 > m_2$, i.e. when the TR node is placed closer to the transmitter.
- For SIMO system models, the proposed SIMO system model performed better than the conventional SIMO model by approximately 2dB. Also the proposed SIMO model gives the best performance as long as $m_1 > m_2$ and the performance sequence is not affected even when $m_1 = m_2$. We have tested this by using 2 and 3 receive antennas and both models give similar results.

- For MISO system models, the proposed system model gave a better performance than the conventional MISO systems by approximately 1.5dB. With varying fading conditions on the $(T - TR)$ and $(TR - R)$ links, the system gives the best performance when $m_1 = m_2$ as long as the number of transmit antennas is low, for e.g. $N_t = 2$ Fig.4.18. When the number of transmit antennas become larger, for e.g. $N_t > 2$, the performance improves with decreasing value of $'m1'$, Fig. 4.19.
- For MIMO system models, the proposed MIMO model with TR node showed the performance improvement of approximately 1dB. When $N_t = N_r$, a better performance is achieved when $m_1 > m_2$ as long as $N_t \; and \; N_r$ is low. As m_1 is decreased over m_2, the performance starts to fall, for e.g. 2×2. When $N_t \; and \; N_r$ is large but still equal, for e.g. 3×3 system, the variations in performance changes and the best performance is achieved when $m_1 = m_2$ and following the trend of 2×2 model when $m_1 \neq m_2$ giving better results when $m_1 > m_2$. When $N_t > N_r$, the best performance is achieved when $m_1 = m_2$ and the performance starts to decrease with increasing m_1, for e.g. $2 \times 1, 3 \times 2$ system models give similar results as $N_t > N_r$.

Thus, we conclude from the simulations performed that the proposed model definitely performs better than the conventional system models. However, the proposed system shows sensitivity towards the number of transmit and receive antennas used and also the fading conditions of (or the distance between) the $(T - TR)$ and $(TR - R)$ channels links. Careful selection of the number of transmit and receive antennas depending on the fading conditions will definitely result in improved performance. Also, the performance of the system is affected by the distance of the TR node from the transmitter and the receiver.

Chapter 5 – Antenna Selection

In this chapter, we describe the system model for a two-hop DAF relayed system for two cases; firstly when antennas selection is performed only at the transmitter, secondly when antenna selection is performed jointly at the transmitter and the receiver. We compare the performance of the two systems in terms of BER over Nakagami-*m* fading channel. We also analyze the performance of the two systems based on different fading conditions on different channel paths.

5.1 Introduction

Communication systems exploiting multiple antennas at the transmitter and/or the receiver are able to provide both data rates (capacity) and performance (BER). These two main advantages of the MIMO systems can be achieved in two different ways namely diversity methods and spatial multiplexing. Employing diversity methods improves the robustness of the communication systems by exploiting multiple paths between transmit and receive antennas and the performance achieved is in terms of BER. Also when using multiple antennas in a rich scattering environment, it is possible for the receiver to sort out the simultaneously transmitted multiple signals from multiple antennas. Thus by sending parallel independent data streams it is possible to achieve overall system capacities. In other words by resolving these parallel spatial paths very high data rates can be achieved, hence, the name spatial multiplexing.

Apart from the benefits achieved from using MIMO systems, they impose a few drawbacks as well. These include poor link reliability, little advantage of antenna diversity, and the need of sub-optimum detection interfaces at the receiver when large number of antennas is used. Another major problem that arises while using MIMO systems is the increased complexity, leading to increased cost, due to the need of multiple $N_t(N_r)$ RF chains. While deploying multiple antennas at mobile stations such high degree of hardware complexity becomes totally detrimental. Also, the ever rising desire of owning smaller and lighter mobile sets without significant performance loss forces to devolve more processing burden on the transmit side. Therefore, considerable efforts have been put in exploring new MIMO systems that can significantly reduce this complexity but continue to provide similar capacity and performance improvements.

A promising technique to achieve this goal is based on selecting antennas at the transmitter and/or receiver. Antenna selection procedure may involve selecting a single antenna or multiple antennas and can be at the transmitter and/or receiver. Achieving a certain diversity order may be opted as the system design criteria. On the other hand, processing power of the receiver can also be accounted for while determining the number of active antennas that a system can support. Similar to MIMO systems, the advantages of antenna selection at either (or both) ends can be achieved in two different ways namely diversity methods and spatial multiplexing. In this thesis, antenna selection is based on the best available channel state information at the receiver. Since the antenna selection can be performed at the transmitter or receiver or both, we discuss here the process of transmit antenna selection (TAS) for the two-hop DAF system model described in Chapter-4, followed by the joint transmit-receive antenna selection (J-TR-AS) where the system is capable of selecting the required number of antennas at both ends.

5.2 Transmit Antenna Selection

Though the maturely used diversity techniques like MRC, STBC and STTC can achieve a full diversity order, but their implementation in practical systems with higher number of antennas at either end gives rise to certain problems. For example, the diversity order in case of MRC is directly determined by the number of receive antennas alone, thus making it unsuitable, A full code rate cannot be achieved for STBC with $N_t > 2$ due to complex constellations, and STTCs with $N_t > 2$ means a large memory order in order to achieve a full diversity order. Also, in some applications the number of antennas is limited to one or two, for example in hand-held devices, and still a high order of diversity is expected due to higher requirements of Quality-of-Service (QoS). TAS is a promising solution which is capable of achieving a high diversity order with a full code rate. For TAS, a feedback path is required from the receiver to the transmitter. In this thesis we use STBC and MRC for providing diversity and perform the task of TAS based on the feedback path from the TR node to the transmitter. Denoting the antennas selection process as $(N_t, L_t; N_r)$ where N_t is the total number of transmit antennas, L_t is the number of transmit antennas selected and N_r is the total number of receive antennas, we perform TAS based on the following system models:

- $(N_t, 1; 1)$ i.e. single TAS with single N_r forming an equivalent SISO system.
- $(N_t, L_t; 1)$ i.e. multiple TAS with single N_r forming an equivalent MISO system.
- $(N_t, 1; N_r)$ i.e. single TAS with multiple N_r forming an equivalent SIMO system.
- $(N_t, L_t; N_r)$ i.e. multiple TAS with multiple N_r forming an equivalent MIMO system.

5.2.1 Proposed TAS System and Channel Model

Assuming that the channel statistics are not varying too fast, and that the TR node is placed in between and in line with the transmitter and the receiver, the channel power gains

are calculated and the transmit antennas corresponding to the maximum channel power gain is selected for transmission. The most suitable L_t antennas out of N_t transmit antennas are chosen assuming that there are L_t RF chains and N_t transmit antennas, and $L_t < N_t$. The phase and amplitude of the transmit signals have to be such that their superposition at the receiver provides the maximum received SNR. In doing so, the L_t transmit antennas with highest channel gain are chosen. On similar basis, TAS is performed for the two-hop DAF system where an additional TR node is also used for transmission except that now the feedback from the TR node to the transmitter is taken into account for TAS. We call this system as TAS-TR. The selection criteria is based on the maximum channel power gains associated with each channel path formed between every transmit antenna and TR node. Also pilot symbols are used to provide feedback from the TR node to the transmitter. We explain this in detail in the following sections.

Pilot symbols are used to aid the TAS process. Known pilot symbols of fixed length are transmitted through all the available transmit antennas to the TR node only and not to the available receive antennas. At the TR node, the power associated with each channel path is calculated and the channel paths with maximum power are sorted. Depending on the number of transmit antennas to be selected, the knowledge of the channel paths with maximum power are sent back to the transmitter via a feedback path. The data transmissions now takes place over those transmit antennas only which showed the maximum channel powers. During the whole TAS process, we account for the channel powers when the pilot symbols are sent from the transmitter to the TR node only and not knowing the channel powers from the TR node to the receiver as there is no pilot symbol transmission from the TR node to the receiver, and also no pilot symbol transmission from the transmitter directly to the receiver.

Considering the system model shown in Fig. 4.3, N_t transmit antennas sends the pilot symbols to the TR node over the Nakagami-m fading channel h_1. Then the received pilot sequence at the TR node can be expressed as

$$y_p = \sqrt{E_b} x_p h_1 + n_p \tag{5.1}$$

where x_p is the pilot symbol sequence, h_1 is the channel coefficients between the transmitter and the TR node $(T - TR)$, and n_p is the additive white noises with zero mean and variance equal to N_0 associated with x_p. Here, h_1 is the $N_t \times 1$ channel matrix whose entries are the fading coefficients $h_{i,1}, i = 1, \dots, N_t$. Each transmit antenna is indexed from $1,2, \dots, t$ for simplicity such that the representation is now

$$N_1 \to 1, N_2 \to 2, \dots, N_t \to t \tag{5.2}$$

At the TR node, the channel power gains are calculated. Let P_i represent the channel power gain associated with transmit antenna i, then it can be calculated as

$$P_i = |h_i|^2, \quad 1 \leq i \leq N_t \tag{5.3}$$

The channel power gains P_i from N_t transmit antennas are then re-arranged in descending order of magnitude and expressed as

$$P_1 > P_2 > \cdots > P_{N_t} \tag{5.4}$$

Also the corresponding indexes from $1\ to\ t$ are rearranged in order with the corresponding channel power gains. For example, if the channel power gain P_i is for the channel path $h_{31}, (i = 3)$, i.e. from the third transmit antenna to the TR node, then the corresponding index term is 3. The channel information and the index term information is fed back to the transmitter. Since these index numbers refer to the sequence number of transmit antennas, the transmit antennas selection takes place and the data transmission takes place over the corresponding channel coefficient. The whole TAS process is summarized in Table 5.1

Table 5.1 Summary of the TAS process

Transmit Antennas, N_t	Transmit Antennas Indexes, t	Channel coefficients, h_1	Channel Power Gains, P_i	P_i rearranged in descending order	Corresponding Index terms	Selected Transmit Antennas, L_t	Corresponding channel coefficients
N_1	1	h_1	$\|h_1\|^2$	$\|h_4\|^2$	4	N_4	h_4
N_2	2	h_2	$\|h_2\|^2$	$\|h_{N_t}\|^2$	t	N_t	h_{N_t}
⋮	⋮	⋮	⋮	⋮	⋮	⋮	⋮
N_i	i	h_i	$\|h_i\|^2$	$\|h_1\|^2$	1	N_1	h_1
⋮	⋮	⋮	⋮	⋮	⋮	⋮	⋮
N_t	t	h_{N_t}	$\|h_{N_t}\|^2$	$\|h_i\|^2$	i	N_i	h_i

Thus, if a single antennas needs to be selected the transmit antenna with the maximum channel power gain is selected, if more than one transmit antenna (say $L_t = 3$) needs to be selected the first three channel power gains from the rearranged P_i sequence is selected and based on the transmit antenna indexes, the corresponding transmit antennas are selected for transmission. The simplicity of the whole process can be compared to the conventional TAS process as in the latter the channel power gains are dependent on the number of receive antennas as

$$P_i^c = \sum_{j=1}^{N_r} |h_{i,j}|^2, \quad 1 \le i \le N_t \tag{5.5}$$

where c in the superscript refers to the conventional TAS model. The channel power gains of all the channel paths from each transmitter to each receiver are calculated to form the subsets since the selection procedure involves selecting a subset of the transmit and/or receive antennas that maximizes the received SNR. In other words, a total of $N_t \times N_r$ channel power gains needs to be calculated in order to form a total of N_t subsets, each subset of dimension

$1 \times N_r$, to select L_t transmit antennas. Keeping track of all the channel information and subset formation makes the whole conventional TAS system a complicated process. By using an additional TR node, only $N_t \times 1$ channel power gains needs to be calculated to form N_t subsets and each subset is of dimension 1×1 to select L_t transmit antennas, thus, making TAS much simpler. Also, the TAS-TR scheme is not dependent on the number of receive antennas, thus, varying the number of receive antennas does not affect the complexity of the system unlike the conventional TAS scheme which is dependent on the number of available receive antennas. For simplicity we will call the conventional TAS system as TAS. This is discussed in detail in the next sections.

5.2.1.1 TAS with single Receive Antenna i.e. $(N_t, L_t; 1)$.

We discuss both the TAS and the TAS-TR scheme here when there are N_t transmit antennas and a single receive antenna. Considering the MIMO system explained in Fig 4.1, Fig. 5.1 shows the conventional TAS scheme where the feedback information for the antennas selection is received from the receiver.

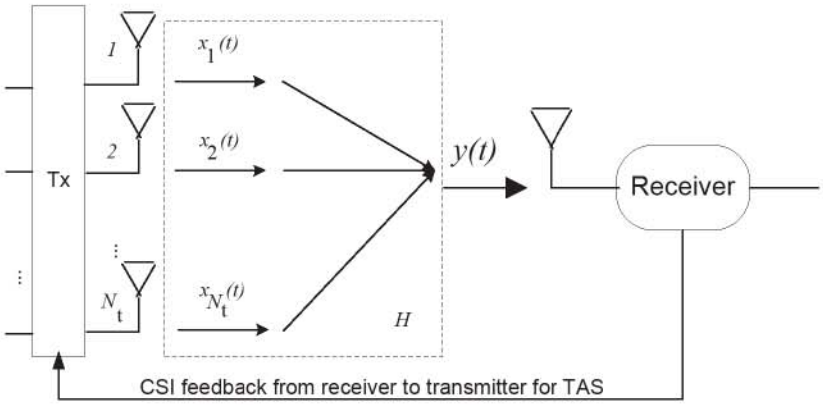

Fig. 5.1 TAS scheme with single receive antenna and feedback from the receiver

A sequence of known pilot symbols is sent by the transmitter and at the receiver the channel power gains are calculated using (5.5). Thus, with N_t transmit antennas and a single receive antennas, the channel matrix H can be expressed as

$$H = \begin{bmatrix} h_1 \\ h_2 \\ \vdots \\ h_{N_t} \end{bmatrix} \tag{5.6}$$

and the channel power gains can be expressed as

$$P_i^c = \begin{bmatrix} |h_{1,1}|^2 \\ |h_{2,1}|^2 \\ \vdots \\ |h_{N_t,1}|^2 \end{bmatrix} \tag{5.7}$$

These channel power gains are then arranged in their descending order using (5.4) and the transmit antenna corresponding to the maximum channel power is selected for transmission when selecting single transmit antenna. For selecting multiple transmit antennas, the first L_t transmit antennas corresponding to the first L_t number of channel power gains are selected for transmission. Fig. 5.2 shows the TAS-TR system model when the feedback to the receiver is provided by the TR node and not by the receiver. In this case the pilot symbols are sent only to the TR node and not to the receiver and the channel power gains are calculated at the TR node.

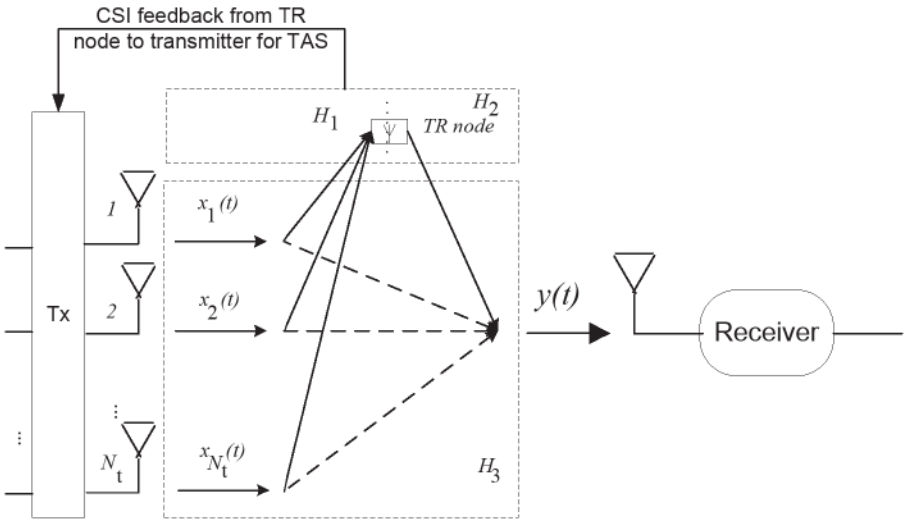

Fig. 5.2 Proposed TAS scheme with single receive antenna and feedback from the TR node

Thus, considering that the pilot symbols sent to the TR node are transmitted over channel H_1 expressed as

$$H_1 = \begin{bmatrix} h_{1_1} \\ h_{1_2} \\ \vdots \\ h_{1_{N_t}} \end{bmatrix} \tag{5.8}$$

The channel power gains are calculated using (5.3) as

$$P_i = \begin{bmatrix} |h_{1_1}|^2 \\ |h_{1_2}|^2 \\ \vdots \\ |h_{1_{N_t}}|^2 \end{bmatrix} \tag{5.9}$$

5.2.1.2 TAS with multiple Receive Antennas i.e. $(N_t, L_t; N_r)$.

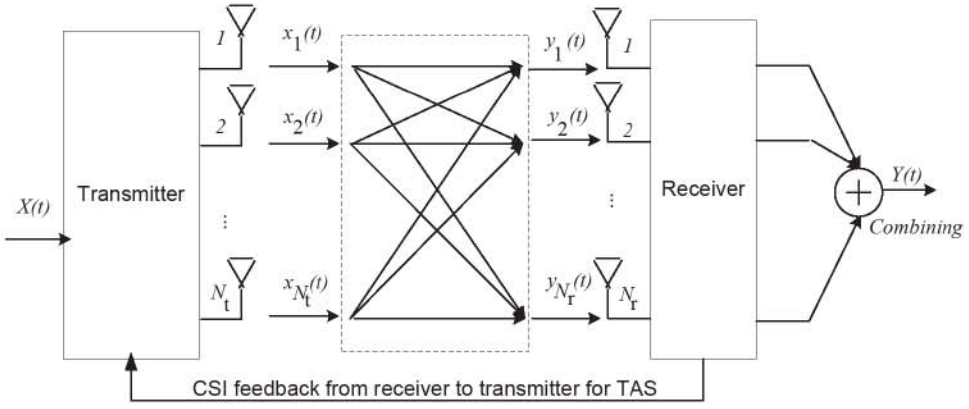

Fig. 5.3 TAS scheme with multiple Receive antennas and feedback from the receiver

When there are multiple receive antennas, the process of TAS becomes complex as can be seen from (5.5). With N_t transmit and N_r receive antennas, the pilot symbols are transmitted over channel H given by

$$H = \begin{bmatrix} h_{1,1} & \cdots & h_{1,N_r} \\ \vdots & \ddots & \vdots \\ h_{N_t,1} & \cdots & h_{N_t,N_r} \end{bmatrix} \tag{5.10}$$

Thus, the channel power gains according to (5.5) can be calculated as

$$P_i^c = \begin{bmatrix} |h_{1,1}|^2 + |h_{1,2}|^2 + \cdots + |h_{1,N_r}|^2 \\ |h_{2,1}|^2 + |h_{2,2}|^2 + \cdots + |h_{2,N_r}|^2 \\ \vdots \\ |h_{N_t,1}|^2 + |h_{N_t,2}|^2 + \cdots + |h_{N_t,N_r}|^2 \end{bmatrix} \tag{5.11}$$

It can be seen from (5.11) that the channel power gains from each transmit antenna to every receive antennas needs to be calculated to form the subsets for TAS. This process adds to the complexity of the whole system. Fig. 5.4 shows the TAS-TR MIMO system model.

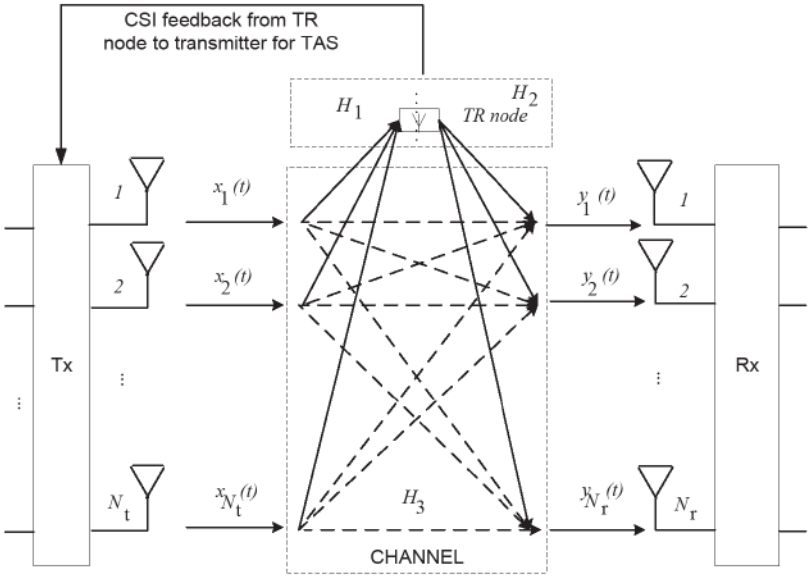

Fig. 5.4Proposed TAS scheme with multiple Receive antennas and feedback from the TR node

The pilot symbols are sent to the TR node over channel path H_1 as given by (5.8) and the channel power gains are calculated using (5.9). Thus, by comparing (5.9) and (5.11), it can be seen that the complexity of the TAS process decreases when using an additional TR node. To further reduce the complexity uncoded but modulated pilot symbols are used.

5.3 Joint Transmit and Receive Antenna Selection

Antenna selection can be performed at both transmit and receive end simultaneously also. Most of the research on antenna selection processes has been carried out with selecting antennas at either end [204], [205]. Joint transmit/receive antenna selection is a quite complex task as it requires to choose a subset of the rows and columns of H, where H is the $N_t \times N_r$ overall channel matrix, such as to maximize the sum of the squared magnitudes of transmit-receive channel gains [174]. The problem that occurs is selecting the best receivers and then best transmitters may not necessarily result in the overall best possible choice. Thus efficient joint transmit/receive antenna selection requires systematic solution apart from exhaustive search for antenna selection. For the system model discussed in chapter-4, we discuss the process of Joint Transmit and Receive Antennas Selection based on the maximum channel power gains obtained by using pilot symbols.

5.3.1 Proposed Joint Transmit-Receive Antenna Selection System and Channel Model

Fig. 5.5 shows the system model for the Joint Transmit-Receive Antenna Selection (J-TR-AS) process.

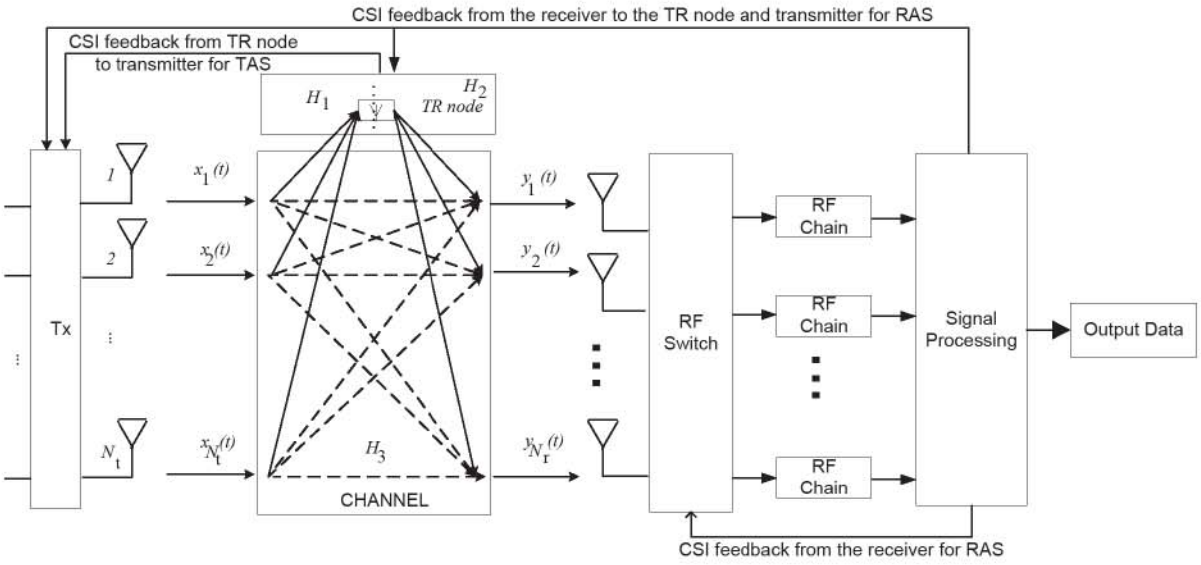

Fig. 5.5 Proposed (J-TR-AS) scheme for MIMO System with additional TR node

Uncoded pilot symbols are sent to the TR node where the process of TAS takes place in a similar way as explained in the previous section. The pilot symbols are then transmitted from the TR node to the receiver. At the receiver, the channel power gains are calculated and the receive antennas corresponding to the maximum channel power gains are selected. For TAS, the feedback from the TR node is provided to the transmitter only. During RAS, the feedback is provided to the RF switch at the receiver for receive antennas selection and the feedback is also provided from the receiver to the transmitter and the TR node so that they have the information about which channel paths to follow. Similar to TAS-TR, in J-TR-AS, the pilot symbols are never sent directly to the receiver. This reduces the overall computational complexity in case of MIMO systems while calculating the channel power gains for all the RF links from N_t transmitters to N_r receivers.

5.3.1.1 Joint Single Transmit Single Receive AS $(N_t, 1; N_r, 1)$

Considering x_p is the known pilot sequence transmitted by N_t transmit antennas to the TR node over the Nakagami-*m* fading channel h_1. Then the received pilot sequence at the TR node is given by (5.1). At the TR node, the channel power gains are calculated according to

(5.3) and the transmitter corresponding to maximum channel power gain is selected for transmission. The pilot symbols are then forwarded to the receiver over channel path h_2 which is a $1\times N_r$ channel matrix containing the CSI of the RF links from the TR node to N_r receive antennas as

$$h_2 = \left[h_{21}\ h_{22}\ \ldots h_{2,N_r}\right] \tag{5.12}$$

The channel power gains are calculated following (5.3) and the receiver corresponding to the maximum channel power gain is switched on for reception. This information is provided as the feedback to the TR node and the transmitter as well and they now know which RF link to follow. The whole process can be summarized as follows:

$$h_1 = \begin{bmatrix} h_{11} \\ h_{12} \\ \vdots \\ h_{1,N_t} \end{bmatrix}, P_i = |h_i|^2, \text{and } P_{TAS} = max|h_i|^2, \quad 1 \le i \le N_t \tag{5.13}$$

$$h_2 = \left[h_{21}\ h_{22}\ \ldots h_{2,N_r}\right], P_j = \left|h_j\right|^2, \text{and } P_{RAS} = max\left|h_j\right|^2, 1 \le j \le N_r \tag{5.14}$$

The data symbols are now transmitted by the selected transmit antennas over the corresponding channel link and is received over the selected receive antenna following the corresponding channel link via the TR node. For the direct transmission between the transmitter and the receiver, the data transmission takes place over the channel path h_3. The system model explained in this section forms an equivalent SISO system model after J-TR-AS.

5.3.1.2 Joint Multiple Transmit Single Receive AS $(N_t, L_t; N_r, 1)$

After arranging the channel power gains of all the channel links in the channel matrix h_1 in descending order, the first L_t transmit antennas with maximum channel power gains are selected out of the total available N_t transmit antennas and the receive antenna corresponding to the maximum channel power gain in the h_2 channel matrix is selected at the receiver. This forms an equivalent MISO model and the channel matrices h_1, h_2, and h_3 in this case are

$$h_1 = \begin{bmatrix} h_{11} \\ h_{12} \\ \vdots \\ h_{1,L_t} \end{bmatrix}_{TAS}, h_2 = [h_{21}]_{RAS}, \text{and } h_3 = \begin{bmatrix} h_{31} \\ h_{32} \\ \vdots \\ h_{3,L_t} \end{bmatrix}_{L_t \times L_r} \quad (5.15)$$

5.3.1.3 Joint Single Transmit Multiple Receive AS $(N_t, 1; N_r, L_r)$

The channel power gains of the channel coefficients of matrices h_1 and h_2 are rearranged in descending order. Then the transmit antenna with maximum channel power gain is selected out of the total available N_t transmit antennas and the first L_r receive antennas with maximum channel power gains are selected out of the total available N_r receive antennas. This forms an equivalent SIMO system model. The channel matrices h_1, h_2, and h_3 in this case are

$$h_1 = [h_{11}]_{TAS}, h_2 = \left[h_{21}\ h_{22} \dots h_{2,L_r}\right]_{RAS}, h_3 = \left[h_{31}\ h_{32} \dots h_{3,L_r}\right]_{L_t \times L_r} \quad (5.16)$$

5.3.1.4 Joint Multiple Transmit Multiple Receive AS $(N_t, L_t; N_r, L_r)$

After arranging the channel power gains of all the channel links in the channel matrices h_1 and h_2 in descending order, the first L_t transmit antennas with maximum channel power gains are selected out of the total available N_t transmit antennas and the first L_r receive antennas with maximum channel power gains are selected out of the total available N_r receive antennas. This forms an equivalent MIMO system model. The channel matrices h_1, h_2, and h_3 in this case are

$$h_1 = \begin{bmatrix} h_{11} \\ h_{12} \\ \vdots \\ h_{1,L_t} \end{bmatrix}_{TAS}, h_2 = \left[h_{21}\ h_{22} \dots h_{2,L_r}\right]_{RAS}, h_3 = \begin{bmatrix} h_{1,1} & \cdots & h_{1,L_r} \\ \vdots & \ddots & \vdots \\ h_{L_t,1} & \cdots & h_{L_t,L_r} \end{bmatrix} \quad (5.17)$$

5.4 Performance Analysis

In this section we present some simulation results to illustrate the error performance of the TAS-TR and J-TR-AS schemes. We present the results when we select one, two, three antennas out of the ten available transmit antennas based on the maximum power associated with each channel path. We testify the TAS of the proposed model for various system models like SISO, SIMO, MISO, and MIMO with BPSK and QPSK modulation over Nakagami-m fading channel for different fading parameter $'m'$.

Based on the results obtained in Chapter-4 for different system models, we choose the fading parameter depending on the type of equivalent model as a result of antennas selection. By equivalent System models, we mean the system models after antennas selection. For example, when the number of transmit antennas is ten and number of receive antennas is one and we select one out of 10 transmit antennas based on TAS, then the equivalent system model after antenna selection is a SISO system model. Thus, we select the fading parameter for $(T-TR)$ and $(TR-R)$ channel paths accordingly.

5.4.1 Results With Transmit Antenna Selection

We use uncoded pilot symbols for the antenna selection process. The use of pilot symbols simplifies the whole antenna selection process in terms of computational complexity. When the number of transmit antennas is high, no complexity is added at the transmitter to encode the pilot symbols before transmission, hence, the proposed TAS scheme works for any number of antennas in the transmitter array. Firstly, we present the simulation results for different fading conditions when TAS is performed at the transmitter when no TR node is used. Then we compare the equivalent system models with the corresponding system models. By equivalent system models we refer to the system models formed after TAS and

by corresponding system models we refer to the system models without TAS. For convenience we name the system models as follows:

System-1 – System models with no TR node but TAS using pilot symbols.

System-2 – System models with TR node and TAS using pilot symbols.

System-3 – System models with TR node and J-TR-AS using pilot symbols.

Pilot sequence of fixed length 4 is transmitted over Nakagami-*m* faded channel with *m=1* using ten transmit antennas and one receive antennas, out of which only one transmit antenna is selected based on the maximum associated channel power. We have performed the simulations for BPSK and QPSK modulation. However, the defined system is capable to perform for higher values of 'M'-PSK modulation schemes as well.

5.4.1.1 BERs with TAS $(N_t, L_t; N_r)$

With single antenna available at the receiver, the equivalent system model for System-1 after single TAS is the SISO model. Fig. 5.6 (a) shows the BERs for the equivalent SISO system model for System-1 with different fading parameters, *m=1,2, and* 5 for BPSK modulated data sequences and Fig. 5.6 (b) shows the BERs for the same system model with similar values of *'m'* with QPSK modulation.

With multiple antennas at the receiver, Fig. 5.7 shows the BERs with single TAS, thus, forming an equivalent SIMO system. Fig. 5.7 (a) shows the BERs for the equivalent SIMO system model for System-1 with different fading parameters, *m=1,1.5,2* for BPSK modulated data sequences and Fig. 5.7 (b) shows the BERs for the same system model with similar values of *'m'* with QPSK modulation. The simulation results presented in Fig. 5.7 are for $N_r = 2,3$ and can be obtained for any $N_r > 3$.

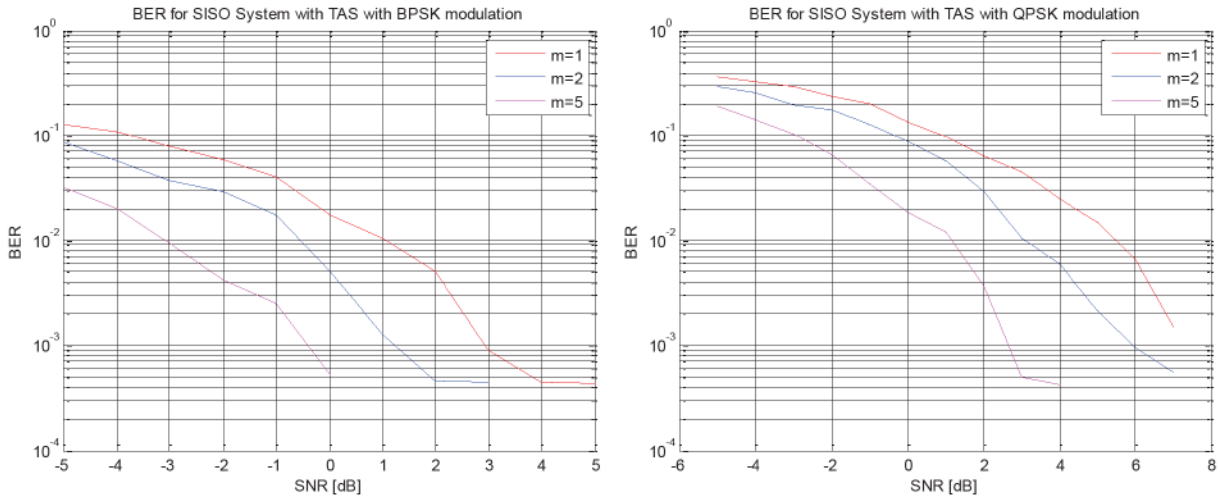

Fig.5.6 BER for (10,1;1) TAS scheme

(a) BPSK modulation and (b) QPSK modulation; m=1,2,5.

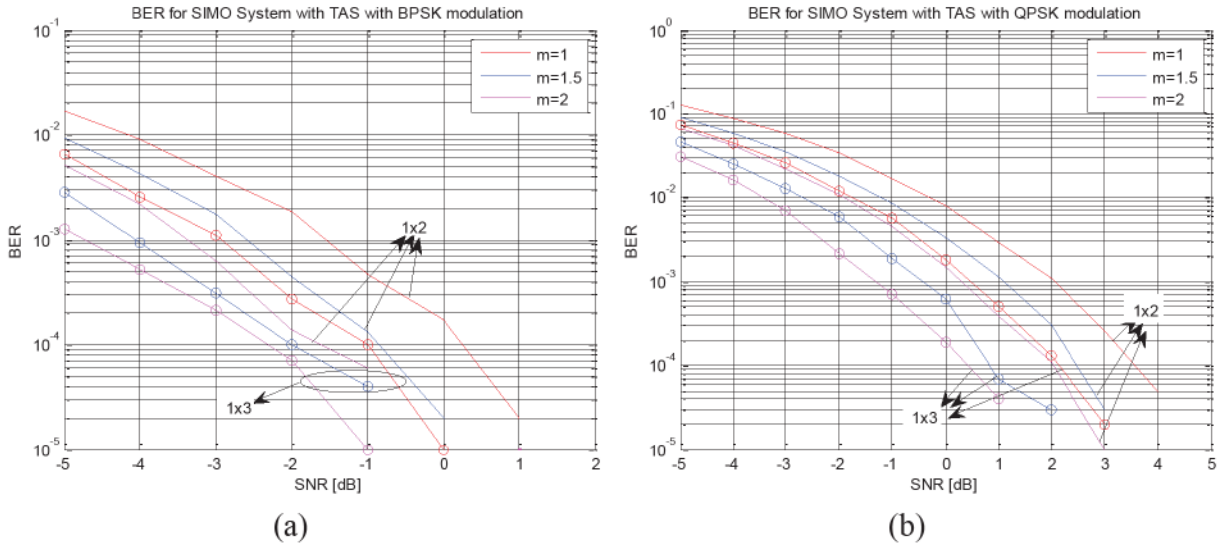

Fig.5.7 BER for (10,1;N_r) TAS scheme

(a) BPSK modulation and (b) QPSK modulation; m=1,1.5,2 and $N_r = 2,3$

With single receive antenna and multiple TAS, Fig. 5.8 shows the BERs of the equivalent MISO system model for System-1. Fig. 5.8 (a) shows the BERs for the equivalent MISO system model with *m=1,1.5,2* for BPSK modulated data sequences and Fig. 5.8 (b) shows the BERs for the same system model with similar values of *'m'* with QPSK

modulation. We have considered here $L_t = 2,3$ but the results can be obtained for $L_t > 3$ also.

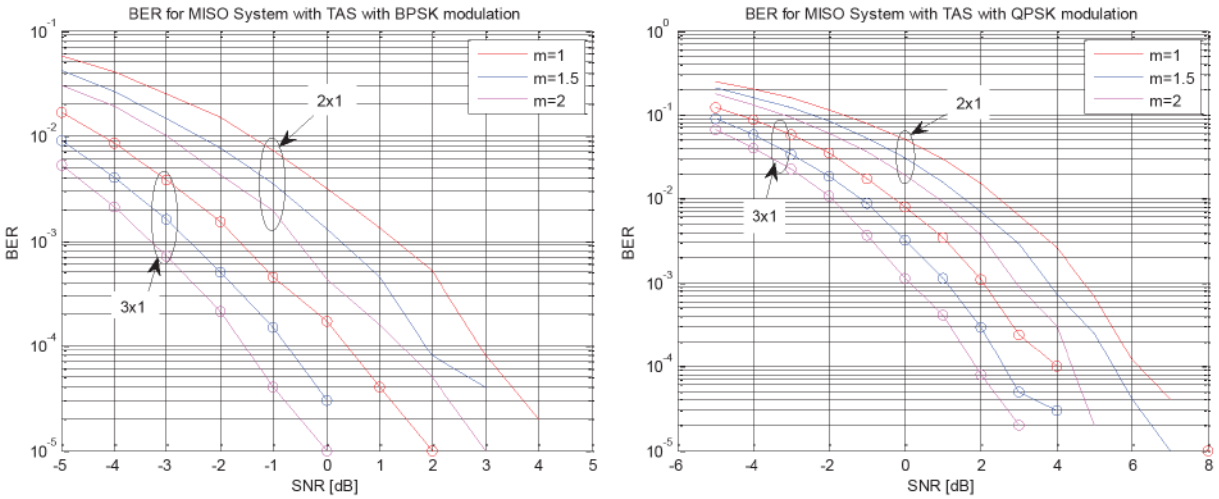

(a) (b)

Fig.5.8 BER for (10,L_t;1) TAS scheme

(a) BPSK modulation and (b) QPSK modulation; m=1,1.5,2, $L_t = 2,3$ and $N_r = 1$

With multiple receive antennas and multiple TAS, Fig. 5.9 shows the BERs for the equivalent MIMO system model for System-1.

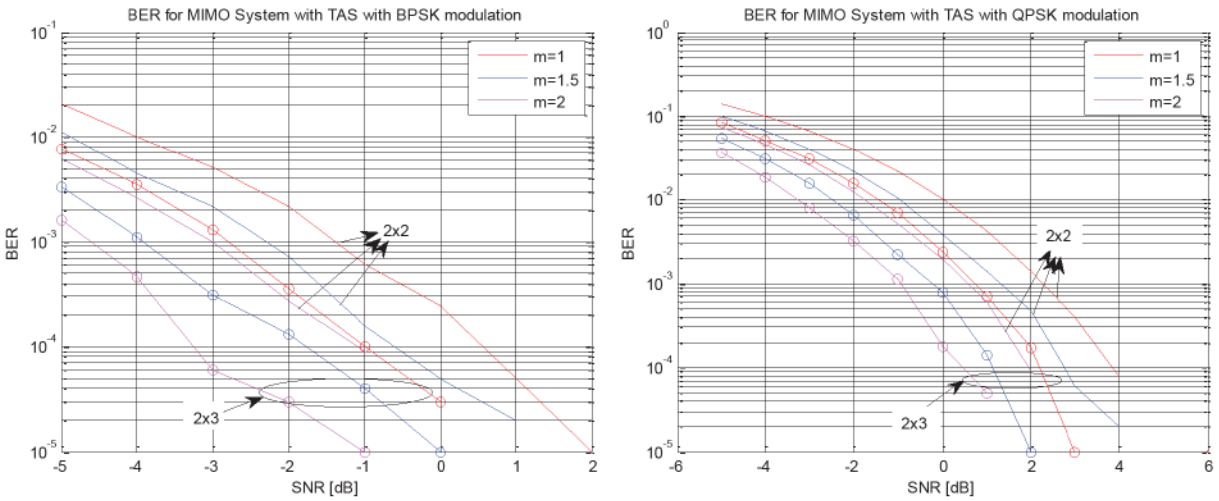

(a) (b)

Fig.5.9 BER for (10,L_t;N_r) TAS scheme

(a) BPSK modulation (b) QPSK modulation; m=1,1.5,2, $L_t = 2,3$, $N_t = 2$ and $N_r = 2,3$

Fig. 5.9 (a) and (b) shows the BERs for the equivalent MIMO system with *m=1,1.5,2* for BPSK and QPSK modulated data sequences, respectively. Here we have obtained the simulation results for 2×2 and 2×3 systems can be easily extended to any number of N_t, L_t, and N_r.

It is well known that the BER performance varies with different fading parameters *'m'*. By performing the simulations of the system models described in Fig. 5.6 – Fig. 5.7, we have successfully verified that the BERs improves with higher values of the fading parameter *'m'* with TAS. Fig. 5.7 – Fig. 5.9 compares the BERs with different number of transmit and receive antennas available and different number of transmit antennas selected. It can be observed that a better performance is achieved as more transmit and /or receive antennas are used.

5.4.1.2 BERs of TAS with TR node and its comparison with TAS without TR node.

We compare the performance of the TAS for a two-hop DAF relay system with a conventional wireless system with TAS. The fading parameter for the conventional system is $m = 1$ and the fading parameter for the $(T - TR)$ and $(TR - R)$ channel paths for the relayed system is also $m_1 = m_2 = 1$. Thus for convenience we will write the fading parameter as $m = 1$ in general for all the channel paths involved within this section only. The length of pilot symbols is 4. The total length of data sequence is 10^3 divided into 10 frames each of length 100. The pilot sequence is transmitted over N_t available transmit antennas to the TR node. At the TR node, the channel power gains of all the $N_t \times 1$ channel paths are calculated and arranged in descending order. This information is provided to the transmitter via a feedback path and the transmit antenna indexed with the channel path with maximum channel power gain is selected for transmission.

Fig. 5.10 compares the BER for TAS-TR when TAS is performed over (10,1;1) schemes. In this case, a single transmit antennas with maximum channel power gain is selected for transmission. The selected transmit antennas transmits data bits to the TR node and to the receiver following the process explained in chapter-4. It can be seen that the TAS-TR process over the (10,1;1) scheme through TR node gives an increased performance of approximately 1dB as compared to the baseline approach of TAS. The performance gains are better at lower SNR values and the performance improvement is less than 1dB at higher SNR values. Fig. 5.10 (a) and (b) compares the BER for BPSK and QPSK modulation and shows similar improvements in terms of BER over TAS scheme.

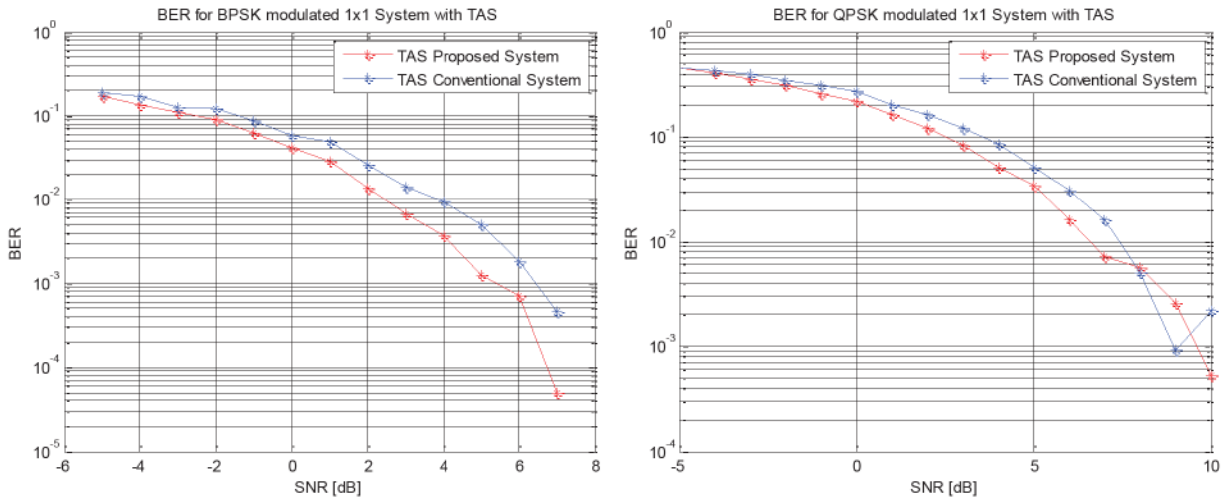

(a) (b)

Fig.5.10 BER of (10,1;1) conventional TAS/STBC scheme and (10,1;1) proposed TAS/STBC scheme with (a) BPSK modulation and (b) QPSK modulation; m=1.

Fig. 5.11 shows the BER when L_t transmit antennas are selected out of N_t transmit antennas available and a single receive antennas. The simulations are carried out for the wireless model with $L_t = 2$ and encoder matrix G_2^* with rate, $R = 1$ and with $L_t = 3$ and encoder matrix G_3^* with rate $R = 1/2$, respectively. The sequence being transmitted over Nakagami-m fading channel with $m = 1$ and BPSK and QPSK modulated. Fig. 5.11 (a)

shows the BER with BPSK modulation and Fig. 5.11 (b) shows the BER with QPSK modulation. It can be observed that the TAS for two-hop DAF relay system showed an improved performance of approximately 0.5dB at lower SNR values and slightly over 1dB at higher SNR values when compared to TAS process. Also it can be seen that the performance is improved when more transmit antennas are selected.

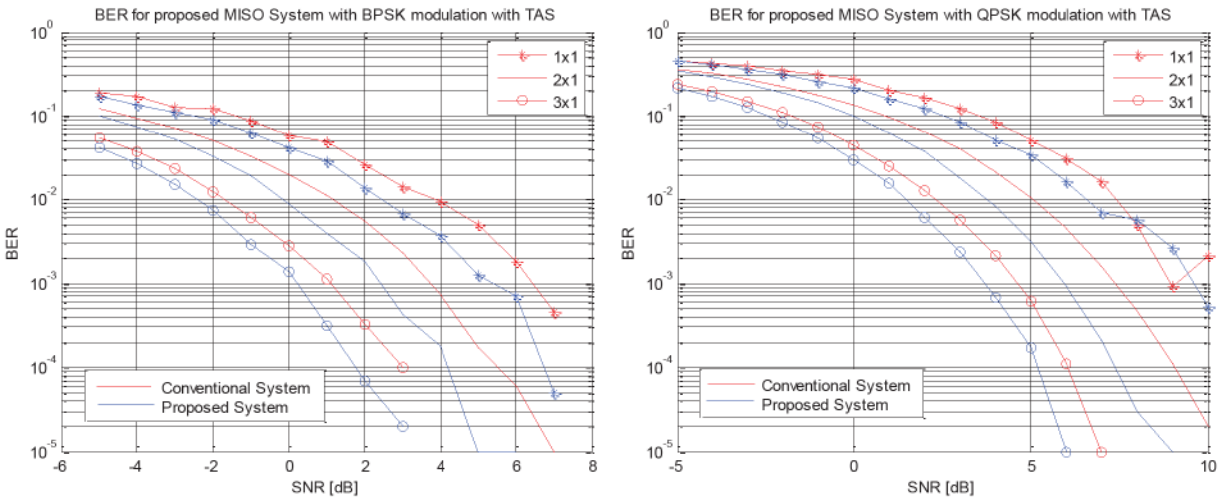

(a) (b)

Fig.5.11 The simulation BER for (10,1;1), (10,2;1), and (10,3;1) conventional and proposed TAS scheme, respectively, with (a) BPSK modulation,(b) QPSK modulation; m=1.

Fig. 5.12 shows the BER when a single transmit antenna is selected out of N_t transmit antennas available and with N_r receive antennas. The sequence being transmitted over Nakagami-*m* fading channel with $m = 1$ and BPSK and QPSK modulated and the signal is received over $N_r = 1,2,3\ and\ 4$ receive antennas. Fig. 5.12 (a) shows the BER with BPSK modulation and Fig. 5.12 (b) shows the BER with QPSK modulation. It can be observed that the TAS for two-hop DAF relay system showed an improved performance of approximately 1dB at lower SNR values and slightly over 1dB at higher SNR values when compared to TAS process with multiple receive antennas. Also it can be seen that the performance is improved when the number of receive antennas are increased from 1 to 4.

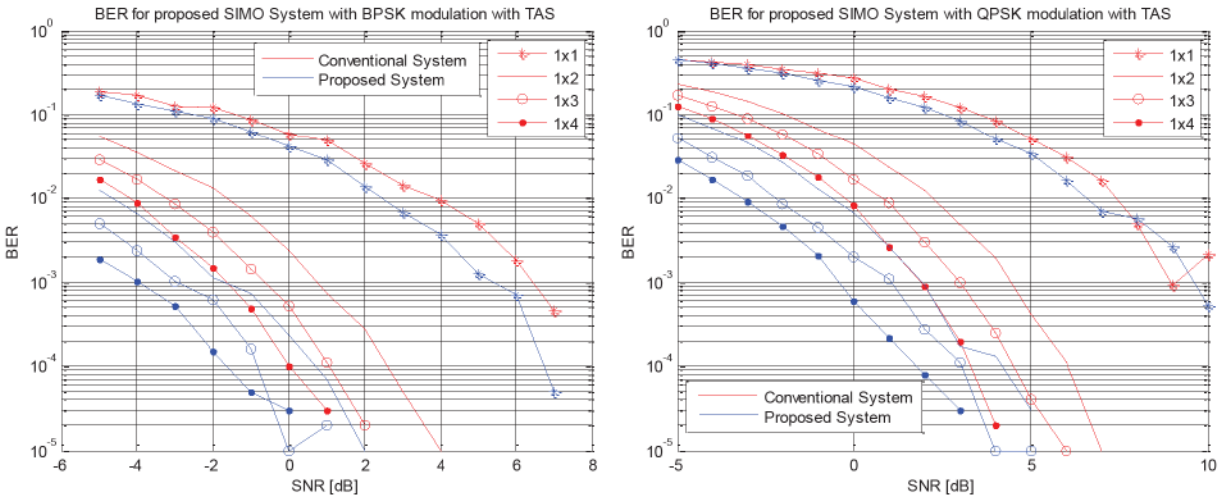

(a) (b)

Fig.5.12 The simulation BER for (10,1;1), (10,1;2), (10,1;3), (10,1;4) conventional and proposed TAS scheme, respectively, with (a) BPSK modulation,(b) QPSK modulation; m=1

Fig. 5.13 plots the BER for the (10,2;2), (10,2;3), (10,3;2), and (10,3;3) schemes over Nakagami-*m* fading channel with $m = 1$ with BPSK and QPSK modulation and compares the simulation BER of the proposed scheme with the existing TAS/STBC schemes.

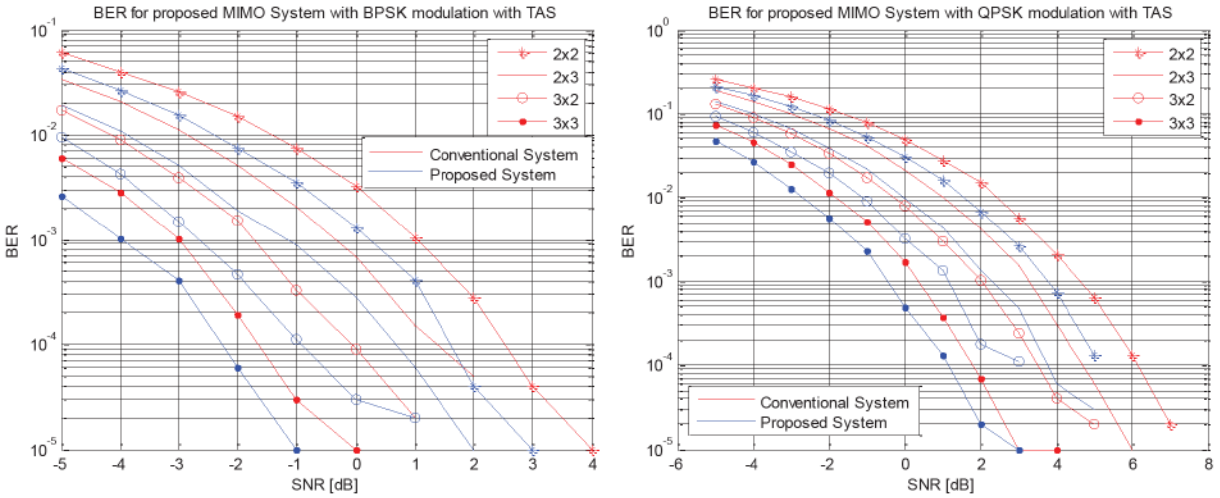

(a) (b)

Fig.5.13 The simulation BER for (10,2;2), (10,2;3), (10,3;2), and (10,3;3) conventional and proposed TAS scheme, respectively, with (a) BPSK modulation,(b) QPSK modulation; m=1.

It can be seen from Fig. 5.13 that the TAS for two-hop amplify-decode-forward relayed system shows better performance over the existing TAS scheme by approximately 1dB when multiple antennas selected at the transmitter with multiple antennas at the receiver. Also as more transmit and receive antennas are used, the BER improves.

5.4.1.3 BER variations of TAS-system with TR node in different fading conditions.

In Chapter-4, the performance of the two-hop DAF relay system based on the placement of the TR node between the transmitter and the receiver was analysed. It was concluded that based on the number of transmit and receive antennas available, placing the TR node nearer or farther from the transmitter gave variations in the BERs. In the previous section, the performance of the two-hop DAF relay system with TAS was simulated and analysed when the fading parameter (or the fading conditions) for the $(T-TR)$ and $(TR-R)$ channel paths were assumed to be same. This section analyses the performances of the proposed system model when the fading conditions on the $(T-TR)$ and $(TR-R)$ channel paths are different. The fading parameter m_1 refers to the fading conditions of the $(T-TR)$ channel path and the fading parameter m_2 refers to the fading conditions of the $(TR-R)$ channel path. The BER are now analysed as m_1 and m_2 takes different values. Table 5.2 summarizes some of the fading parameter values for which simulations have been performed for different system models.

Table 5.2 Equivalent system models and their corresponding fading parameters.

TAS, $(N_t, L_t; N_r)$	Equivalent System Model	Fading Parameter ' $'m'$
$(N_t, 1; 1)$	SISO	1. $m_1 = m_2 = 2$ 2. $m_1 = 0.7, m_2 = 3.3$ 3. $m_1 = 3.3, m_2 = 0.7$ 4. $m_1 = 1, m_2 = 3$ 5. $m_1 = 3, m_2 = 1$
$(N_t, L_t; 1)$ $L_t = 2,3$	MISO	1. $m_1 = m_2 = 1$ 2. $m_1 = 0.7, m_2 = 1.3$ 3. $m_1 = 1.3, m_2 = 0.7$
$(N_t, 1; N_r)$ $N_r = 2$	SIMO	1. $m_1 = m_2 = 1$ 2. $m_1 = 0.8, m_2 = 1.2$ 3. $m_1 = 1.2, m_2 = 0.8$
$(N_t, L_t; N_r)$ $L_t = 2,3$ $N_r = 2,3$	MIMO	1. $m_1 = m_2 = 1$ 2. $m_1 = 0.8, m_2 = 1.2$ 3. $m_1 = 1.2, m_2 = 0.8$

Fig. 5.14 (a) shows the simulations results for $(N_t, 1; 1)$ system with different fading parameter as mentioned in Table 5.2. It can be observed that the best performance is achieved when $m_1 = m_2 = 2$, that is when the TR node is placed at equidistant from the transmitter and the receiver. This is in accordance with the two-hop DAF relay system without TAS as proved in chapter-4. But if we compare Fig. 4.14 (ii) and Fig. 5.14 (a), we observe that while a better performance is achieved with $m_1 > m_2$ (when $m_1 = m_2$ is not possible) in the former case, in the latter case a better performance is achieved when $m_2 > m_1$. This can be explained as follows. The performance of the system under consideration is affected by the fading conditions of the $(T - TR)$ and $(TR - R)$ channel paths which is based on the distance of the TR node from the transmitter and the receiver and on the number of available

transmit and receive antennas. With no TAS, the added diversity path by the TR node at the receiver over powered the degradation of the signal due to larger distance between the TR node and the receiver. Thus the system model with no TAS gave better performance when $m_1 > m_2$. When TAS was performed, the antenna was selected based on the maximum channel power gain and the data was sent over this known channel. Thus even though the fading conditions on the $(T - TR)$ channel path was worse than the fading conditions on the $(TR - R)$ channel path, TAS compensated for the loss due to fading thus giving better performance when $m_2 > m_1$ rather than with $m_1 > m_2$. Thus, it can be concluded that the effects of TAS are stronger than the fading effects thus giving better performance.

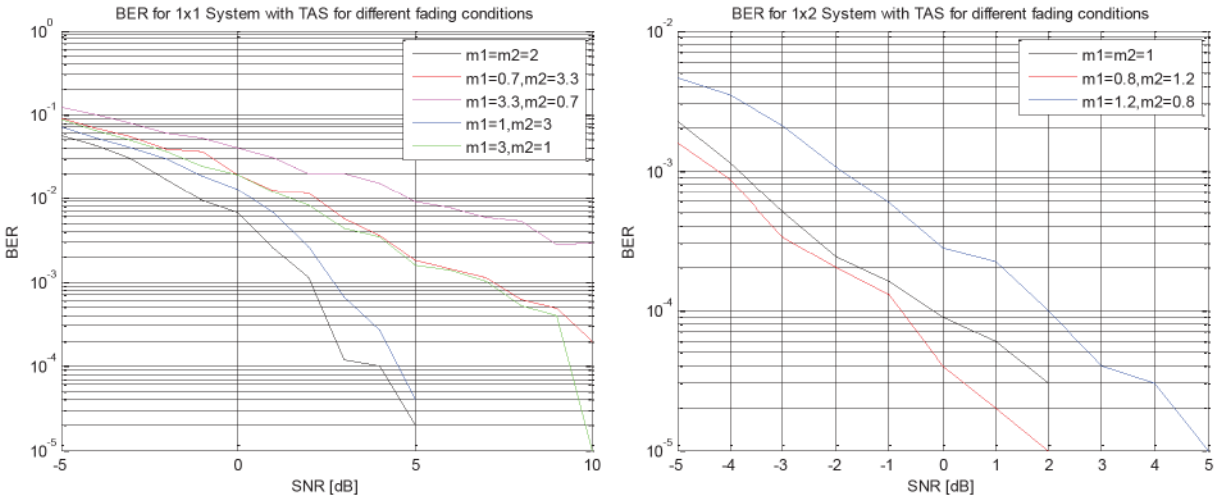

(a) (b)

Fig.5.14 BER for proposed TAS scheme in various fading conditions with BPSK modulation (a) $(N_t, 1; 1)$*,(b)* $(N_t, 1; 2)$.

Fig. 5.14 (b) shows the BER for $(N_t, 1; 2)$ scheme for different values of m_1 and m_2 as mentioned in Table 5.2. It is observed that the best performance is achieved when $m_2 > m_1$ which is similar to the SIMO system model discussed and analysed in Chapter-4. The explanation is similar to $(N_t, 1; 1)$ scheme except that in this case a better performance is achieved with $m_2 > m_1$ than $m_2 = m_1$ due to the fact lower fading parameter, TAS and

increased number of receive antennas help in gaining better performance when the TR node is placed closer to the receiver than when placing it at equidistance from the transmitter and the receiver.

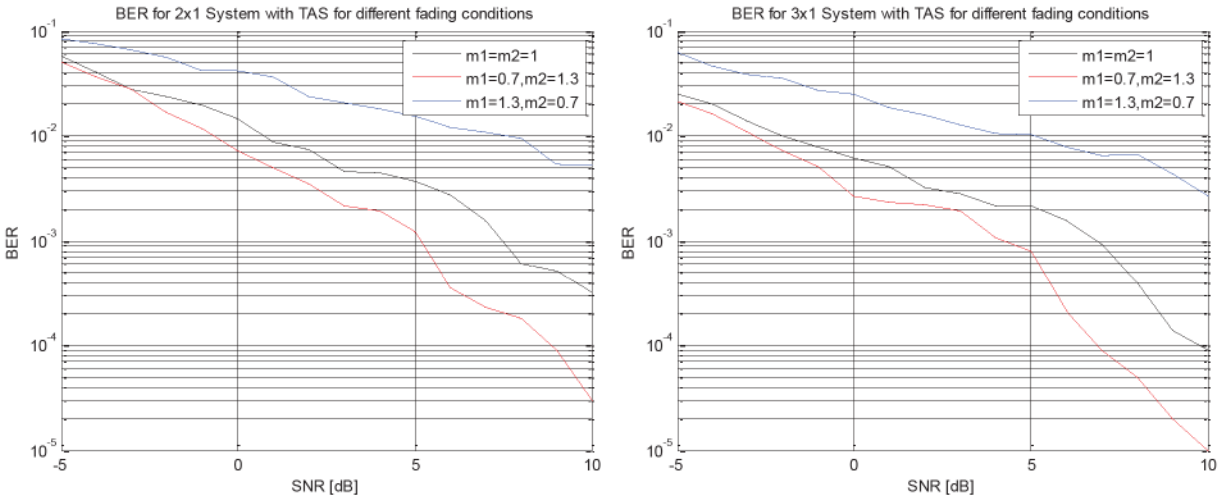

(a) (b)

Fig.5.15 BER for proposed TAS scheme in various fading conditions with BPSK modulation (a) $(N_t, 2; 1)$*,(b)* $(N_t, 3; 1)$.

Fig. 5.15 shows the BER for $(N_t, L_t; 1)$ scheme for different values of m_1 and m_2 as mentioned in Table 5.2. Fig. 5.15 (a) shows the BER when $L_t = 2$ and Fig. 5.15 (b) shows the BER when $L_t = 3$. It is observed that again the best performance is achieved when $m_2 > m_1$ in both the cases which is similar to the SIMO system model discussed earlier. The explanation is similar to $(N_t, 1; 2)$ scheme that lower fading parameter, higher number of transmit antennas selected helps in gaining better performance when the TR node is placed closer to the receiver than when placing it at an equidistance from the transmitter and the receiver. Also the poorer fading conditions on the $(T - TR)$ channel path is over shadowed by the data transmission taking place over the channel paths with maximum channel power gains thus improving performance.

Fig. 5.16 shows the BER for the $(N_t, L_t; N_r)$ scheme for different values of m_1 and m_2 as mentioned in Table 5.2. Fig. 5.16 (a) shows the BER when $L_t = 2; N_r = 2$ and Fig. 5.16 (b) shows the BER when $L_t = 3; N_r = 3$. It shows similar results when compared to the schemes previously discussed that the best performance is achieved when $m_2 > m_1$.

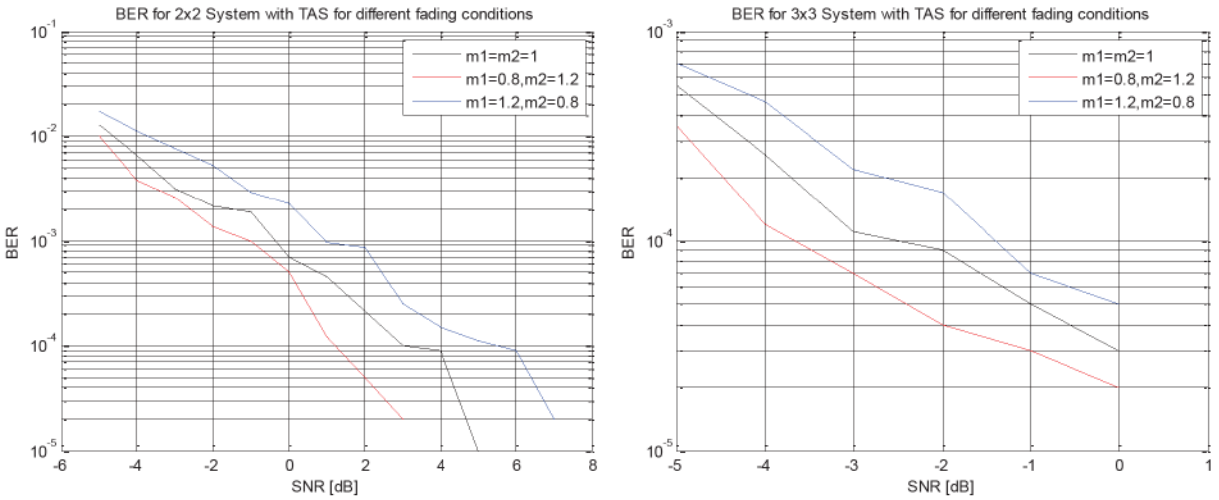

(a) (b)

Fig.5.16 BER for proposed TAS scheme in various fading conditions with BPSK modulation (a) $(N_t, 2; 2)$*,(b)* $(N_t, 3; 3)$.

In all the case the worst performance is achieved when $m_1 > m_2$. When $m_1 > m_2$, the TR node is placed closer to the transmitter and the channel path between the TR node and the receiver suffers from poorer fading conditions. Further, TAS helps compensate for the fading conditions between the transmitter and the TR node and thus the fading conditions between the $(TR - R)$ channel path remains unaccounted for. On the other hand, when $m_2 > m_1$, fading conditions on the $(TR - R)$ channel path are better than the fading conditions on $(T - TR)$ channel path. TAS helps in reducing the poorer fading effects on the $(T - TR)$ channel path, and though the $(TR - R)$ channel path remains accounted, due to higher values of *'m'* it is already suffering from less sever fading as compared to the amount of fading when $m_1 > m_2$. Thus better performance is achieved when $m_2 > m_1$ as compared

to when $m_1 > m_2$. We have presented the simulation results for BPSK modulation alone when dealing with different fading conditions and their achievement for higher MPSK modulation schemed are straight forward.

5.4.2 Joint Transmit-Receive Antenna Selection

In this section we present the simulation results when joint antenna selection is performed at the transmitter and the receiver for a two-hop DAF relay system based on pilot symbols. We present the results for only QPSK modulation. However, extension to other MPSK schemes is straight forward. We have used the following representations for the three systems under analysis in Fig. 5.17:

- **J-TR-AS** represents a two-hop DAF system model with Joint transmit and receive antennas selection.
- **TAS-TR** represents a two-hop DAF system model with only transmit antennas selection.
- **TAS** represents the baseline system models with transmit antenna selection.

We first compare the BERs of J-TR-AS, TAS-TR and TAS and account for the performance improvements in terms of dB.

5.4.2.1 BER variations of JAS-system with TR node

Fig. 5.17 (a) compares the BER of J-TR-AS for (10,1;10,1), TAS-TR for (10,1;1), and TAS for (10,1;1) with QPSK modulation, i.e. single antennas is selected in all the three case. It can be seen that at lower SNRs, J-TR-AS gives an approximately 2dB improvement in performance as compared to TAS-TR while at higher SNRs, the performance improvement is slightly less than 1dB when compared to TAS-TR.

Fig. 5.17 (b) compares the BER for J-TR-AS for *(10,1;10,2), (10,1;10,3), and* TAS-TR, and TAS for *(10,1;2) and (10,1;3)*, thus forming an equivalent system models of (1×2)

and (1×3), respectively. It can be concluded from the simulation results that the joint selection of antennas at both transmitter and receiver shows a performance improvement of approximately 2dB as compared to TAS-TR for a general case of SIMO system model.

Fig. 5.17 (c) compares the BER for J-TR-AS for *(10,2;10,1), (10,3;10,1),* and, TAS-TR, and TAS for *(10,2;1), and (10,3;1)*. Thus, when performing joint selection, multiple antennas are selected at the transmitter and a single antenna is selected at the receiver, and while performing TAS alone multiple antennas are selected at the transmitter while the number of receive antennas is fixed to one giving an equivalent MISO system. We present here the BER results when only two and three transmit antennas are available i.e. for (2×1) and (3×1) systems, respectively. The simulation results can be easily extended to higher number of selection of antennas at the transmitter following the orthogonality principle of STBCs. It can be seen that J-TR-AS gives better BERs giving an overall performance improvement of approximately 2dB when compared to TAS-TR and approximately 4dB when compared to TAS.

Fig. 5.17 (d) compares the BERs for J-TR-AS for *(10,2;10,2), (10,2;10,3), (10,3;10,3)* and, TAS-TR, and TAS for *(10,2;2), (10,2;3) and (10,3;3)* forming an equivalent MIMO system. We have presented the results for an equivalent (2×2), (2×3), and (3×3), systems, respectively and it has been concluded that J-TR-AS process outperformed TAS by approximately 2dB and by approximately 3.5 dB when compared to TAS.

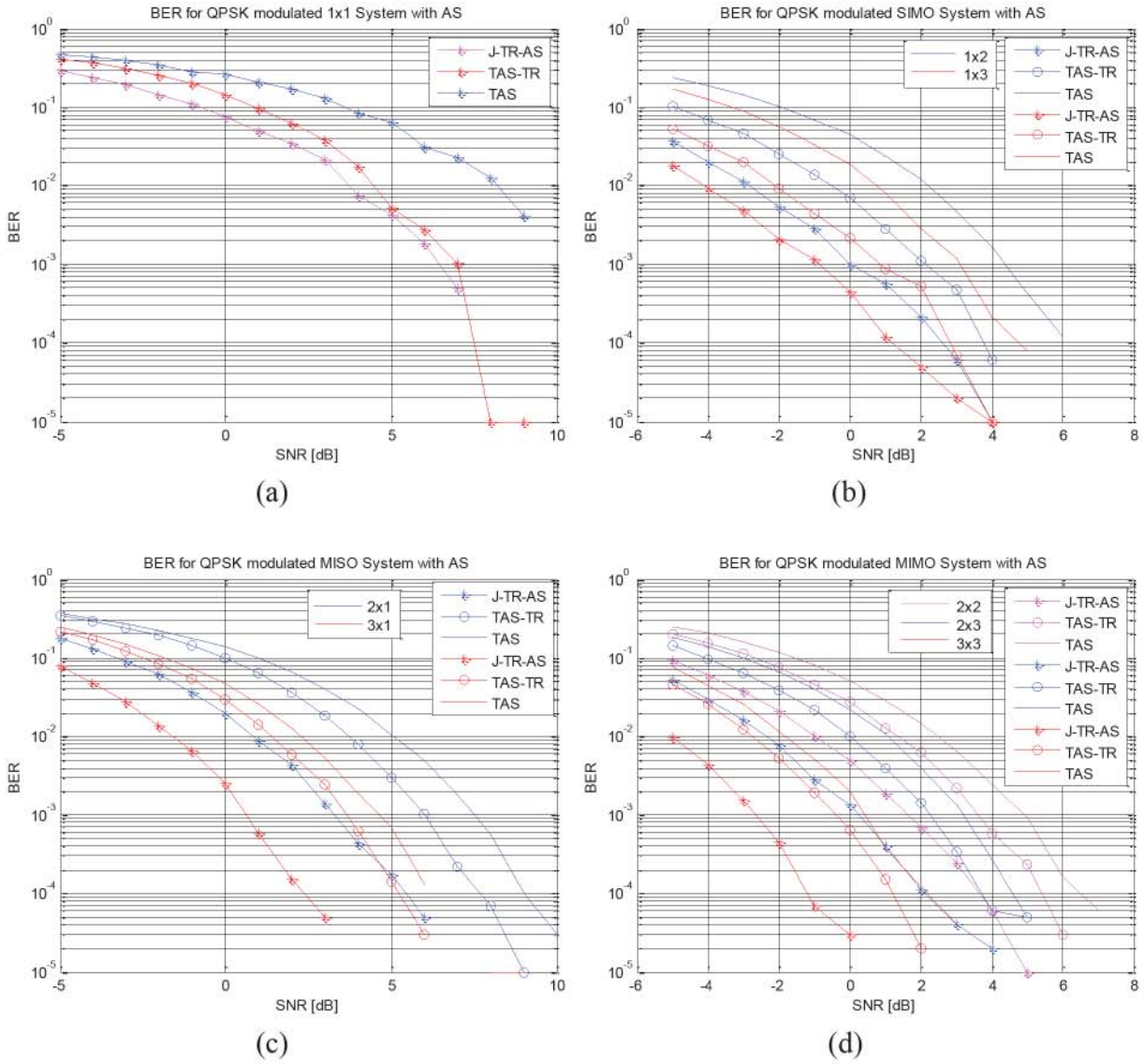

Fig.5.17 BER comparison of J-TR-AS, TAS-TR, and TAS schemes with QPSK modulation for,

(b) Equivalent SISO systems (b) Equivalent SIMO systems

(d) Equivalent MISO systems (d) Equivalent MIMO systems

5.4.2.2 BER variations of JAS-system with TR node in different fading conditions.

Fig. 5.18 - Fig. 5.20 plots the BERs for the various systems in different fading conditions. Table 5.3 summarizes the values of fading parameters m_1 and m_2 for different system models. Monte Carlo simulations have been performed for the J-TR-AS system to show the variations in the performance of the two-hop DAF system based on the placement of the TR node between the transmitter and the receiver. The fading parameters m_1 and m_2

can take value from $0.65 \leq m \leq 10$, while the sum $(m_1 + m_2)$ is always considered as integer. The simulations carried here have been performed when $(m_1 + m_2) = 1$ in all the cases and m_1 and m_2 taking arbitrary real values. These simulations results can be easily extended to other values of fading parameters m_1 and m_2.

Table 5.3 Equivalent system models and their corresponding fading parameters.

J-TR-AS, $(N_t, L_t; N_r, L_r)$	**Equivalent System Model**	**Fading Parameter** $'m'$
$(N_t, 1; N_r, 1)$	SISO	1. $m_1 = m_2 = 1$ 2. $m_1 = 1.2, m_2 = 0.8$ 3. $m_1 = 0.8, m_2 = 1.2$
$(N_t, L_t; N_r, 1)$ $L_t = 2, L_r = 1$	MISO	1. $m_1 = m_2 = 1$ 2. $m_1 = 1.2, m_2 = 0.8$ 3. $m_1 = 0.8, m_2 = 1.2$
$(N_t, 1; N_r, L_r)$ $L_t = 1, L_r = 2,3$	SIMO	1. $m_1 = m_2 = 1$ 2. $m_1 = 1.2, m_2 = 0.8$ 3. $m_1 = 0.8, m_2 = 1.2$
$(N_t, L_t; N_r, L_r)$ $L_t = 2,3; L_r = 2,3$	MIMO	1. $m_1 = m_2 = 1$ 2. $m_1 = 1.2, m_2 = 0.8$ 3. $m_1 = 0.8, m_2 = 1.2$

It can be seen from these figures that with J-TR-AS, the best performance is achieved when the TR node is placed at equidistant from the transmitter and the receiver in all the cases. This can be explained on the basis that for both the channel paths i.e. $(T - TR)$, and $(TR - R)$, the transmission takes place over the best channel path selected, thus irrespective of the distance of the TR node from either end, the fading effects of both the channel paths are overlooked by the antennas selection process. Also, it can be noted though having different values of fading parameters gave poorer performance as compared to when the

fading parameters are same, placing TR node closer to either ends gave almost same levels of performance in all the cases.

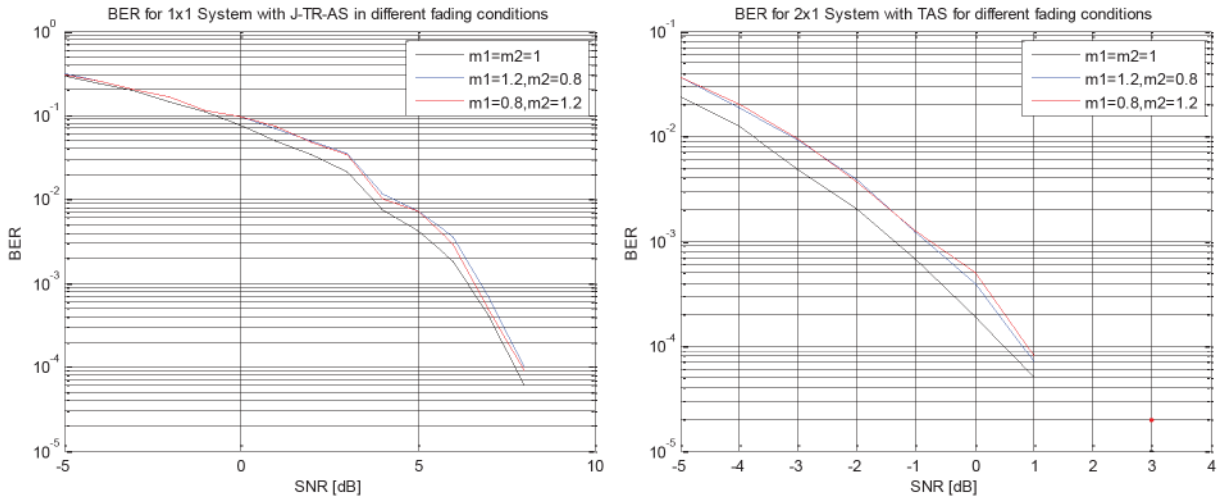

(a) (b)

Fig.5.18 BER for J-TR-AS with different fading parameter values,

(a) (10,1; 10,1) *(b)* (10,2; 10,1).

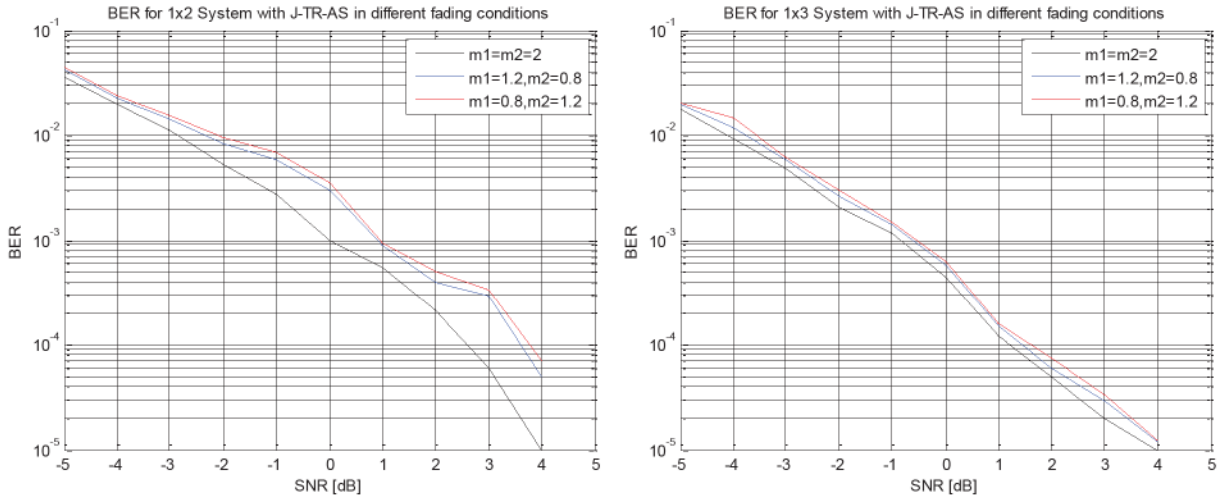

(a) (b)

Fig.5.19 BER for J-TR-AS with different fading parameter values,

(a) (10,1; 10,2) *(b)* (10,1; 10,3).

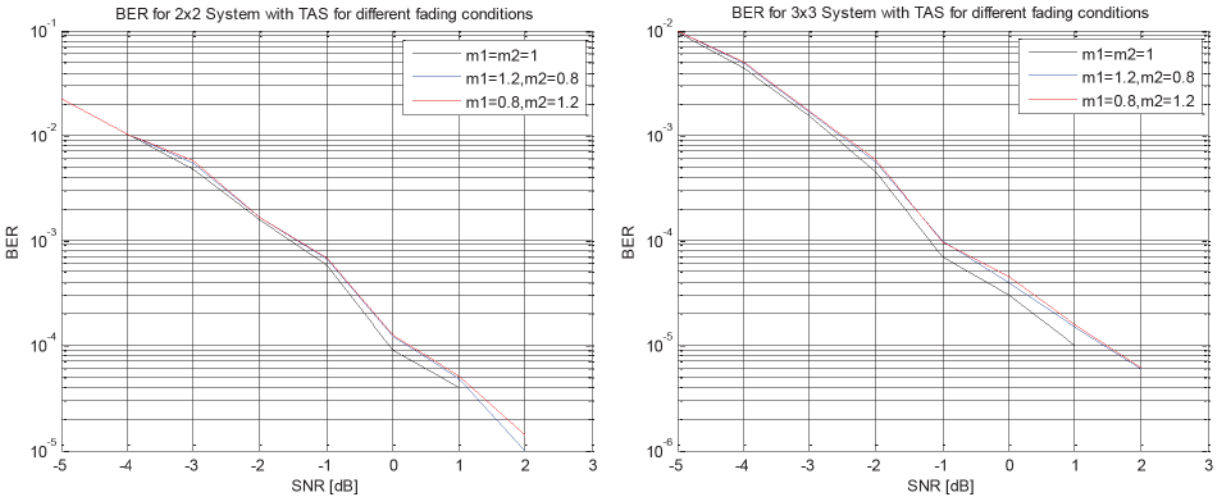

(a) (b)

Fig.5.20 BER for J-TR-AS with different fading parameter values,

(a) $(10{,}2;10{,}2)$ *(b)* $(10{,}3;10{,}3)$.

5.5 Chapter Summary and Conclusion

We have discussed three systems in this chapter, named as TAS, TAS-TR, and J-TR-AS. We have calculated their BERs and compared their levels of performance in various fading conditions.

Firstly, we performed Monte Carlo simulations for TAS, where single or multiple transmit antennas were selected out of the total N_t transmit antennas available. At the receiver there were either single or multiple antennas available. This gave us the equivalent SISO, SIMO, MISO, MIMO system models with TAS. MPSK modulation for *M = 2, and 4*, was considered. When a single transmit antenna was selected, the transmission over the selected transmit antenna was totally uncoded. However, when multiple transmit antennas were selected, the transmission was based on STBC with their orthogonality principle fulfilled. Similarly, when a single receive antenna was available, the data was received without any receive diversity exploited. And with multiple antennas available at the receiver MRC was performed at the receiver to combine the signals received over multiple receive antennas. The simulations were performed over Nakagami-*m* fading channel with different fading parametric values. We obtained the BERs for the simulations performed depending on the number of transmit antennas selected and the number of receive antennas available. We concluded that as the fading parameter decreased, the performance of the system improved. This was a consistent result obtained for different system models and was in accordance with the theoretical concept associated with the Nakagami-*m* fading parameters.

We then extended the process of TAS to a two-hop DAF system model. We carried out the simulations when single transmit antenna was selected. At the receiver, N_r were available for receiving the data symbols, thus forming an equivalent SIMO system model. An equivalent SISO system model is a special case of this when $N_r = 1$. Thus only a single antennas was activated during transmission and rest of the transmit antennas stayed in an

inactive mode. The knowledge of CSI of $(T-TR)$ channel path was the only available feedback to the transmitter for TAS. The destination had almost no knowledge of the CSI of $(T-TR)$ channel path thus no feedback was provided from the receiver to the transmitter. This kept the complexity of the overall system lowered due to single feedback path available at the transmitter. Unlike TAS, in TAS-TR MRC was performed in all the case even when there was only a single receive antennas available as the signals from the TR node and from the transmitter needed to be MRC combined. We noticed significant improvement in the BERs of the TAS-TR when compared to TAS. It was due to added diversity at the transmitter and the receiver due to an additional TR node. Antenna Selection further enhanced the performance of the overall system.

We further expanded the system model by performing antenna selection at both the transmitter and the receiver. We obtained the BERs for the cases when single transmit and receive antennas were selected followed by multiple transmit and receive antenna selection. The BERs for various system models after J-TR-AS were compared. As observed in Chapter-4 that by increasing the number of antennas at either end increased the performance, J-TR-AS gave similar results which proved the consistency of the results obtained for two-hop DAF with J-TR-AS with that of the baseline models. We further compared the BERs for TAS, TAS-TR, and J-TR-AS and noticed that joint selection at both ends gave the best overall performance.

For TAS-TR and J-TR-AS, we observed the sensitivity of the two systems in different fading conditions and noticed that the placement of the TR node between the transmitter and the receiver affected the performance of the system. We summarize the performance of various system models based on the fading channel parameter in Table 5.4 for TAS-TR and in Table 5.5 for J-TR-AS.

Table 5.4 Summary of equivalent system models for TAS-TR and their performance based on different values of fading parameter $'m'$.

TAS, $(N_t, L_t; N_r)$	**Equivalent System Model**	**Fading Parameter ' m'**	**Analysis**
$(N_t, 1; 1)$	SISO	1. $m_1 = m_2 = 2$ 2. $m_1 = 0.7$, $m_2 = 3.3$ 3. $m_1 = 3.3$, $m_2 = 0.7$ 4. $m_1 = 1, m_2 = 3$ 5. $m_1 = 3, m_2 = 1$	Best performance is achieved with $m_1 = m_2$. When $m_1 \neq m_2$, best performance is achieved when $m_2 > m_1$, i.e. when TR node is placed closer to the receiver, for both the cases when m_1 and m_2 are arbitrary real numbers and when m_1 and m_2 are integers.
$(N_t, L_t; 1)$ $L_t = 2,3$	MISO	1. $m_1 = m_2 = 1$ 2. $m_1 = 0.7$, $m_2 = 1.3$ 3. $m_1 = 1.3$, $m_2 = 0.7$	Best performance is achieved with $m_2 > m_1$. The performance starts to decline as m_1 is increased and m_2 is decreased.
$(N_t, 1; N_r)$ $N_r = 2$	SIMO	1. $m_1 = m_2 = 1$ 2. $m_1 = 0.8$, $m_2 = 1.2$ 3. $m_1 = 1.2$, $m_2 = 0.8$	Best performance is achieved with $m_2 > m_1$. The performance starts to decline as m_1 is increased and m_2 is decreased.
$(N_t, L_t; N_r)$ $L_t = 2,3$ $N_r = 2,3$	MIMO	1. $m_1 = m_2 = 1$ 2. $m_1 = 0.8$, $m_2 = 1.2$ 3. $m_1 = 1.2$, $m_2 = 0.8$	Best performance is achieved with $m_2 > m_1$. The performance starts to decline as m_1 is increased and m_2 is decreased.

Except for equivalent SISO models, which gives the best performance when $m_1 = m_2$, a consistency of results is observed when dealing with different fading conditions for

TAS-TR and the best performance is achieved when $m_2 > m_1$. For J-TR-AS all the system models give consistent results in different fading conditions. The best achievement is always achieved $m_1 = m_2$. When $m_1 \neq m_2$, the performance is not affected with $m_1 > m_2$ or vice-versa

Table 5.5 Summary of equivalent system models for J-TR-AS and their performance based on different values of fading parameter $'m'$.

J-TR-AS, $(N_t, L_t; N_r, L_r)$	**Equivalent System Model**	**Fading Parameter $'m'$**	**Analysis**
$(N_t, 1; N_r, 1)$	SISO	1. $m_1 = m_2 = 1$ 2. $m_1 = 1.2$, $m_2 = 0.8$ 3. $m_1 = 0.8$, $m_2 = 1.2$	Best performance is achieved with $m_1 = m_2$. When $m_1 \neq m_2$, the performance is not affected with $m_1 > m_2$ or vice-versa
$(N_t, L_t; N_r, 1)$ $L_t = 2, L_r = 1$	MISO	1. $m_1 = m_2 = 1$ 2. $m_1 = 1.2$, $m_2 = 0.8$ 3. $m_1 = 0.8$, $m_2 = 1.2$	Best performance is achieved with $m_1 = m_2$. When $m_1 \neq m_2$, the performance is not affected with $m_1 > m_2$ or vice-versa
$(N_t, 1; N_r, L_r)$ $L_t = 1, L_r = 2,3$	SIMO	1. $m_1 = m_2 = 1$ 2. $m_1 = 1.2$, $m_2 = 0.8$ 3. $m_1 = 0.8$, $m_2 = 1.2$	Best performance is achieved with $m_1 = m_2$. When $m_1 \neq m_2$, the performance is not affected with $m_1 > m_2$ or vice-versa
$(N_t, L_t; N_r, L_r)$ $L_t = 2,3; L_r = 2,3$	MIMO	1. $m_1 = m_2 = 1$ 2. $m_1 = 1.2$, $m_2 = 0.8$ 3. $m_1 = 0.8$, $m_2 = 1.2$	Best performance is achieved with $m_1 = m_2$. When $m_1 \neq m_2$, the performance is not affected with $m_1 > m_2$ or vice-versa

Chapter 6 – Joint Antenna Selection and Channel Estimation

Channel impairment is one of the major factors affecting the performance of wireless communication systems. In this chapter, we focus on estimating the channel to help improve the performance of the system. The purpose of this chapter is twofold:

1. Firstly, we present a feedback based method of channel estimation that provides the fading channel estimates and its approximate auto-regressive (AR) parameters. Depending on the use of preambles in the data structure and the generation of channel coefficients two algorithms have been discussed;
   - The Auto-Regressive Channel Approximation (ARA) algorithm which is bandwidth efficient and
   - The Joint LS Estimation and AR Channel Approximation (LS-ARA) algorithm which uses more bandwidth but shows better performance in terms of bit-error-rates (BER) as compared to the ARA algorithm.
2. Secondly, we present a joint channel estimation and antenna selection process based on one of the channel estimation algorithms developed that performs better in terms of improved bit error rates. We call this algorithm as J-AR-LS-AS.

First order Auto-regressive process is used to estimate and approximate the channel variations occurring in between the frames. Least Square Estimation algorithm is used to obtain the initial estimates of the fading channel followed by the AR process to approximate the channel coefficients.

6.1 Introduction

Signaling over a wireless channel is severely affected by the environmental radio propagation effects as the channel state may change within a very short time span. In most of the cases, it is assumed that the channel be constant and known prior [210]. However, such assumptions may not be feasible in real scenarios and there is always a need to estimate the channel state information (CSI). Typically when no CSI is available at the receiver, it becomes necessary to estimate and/or approximate the variations in the amplitude and the phase of the channel occurring as a factor of time. One way to deal with this situation is by taking advantage of the training-based methods, also known as pilot symbol assisted modulation (PSAM) [159].

Training based methods are readily available in the literature for single/multiple transmit/receive antenna systems [170], [211]. These methods are the most popularly used as they can be applied to any communication system with ease and proves quite effective in precisely compensating for the channel distortions. Pilot symbols known to the receiver are embedded into the frame and are transmitted over the channel. The receiver then uses this known sequence to reconstruct the transmitted waveform irrespective of the fact that the receiver might not have direct access to the transmitted signal. The channel is identified at the receiver by exploiting this known training sequence. In this chapter, we have focused on performing the following tasks:

1. **Development of Feedback based channel estimation algorithms** – In this the focus is on the family of training based channel identification algorithms considering a wireless transmission scheme where a constant and known training sequence is repeatedly inserted within the frames. A quasi-static Nakagami-*m* fading channel is considered for transmission. The channel variations remain constant over the entire frame but occur from one frame to another. In order to keep the complexity of the algorithm lower, first order

Auto-Regressive (AR) process has been used for modeling the fading process because the complexity of the filter increases with the order of the AR process. Assuming that very little channel knowledge is available at the receiver and no CSI at the transmitter, two algorithms have been proposed based on channel feedback to the transmitter. Thus, the discussions are on

- The development of a channel estimation algorithm to suit a wireless communication system with lower bandwidth availability where the pilot sequence is used only once, and
- The channel approximation and estimation algorithm for the communication systems with the availability of extra bandwidth where the pilot sequence can be inserted before every frame transmission.

Also, based on the availability of the BW at a particular time of transmission the pilot symbols can be inserted in or cut-off from the data sequence following a simple switch mechanism.

2. **Joint Antennas Selection and Channel Estimation** – In chapter – 5, the antenna selection process considering $(T - TR)$ and $(TR - R)$ channel paths only was discussed. The direct $(T - R)$ channel path was not considered in order to reduce the complexity involved in forming and selecting the $(L_t \times L_r)$ subsets for antenna selection. Thus, the CSI of this path remains unknown unless assuming perfect CSI for this direct channel path. This problem can be solved by performing the task of channel estimation on the direct $(T - R)$ channel paths to gain the channel knowledge. LS algorithm has been used for channel estimation of the direct path. The channel paths $(T - TR)$ and $(TR - R)$ need not be estimated as the antennas selection is already based on the channel paths with maximum power gains. This is discussed in detail in Section 6.3.

6.2 The Proposed Channel Estimation Algorithms

The Nakagami-*m* fading channel model used here is modeled based on the auto-regressive (AR) process. In the first case, a preamble is used to provide the initial channel estimates and CSI for frame transmission is approximated using the AR process. The channel is updated after every frame transmission and is provided to the transmitter as a feedback. This algorithm works well in scenarios where very little CSI is available and also very little bandwidth is wasted due to the use of once only pilot symbols. In the second case, a better approximation of the channel is provided by periodically inserting the preamble into the data sequence just before every frame transmission. The pilot symbols contained in the preamble provides the channel estimation and the channel is approximated using AR process for every frame. Thus, the AR parameters are estimated and are available to the transmitter via a feedback path. The whole data sequence is divided into L frames of length l. Each frame contains a particular sequence of data. Since the channel is quasi-static, the channel variation occurring from one frame to another is dependent on the channel state information of the previous frame obtained auto-regressively.

6.2.1 Auto-Regressive Channel Approximation (ARA) Algorithm

In this section, the first algorithm referred to as Auto-Regressive Channel Approximation (ARA) algorithm is presented.

Algorithm 1: AR Channel Approximation Algorithm (ARA)

1: **INPUT**: X_p, h_p, n_p,X_d, n_d, n_{AR}
2: **BEGIN**
3: Compute pilot sequence reception
4: Estimate the channel associated with pilot symbol transmission ($\boldsymbol{h_p}$) using LS channel estimator
5: Provide estimated channel feedback to the transmitter
6: **FOR** each frame transmitted **DO**
7: Provide the channel statistics for frame transmission
8: Compute the output received at the receiver
9: Compute the AR channel parameters
10: Update the channel statistics
11: **END FOR**
12: **END ARA**

Fig. 6.1 outlines the proposed algorithm based on the frame structure explained in Algorithm 1.

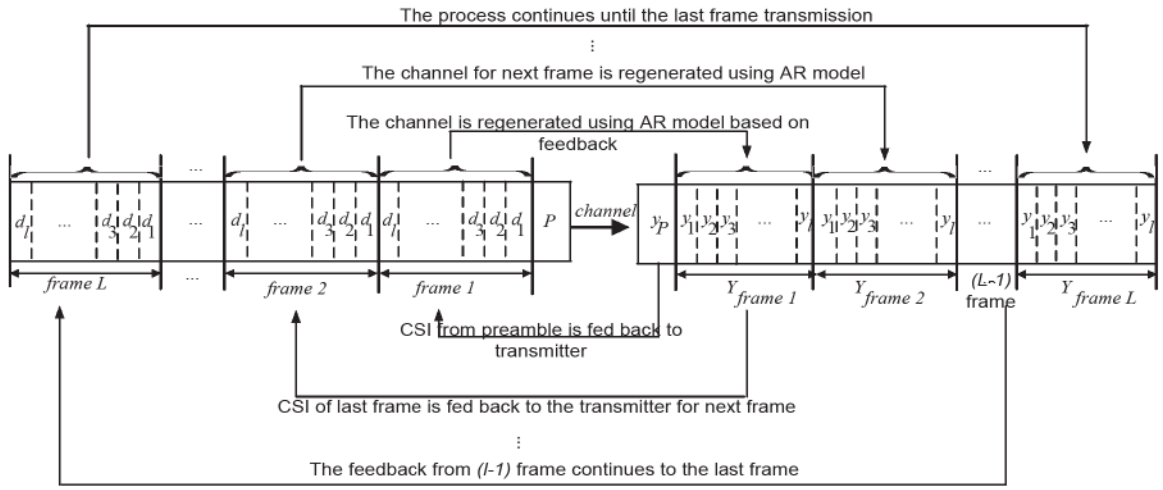

Fig. 6.1 Frame structure for Algorithm 1

It is assumed that the data sequence is divided into L frames and a preamble is attached only once at the start of data transmission. The transmission takes place with very little CSI available at the receiver and no knowledge at the transmitter.

The preamble is sent only once during the whole data transmission and not with every frame. The CSI associated with the preamble is exploited for channel estimation using LS channel estimator. The estimated channel knowledge is fed back to the transmitter where it is used for generating channel coefficients using the AR process. The frame is sent over the channel and the CSI associated with the AR generated channel coefficients are exploited at the receiver for receiving the frame. Thus the channel information attached with the previous transmitted frame is used to generate channel coefficients based on AR process, which are further used for next frame transmission. The process continues until the last frame transmission takes place. The detailed version of the frame structure explaining complete data transmission and the channel generation process are shown in Fig.6.1. The pilot sequence received at the receiver is computed based on the input parameters as follows

$$Y_p = h_p X_p + n_p \tag{6.1}$$

where $X_p = [x_{p1}\ x_{p2} \ldots x_{pp}]$ is the known pilot sequence

h_p is the channel associated with pilot symbol transmission

Y_p is the received pilot sequence.

n_p is the noise vector affecting the preamble transmission.

At any time instant t, pilot symbols are transmitted over Nakagami-*m* faded channel. At the receiver it is observed as Y_p. LS channel estimation takes place based on the LS algorithm according to which $h_{p_{LS}} = x^{\#}y$, where $x^{\#} = (x^H x)^{-1}x^H$ denotes the pseudo-inverse of x, and $h_{p_{LS}}$ is the channel estimate, which gives

$$h_{p_{LS}} = (x^H x)^{-1}x^H y \tag{6.2}$$

This estimated channel information $h_{p_{LS}}$ is sent back to the transmitter as a feedback h_d such that $h_d = h_{p_{LS}}$. The first frame transmission takes place over this LS estimated h_d. The output of the transmitted frame is computed based on the input parameters as follows

$X_d = [x_{d1}\ x_{d2}\ ...\ x_{dl}]$ is the data transmission vector

h_d is the channel feedback after estimation

Y_d is the received data sequence.

n_d is the noise vector affecting the transmission of data symbols,

Both the preamble matrix X_p and the data matrix X_d is assumed to be affected by different channels such that the receiver observes the data matrix as

$$Y_d = h_d X_d + n_d \tag{6.3}$$

The channel information h_d is now provided to the transmitter as a feedback such that $h_{t-1} = h_d$ where it is exploited to approximate the new channel statistics based on AR process as

$$h_{AR} = \sqrt{\alpha} h_{t-1} + \sqrt{1-\alpha^2} n_{AR} \tag{6.4}$$

Thus, the AR channel coefficients are generated based on the channel information obtained from the previously transmitted frame and the channel is now update as $h_d = h_{AR}$ for next frame transmission.

6.2.2 Joint LS Estimation and AR Channel Approximation (LS-ARA) Algorithm

In this section, another algorithm referred to as Joint LS Estimation and AR Channel Approximation (LS-ARA) is presented.

Algorithm 2: Joint LS Estimation and AR Channel Approximation Algorithm (LS-ARA)

1: **INPUT**: X_p, h_p, n_p,X_d, n_d, n_{AR}
2: **BEGIN**
3: **FOR** each frame transmitted **DO**
4: Compute pilot sequence reception
5: Estimate the channel associated with pilot symbol transmission (h_p)
6: Provide estimated channel feedback to the transmitter
7: Compute the output received a**t the rece**iver
8: Compute the AR channel parameters
9: Update the channel statistics for h_p
10: **END FOR**
11: **END LS-ARA**

Fig. 6.2 outlines the algorithm based on joint channel estimation and approximation as explained in Algorithm 2.

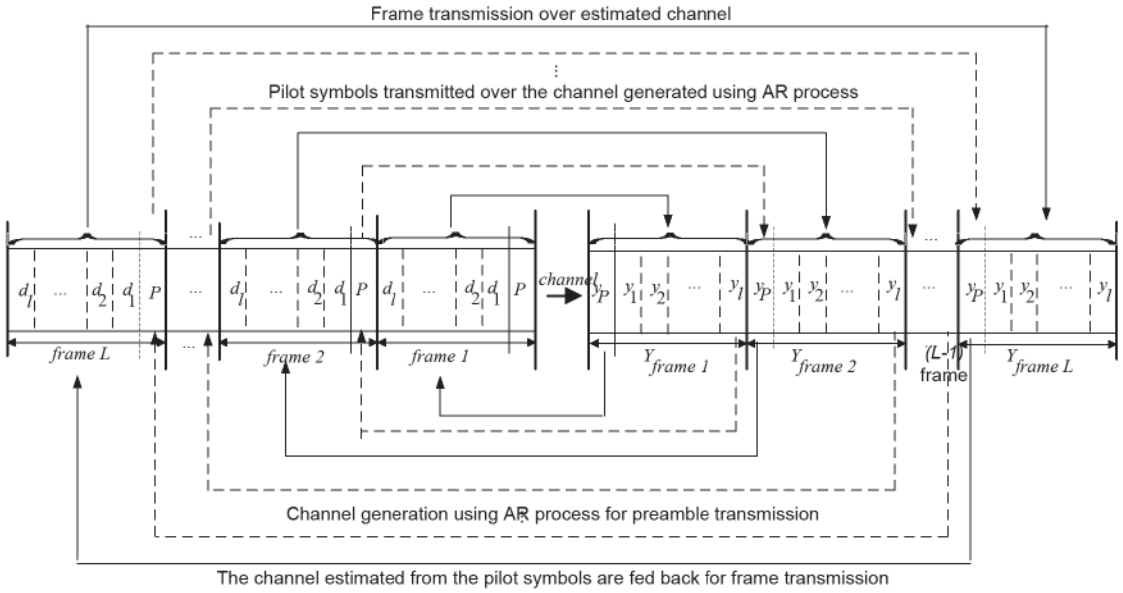

Fig. 6.2 Frame structure for Algorithm 2

The main idea of LS-ARA is to obtain a better approximation of the channel. The pilot symbols contained in the preamble are inserted periodically into the data sequence just before every frame transmission. When the first sequence of pilot symbols is transmitted, it provides an estimate of the channel. The frame transmission takes place over these estimated CSI which is now available at the transmitter as a feedback. When the frame transmission is

complete, the CSI associated with the frame is available for the next preamble where the channel is approximated using AR process. The pilot symbols are then sent over this newly approximated channel which is then estimated at the receiver and feedback to the transmitter for frame transmission. The process follows until the last frame transmission. In this way the channel is estimated as well as approximated thus giving better performance. The detailed version of the frame structure explaining complete data transmission process is shown in Fig.6.2. The dotted lines show pilot symbols transmission and the channel feedback to the preamble and bold line shows frame transmission and the associated channel feedback for frame transmission.

The process is similar as explained earlier for Algorithm 1 except that for Algorithm 1, the channel statistics are updated as $h_d = h_{AR}$ and the next frame transmission occurs according to (6.3) whereas for Algorithm 2 the channel information is updated for h_p according to $h_p = h_{AR}$ which is further used for transmitting pilot symbols and to estimate the AR parameters. While Algorithm 1 explains the channel approximations carried out using AR-process, Algorithm 2 explains the joint process of generation and estimation of the AR parameters using pilot symbols based LS estimator.

6.3 Joint Antenna Selection and Channel Estimation

The simulation results as presented in Section 6.4.1 obtained for the two algorithms developed in Section 6.2 shows that Algorithm-2 performs better than Algorithm-1 when compared in terms of the bit error rates. The focus is on using the LS-ARA algorithm for channel estimation. However, channel estimation based on the simple LS algorithm for the is also performed for the sake of comparison with the LS-ARA algorithm.

In chapter – 5, the process of joint transmit-receive antenna selection for the two-hop DAF relay based system was discussed. The $(T - TR)$ channel path was considered for transmit antenna selection and $(TR - R)$ channel path for receive antenna selection. Due to the use of a single antenna relay at the TR node, the TAS and RAS tasks via these two channel paths, respectively, were simplified. The direct path between the transmitter and the receiver was not considered for antenna selection due to the complexity involved in calculating the channel power gains from each transmit antenna to every receive antennas to form the subsets for antenna selection, as given by (5.11). Thus, we utilize the $(T - TR - R)$ channel path for antenna selection and the $(T - R)$ channel path for channel estimation of the direct path. The whole process is as explained:

As explained in Chapter – 5, pilot symbols are used for performing antenna selection. At the TR node, the channel power gains are calculated and the information is sent back to the transmitter and the antennas are selected. Similar process is performed at the receiver side for selecting the receivers. In this whole duration, no communication takes place between the transmitter and the receiver over the direct path. Also, the transmitter and the receiver receives the CSI of all the channel paths from $(T - TR)$ and $(TR - R)$ but no accurate information is still available at either end for the direct $(T - R)$ channel path. So, the question here arises, how to utilize this $(T - R)$ channel path?

One solution is utilizing this for the same task of antenna selection. But the complexity involved in this task is too much because of the subset formation form each transmit to every receive antenna. Another solution is to utilize this for channel estimation of the direct path. Based on this, we developed a Joint Antenna Selection and Channel Estimation Algorithm (J-AR-LA-AS), where the channel estimation is based on the LS-ARA Algorithm described in Section 6.2.2.

6.3.1 Joint Antenna Selection and Channel Estimation Algorithm (J-AR-LS-AS) Based on LS-ARA Algorithm

For channel estimation, one way is to transmit pilot symbols over all the N_t transmit antennas, performing LS estimation and providing CSI to the transmitter, then, transmitting information over the estimated channel and the selected antennas. However, this involves complexity as the channel estimates need to be obtained for the $N_t \times N_r$ channel paths. A less complex way is to wait for the feedback from the TR node. Once the transmit antennas are selected, transmit the pilot symbols over the selected transmitters. In the meantime, the receive antennas are selected and the pilot symbols are received over the selected receive antennas only, thus reducing the complexity of channel estimation from $N_t \times N_r$ channel paths to $L_t \times L_r$ channel paths. The J-AR-LS-AS is presented below:

Algorithm 3: Joint Antenna Selection and Channel Estimation Algorithm (J-AR-LS-AS)

1: **INPUT**: $X_p, h_1, h_2, h_3, n_{1p}, n_{2p}, n_{3p}$
$X_d, n_d, h_1, h_2, n_{AR}$
2: **BEGIN**
3: **FOR** each frame transmitted **DO**
4: Transmit $\boldsymbol{X_p}$ to TR node over $\boldsymbol{h_1}$
5: Receive Pilot Symbols $\boldsymbol{y_{1p}}$
6: Compute channel power gains of $\boldsymbol{h_1}$ and arrange in descending order
7: Select $\boldsymbol{L_t}$ transmit antennas out of $\boldsymbol{N_t}$ total available for data transmission
8: Transmit $\boldsymbol{X_p}$ over $\boldsymbol{h_3}$ using the selected $\boldsymbol{L_t}$ transmit antennas
9: At the same time, transmit $\boldsymbol{y_{1p}}$from the TR node to the receive over $\boldsymbol{h_2}$
10: Estimate the channel associated with pilot symbol transmission at the receiver using LS algorithm.
11: At the same time calculate the channel power gains associated with $\boldsymbol{h_2}$
12: Provide estimated channel feedback from the receiver to the transmitter.
13: Using the same feedback path provide information about the calculated channel power gains to the transmitter. Also provide feedback to the TR node for receive antenna selection.
14: The transmitter now has the knowledge about $\boldsymbol{L_t}$ transmit, $\boldsymbol{L_r}$ receive antennas selected and the estimated channel $\boldsymbol{h_3}$
15: The TR node and the receiver has the knowledge of $\boldsymbol{L_r}$ receive antennas selected
16: Transmit information $\boldsymbol{X_d}$ to the TR node over $\boldsymbol{h_1}$ and to the receiver over estimated $\boldsymbol{h_{3p}}$ using $\boldsymbol{L_t}$ transmit antennas to the $\boldsymbol{L_r}$ receive antennas
17: Compute the output received at the receiver and combine using MRC as explained in Chapter-3
18: Compute the AR channel parameters
19: Update the channel statistics for $\boldsymbol{h_3}$
20: **END FOR**
21: **END J-AR-LS-AS**

The Antenna Selection process is explained in detail in Chapter – 5 and the LS-ARA Algorithm is described in Section 6.2.2. It is worthwhile to mention here that while performing the task of channel estimation, the CSI available from the previous frame is used to auto-regressively approximate the CSI for the next frame. As explained in Section 6.2.2, it uses a little extra bandwidth but provides better estimates of the channel. For comparison, we have presented simulation results for the case when the pilot symbols are estimated using LS algorithm but are not auto-regressively regenerated. This is referred to as J-LS-AS Algorithm.

This algorithm is similar to Algorithm 3 except that Steps 18 and 19 are not performed. Also for every frame transmission it is assumed that some partial CSI is available at the transmitter unlike in J-AR-LS-AS where the CSI for every next frame transmission is obtained from the previous frame transmitted.

6.4 Performance Analysis

In this section we first compare the simulation results obtained from the approximation and estimation of AR fading channel parameters. We then perform MATLAB simulations to obtain BER for the two-hop DAF relay system with joint antenna selection and channel estimation based on the channel estimation algorithm that gives better BERs. The channel under consideration is quasi-static Nakagami-*m* fading channel and the modulation considered is BPSK and QPSK.

6.4.1 Comparison of the Developed Channel Estimation Algorithms

The following parameters have been used for the simulations.

Table 6.1. Set of Simulation Parameters used

Parameters	**Types/Values**
Channel Type	Quasi-Static
Channel Statistics	Nakagami-*m*
Fading parameter, *m*	1
Number of frames	10^5
Frame Length	100
Pilot Length	4
Modulation Type	BPSK and QPSK
Max. Doppler Frequency, f_d	250 Hz
Symbol Frequency, f_s	5 ksps
Doppler Rate, $f_d T_s$	0.05

The parameters used in this thesis are quite close to the ones used in [212]. Since in [212], Rayleigh fading is considered, so the fading parameter $m = 1$ is used to provide close comparisons of the results obtained. The coefficient α is related to the Doppler spread f_d according to the first order approximation of Jakes channel model as $\alpha = J_0(2\pi f_d T_s)$ where $f_d T_s$ is used as the measure for fading rate. Typically its value falls in the range of (0.01-0.1).

In the first algorithm, very little channel knowledge is known which is approximated using the LS estimator and the channel is approximated using first order AR channel simulator given by (6.4). In the second algorithm the AR channel parameters are approximated and estimated based on the channel statistics available from the pilot symbols.

Fig. 6.3 plots the bit-error-rates (BER) of the simulation results for Algorithm 1 for BPSK and QPSK modulation. To obtain these results, the pilot sequence was sent only once with the first frame during the start of data transmission. The channel was estimated using the LS algorithm and the CSI was fed back to the transmitter. For the rest of the frames, the CSI was auto-regressively recovered, as explained in Section 6.2.1, and fed back to the transmitter until all the frames were transmitted. For comparison, the BER when the channel is perfectly known is also shown.

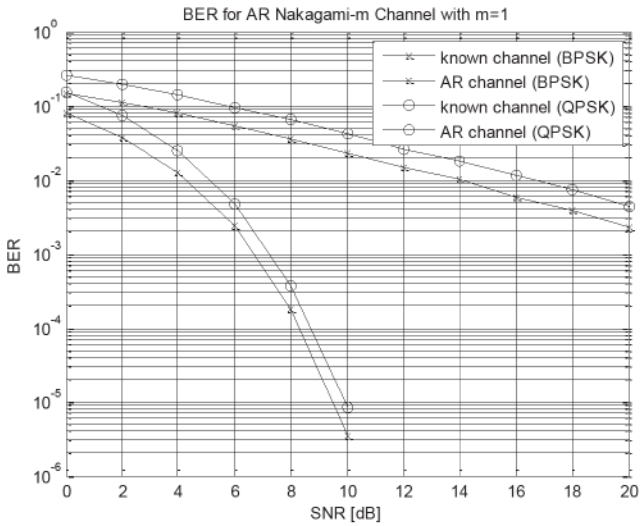

Fig. 6.3 BER Performance of the Algorithm-1

Fig. 6.4 plots the BER of the two algorithms for BPSK and QPSK modulation and compares their performance. While simulating Algorithm 2, the pilot sequence was inserted periodically at the start of each frame and the channel was estimated at the receiver using the pilot sequence based on LS algorithm. The data transmission took place over these estimated channel coefficients. For the pilot sequence transmission of the second frame, the CSI is

approximated using the AR process and then transmitted over these newly generated channel coefficients which are again LS estimated at the receiver and fed back to the transmitter for data transmission as explained in Section 6.2.2. The process continued until all the frames were transmitted and the bit errors were averaged over the entire data sequence.

It can be observed that when the pilot symbols are periodically inserted in between the data sequence, the system shows an improved performance of around 2dB at an average SNR in terms of BER as compared to when the pilot symbols were inserted just once at the start of the data sequence. This can be explained on the basis as described in section 6.2 that while Algorithm 1 focuses mainly on the approximation of the channel statistics, Algorithm 2 considers approximating the AR parameters of the pilot sequence along with estimating the channel coefficients for transmitting data sequence. Thus Algorithm 2 proves to provide a better performance that algorithm 1 when the channel statistics are periodically estimated.

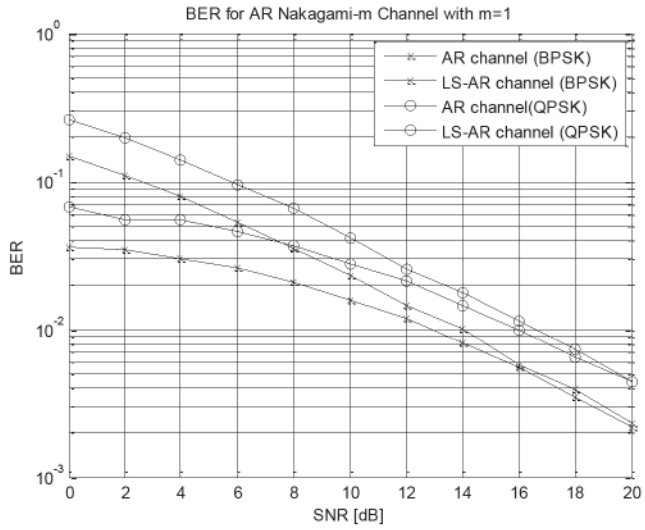

Fig. 6.4 BER Performance of the Algorithm-2 and its comparison with Algorithm-1

At lower SNR values, Algorithm 2 shows a very high performance improvement over Algorithm 1 whereas at higher SNR values, the performance of the two algorithms appears to be quite similar with a very little improvement from Algorithm 2.

Fig. 6.5 plots the frame-error-rates (FER) for Algorithm 1 and the known channel and Fig. 6.6 plots the FER for Algorithm 1 and Algorithm 2 for BPSK and QPSK modulation. The comparisons are in accordance with the description of the two algorithms.

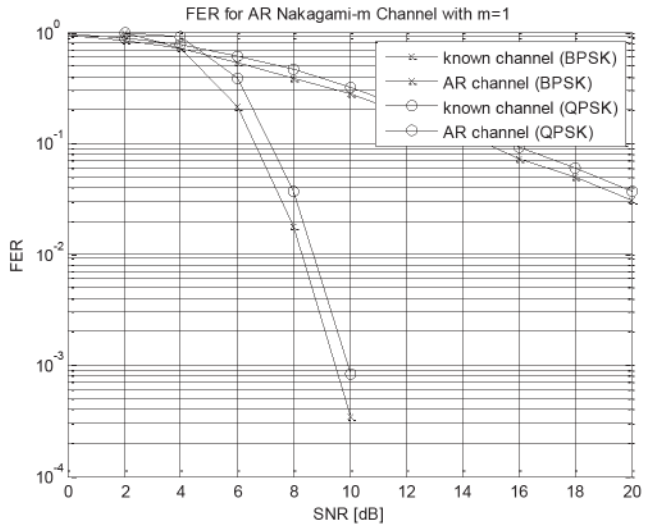

Fig. 6.5 FER Performance of the Algorithm-1

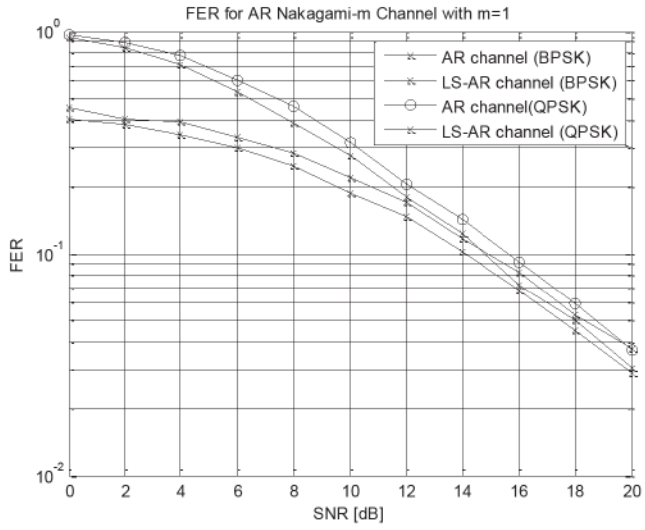

Fig. 6.6 FER Performance of Algorithm-2 and its comparison with Algorithm-1.

The BER and FER for the two algorithms have been summarized in Table 6.2 for QPSK and BPSK modulation and it can be seen that as the SNR increases the BER decreases. The BER for Algorithm 2 has lower values than Algorithm 1 at different SNR values.

Table 6.2. BER and FER at different SNR values

SNR	BPSK		QPSK	
	BER	FER	BER	FER
2dB				
Known channel	0.0374	0.9778	0.0736	0.9995
AR Channel	0.1085	0.8417	0.1955	0.8897
LS-AR Channel	0.0348	0.3841	0.0556	0.4021
6dB				
Known channel	0.0023	0.2114	0.0047	0.3807
AR Channel	0.0525	0.5350	0.0948	0.6064
LS-AR Channel	0.0259	0.2983	0.0459	0.3350
10dB				
Known channel	$3.4\text{x}10^{-6}$	0.0003	$8.2\text{x}10^{-6}$	0.0008
AR Chanel	0.0232	0.2763	0.0416	0.3416
LS-AR Channel	0.0157	0.1868	0.0275	0.2200

In [212], the simulation is done for BPSK over Rayleigh faded channel. We have approximated the BER at different values based on Fig. 6 in [212] and summarized them in Table 6.3. The BER values for the two proposed algorithms are also shown in Table 6.3. It can be seen that the BER values of the two proposed algorithms are lower in comparison to the BER values given in [212] at the same SNR in approximately the same fading environment.

Table 6.3. BER comparison at different SNR values

SNR	10dB	15dB	20dB
Ref. [5]	0.0391	0.0297	0.0163
AR Channel	0.0224	0.0078	0.0023
LS-AR Channel	0.0163	0.0065	0.0022

6.4.2 BER Calculations for Joint Antenna Selection and Channel Estimation Algorithm (J-AR-LS-AS)

In this section we present the simulation results obtained from MATLAB modeling of Algorithm 3. Before that we present a few simulation results for the case when the channel estimates are obtained using only the LS algorithm at the receiver and the channel estimates are not auto-regressively regenerated as in LS-ARA algorithm. For convenience we name it as J-LS-AS Algorithm. Then we present the simulation results obtained by modeling J-AR-LS-AS Algorithm and compare its performance with the J-LS-AS Algorithm. The parameters used for the simulations are summarized in Table 6.4.

Table 6.4 Set of Simulation Parameters used

Parameters	**Types/Values**
Channel Statistics	Nakagami-m
Fading parameter, m	varying
Number of frames	10^3
Frame Length	100
Pilot Length	4
Modulation Type	QPSK (other MPSK schemes can be used)
Max. Doppler Frequency, f_d	250 Hz
Symbol Frequency, f_s	5 ksps
Doppler Rate, $f_d T_s$	0.05

6.4.2.1 BERs of J-LS-AS and its comparison with JAS

Fig. 6.7 presents the BERs for the J-LS-AS for a$(N_t, 1; N_r, 1)$ system. For the direct channel path for JAS, it was assumed that partial CSI is available at the transmitter whereas for the J-LS-AS, the direct channel path was estimated using LS algorithm. Better BERs are achieved when the channel is estimated though marginally as can be seen from Fig. 6.7 (a). Performance improvement of approximately 0.5 dB is achieved at lower SNRs. However, at

higher SNRs, the performance improvement is just below 0.5dB. In Fig. 6.7 (b), we have presented the BERs for J-LS-AS for different fading parameter *'m'*. As shown in Appendix A.1, the BER improves with lower values of *'m'*, it can be seen that when $m_1 = m_2 = 2$, the system performs better as compared to the case when $m_1 = m_2 = 1$. This is in accordance with the fact that lower fading parameter means less fading and improved performance. However, when $m_1 \neq m_2$, better performance is achieved when $m_1 > m_2$, i.e., the channel fading between $(T - TR)$ is less that the fading between $(TR - R)$ channel path.

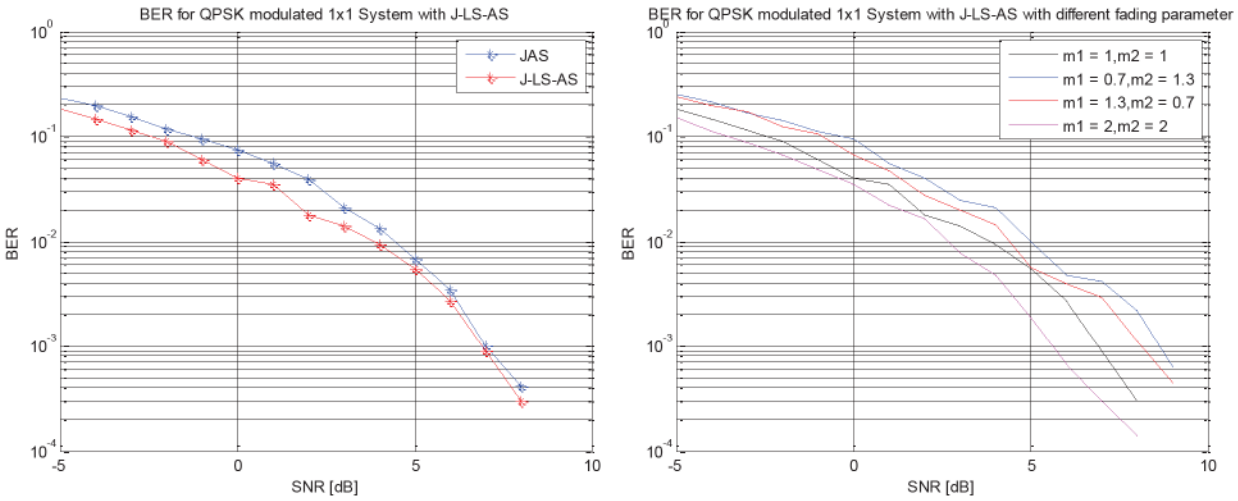

(a) (b)

Fig. 6.7 BER for J-LS-AS Algorithm for $(N_t, 1; N_r, 1)$ *QPSK system*

(a) Comparison with JAS for m=1 (b) Comparison in different fading conditions

Fig. 6.8 presents the BERs for the J-LS-AS for a$(N_t, 1; N_r, L_r)$ system. Performance improvement of approximately 0.7dB is achieved at higher SNRs. In different fading conditions, similar results are obtained as in Fig. 6.7 (b). The best performance is achieved when $m_1 = m_2$. When $m_1 \neq m_2$, better performance is achieved when the $m_1 > m_2$.

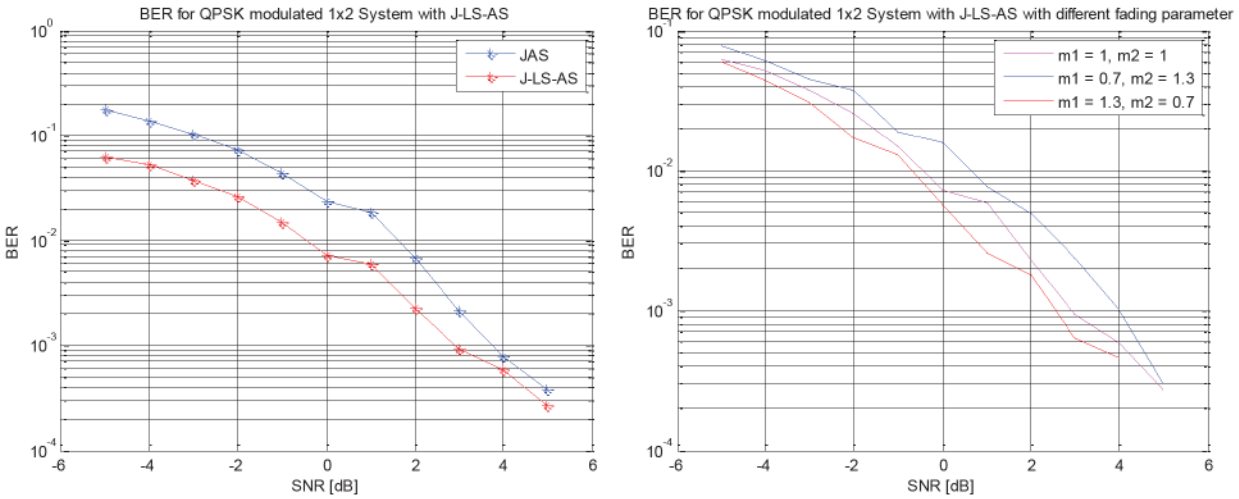

(a) (b)

Fig. 6.8 BER for J-LS-AS Algorithm for $(N_t, 1; N_r, L_r)$ QPSK system

(a) Comparison with JAS for m=1 (b) Comparison in different fading conditions

Fig. 6.9 presents the BERs for the J-LS-AS for a $(N_t, L_t; N_r, L_r)$ system. Marginal performance improvements can be seen with channel estimation when comparing the two systems. In different fading conditions, the best performance is achieved when $m_1 > m_2$ unlike in $(N_t, 1; N_r, 1)$ and $(N_t, 1; N_r, L_r)$ systems where the best performance is achieved with $m_1 = m_2$. The performance degraded when $m_1 < m_2$ as can be seen from Fig. 6.9 (b)

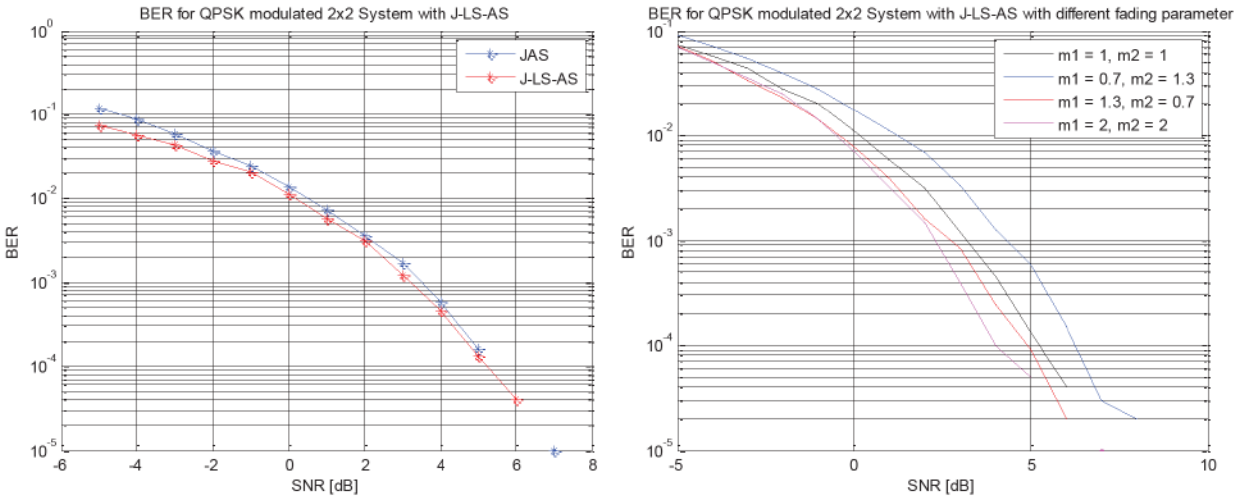

(a) (b)

Fig. 6.9 BER for J-LS-AS Algorithm for $(N_t, L_t; N_r, L_r)$ QPSK system

(a) Comparison with JAS for m=1 (b) Comparison in different fading conditions

6.4.2.2 BERs of J-AR-LS-AS and its comparison with J-LS-AS and JAS.

In this section the simulation results for the J-AR-LS-AS model are presented and are compared with the J-LS-AS and JAS models. The simulations were performed following Algorithm 3 where the channel coefficients for pilot symbol transmission were regenerated using first order auto-regressive process. The performance improvement can be seen from Fig. 6.10 (a) in terms of BER. Though at lower SNRs, there is very little improvement in BERs but at higher SNRS, performance improvement of approximately 1dB was achieved. In Fig. 6.10 (b), we have tested the performance of the system in different fading conditions. We can see that the best performance is achieved when $m_1 = m_2$. When $m_1 \neq m_2$, better performance is achieved when $m_1 > m_2$, which is in accordance with the results obtained with J-LS-AS in different fading conditions.

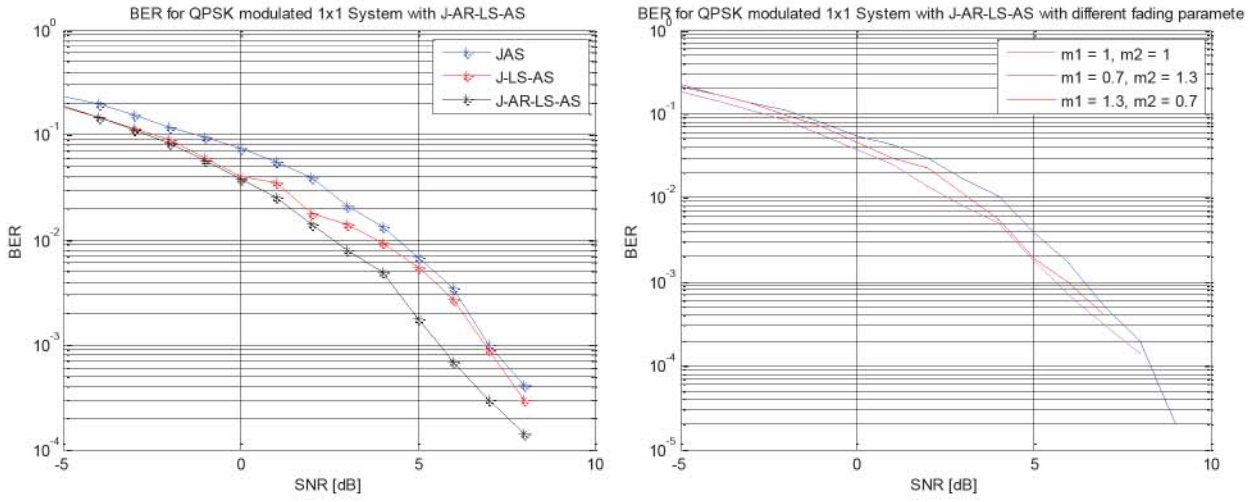

(a) (b)

Fig. 6.10 BER for J-AR-LS-AS Algorithm for $(N_t, 1; N_r, 1)$ *QPSK system*

(a) Comparison with J-LS-AS and JAS for m=1

(b) Comparison in different fading conditions

Simulation Results for $(N_t, L_t; N_r, L_r)$ QPSK system with J-AR-LS-AS are presented in Fig. 6.11. A performance improvement of approximately 0.9dB has been achieved when

the channel coefficients are regenerated using AR process when compared to the channel estimation using LS algorithm alone. In Fig. 6.11 (b), BERs in different fading conditions are plotted and the graph shows that the best performance is achieved when $m_1 = m_2$ and the performance degrades as m_1 is decreased over m_2.

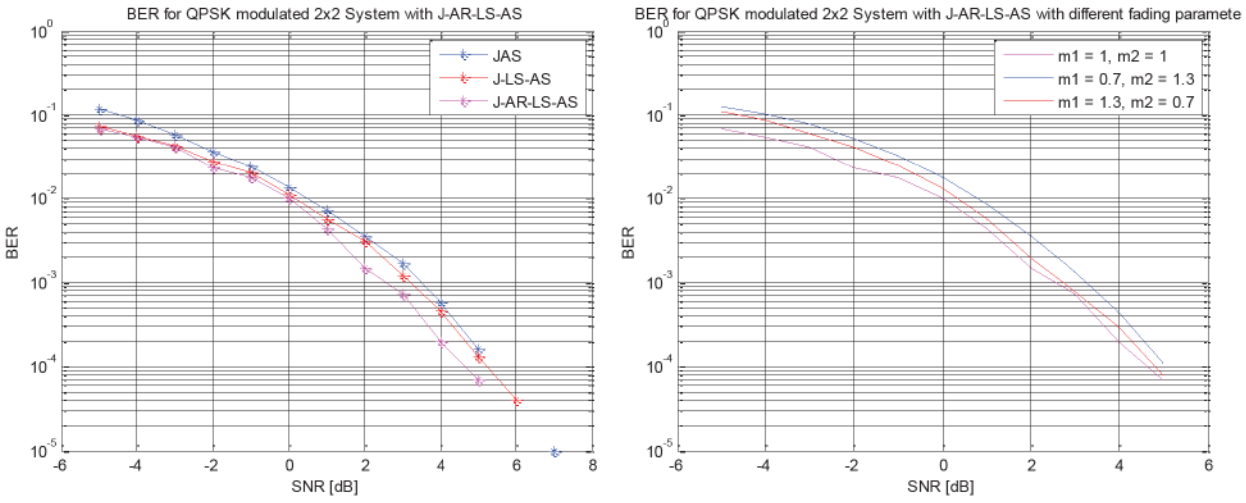

(a) (b)

Fig. 6.11 BER for J-AR-LS-AS Algorithm for $(N_t, L_t; N_r, L_r)$ QPSK system

(a) Comparison with J-LS-AS and JAS for m=1

(b) Comparison in different fading conditions

6.5 Summary and Conclusions

In this chapter we have presented a feedback based method for channel approximation based on AR process followed by channel estimation of AR parameters for quasi-static channels. As the proposed methods are based on the fact that very little channel knowledge is available, pilot symbols have been used to exploit this channel information which is provided to the AR simulator for channel coefficients approximation. These pilot symbols are further used for estimating the AR channel coefficients for every frame. Since the pilot symbols are used only once in Algorithm 1 at the start of the data transmission no wastage of bandwidth takes place. However, in Algorithm 2, pilot symbols are inserted periodically in between the data sequence before the transmission of every frame. It can be concluded from the simulation results that more robust channel state information is achieved when pilot symbols are periodically inserted as it provides provision for estimation of the AR parameters thus improving the BER as compared to the channel statistics of Algorithm 1 for same amount of SNR. Hence a trade-off between the available bandwidth and the bit error rates needs to be maintained when considering the two algorithms. We have further used Algorithm 2 to estimate the channel for the direct path for a two-hop DAF relay system. By using the direct path for channel estimation rather than antenna selection, the complexity of the system has been reduced. The simulation results present here are for QPSK modulation, however, they can be easily elaborated to higher PSK constellations for different values of fading parameter $'m'$. For simplicity, the channel coefficients in this chapter were approximated based on the first order AR process only. In future, the algorithms presented in this paper can be elaborated for higher order AR process and also the data can be modulated using other complex modulation schemes to fit the needs of the advanced wireless communication systems.

Chapter 7 – Conclusions and Future Directions

In this chapter we present the main contributions of the thesis and suggest future work.

7.1 Summary of Contributions

This research has addressed areas of transmit and receive diversity to combat the effects of channel fading, relay transmission for increased diversity, effects of channel fading on the performance of the relay systems, antenna selection for improved cost and complexity and channel estimation and modeling for further enhancing the performance in wireless communication systems. A union of these areas led to the following major contributions:

An extensive literature survey on the various components required for designing a wireless system model was conducted. Nakagami-*m* distribution provided the best fit for our system model where we have considered the performance based on the movements of the relay node. OSTBC at the transmitter proved to be more efficient in terms of their lower complexity while coding at the transmitter and decoding at the receiver. MRC at the receiver further aided in improving BERs as it is the best combining techniques in terms of improved

BER. MIMO systems are a proven method for excellent performance enhancements in terms of data transmission rate and interference reduction, but they have the drawback of increased cost and power. Relay transmission has proven to provide increased diversity with lower associated cost and power. Antenna Selection strategies have provided another insight in to the cost effectiveness of the MIMO wireless systems so we use them to further enhance the performance of the system. The transmission take place over a wireless channel there is some information associated with this channel known as channel state information (CSI). Assuming that CSI is always known is a hypothetical case. In real-time applications, CSI needs to be calculated. There are a range of channel estimation algorithms available in literature. LS algorithm is the simplest of them all which requires less power and still effective so we concentrated on using LS algorithm for channel estimation.

An extensive literature review on MIMO systems and relay transmission provided directions for this research. As the demand for reliable and efficient communication systems increases, the major concern comes up to minimize the error probability of the received signal. By making efficient use of power and available bandwidth on one hand and minimize the system complexity on the other hand, the cost and processing time of the overall wireless communication system can be significantly reduced. A simplified two-hop hybrid relay system was successfully developed which utilized less energy as compared to the conventional system model with same of transmit and receive antennas. The developed system performed better than the existing conventional systems. The developed system is adaptive to any number of transmit and receive antennas, thus, in practice can be used for either of the SISO, SIMO, MISO, and MIMO system models. Use of OSTBC at the transmitter for encoding kept the complexity of coding the signals to a low and the use of maximum likelihood decision decoding kept the complexity of decoding the received bits to low at the receiver. Use of MRC gave the best possible results in terms of BER. The

developed is sensitive to fading conditions and even a slight change in the fading conditions affected the performance of the system, thus, the developed system is capable of working under different fading conditions. However, different system models with different number of antenna elements behaved differently based on whether the TR node was moved towards the source or the destination. Thus, the system is also sensitive to the number of available antennas elements at either end.

Antenna selection techniques proved their promising solution to high cost MIMO systems using multiple expensive RF chains. For the same reasons, antennas selection techniques can be applied to relay transmission with multiple antennas at the source at the destination. Unlike antenna selection in conventional MIMO systems, where the feedback path from the destination to the source is provided to carry information about the antennas to be selected, in this thesis, we have provided the feedback path from the relay to the source. This reduced the computational complexity of calculating the subsets from each transmit to each receive antenna thus reducing the processing power. Through simulations it has been proved that TAS on two-hop hybrid relay systems performed better than the TAS on the conventional wireless systems in terms of improved BER. The J-TR-AS further performed better than the TAS on two-hop hybrid relay systems. The developed TAS and J-TS-AS for the two-hop hybrid relay systems in this thesis are adaptive to any number of transmit and receive antennas. In this thesis, we have provided antennas selection with ten transmit and receive antennas out of which we were capable of selecting one, two, three transmit/receive antennas. Till date no antenna selection has been done with such high number of transmit and receive antennas. The developed TAS and J-TS-AS for the two-hop hybrid relay systems are also adaptive to various fading conditions as has been proved through simulations. Overall, we have successfully developed a simplified TAS and J-TS-AS for the two-hop hybrid relay systems which is less complex than the existing antenna selection techniques, uses less power

at the relay, works in different fading conditions, is adaptive to any number of transmit and receive antennas and above all gives improved performance.

Channel Estimation Algorithms has proved that transmission over a known channel gives better results. Since there is an existing feedback path in the system for the purpose of selection of antennas, we decided to utilize this path for providing CSI to the transmitter. For this purpose, we developed two feedback based channel estimation algorithms depending on the use of preambles in the data structure and the generation of channel coefficients using LS algorithm. Since we have assumed a quasi-static channel, the variations in channel after every frame transmission have been approximated using first order auto-regressive process. The Auto-Regressive Channel Approximation (ARA) algorithm proved to be bandwidth efficient where the pilot symbols are inserted only once at the start of data transmission. We also call this algorithm as Algorithm – 1, and the Joint LS Estimation and AR Channel Approximation (LS-ARA) algorithm gave better performance in terms of bit-error-rates (BER) as compared to the ARA algorithm but used more bandwidth as the pilot symbols were periodically inserted before every frame transmission and is called as Algorithm – 2. It was concluded from the simulation results that more robust channel state information was achieved when pilot symbols were periodically inserted as it provided provision for estimation of the AR parameters thus improving the BER as compared to the channel statistics of Algorithm 1 for same amount of SNR.

We have further used Algorithm 2 to estimate the channel for the two-hop DAF relay system. Antenna Selection used only the source-relay-destination path and in the mean time the direct source-destination path remained idle. So we used this direct path for channel estimation. By using the direct path for channel estimation rather than antenna selection, the complexity of the system was reduced. Thus, we developed a joint channel estimation and antenna selection process based on a simple LS algorithm which uses the first order AR

process for approximating the CSI for every next frame based on the CSI from the previous frame transmission. We called this algorithm as J-AR-LS-AS and it proved to perform better when CSI was performed in terms of improved bit error rates. The J-AR-LS-AS system also proved to be sensitive to changes in the fading conditions between the source-relay channel path and the relay-destination channel path, thus, adaptive to work under different fading conditions.

7.2 Suggestion for Further Study

The development of the two-hop hybrid relay with applied antenna selection techniques and channel estimation appeared to perform better with improved BER, less computational complexity, lower power consumption thus giving better quality, wider coverage and more services. Though this development gave a better insight into the performance of the relay based transmission systems, there are still many issues to be resolved.

- We have assumed that the Nakagami-m fading coefficients are i.i.d. However, in practical situation, the correlation between the fading coefficients still exists because of the physical limitations for smaller device forcing the antennas to be spaced closely. The correlation may significantly influence the performance of transmission system. It is worth further investigating into error performance over correlated Nakagami-*m* fading channels.
- The evaluations in this thesis are based on statistical Nakagami-*m* fading channels which can be further elaborated and performed using measurement-based channel models for sub-urban and urban environments like geometric channel models which are more capable in changing environments and hence are more accurate.
- In this thesis, we have focused on MPSK family of modulation and it is worth trying the system with other modulation schemes like PSAM, QAM etc. to have an insight into the change in performance levels.
- In order to satisfy the increasing demands of the growing number of users on data rates, the mobile communication system needs to be designed in a way to send bits faster within a given bandwidth. The main aim of the next generation mobile communications system is to seamlessly integrate a wide variety of communication services such as high

speed data, video and multimedia traffic as well as voice signals. Hence a search lies for higher spectral efficiency.

- So far, all the works presented in this thesis have focused on the flat fading case where only spatial diversity is available. However, future wireless communication systems will transmit information with symbol duration much smaller than the channel delay spread and consequently frequency-selectivity will arise in the channel. Future work will look at system model capable of performing over frequency selective channels that can exploit both spatial and multipath diversity.
- As we have focused on flat fading channels, the ISI between the symbols have been ignored. In future, relay transmission systems employing orthogonal frequency division multiplexing (OFDM) space-time coding with single carrier frequency domain equalization (SC-FDE) techniques can be used which account for ISI as well. Both the schemes work in frequency-selective environments and have the advantage of lower processing complexity.
- In channel estimation, training–based channel estimation is used. However, the available bandwidth will be occupied by training sequence. The future research might be the inclusion of blind channel estimation for possible improvement in the system.

References

[1] J. H. Winters, "On the capacity of radio communication systems with diversity in a Rayleigh fading environment," *IEEE J. Select. Areas Commun.*, vol. 5, pp. 871–878, June 1987.

[2] I. E. Telatar, "Capacity of multi-antenna Gaussian channels," *Europ. Trans. Telecommun.*, vol. 10, no. 6, pp. 585–595, Nov./Dec. 1999.

[3] G. J. Foschini and M. J. Gans, "On limits of wireless communications in a fading environment when using multiple antennas," *Wireless Pers. Commun.*, vol. 6, no. 3, pp. 311–335, Mar. 1998.

[4] G. J. Foschini, "Layered space-time architecture for wireless communication in a fading environment when using multi-element antennas," *Bell Labs Tech. J.*, vol. 1, no. 2, pp. 41–59, Autumn 1996.

[5] E. C. Van Der Meulen, "Three terminal communication channels," *Advances in Applied Probability*, vol. 3, no. 1, pp.120 – 154, Spring 1971.

[6] T. M. Cover, and A. A. El Gamal, "Capacity theorems for the relay channel," *IEEE Trans. on Inform. Theory,* vol. 25, no. 5, pp. 572 – 584, 1979.

[7] J. N. Laneman, D. N. C. Tse, and G. W. Wornell, "Cooperative diversity in wireless networks: Efficient protocols and outage behavior," *IEEE Trans. on Inform. Theory*, vol. 50, no. 12, pp. 3062 – 3080, 2004.

[8] K. Loa, C. C. Wu, S. T. Sheu, Y. Yuan, M. Chion, D. Huo, and L. Xu, "IMT-advanced relay standards," *IEEE Communications Magazine*, vol. 48, no. 8, Aug. 2010.

[9] Z. Rui, Y. Fei, and Y. L. Xi, "Relay-Assisted Cooperative Communication Networks," *ZTE Communications magazine*, no. 3, 2008.

[10] M. R. Souryal, and B. R. Vojcic, "Performance of amplify-and-forward and decode-and-forward relaying in Rayleigh fading with turbo codes," in Proc. IEEE International

Conference on Acoustics, Speech and Signal Processing (ICASSP 2006), pp. IV - IV, 14-19 May 2006.

[11] T. A. Tsiftsis, G. K. Karagiannidis, P. T. Mathiopoulos, and S. A. Kotsopoulos, "Nonregenerative dual-hop cooperative links with selection diversity," *EURASIP Journal on Wireless Commun. and Networking*, vol. 2006, Article ID 17862, 8 pages, 2006.

[12] H. A. Suraweera, R. H. Y. Louie, Y. Li, G. K. Karagiannidis, and B. Vucetic, "Two hop amplify-and-forward transmission in mixed Rayleigh and Rician fading channels," *IEEE Commun. Letters*, vol. 13, no. 4, pp. 227–229, 2009.

[13] M. O. Hasna, and M. S. Alouini, "Performance analysis of two-hop relayed transmissions over Rayleigh fading channels," *in Proc. 56th IEEE Vehicular Technology Conference, 2002. VTC 2002-Fall,* vol.4, pp. 1992 – 1996, 2002.

[14] I. H. Lee, and D. Kim, "End-to-end BER analysis for dual-hop OSTBC transmissions over Rayleigh fading channels" *IEEE Trans Commun.*, vol. 56, pp. 347 ‐ 351, 2008.

[15] R. H. Y. Louie, Y. Li, and B. Vucetic, "Performance analysis of beamforming in two hop amplify and forward relay networks," *in Proc. of the IEEE International Conf. on Commun. (ICC '08),* pp. 4311–4315, Beijing, China, 2008.

[16] S. Chen, W. Wang, X. Zhang, and Z. Sun, "Performance analysis of OSTBC transmission in amplify-and-forward cooperative relay networks," *IEEE Trans. on Veh. Tech.*, vol. 59, no. 1, pp. 105–113, 2010.

[17] N. C. Beaulieu, and J. Hu, "A closed-form expression for the outage probability of decode-and-forward relaying in dissimilar Rayleigh fading channels," *IEEE Commun. Letters,* vol. 10, no. 12, pp. 813 – 815, 2006.

[18] I. H. Lee, and D. Kim, "BER analysis for decode-and-forward relaying in dissimilar Rayleigh fading channels," *IEEE Commun. Letters*, vol. 11, no. 1, pp. 52 – 54, 2007.

[19] Q. Zhao, and H. Li, "Performance analysis of an amplify-based differential modulation for wireless relay networks under Nakagami-m fading channels," *in Proc. IEEE 6th Workshop on Signal Processing Advances in Wireless Communications, (SPAWC'05),* New York, NY, USA, Piscataway, NJ, USA, pp. 211 – 215, 5 – 8 Jun, 2005.

[20] B. Maham, and A. Hjørungnes, "Asymptotic performance analysis of amplify-and-forward cooperative networks in a Nakagami-m fading environment," *IEEE Commun. Letters*, vol. 13, no. 5, pp. 300 – 302, May 2009.

[21] S. Ikki, and M. H. Ahmed, "Performance Analysis of Cooperative Diversity Wireless Networks over Nakagami-m Fading Channel," *IEEE Commun. Letters*, vol. 11, no.4, pp. 334 – 336, April 2007.

[22] S. Ikki, and M. H. Ahmed, "Performance Analysis of Decode-and-Forward Cooperative Diversity Using Differential EGC over Nakagami-m Fading Channels," 69th IEEE Veh. Tech. Conf., 2009. VTC Spring 2009, pp. 1 – 6, Barcelona, Spain, 26 – 29 April 2009.

[23] G. Chuai, X. Li, S. Liu, Y. Hu and F. Shi, "Closed-form expressions for outage probability of decode-and-forward relaying over Nakagami-m fading channels," *The Journal of China Universities of Posts and Telecommunications*, vol. 17, no. 2, pp. 72 – 75, April 2010.

[24] T. Q. Duong, V. N. Q. Bao, and H. J. Zepernick, "On the performance of selection decode-and-forward relay networks over Nakagami-m fading channels," *IEEE Commun. Letters*, vol. 13, no. 3, pp. 172 – 174, March 2009.

[25] X. Bao and J. Li, "Efficient message relaying for wireless user cooperation: decode-amplify-forward (DAF) and hybrid DAF and coded-cooperation," *IEEE Trans. on Wireless Commun.*, vol. 6, no. 11, pp. 3975 – 3984, 2007.

[26] G. Y. Li, Z. Xu, C. Xiong, C. Yang, S. Zhang, Y. Chen, and S. Xu, "Energy-Efficient Wireless Communications: Tutorial, Survey, and Open Issues", 2011.

[27] B. Badic, T. O'Farrell, P. Loskot, and J. He, "Energy efficient radio access architectures for green radio: large versus small cell size deployment," *in Proc. IEEE Veh. Technol. Conf. (VTC'09 Fall),* Sept. 2009.

[28] V. Tarokh, H. Jafarkhani, and A. R. Calderbank, "Space-time block codes from orthogonal designs," *IEEE Trans. on Inform. Theory*, vol. 45, pp. 1456 – 1467, July 1999.

[29] A. Yilmaz, and O. Kucur, "Error performance of joint transmit and receive antenna selection in two hop amplify-and-forward relay system over Nakagami-m fading channels," *IEEE 21st International Symposium on Personal Indoor and Mobile Radio Communications (PIMRC),* pp. 2198 – 2203, 26-30 Sept. 2010.

[30] A. Sendonaris, E. Erkip, and B. Aazhang, "User cooperation diversity. Part I. System description," *IEEE Trans. Commun.*, vol. 51, no. 11, pp.1927 – 1938, Nov. 2003.

[31] A. Sendonaris, E. Erkip, and B. Aazhang, "User cooperation diversity. Part II. Implementation aspects and performance analysis," *IEEE Trans. Commun.*, vol. 51, no. 11, pp. 1939 – 1948, Nov. 2003.

[32] J. N. Laneman and G. Wornell, "Distributed space-time coded protocols for exploiting cooperative diversity in wireless networks," in *IEEE GLOBECOM 2002*, vol. 1, no. 11, Taipei, Taiwan, R.O.C., pp. 77 – 81, Nov. 2002.

[33] A. Scaglione and Y.-W. Hong, "Opportunistic large arrays: Cooperative transmission in wireless multi-hop ad hoc networks for the reach back channel," *IEEE Trans. Signal Process.*, vol. 51, no. 8, pp. 2082 – 2092, Aug. 2003.

[34] M. Janani, A. Hedayat, T. E. Hunter, and A. Nosratinia, "Coded cooperation in wireless communications: Space-time transmission and iterative decoding," *IEEE Trans. Signal Process.*, vol. 52, no. 2, pp. 362 – 371, Feb. 2004.

[35] H. Sato, "Information transmission through a channel with relay," *Tech.Rep.* B76-7, The Aloha System, University of Hawaii, Honolulu, March 1976.

[36] Y. Zhao, R. Adve, and T. Lim, "Improving amplify-and-forward relay networks: Optimal power allocation versus selection," *IEEE Trans. on Wireless Commun.*, vol. 6, pp. 3114 – 3123, 2007.

[37] A. Bletsas, H. Shin, and M. Win, "Outage optimality of opportunistic amplify-and-forward relaying," *IEEE Commun. Letters*, vol. 11, pp. 261 – 263, 2007.

[38] A. Bletsas, A. Khisti, D. Reed, and A. Lippman, "A simple cooperative diversity method based on network path selection," *IEEE Journal on Selected Areas in Commun.,* vol. 24, no. 3, pp. 659–672, March 2006.

[39] Y. Sun, Z. Mao, X. Zhong, Y. Xiao, S. Zhou, and N. B. Shroff, "Optimal Distributed Power Allocation for Decode-and-Forward Relay Networks," 1201.0320v1 [cs.IT] 1 Jan 2012.

[40] D. S. Michalopoulos and G. K. Karagiannidis, "Distributed switch and stay combining (DSSC) with a single decode and forward relay," *IEEE Commun. Letters*, vol. 11, no. 5, pp. 408 - 410, May 2007.

[41] S. Ikki and M. H. Ahmed, "Performance analysis of cooperative diversity using equal gain combining (EGC) technique over Rayleigh fading channels," *Proc. IEEE ICC*, pp. 5336 – 5341, Jun. 2007.

[42] Y. C. Ko, M. S. Alouini, and M. K. Simon, "Analysis and optimization of switched diversity systems," *IEEE Trans. on Veh. Tech.*, vol. 49, no. 5, pp. 1813 – 1831, Sep. 2000.

[43] Y. C. Ko, M. S. Alouini, and M. K. Simon, "Correction to analysis and optimization of switched diversity systems," *IEEE Trans. on Veh. Tech.*, vol. 51, no. 1, pp. 216 – 216, Jan. 2002.

[44] P. A. Anghel and M. Kaveh, "Exact symbol error probability of a cooperative network in a Rayleigh-fading environment," *IEEE Trans. on Wireless Commun.*, vol. 3, no. 5, pp. 1416 – 1421, Sep. 2004.

[45] H. A. Suraweera, G. K. Karagiannidis and P. J. Smith "Performance analysis of the dual-hop asymmetric fading channel," *IEEE Trans. on Wireless Commun.*, vol. 8, no. 6, pp. 2783 – 2788, Jun. 2009.

[46] D. A. Zogas, G. K. Karagiannidis, N. C. Sagiasz, T. A. Tsiftsis, P. T. Mathiopoulost and S. A. Kotsopoulos, "Dual hop wireless communications over Nakagami fading," *Proc. IEEE VTC*, vol. 4, pp. 2200-2204, Feb. 2005.

[47] G. K. Karagiannidis, D. A. Zogas, N. C. Sagias, T. A. Tsiftsis, and P. T. Mathiopoulos, "Multihop communications with fixed-gain relays over generalized fading channels," *Proc. IEEE Globecom*, vol. 1, pp. 36 - 40, Nov. 2004.

[48] H. Katiyar and R. Bhattacharjee, "Performance of MRC combining multi-antenna cooperative relay network," *Elsevier's International Journal of Electronics and Commun. (AEU),* Aug.2009.

[49] H. Katiyar and R. Bhattacharjee, "Outage performance of two-hop multi-antenna cooperative relaying in Rayleigh fading channel," *Electronics Letters*, vol. 45, no. 17, pp. 881 – 883, Aug. 2009.

[50] H. Katiyar and R. Bhattacharjee, "Performance of two-hop regenerative relay network under correlated Nakagami-m fading at multi-antenna relay," *IEEE Commun. Letters*, vol. 13, no. 10, Oct. 2009.

[51] H. Katiyar and R. Bhattacharjee, "Performance of regenerative relaying at uplink of multi-antenna access point in Nakagami-m fading," *Proc. NCC*, pp. 165 – 169, Jan. 2009.

[52] P. Popovski and H. Yomo, "Physical network coding in two-way wireless relay channels," *in Proc. IEEE Int. Control Conf.*, pp. 707–712, Jun. 2007.

[53] B. Rankov and A.Wittneben, "Spectral efficient protocols for half-duplex fading relay channels," *IEEE J. Sel. Areas Commun.,* vol. 25, no. 2, pp. 379–389, Feb. 2007.

[54] T. J. Oechtering, C. Schnurr, I. Bjelakovi´c, and H. Boche, "Broadcast capacity region of two-phase bidirectional relaying," *IEEE Trans. Inf. Theory*, vol. 54, no. 1, pp. 454 – 458, Jan. 2008.

[55] S. J. Kim, P. Mitran, and V. Tarokh, "Performance Bounds for Bi-Directional Coded Cooperation Protocols," arXiv: 0703017.

[56] C. E. Shannon, "Two-way communication channels," *in Proc. 4th Berkeley Symp. Math Stat. Prob.*, vol. 1, pp. 611 – 644, 1961.

[57] T. S. Han, "A general coding scheme for the two-way channel," *IEEE Trans. Inf. Theory,* vol. IT-30, no. 1, pp. 35 – 44, Jan. 1984.

[58] B. Rankov and A. Wittneben, "Achievable rate regions for the two way relay channel," *in Proc. IEEE Int. Symp. Inf. Theory*, pp. 1668–1672, Jul. 2006.

[59] C. K. Ho, R. Zhang, and Y. C. Liang, "Two-way relaying over OFDM: Optimized tone permutation and power allocation," *in Proc. IEEE Int. Control Conf*, pp. 3908–3912., May 2008.

[60] Y. C. Liang and R. Zhang, "Optimal analogue relaying with multi-antennas for physical layer network coding," *in Proc. IEEE Int. Control Conf.*, pp. 3893 – 3897, May 2008.

[61] T. J. Oechtering, and H. Boche, "Bidirectional regenerative half-duplex relaying using relay selection," *IEEE Trans. on Wireless Commun*., vol. 7, no. 5, May 2008.

[62] O. Munoz, A. Augustin, and J. Vidal, "Cellular capacity gains of cooperative MIMO transmission in the downlink," *in Proc. IZS, (Zurich, Switzerland),* pp. 22 – 26, Feb. 2004.

[63] T. J. Oechtering and A. Sezgin, "A new cooperative transmission scheme using the space-time delay code," *in Proc. ITG Workshop on Smart Antennas*, (Munich, Germany), pp. 41 – 48, Mar. 2004.

[64] J.N.Laneman, G.W.Wornell, and D.N.C.Tse, "An efficient protocol for realizing co-operative diversity in wireless networks," *in Proc. of IEEE International Symposium on Inform. Theory*, Washington DC, USA, Jun. 2001.

[65] S. Borade, L. Zheng, and R. Gallager, "Amplify-and-Forward in Wireless Relay Networks: Rate, Diversity, and Network Size," IEEE Trans. on Inform. Theory, vol. 53, no.10, pp. 3302 – 3318, Oct. 2007.

[66] S. Agnihotri, S. Jaggi, and M. Chen, "Amplify-and-Forward in Wireless Relay Networks," arXiv:1105.2760v2 [cs.IT] 1 Jun 2011.

[67] D.-Wu Yue, and H. H. Nguyen, "Performance of orthogonal wireless relay networks with multiple SNR-thresholds and multiple hard-decision detections," in Proc. of the 28th IEEE conference on Global telecommunications GLOBECOM'09, IEEE Press Piscataway, NJ, USA, 2009.

[68] T Himsoon, W Siriwongpairat, W Su, and K Liu, "Differential modulation with threshold-based decision combining for cooperative communications," *IEEE Trans Signal Process*., vol. 55, pp. 3905 – 3923, 2007.

[69] D Chen, and J Laneman, "Modulation and demodulation for cooperative diversity in wireless systems," *IEEE Trans Wireless Commun*., vol. 5, pp. 1785 – 1794, 2006.

[70] J Hu, and N. Beaulieui, "Performance analysis of decode-and-forward relaying with selection combining," *IEEE Commun Letters*, vol. 11, no. 6, pp. 489 – 491, 2007.

[71] M. Selvaraj, and R Mallik, "Error analysis of the decode and forward protocol with selection combining," *IEEE Trans Wireless Commun*., vol. 8, no. 6, pp. 3086 – 3094, 2009.

[72] M. Selvaraj, and R Mallik, "Scaled selection combining based cooperative diversity system with decode and forward relaying," *IEEE Trans Veh. Technol.*, vol. 59, no. 9, pp. 4388 – 4399, 2010.

[73] S Ikki, and M. Ahmed, "Performance analysis of generalized selection combining for decode-and-forward cooperative-diversity networks," *Proc. of IEEE Veh. Technol. Conf.*, pp 1 – 5, 2010.

[74] H. X. Nguyen and H. H. Nguyen, "Selection combining for non-coherent decode-and-forward relay networks," *EURASIP Journal on Wireless Commun. and Networking*, 2011:106 doi:10.1186/1687-1499-2011-106, 2011.

[75] B. Can, H. Yomo, and E. De Carvalho, "Hybrid forwarding scheme for cooperative relaying in OFDM based networks," *in Proc. IEEE International Conf. on Commun.*, vol. 10, pp. 4520 – 4525, Istanbul, Turkey, June 2006.

[76] T. Q. Duong and H.-J. Zepernick, "On the Performance Gain of Hybrid Decode-Amplify-Forward Cooperative Communications," *EURASIP Journal on Wireless Commun. and Networking*, vol. 2009, Article ID 479463, 10 pages, 2009. doi:10.1155/2009/479463

[77] T. Q. Duong and H.-J. Zepernick, "Hybrid decode-amplify-forward cooperative communications with multiple relays," Proc. IEEE conference on Wireless Commun. and Networking Conference (WCNC), pp. 273 – 278, 2009.

[78] M. O. Hasna and M. S. Alouini, "A Performance Study of Dual-Hop Transmissions With Fixed Gain Relays," *IEEE Trans. Wireless Commun.*, vol. 3, no. 6, pp. 1963 – 1968, Nov. 2004.

[79] D. B. da Costa and M. D. Yacoub, "Dual-hop transmissions with semi-blind relays over Nakagami-m fading channels," *Electron. Lett.*, vol. 44, no. 3, pp. 214 – 216, Dec. 2007.

[80] M. O. Hasna and M. S. Alouini, "End-to-end performance of transmission systems with relays over Rayleigh fading channels," *IEEE Trans. on Wireless Commun.*, vol. 2, no. 6, pp. 1126 – 1131, 2003.

[81] H. Q. Huynh, S. I. Husain, J. Yuan, A. Razi, and H. Suzuki, "Performance Analysis of Multibranch Dual-Hop Nonregenerative Relay Systems with EGC in Nakagami-*m* Channels," Research Article EURASIP Journal on Wireless Commun. and Networking, vol. 2010, Article ID 835498, 11 pages doi:10.1155/2010/835498.

[82] S. Yang and J.-C. Belfiore, "Diversity of MIMO multihop relay channels," submitted to *IEEE Trans. Inform. Theory*. [Online]. Available: http://arxiv.org/abs/0708.0386

[83] S. Yeh and O. Leveque, "Asymptotic capacity of multi-level amplify-and-forward relay networks," *in Proc. IEEE ISIT'07*, June 2007.

[84] A. ¨Ozg¨ur, O. L´ev^eque, and D. N. C. Tse, "Hierarchical cooperation achieves optimal capacity scaling in ad hoc networks," *IEEE Trans. Inform. Theory*, vol. 53, pp. 3549 – 3572, Oct. 2007.

[85] N. Fawaz, K. Zarifi, M. Debbah, and D. Gesbert, "Asymptotic Capacity and Optimal Precoding in MIMO Multi-Hop Relay Networks," IEEE Trans. on Inform. Theory, vol. 57, no. 4, pp. 2050 – 2069, April 2011.

[86] W. Jaafar, W. Ajib, and D. Haccoun, "On the performance of multi-hop wireless relay networks," *Wireless Commun. and Mobile Computing*, doi: 10.1002/wcm.1246, 2011

[87] R. W. Simons, "Guglielmo Marconi and Early Systems of Wireless Communication," *GEC Review*, vol. 11, no. 1, 1996.

[88] F. Adachi, "Wireless Past and Future – Evolving Mobile Communications Systems", *IEICE Trans. Fundamentals*, vol. E84-A, no. 1, Jan. 2001.

[89] K. L. Du and M. N. S. Swamy, "Wireless Communication Systems, 1st Edition, Cambridge University Press, 2009.

[90] A. Goldsmith, "Wireless Communication," Cambridge University Press 2005.

[91] J. M. Steber, "PSK Demodulation (Part I)," the Communications Edge, WJ Communications Inc., 2001.

[92] J. G. Proakis, "Digital Communications," McGraw-Hill International, 4th edition, 2001.

[93] M. Schwartz, "Information Transmission, Modulation and Noise," McGraw Hill, New York, 1980.

[94] T. S. Rappaport, "Wireless Communications, Principles and practices," Second Edition.

[95] F. Belloni, "Fading Models," Post Graduate course in Radio Communications, Autumn, 2004.

[96] M. K. Simon and M. S. Alouini, "A Unified Approach to Performance Analysis of Digital Communications over Fading Channels," *Proc. IEEE*, vol. 86, no. 9, pp. 1860 – 1877, Sep. 1998.

[97] H. Bai, H. Aerospace, M. Atiquzzaman, "Error Modeling Schemes for Fading Channels in Wireless Communications: A survey," *IEEE communications Surveys & Tutorials*, vol. 5, no. 2, Fourth Quarter 2003.

[98] F. Babich and G. Lombardi, "Statistical Analysis and Characterization of the indoor Propagation Channel," *IEEE Trans. Comm*., vol. 48, no. 3, pp 455 – 464, Mar. 2000.

[99] W. C. Jakes, "Microwave Mobile Communications," New York, John Wiley, 1974.

[100] Bernard Sklar, "Rayleigh Fading Channels in Mobil Digital Communication Systems, Part I: Characterization," *IEEE Comm. Magazine*, vol. 35, no. 7, pp. 90 – 101, 1997.

[101] J. Li, A. Bose and Y. Q. Zhai, "Rayleigh Flat Fading Channels' Capacity," *Proc. 3rd IEEE Annual Commun. Networks and Services Research Conf.*, 2005.

[102] H. Shin and J. H. Lee, "On the Error Probability of Binary and M-ary signals in Nakagami-m Fading Channels," *IEEE Trans. Comun*., vol. 52, no.4, April 2004.

[103] J. Luo, J. R. Zeidler, "A Statistical Simulation Model for Correlated Nakagami Fading Channels," Electrical and Computer Engineering Department, University of California, San Diego, 9500 Gilman Drive, La Jolla, CA 92093-0407, USA.

[104] N. C. Beaulieu and C. Cheng, "An Efficient Procedure for Nakagami-m Fading Simulation," *Proc. IEEE GLOBECOMM*, pp. 3331-3342, Nov. 2000.

[105] B.N. Getu and J.B. Andersen, "BER and spectral efficiency of a MIMO system," *Proc. 5th Int. Symp. on Wireless Personal Multimedia Commun*., vol. 2, pp. 397 – 401, Honolulu, Oct. 2002.

[106] S. W. Kim, D. S. HA and J. H. Kim,"'Performance Gain of Smart Antennas with diversity combining at handsets for the 3GPP WCDMA system," *13th International Conf. on Wireless Commun. (Wireless 2001)*, Calgary, Alberta, Canada, July 2001.

[107] A. Paulraj, R. Nabar, and D. Gore, "Introduction to space-time wireless communications," *Cambridge University Press*, UK, 2003.

[108] H. Hourani, "An Overview of Diversity Techniques in Wireless Communication Systems," *Postgraduate Course in Radio Communications*, 2004 – 2005.

[109] B. Vucetic, and J. Yuan, "Space-time coding," New York, *John Wiley & Sons,* 2003.

[110] S. N. Diggavi, N. Al-Dhahir, A. Stamoulis, and A. R. Calderbank, "Great Expectations: The Value of Spatial Diversity in Wireless Networks," *Proc. IEEE*, vol. 92, no. 2, Feb. 2004.

[111] V. Tarokh, N. Seshadri, and A. R. Calderbank, "Space-Time Codes for High Data Rate Wireless Communication: Performance Criteria and Code Construction," *IEEE Trans. Inform. Theory*, pp. 744 – 764, Mar. 1998.

[112] E. G. Larsson and P. Stoica, "Space-time block coding for wireless communications," Cambridge, *UK: Cambridge University Press*, 2003.

[113] N. Seshadri, V. Tarokh, and A. R. Calderbank, "Space-Time Codes for Wireless Communication: Code Construction," *AT&T Labs-Research*.

[114] K. E. Baddour and N. C. Beaulieu, "Auto-regressive Models for fading channel Simulation," *IEEE Trans. on Wireless Commun*., vol. 4, no. 4, pp. 1650 – 1662, July 2005.

[115] V. Tarokh, A. Naquib, N. Seshadri, and A. R. Calderbank, "Space-Time Codes for High Data Rate Wireless Communication: Performance Criteria in the Presence of Channel Estimation Errors, Mobility and Multiple Paths".

[116] G. J. Foschini amd M. J. Gans, "On Limits of Wireless Communications in a Fading Environment when using Multiple Antennas," *Wireless Personal Commun*., vol. 6, no. 3, pp. 311 – 335, Mar. 1998.

[117] Z. Safar, and K. J. R. Liu, "Systematic Design of Space-Time Trellis Codes for Diversity and Coding Advantages," *EURASIP Journal on Applied Signal Processing*, pp. 221 – 235, 2002-2003.

[118] S. Sandhu, R. Heath, and A. Paulraj, "Space-Time Block Codes versus Space-Time Trellis Codes," *IEEE,* 2001.

[119] S. M. Alamouti, "A Simple Transmit Diversity Technique for Wireless Communications," *IEEE Journal on Select Areas in Commun*., vol. 16, pp. 1451 – 1458, 1998.

[120] J. C. Guey, M. P. Fitz, M. R. Bell, and W. Y. Kuo, "Signal design for transmitter diversity wireless communication systems over Rayleigh fading channels," *IEEE Veh. Tech. Conf*., vol. 1, pp. 136 – 140, April 1996.

[121] G. J. Foschini, "Layered space-time architecture for wireless communication in a fading environment when using multiple antennas," *Bell Labs Technical Journal*, vol. 1, no. 2, pp. 41 – 59, Sept. 1996.

[122] Y. Hong, J. Yuan, Z. Chen, and B. Vucetic, "Space-Time Turbo Trellis Codes for Two, Three, and Four Transmit Antennas," *IEEE Trans. on Veh. Tech.*, vol. 53, no. 2, March 2004.

[123] Y. Sasazaki and T. Ohtsuki, "Design Criteria for Space-Time Trellis Codes Based on Product Distance Distribution and Trace Distribution in Fast Fading Channels," *Electronics and Commun. in Japan Part 1*, vol. 88, no. 11, 2005.

[124] S. Jiang and R. Kohno, "A New Space-Time Multiple Trellis Coded Modulation Scheme UsingTransmit Symbol Phase Rotation," *Wireless Personal Commun.,* vol. 35, pp. 153 – 171, Springer 2005.

[125] O. Tirkkonen, and A. Hottinen, "Square-Matrix Embeddable Space-Time Block Codes for complex Signal Constellations," *IEEE Trans. on Inform. Theory*, vol. 48, no. 2, pp. 384 – 395, Feb. 2002.

[126] C. Yuen, Y. L. Guan, and T. T. Tjhung, "On the Search for High-Rate Quasi-Orthogonal Space-Time Block Code," *Inter. Journal of Wireless Information Networks*, vol. 13, no. 4, pp. 329 – 340, Oct. 2006.

[127] F. Oggier, G. Rekaya, and J. C. Belfiore, "Perfect Space-Time Block Codes," *IEEE Trans. on Inform. Theory,* vol. 52, no. 9, pp. 3885 – 3902, Sept. 2006.

[128] V. Tarokh and H. Jafarkhani, "A differential detection scheme for transmit diversity," *IEEE Journal on Sel. Areas in Comm.*, vol. 18, pp. 1169 – 1174, July 2000.

[129] B. L. Hughes, "Differential Space-Time Modulation," *IEEE Trans. Inform. Theory*, vol. 46, no. 7, Nov. 2000.

[130] A.M.D. Turkmani, A.A. Arowogolu, P.A. Jefford, and C.J. Kellent, "An Experimental Evaluation of Performance of Two-Branch Space and Polarization Diversity Schemes at 1800 MHz," *IEEE Trans. Veh. Tech.*, vol. 44, no.2, pp. 318 – 326, May 1995.

[131] L. Yue, "Analysis of Generalized Selection Combining Techniques," *Proc. Of Veh. Tech. Conf., VTC – Tokyo*, vol. 2, pp. 1191 – 1195, 2000.

[132] N. Kong and L. B. Milstein, "SNR of generalized diversity selection combining with nonidentical Rayleigh fading statistics," *IEEE Trans. Commun.*, vol. 48, pp. 1266 – 1271, Aug. 2000.

[133] X. Zhang and N. C. Beaulieu, "Performance analysis of generalized selection combining in generalized correlated Nakagami-m fading," *IEEE Trans. Commun.*, vol. 54, pp. 2103 – 2112, Nov. 2006.

[134] … "Maximal Ratio Combining with Correlated Rayleigh Fading Channels," EE359: Wireless Communications, Dec. 7, 2002

[135] P. Lombardo, F. Fedele, and M. M. Rao, "MRC Performance for Binary Signals in Nakagami Fading with General Branch Correlation," *IEEE Trans. on Commun.*, vol. 47, no. 1, pp. 44 – 50, Jan. 1999.

[136] A. Shah and A. M. Haimovich, "Performance analysis of maximal ratio combining and comparison with optimum combining for mobile radio communications with co-channel interference," *IEEE Trans. Veh. Technol.*, vol. 49, pp. 1454 – 1463, July 2000.

[137] V. A. Aalo, T. Piboongungon, and G. Efthymoglou, "Another look at the performance of MRC schemes in Nakagami-m fading channels with arbitrary parameters," *IEEE Trans. Commun.*, vol. 53, pp. 2002 – 2005, Dec. 2005.

[138] W. Li, H. Zhang, and T. A. Gulliver, "Capacity and Error Probability for Maximal Ratio Combining Reception over Correlated Nakagami Fading Channels," *Wireless Personal Commun.*, vol. 37, pp. 73 – 89, 2006.

[139] A. Annamalai, V. Ramanathan and C. Tellambura, "Analysis of Equal Gain Diversity Receiver in Correlated Fading Channels," *Proc. IEEE Veh. Technol. Conf.,* vol. 4, pp. 2038 – 2041, Fall 2002.

[140] M. S. Alouini and M. K. Simon, "Performance analysis of coherent equal gain combining over Nakagami-m fading channels," *IEEE Trans. Veh. Technol.*, vol. 50, pp. 1449 – 1463, Nov. 2001.

[141] Y. Song, S. D. Blostein, and J. Cheng, "Exact outage probability for equal gain combining with cochannel interference in Rayleigh fading," *IEEE Trans. Wireless Commun.,* vol. 2, pp. 865 – 870, Sept. 2003.

[142] J. Boyer, D. D. Falconer, and H. Yanikomeroglu, "Multihop diversity in wireless relaying channels," *IEEE Trans. Commun*., vol. 52, no.10, pp. 1820 – 1830, Oct. 2004.

[143] S. Ikki, and M. H. Ahmed, "Performance of Decode-and-Forward Cooperative Diversity Networks over Nakagami-m Fading Channels," *in Proc. IEEE GLOBECOM'07*, pp. 4328 – 4333, Nov. 2007.

[144] L. Cao, D. C. Yang, H. W. Yang, C. Feng and X. Zhang, "Asymptotic performance of amplify-and-forward MIMO relaying with transmit antenna selection," *SCIENCE CHINA Information Sciences*, vol. 53, no. 12, pp. 2631 – 2641, Dec. 2010.

[145] Y. Fan, and J. Thompson, "MIMO configurations for relay channels: Theory and practice," *IEEE Trans Wireless Commun.,* vol. 6, pp. 1774 – 1786, 2007.

[146] T. Q. Duong and H. J. Zepernick, "On the Performance Gain of Hybrid Decode-Amplify-Forward Cooperative Communications" *EURASIP Journal on Wireless Communications and Networking, Volume 2009 (2009)*, Article ID 479463, 10 pages.

[147] B. M. Hochwald and T. L. Marzetta, "Unitary space-time modulation for multiple-antenna communications in Rayleigh flat fading," *IEEE Trans. Inform. Theory*, vol. 46, pp. 543 – 564, March 2000.

[148] B. M. Hochwald, and W. Sweldens, "Differential Unitary Space-Time Modulation," *IEEE Trans. on Commun.*, vol. 48, no. 12, Dec. 2000.

[149] J. Liu, J. Li, H. Li, and E. G. Larsson, "Differential Space-Code Modulation for Interference Suppression," *IEEE Trans. on Signal Proc.*, vol. 49, no. 8, Aug. 2001.

[150] R. Schober, and L. H. J. Lampe, "Differential Modulation Diversity" *IEEE Trans. on Veh. Tech.*, vol. 51, no. 6, pp. 1431 – 1444, Nov 2002.

[151] C. B. Peel, and A. L. Swindlehurst, "Performance of Unitary Space-Time Modulation in a Continuously Changing Channel," *IEEE*, 2001

[152] C. B. Peel, and A. L. Swindlehurst, "Performance of Unitary Space-Time Modulation in Rayleigh Fading," *International Conf. on Commun.*, 2001

[153] C. Cozzo, and B. L. Hughes, "Joint Channel Estimation and Data Detection in Space-Time Communications," *IEEE Trans. on Commun.*, vol.51, no. 8, Aug. 2003.

[154] C. Cozzo, and B. L. Hughes, "An Adaptive Receiver for Space-Time Trellis Codes Based on Per-Survivor Processing," *IEEE Trans. on Commun.*, vol.50, no. 8, Aug. 2002.

[155] Z. Liu, X. Ma, and G. B. Giannakis, "Space Time Coding and Kalman filtering for time-selective fading channels," *IEEE Trans. Commun.*, vol. 50, no. 2, pp. 183 – 186, Feb. 2002

[156] R. Raheli, A. Polydoris, and C. Tzou, "Per-survivor processing: a general approach to MLSE in uncertain environment," *IEEE Trans. Commun.*, vol. 43, pp. 354 – 364, Feb. /Mar/Apr. 1995.

[157] Y. Xue and X. Zhu, "PSP decoder for space-time trellis code based on accelerated self-tuning LMS algorithm," *Electronic Letters*, vol. 36, no. 17, pp. 1472 – 1474, Aug. 2000.

[158] M. Nicoli, S. Ferrara, and U. Spagnolini, "Soft-Iterative Channel Estimation: Methods and Performance Analysis," *IEEE Trans. on Signal Processing*, vol. 55, no. 6, June 2007.

[159] P. Kadlec, P. Kejik, and Z. Raide, "Comparison of Pilot Symbol Embedded Channel Estimation Algorithms," *Radioengineering*, vol. 18, no. 4, pp. 485 – 490, Dec. 2009.

[160] M. J. Omidi, S. Pasupathy, and P. G. Gulak, "Joint Data and Kalman Estimation for Rayleigh Fading Channels," *Wireless Personal Communications*, vol. 10, 1999.

[161] M. Tuchler, R. Otnes and A. Schmidbauer, "Performance of Soft Iterative Channel Estimation in Turbo Equalization," *in Proc. IEEE ICC*, vol. 3, pp. 1858 – 1862, Apr. – May 2002,

[162] H. Mai, A. G. Burr and S. Hirst, "Iterative channel estimation for turbo equalization," *in Proc. IEEE PIMRC*, vol. 2, pp. 1327 – 1331, Sep. 2004.

[163] L. M. A. Jalloul and R. M. Misra, "Data aided channel estimation for wideband CDMA," *IEEE Trans. Wireless Comm.*, vol. 4, no. 4, pp. 1622 – 1634, Jul. 2005.

[164] T. Zemen, "Multi user communication over time-variant channels," PhD dissertation, Vienna Univ. Trach., Vienna, Austria, 2004.

[165] T. Zemen, M. Loncar, J. Wehinger, C. Mecklenbrauker and R. Muller, "Improved channel estimation for iterative receivers," *in Proc. IEEE GlobeComm*, vol. 1, pp. 257 – 261, Dec. 2003.

[166] A. Lampe, "Iterative multi user detection with integrated channel estimation for coded DS-CDMA," *IEEE Trans. Commun.*, vol. 50, no. 8, pp. 1217 – 1223, Aug. 2002

[167] A. F. Molisch and M. Z. Win, "MIMO Systems with Antenna Selection," *IEEE Microwave Magazine*, March 2004.

[168] X. M. Chen, and P. A. Hoecher, "Design Considerations of Adaptive Trellis-Based Blind Sequence Estimators".

[169] O. Rousseaux, G. Leus, P. Stoica, and M. Moonen, "Training Based Maximum Likelihood Channel Identifications".

[170] S. Zhang, P. Y. Kam, and P. Ho, "Performance of Pilot-Symbol-Assisted-Modulation with Transmit-Receive Diversity in Nonselective Rayleigh Fading Channels," *IEEE*, 2004.

[171] R. Visoz, and A. O. Berthet, "Iterative Decoding and Channel Estimation for Space-Time BICM over MIMO Block fading Multipath AWGN Channel," *IEEE Trans. on Commun.*, vol. 51, no. 8, Aug. 2003.

[172] J. Wehinger, R. R. Muller, M. Loncar and C. F. Mecklenbrauker, "Performance of iterative CDMA receivers with channel estimation in multipath environments," *presented at the IEEE 26th Asilomar CSSC*, Pacific Grove, CA, Nov. 2 – 6, 2002.

[173] X. Wautelet, C. Hezret, A. Dejonghe, and L. Vandendorpe, "MMSE-based and EM Iterative Channel Estimation Methods," *Proc. Symposium IEEE Benelux Chapter on Commun. and Vehicular Tech.*, 2003.

[174] A. Kocian and B. H. Fleury, "EM-based joint data detection and channel estimation of DS-CDMA signals," *IEEE Trans. Commun.*, vol. 51, no. 10, pp. 1709 – 1720, Oct. 2003.

[175] Y. Li, C. N. Georghiades, and G. Huang, "Iterative Maximum-Lekelihood Sequence Estimation for Space-Time Coded Systems," *IEEE Trans. on Commun.,* vol. 49, no. 6, Jun. 2001.

[176] E. Panayirci, U. Aygolii, and A. E. Pusane, "Sequence Estimation with Transmit Diversity for Wireless Communications," *AEU Int. Journal on Electron. Commun.*, vol. 57, no. 5, Sept. 2003.

[177] E. Chiavaccini, and G. M. Vitetta, "An EM-based MAP Detector for CPM Signals Transmitted over Frequency-Flat Fading Channels," *IEEE*, 2001

[178] C. Cozzo, and B. L. Hughes, "Joint Channel Estimation and Data Symbol Detection in Space-Time Communications," *IEEE*, 2000.

[179] R. Otnes and M. Tüchler, "Iterative channel estimation for turbo equalization of time-varying frequency-selective channels," *IEEE Trans. Wireless Commun.*, vol. 3, no. 6, pp. 1918 – 1923, Nov. 2004.

[180] H. Shen, and A. P. Suppappola, "Diversity and Channel Estimation Using Time-Varying Signals and Tine-Frequency Techniques," *IEEE Trans. on Signal Processing*, vol. 54, no. 9, Sept. 2006.

[181] R. A. Ziegler and J. M. Coffi, "Estimation of time-varying digital radio channels," *IEEE Trans. on Vehicular Technology*, vol. 4, no. 2, pp. 134 – 151, May 1992.

[182] J. H. Kotecha, P. M. Djuric, "Blind sequential Detection for Rayleigh Fading channels using Hybrid Monte Carlo-Recursive Identification Algorithms," *Signal Processing*, vol. 84, no. 5, pp 825 – 832, May 2004.

[183] A. Barbieri, A. Piemontese and G. Colavolpe, "On the ARMA approximation for frequency-flat Rayleigh Fading Channels," *International Symposium on Information Theory (ISIT2007),* Nice, France, June 24 – 29, 2007.

[184] S. W. Kim and E. Y. Kim, "Optimum Receive Antenna Selection Minimizing Error Probability," *IEEE*, pp. 441 – 447, 2003

[185] S. Sanayei and A, Nostratinia, "Antenna Selection in MIMO Systems," *IEEE Commun. Magazine*, Oct. 2004.

[186] A. F. Molisch, "MIMO Systems with Antenna Selection – an Overview," *MERL*, August 2003.

[187] Y. Wang, G. Shen, H. Yu, S. Liu, and J. W. Chong, "Exact BER Expression for Alamouti Scheme with Joint Transmit and Receive Antenna Selection," *IEEE*, pp. 1328 – 1331, 2007.

[188] A. Ghrayeb and T. M. Duman, "Performance Analysis of MIMO Systems with Antenna Selection over Quasi-Static Fading Channels," *IEEE Trans. on Veh. Tech.*, vol. 52, no. 2, pp. 281 – 288, March 2003.

[189] S. Chen, W. Wang, X. Zhang, and D. Zhao, "Performance of Amplify-and-Forward MIMO Relay Channels with Transmit Antenna Selection and Maximal-Ratio-Combining," *Proceeding WCNC, IEEE*, 2009.

[190] L. Yang and J. Qin, "Performance of Alamouti Scheme with Transmit Antennas Selection for M-ray Signals," *IEEE Trans. on Wireless Commun.*, vol. 5, no. 12, pp. 3365 – 3369, Dec. 2006.

[191] P. Shang, G. Zhu, and G. Shu, "Low Complexity Antenna Selection Algorithms for Downlink Distributed MIMO Systems," *Journal of Networks*, vol. 5, no. 4, pp. 467 – 474, Apr. 2010.

[192] G. Lebrun, S. Spiteri, and M. Faulkner, "MIMO Complexity Reduction through Antenna Selection".

[193] W. Xie, L. Xie, J. Zhan, and S. Liu, "A Novel Antenna Selection Algorithm for MIMO Systems under Correlated Channels," *6th IEEE International Conference on ITS Telecommunications Proc.*, pp. 461 – 464, 2006.

[194] A. Gorokhov, D. Gore, and A. Paulraj, "Receive Antenna Selection for MIMO Flat-Fading Channels: Theory and Algorithms," *IEEE Trans. on Information Theory*, vol. 49, no. 10, pp. 2687 – 2696, Oct. 2003.

[195] S. Sanayei, and A. Nosratinia, "Capacity of MIMO Channels with Antenna Selection," Feb. 2005.

[196] S. R. Meraji, "Performance Analysis of Transmit Antenna Selection in Nakagami-m Fading Channels," *Wireless Personal Communications*, vol. 43, pp. 327 – 333, Springer 2006.

[197] D. Senaratne and C. Tellambura, "Unified Performance Analysis of Two Hop Amplify and Forward Relaying," *Proc. IEEE Commun. Society*, ICC 2009.

[198] L. Cao, X. Zhang, Y. Wang and D. Yang, "Transmit Antenna Selection Strategy in Amplify-and-Forward MIMO Relaying," *Proc. IEEE Commun. Society*, WCNC 2009.

[199] L. L. Yang, H. H. Chen, "Error Probability of Digital Communications Using Relay Diversity over Nakagami-m Fading Channels," *IEEE Trans. on Wireless Commun.*, vol. 7, no. 5, May, 2008.

[200] H. Shin and J. H. Lee, "On the Error Probability of Binary and M-ary signals in Nakagami-m Fading Channels," *IEEE Trans. on Commun.*, vol. 52, no.4, April 2004.

[201] A. Annamalai and C. Tellambura, "Error Rates for Nakagami-m Fading Multi Channel Reception of Binary and M-ary signals," *IEEE Trans. On Commun.*, vol. 49, no. 1, 2001.

[202] I. Gradshteyn and I. Ryzhik, "Table of Integrals, Series and Products," 7th Edition, San Diego, CA: Academic 2007.

[203] X. Feng and Y. Dianwu, "Exact Error Probability of Orthogonal Space-time Block Codes over Flat Fading Channels," *Journals of Electronics (China),* vol. 24, no. 4, July 2007.

[204] A. Kuhne, A. Klein, "Transmit Antenna Selection and OSTBC in adaptive multiuser OFDMA systems with different user priorities and imperfect CQI," 2010 International ITG Workshop on Smart Antennas (WSA), pp.218 – 225, 23 – 24 Feb. 2010.

[205] Z. Chen, Z. Chi, Y. Li, and B. Vucetic, "Error performance of maximal-ratio combining with transmit antenna selection in flat Nakagami-m fading channels," *IEEE Trans. on Wireless Commun.*, vol.8, no.1, pp. 424 – 431, Jan. 2009

[206] A. F. Coşkun, O. Kucur, and I. Altunbaş, "Performance of space-time block codes with transmit antenna selection in Nakagami-m fading channels," Wireless Conference (EW), 2010 European, pp. 171 – 176, 12-15 April 2010.

[207] K. T. Phan and C. Tellambura. "Receive Antenna Selection Based on Union-Bound Minimization Using Convex Optimization," *IEEE Signal Processing Letters*, vol. 14, no. 9, pp. 609 – 612, Sept. 2007.

[208] V. Kristem, N. B. Mehta, and A. F. Molisch, "A Novel Energy-Efficient Training Method for Receive Antenna Selection," 2010 IEEE International Conf. on Commun. (ICC), pp.1 – 5, 23 – 27 May 2010.

[209] B. H. Wang, H. T. Hui, and M. S. Leong, "Global and Fast Receiver Antenna Selection for MIMO Systems," *IEEE Transactions on Commun.*, vol. 58, no. 9, pp. 2505 – 2510, Sept. 2010.

[210] S. Sharma, D. Engles and S.S. Pathak, "Performance of Rotated Constellation and Trellis Coded Modulation with Channel State Information Errors :MIMO Systems," *Proc. International MultiConference of Engineers and Computer Scientists 2008*, vol. II, IMECS 2008, Hong Kong, 19-21 March, 2008.

[211] M. W. Numan, M. T. Islam, and N. Misran, "Performance And Complexity Improvement of Training Based Channel Estimation in MIMO Systems," *Progress In Electromagnetics Research C*, vol. 10, pp. 1 – 13, 2009.

[212] A. Jamoos, E. Grivel, N. Christov, and M. Najim, "Estimation on autoregressive fading channels based on two cross-coupled H_∞ filters," *SIViP*, vol. 3, pp 209 – 216, 2009.

APPENDIX A

A.1 System and Channel Model when $N_t = 3$ and $N_r = 1$

A.1.1 Encoding Algorithm: Coding and Modulation

For $N_t = 3$ and $N_r = 1$ the encoder matrix G_3^* is described as

$$G_3^* = \begin{bmatrix} x_1 & -x_2 & -x_3 & -x_4 & x_1^* & -x_2^* & -x_3^* & -x_4^* \\ x_2 & x_1 & x_4 & -x_3 & x_2^* & x_1^* & x_4^* & -x_3^* \\ x_3 & -x_4 & x_1 & x_2 & x_3^* & -x_4^* & x_1^* & x_2^* \end{bmatrix} \quad \text{(A.1)}$$

where the four complex set of symbols x_1, x_2, x_3 and x_4 at the encoder input are taken at a time and transmitted by three transmit antennas in eight symbol periods, hence giving the transmission rate $R = 1/2$,

A.1.2 Combining

We define the channel paths H_1, H_2, H_3 for the $(T - TR)$, $(TR - R)$, and $(T - R)$ links, respectively, as

$$H_1 = \begin{bmatrix} h_{11} \\ h_{12} \\ h_{13} \end{bmatrix} \quad \text{(A.2)}$$

$$H_2 = [h_{21}] \quad \text{(A.3)}$$

$$H_3 = \begin{bmatrix} h_{31} \\ h_{32} \\ h_{33} \end{bmatrix} \quad \text{(A.4)}$$

The signal received at the TR node sees a complex weighted version of the $N_t = 3$ simultaneously transmitted signals weighted by fade coefficients and noisy superposition of the signals corrupted by Nakagami-*m* fading and is given by

$$y_{(T-TR)}^1 = \sqrt{\frac{E_b}{3}} [x_1 \quad x_2 \quad x_3] \begin{bmatrix} h_{11} \\ h_{12} \\ h_{13} \end{bmatrix} + n_{11} = \sqrt{\frac{E_b}{3}} (x_1 h_{11} + x_2 h_{12} + x_3 h_{13}) + n_{11} \quad \text{(A.5)}$$

$$y_{(T-TR)}^{2} = \sqrt{\frac{E_b}{3}}[-x_2 \quad x_1 \quad -x_4]\begin{bmatrix} h_{11} \\ h_{12} \\ h_{13} \end{bmatrix} + n_{12} = \sqrt{\frac{E_b}{3}}(-x_2 h_{11} + x_1 h_{12} - x_4 h_{13}) + n_{12} \quad \text{(A.6)}$$

$$y_{(T-TR)}^{3} = \sqrt{\frac{E_b}{3}}[-x_3 \quad x_4 \quad x_1]\begin{bmatrix} h_{11} \\ h_{12} \\ h_{13} \end{bmatrix} + n_{13} = \sqrt{\frac{E_b}{3}}(-x_3 h_{11} + x_4 h_{12} + x_1 h_{13}) + n_{13} \quad \text{(A.7)}$$

$$y_{(T-TR)}^{4} = \sqrt{\frac{E_b}{3}}[-x_4 \quad -x_3 \quad x_2]\begin{bmatrix} h_{11} \\ h_{12} \\ h_{13} \end{bmatrix} + n_{14} = \sqrt{\frac{E_b}{3}}(-x_4 h_{11} - x_3 h_{12} + x_2 h_{13}) + n_{14} \quad \text{(A.8)}$$

$$y_{(T-TR)}^{5} = \sqrt{\frac{E_b}{3}}[x_1^* \quad x_2^* \quad x_3^*]\begin{bmatrix} h_{11} \\ h_{12} \\ h_{13} \end{bmatrix} + n_{15} = \sqrt{\frac{E_b}{3}}(x_1^* h_{11} + x_2^* h_{12} + x_3^* h_{13}) + n_{15} \quad \text{(A.9)}$$

$$y_{(T-TR)}^{6} = \sqrt{\frac{E_b}{3}}[-x_2^* \quad x_1^* \quad -x_4^*]\begin{bmatrix} h_{11} \\ h_{12} \\ h_{13} \end{bmatrix} + n_{16} = \sqrt{\frac{E_b}{3}}(-x_2^* h_{11} + x_1^* h_{12} - x_4^* h_{13}) + n_{16} \quad \text{(A.10)}$$

$$y_{(T-TR)}^{7} = \sqrt{\frac{E_b}{3}}[-x_3^* \quad x_4^* \quad x_1^*]\begin{bmatrix} h_{11} \\ h_{12} \\ h_{13} \end{bmatrix} + n_{17} = \sqrt{\frac{E_b}{3}}(-x_3^* h_{11} + x_4^* h_{12} + x_1^* h_{13}) + n_{17} \quad \text{(A.11)}$$

$$y_{(T-TR)}^{8} = \sqrt{\frac{E_b}{3}}[-x_4^* \quad -x_3^* \quad x_2^*]\begin{bmatrix} h_{11} \\ h_{12} \\ h_{13} \end{bmatrix} + n_{18} = \sqrt{\frac{E_b}{3}}(-x_4^* h_{11} - x_3^* h_{12} + x_2^* h_{13}) + n_{18} \quad \text{(A.12)}$$

during time slots 1, 2,… 8, respectively. Or equivalently as

$$\begin{bmatrix} y_{(T-TR)}^{1} \\ y_{(T-TR)}^{2} \\ y_{(T-TR)}^{3} \\ y_{(T-TR)}^{4} \\ y_{(T-TR)}^{5} \\ y_{(T-TR)}^{6} \\ y_{(T-TR)}^{7} \\ y_{(T-TR)}^{8} \end{bmatrix} = \begin{bmatrix} h_{11} & h_{12} & h_{13} & 0 \\ h_{12} & -h_{11} & 0 & -h_{13} \\ h_{13} & 0 & -h_{11} & h_{12} \\ 0 & h_{13} & -h_{12} & -h_{11} \\ h_{11}^* & h_{12}^* & h_{13}^* & 0 \\ h_{12}^* & -h_{11}^* & 0 & -h_{13}^* \\ h_{13}^* & 0 & -h_{11}^* & h_{12}^* \\ 0 & h_{13}^* & -h_{12}^* & -h_{11}^* \end{bmatrix} \begin{bmatrix} x_1 \\ x_2 \\ x_3 \\ x_4 \end{bmatrix} + \begin{bmatrix} n_{11} \\ n_{12} \\ n_{13} \\ n_{14} \\ n_{15} \\ n_{16} \\ n_{17} \\ n_{18} \end{bmatrix} \quad \text{(A.13)}$$

where $y_{(T-TR)}^{1}, y_{(T-TR)}^{2}, y_{(T-TR)}^{3}, y_{(T-TR)}^{4}, y_{(T-TR)}^{5}, y_{(T-TR)}^{6}, y_{(T-TR)}^{7}$, and $y_{(T-TR)}^{8}$ is the received symbol, h_{11}, h_{12} and h_{13} is the channel, x_1, x_2, x_3 and x_4 is the transmitted symbol, and, $n_{11}, n_{12}, n_{13}, n_{14}, n_{15}, n_{16}, n_{17}$ and n_{18} is the noise during time slots 1, 2… 8, respectively.

Defining $\widetilde{H}_1 = \begin{bmatrix} h_{11} & h_{12} & h_{13} & 0 \\ h_{12} & -h_{11} & 0 & -h_{13} \\ h_{13} & 0 & -h_{11} & h_{12} \\ 0 & h_{13} & -h_{12} & -h_{11} \\ h_{11}^* & h_{12}^* & h_{13}^* & 0 \\ h_{12}^* & -h_{11}^* & 0 & -h_{13}^* \\ h_{13}^* & 0 & -h_{11}^* & h_{12}^* \\ 0 & h_{13}^* & -h_{12}^* & -h_{11}^* \end{bmatrix}$, $\mathcal{N}_1 = \begin{bmatrix} n_{11} \\ n_{12} \\ n_{13} \\ n_{14} \\ n_{15} \\ n_{16} \\ n_{17} \\ n_{18} \end{bmatrix}$, and $y_{(TR-R)} = \begin{bmatrix} y_{(T-TR)}^1 \\ y_{(T-TR)}^2 \\ y_{(T-TR)}^3 \\ y_{(T-TR)}^4 \\ y_{(T-TR)}^5 \\ y_{(T-TR)}^6 \\ y_{(T-TR)}^7 \\ y_{(T-TR)}^8 \end{bmatrix}$

$$y_{(TR-R)} = \widetilde{H}_1 \begin{bmatrix} x_1 \\ x_2 \\ x_3 \\ x_4 \end{bmatrix} + \mathcal{N}_1 \tag{A.14}$$

A.1.3 Decoding and estimating

The transmitted symbols can be estimated by following the LS estimation rule i.e.

$$\hat{y}_{(T-TR)} = y_{(TR-R)}.\, inv(\widetilde{H}_1) \tag{A.15}$$

Thus to calculate $inv(\widetilde{H}_1)$, we first calculate the pseudo inverse of $\widetilde{H}_1$ as

$$inv\left(\widetilde{H}_1\right) = \acute{H}_1 = (\widetilde{H}_1{}^H \widetilde{H}_1)^{-1} \widetilde{H}_1{}^H \tag{A.16}$$

Describing $(\widetilde{H}_1{}^H \widetilde{H}_1)$ and $(\widetilde{H}_1{}^H \widetilde{H}_1)^{-1}$ as

$$\widetilde{H}_1{}^H \widetilde{H}_1 = \begin{bmatrix} h_{11}^* & h_{12}^* & h_{13}^* & 0 & h_{11} & h_{12} & h_{13} & 0 \\ h_{12}^* & -h_{11}^* & 0 & h_{13}^* & h_{12} & -h_{11} & 0 & h_{13} \\ h_{13}^* & 0 & -h_{11}^* & -h_{12}^* & h_{13} & 0 & -h_{11} & -h_{12} \\ 0 & -h_{13}^* & h_{12}^* & -h_{11}^* & 0 & -h_{13} & h_{12} & -h_{11} \end{bmatrix} \begin{bmatrix} h_{11} & h_{12} & h_{13} & 0 \\ h_{12} & -h_{11} & 0 & -h_{13} \\ h_{13} & 0 & -h_{11} & h_{12} \\ 0 & h_{13} & -h_{12} & -h_{11} \\ h_{11}^* & h_{12}^* & h_{13}^* & 0 \\ h_{12}^* & -h_{11}^* & 0 & -h_{13}^* \\ h_{13}^* & 0 & -h_{11}^* & h_{12}^* \\ 0 & h_{13}^* & -h_{12}^* & -h_{11}^* \end{bmatrix} \tag{A.17}$$

Solving (A.17)

$$\widetilde{H}_1{}^H \widetilde{H}_1 = \begin{bmatrix} \mathbb{H} & 0 & 0 & 0 \\ 0 & \mathbb{H} & 0 & 0 \\ 0 & 0 & \mathbb{H} & 0 \\ 0 & 0 & 0 & \mathbb{H} \end{bmatrix} \tag{A.18}$$

where $\mathbb{H} = 2(|h_{11}|^2 + |h_{12}|^2 + |h_{13}|^2)$

$$\widetilde{H_1}^H \widetilde{H_1} = 2(|h_{11}|^2 + |h_{12}|^2 + |h_{13}|^2)I \tag{A.19}$$

$$(\widetilde{H_1}^H \widetilde{H_1})^{-1} = \left(\frac{1}{2(|h_{11}|^2 + |h_{12}|^2 + |h_{13}|^2)}\right) I \tag{A.20}$$

Thus, from (A.15) and (A.16)

$$\hat{y}_{(T-TR)} = (\widetilde{H_1}^H \widetilde{H_1})^{-1} \widetilde{H_1}^H (y_{(TR-R)}) \tag{A.21}$$

$$= (\widetilde{H_1}^H \widetilde{H_1})^{-1} \widetilde{H_1}^H \left(\widetilde{H_1} \begin{bmatrix} x_1 \\ x_2 \\ x_3 \\ x_4 \end{bmatrix} + \mathcal{N}_1 \right) \tag{A.22}$$

$$\hat{y}_{(T-TR)} = \begin{bmatrix} x_1 \\ x_2 \\ x_3 \\ x_4 \end{bmatrix} + (\widetilde{H_1}^H \widetilde{H_1})^{-1} \widetilde{H_1}^H \mathcal{N}_1 \tag{A.23}$$

$$\hat{y}_{(T-TR)} = \begin{bmatrix} x_1 \\ x_2 \\ x_3 \\ x_4 \end{bmatrix} + \dot{n} \tag{A.24}$$

where $\dot{n} = (\widetilde{H_1}^H \widetilde{H_1})^{-1} \widetilde{H_1}^H . \mathcal{N}_1$. The decision rule can be performed following (4.35). Similar to previous section, no error correction is performed at the TR node and the erroneous estimated signal $\hat{x}$ at the TR node is again modulated using MPSK and transmitted to the receiver over the channel path H_2. The signal received at the receiver from the TR node is similar to (4.37) and equalized as per (4.6). The signal received at the receiver directly from the transmitter follows similar combining, demodulating and estimating process such that the received signal in two time slots is given by

$$y_{(T-R)} = \widetilde{H_3} \begin{bmatrix} x_1 \\ x_2 \\ x_3 \\ x_4 \end{bmatrix} + \mathcal{N}_3 \tag{A.25}$$

where $y_{(T-R)} = \begin{bmatrix} y^1_{(T-R)} \\ y^2_{(T-R)} \\ y^3_{(T-R)} \\ y^4_{(T-R)} \\ y^5_{(T-R)} \\ y^6_{(T-R)} \\ y^7_{(T-R)} \\ y^8_{(T-R)} \end{bmatrix}$ is the received symbol, $\begin{bmatrix} x_1 \\ x_2 \\ x_3 \\ x_4 \end{bmatrix}$ is the transmitted block, and, $\mathcal{N}_3 = \begin{bmatrix} n_{31} \\ n_{32} \\ n_{33} \\ n_{34} \\ n_{35} \\ n_{36} \\ n_{37} \\ n_{38} \end{bmatrix}$ is the noise during the time slots 1, 2, …, 8, respectively, from the $(T-R)$. Following (4.40) the estimate of the transmitted symbols is given by

$$\hat{y}_{(T-R)} = (\widetilde{H}_3{}^H \widetilde{H}_3)^{-1} \widetilde{H}_3{}^H (y_{(T-R)}) \tag{A.26}$$

$$\hat{y}_{(T-TR)} = \begin{bmatrix} x_1 \\ x_2 \\ x_3 \\ x_4 \end{bmatrix} + (\widetilde{H}_3{}^H \widetilde{H}_3)^{-1} \widetilde{H}_3{}^H \mathcal{N}_3 \tag{A.27}$$

$$\hat{y}_{(T-TR)} = \begin{bmatrix} x_1 \\ x_2 \\ x_3 \\ x_4 \end{bmatrix} + \ddot{n} \tag{A.28}$$

where $\ddot{n} = (\widetilde{H}_3{}^H \widetilde{H}_3)^{-1} \widetilde{H}_3{}^H . \mathcal{N}_3$, $\widetilde{H}_3$ is the channel matrix and $H_3 = H_1 H_2$ as defined by (4.19). At the receiver, the received signals $\hat{y}_{(TR-R)}$ and $\hat{y}_{(T-R)}$ are combined as

$$Y = sum(\hat{y}_{(TR-R)}, \hat{y}_{(T-R)}) \tag{A.29}$$

Maximum Likelihood demodulation of the signal Y is performed to obtain X following (4.14) and the decision is made in favor of the symbol with minimum distance following (4.42) as

$$X = arg \min_{MPSK_{map_{set}} \in \mathcal{A}} \left(\left| Y - MPSK_{map_{set}} \right|^2 \right) \tag{A.30}$$

APPENDIX B

B.1 System and Channel Model when $N_t = 1$ and $N_r = 3$

We first define the channel paths H_1, H_2, H_3 for the $(T - TR)$, $(TR - R)$, and $(T - R)$ links, respectively, as

$$H_1 = [h_{11}] \tag{B.1}$$

$$H_2 = \begin{bmatrix} h_{21} \\ h_{22} \\ h_{23} \end{bmatrix} \tag{B.2}$$

$$H_3 = \begin{bmatrix} h_{31} \\ h_{32} \\ h_{33} \end{bmatrix} \tag{B.3}$$

The signal $\hat{x}$ as given by (4.8) is now transmitted by the TR node over the channel H_2 to be received by three antenna elements at the receiver. Representing h_{21}, h_{22} and h_{23} as the complex channels between the TR node and $N_r = 1,2,$ and 3 receive antennas, respectively, the signals received at the receiver are given by

$$y_{(TR-R)1} = h_{21}\hat{x} + n_{21} \tag{B.4}$$

$$y_{(TR-R)2} = h_{22}\hat{x} + n_{22} \tag{B.5}$$

$$y_{(TR-R)3} = h_{23}\hat{x} + n_{23} \tag{B.6}$$

where n_{21}, n_{22} and n_{23} are the complex noise added at the three receivers. At the receiver, the two signals are combined using MRC and the matched filter output is given by

$$\tilde{y}_{(TR-R)}(t) = (|h_{21}^2| + |h_{22}^2| + |h_{23}^2|)\hat{x}(t) + \ddot{n}(t) \tag{B.7}$$

where $\ddot{n}(t) = [n_{21}(t) \quad n_{22}(t) \quad n_{23}(t)]^T$ is the complex noise vector.

The signal received at the receiver directly from the transmitter is given by

$$y_{(T-R)1} = h_{31}x + n_{31} \tag{B.8}$$

$$y_{(T-R)2} = h_{32}x + n_{32} \tag{B.9}$$

$$y_{(T-R)3} = h_{33}x + n_{33} \tag{B.10}$$

where n_{31}, n_{32} and n_{33} are the complex noise added at the three receivers. At the receiver, the three signals are combined using MRC and the matched filter output is given by

$$\tilde{y}_{(T-R)}(t) = (|h_{31}^2| + |h_{32}^2| + |h_{33}^2|)x(t) + \ddot{n}(t) \tag{B.11}$$

where $\ddot{n}(t) = [n_{31}(t) \quad n_{32}(t) \quad n_{33}(t)]^{\mathrm{T}}$ is the complex noise vector. At the receiver, the received signals $\hat{y}_{(TR-R)}$ and $\hat{y}_{(T-R)}$ are summed as

$$Y = sum(\hat{y}_{(TR-R)}, \hat{y}_{(T-R)}) \tag{B.12}$$

Maximum Likelihood demodulation of the signal Y is performed following (4.14) and the decision is again made in favor of the symbol with minimum distance to retrieve the signal with minimum number of errors as

$$X = arg\min_{MPSK_{map_{set}} \in \mathcal{A}}(Y_{est}) \tag{B.13}$$

Similar operations can be performed for higher number of receive antennas at the receiver.

APPENDIX C

C.1 SEP expression for two-hop DAF relay system (SISO systems)

For Fig. 4.7 (b), the PDF $p_{\gamma_{(T-R)}}(\gamma)$ of $\gamma_{(T-R)}$ is given by

$$p_{\gamma_{(T-R)}}(\gamma) = \frac{1}{\Gamma(m)}\left(\frac{m}{\overline{\gamma}_{(T-R)}}\right)^{m} \gamma^{m-1} e^{-m\gamma_{(T-R)}/\overline{\gamma}_{(T-R)}} \tag{C.1}$$

and the MGF $(\Lambda_{(\gamma_{(T-R)})}))$ as

$$\Lambda_{(\gamma_{(T-R)})}\left(\frac{-g}{\sin^2(\theta)}\right) = \int_0^{\infty} p_{\gamma_{(T-R)}}(\gamma) e^{s\gamma_{(T-R)}} d\gamma \tag{C.2}$$

$$= \left(1 - \frac{s\overline{\gamma}_{(T-R)}}{m}\right)^{-m} = \left(1 - \frac{g\overline{\gamma}_{(T-R)}}{m\sin^2(\theta)}\right)^{-m} \tag{C.3}$$

$$\Lambda_{(\gamma_{(T-R)})}\left(\frac{-g}{\sin^2(\theta)}\right) = \left(\frac{m\sin^2(\theta)}{g\overline{\gamma}_{(T-R)} + m\sin^2(\theta)}\right)^{m}, m \geq 0.65 \tag{C.4}$$

for a non-negative random variable $\gamma, \gamma \geq 0$ [199].

For the independently Nakagami-m faded $(T - TR)$ and $(TR - R)$ links (as shown in Fig. 4.7 (a)), the PDF $p_{\gamma_{(TR)}}(\gamma)$ can be expressed as [200], (29)]

$$p_{\gamma_{(TR)}}(\gamma) = \int_0^{\gamma} \frac{r^2}{(r-\gamma)^2} \cdot p_{\gamma_{(T-TR)}}\left(\frac{r\gamma}{(r-\gamma)}\right) \cdot p_{\gamma_{(TR-R)}}(r) dr \tag{C.5}$$

By analyzing (C.5), we can see that it involves the pdf terms of $\gamma_{(T-TR)}$ and $\gamma_{(TR-R)}$, thus, following (C.1) the pdfs $p_{\gamma_{(T-TR)}}\left(\frac{r\gamma}{(r-\gamma)}\right)$ and $p_{\gamma_{(TR-R)}}(r)$ can be written as

$$p_{\gamma_{(T-TR)}}\left(\frac{r\gamma}{r-\gamma}\right) = \frac{1}{\Gamma(m_1)}\left(\frac{m_1}{\overline{\gamma}_{(T-TR)}}\right)^{m_1}\left(\frac{r\gamma}{r-\gamma}\right)^{m_1-1} exp\left(\frac{-m_1}{\overline{\gamma}_{(T-TR)}} \cdot \left(\frac{r\gamma}{r-\gamma}\right)\right), \text{ and} \tag{C.6}$$

$$p_{\gamma_{(TR-R)}}(r) = \frac{1}{\Gamma(m_2)}\left(\frac{m_2}{\overline{\gamma}_{(TR-R)}}\right)^{m_2}(r)^{m_2-1} exp\left(\frac{-m_1}{\overline{\gamma}_{(TR-R)}} \cdot r\right), \tag{C.7}$$

respectively. Substituting (C.6) and (C.7) in (C.5) and solving, $p_{\gamma_{(TR)}}(\gamma)$ can be expressed as

$$p_{\gamma_{(TR)}}(\gamma) = \frac{\gamma^{m_1-1}}{\Gamma(m_1)\Gamma(m_2)}\left(\frac{m_1}{\overline{\gamma}_{(T-TR)}}\right)^{m_1}\left(\frac{m_2}{\overline{\gamma}_{(TR-R)}}\right)^{m_2} \times exp\left[-\left(\frac{m_1}{\overline{\gamma}_{(T-TR)}}+\frac{m_2}{\overline{\gamma}_{(TR-R)}}\right)\gamma\right]\int_0^{\infty} r^{m_2-1} \times \left(1+\frac{\gamma}{r}\right)^{m_1+m_2} exp\left[-\left(\frac{m_1\gamma^2}{\overline{\gamma}_{(T-TR)}r}+\frac{m_2 r}{\overline{\gamma}_{(TR-R)}}\right)\right]dr \quad \text{(C.8)}$$

Since we have considered that m_1 and m_2 may or may not be integers but $m_1 + m_2$ is always an integer, (C.8) becomes

$$p_{\gamma_{(TR)}}(\gamma) = \frac{\gamma^{m_1-1}}{\Gamma(m_1)\Gamma(m_2)}\left(\frac{m_1}{\overline{\gamma}_{(T-TR)}}\right)^{m_1}\left(\frac{m_2}{\overline{\gamma}_{(TR-R)}}\right)^{m_2} \times exp\left[-\left(\frac{m_1}{\overline{\gamma}_{(T-TR)}}+\frac{m_2}{\overline{\gamma}_{(TR-R)}}\right)\gamma\right]\sum_0^{m_1+m_2}\binom{m_1+m_2}{k} \times \gamma^k \int_0^{\infty} r^{m_2-k-1} exp\left[-\left(\frac{m_1\gamma^2}{\overline{\gamma}_{(T-TR)}r}+\frac{m_2 r}{\overline{\gamma}_{(TR-R)}}\right)\right]dr \quad \text{(C.9)}$$

Solving further, the pdf of the instantaneous SNR γ in (C.9) can be expressed as

$$p_{\gamma_{(TR)}}(\gamma) = \frac{2\gamma^{m_1+m_2-1}}{\Gamma(m_1)\Gamma(m_2)}\left(\frac{m_1}{\overline{\gamma}_{(T-TR)}}\right)^{m_1}\left(\frac{m_2}{\overline{\gamma}_{(TR-R)}}\right)^{m_2} \times exp\left[-\left(\frac{m_1}{\overline{\gamma}_{(T-TR)}}+\frac{m_2}{\overline{\gamma}_{(TR-R)}}\right)\gamma\right]$$

$$\sum_{k=0}^{m_1+m_2}\binom{m_1+m_2}{k} \times \left(\frac{m_1\overline{\gamma}_{(TR-R)}}{m_2\overline{\gamma}_{(T-TR)}}\right)^{\frac{(m_2-k)}{2}} K_{|m_2-k|}\left(2\gamma_{(TR)}\sqrt{\frac{m_1 m_2}{\overline{\gamma}_{(T-TR)}\overline{\gamma}_{(TR-R)}}}\right), \gamma_{(TR)} \geq 0 \quad \text{(C.10)}$$

Following (C.2), the MGF of $\gamma_{(TR)}$ can be calculated as

$$\Lambda_{(\gamma_{(TR)})}\left(\frac{-g}{\sin^2(\theta)}\right) = \int_0^{\infty} p_{\gamma_{(TR)}}(\gamma) exp\left(\frac{-g\gamma_{(TR)}}{\sin^2(\theta)}\right) d\gamma_{(TR)} \quad \text{(C.11)}$$

Substituting (C.10) into (C.11), the MGF of $\gamma_{(TR)}$ can be written as

$$\Lambda_{(\gamma_{(TR)})}\left(\frac{-g}{\sin^2(\theta)}\right) = \frac{2}{\Gamma(m_1)\Gamma(m_2)}\left(\frac{m_1}{\overline{\gamma}_{(T-TR)}}\right)^{m_1}\left(\frac{m_2}{\overline{\gamma}_{(TR-R)}}\right)^{m_2} \times \sum_{k=0}^{m_1+m_2}\binom{m_1+m_2}{k} \times \left(\frac{m_1\overline{\gamma}_{(TR-R)}}{m_2\overline{\gamma}_{(T-TR)}}\right)^{\frac{(m_2-k)}{2}} \times \int_0^{\infty} \gamma^{m_1+m_2-1} exp\left[-\left(\frac{m_1}{\overline{\gamma}_{(T-TR)}}+\frac{m_2}{\overline{\gamma}_{(TR-R)}}+\frac{g}{\sin^2(\theta)}\right)\gamma\right] \times K_{|m_2-k|}\left(2\gamma_{(TR)}\sqrt{\frac{m_1 m_2}{\overline{\gamma}_{(T-TR)}\overline{\gamma}_{(TR-R)}}}\right) d\gamma_{(TR)} \quad \text{(C.12)}$$

for the limited case when $m_1 + m_2$ is an integer. Using (6.621.3) in [202], which says

$$\int_0^\infty x^{\mu-1} exp(-\alpha x) \times K_\nu(\beta x) dx = \frac{\sqrt{\pi}(2\beta)^\nu}{\left(\mu+\frac{1}{2}\right)^{\mu+\nu}} \frac{\Gamma(\mu+\nu)\Gamma(\mu-\nu)}{\Gamma\left(\mu+\frac{1}{2}\right)} F\left(\mu+\nu; \nu+\frac{1}{2}; \mu+\frac{1}{2}; \frac{\alpha-\beta}{\alpha+\beta}\right) \quad \text{(C.13)}$$

Defining $\alpha = \left(\frac{m_1}{\overline{\gamma}_{(T-TR)}} + \frac{m_2}{\overline{\gamma}_{(TR-R)}} + \frac{g}{\sin^2(\theta)}\right), \beta = 2\sqrt{\frac{m_1 m_2}{\overline{\gamma}_{(T-TR)}\overline{\gamma}_{(TR-R)}}}, \mu = m_1 + m_2, \nu = |m_2 - k|$, (C.13) can be expressed as

$$\Lambda_{(\gamma_{(TR)})}\left(\frac{-g}{\sin^2(\theta)}\right) = \frac{2}{\Gamma(m_1)\Gamma(m_2)}\left(\frac{m_1}{\overline{\gamma}_{(T-TR)}}\right)^{m_1}\left(\frac{m_2}{\overline{\gamma}_{(TR-R)}}\right)^{m_2} \times \sum_{k=0}^{\mu}\binom{\mu}{k} \times \left(\frac{m_1\overline{\gamma}_{(TR-R)}}{m_2\overline{\gamma}_{(T-TR)}}\right)^{\frac{(m_2-k)}{2}}$$
$$\times \frac{\sqrt{\pi}(2\beta)^\nu}{\left(\mu+\frac{1}{2}\right)^{\mu+\nu}} \frac{\Gamma(\mu+\nu)\Gamma(\mu-\nu)}{\Gamma\left(\mu+\frac{1}{2}\right)} \, {}_2F_1\left(\mu+\nu; \nu+\frac{1}{2}; \mu+\frac{1}{2}; \frac{\alpha-\beta}{\alpha+\beta}\right) \quad \text{(C.14)}$$

If $(\Lambda_{(\gamma_{(TR)})})$ and $(\Lambda_{(\gamma_{(T-R)})})$ is the MGF of $\gamma_{(TR)}$ and $\gamma_{(T-R)}$, respectively, then the combined (MGF,$(\Lambda_{\gamma_{eq}})$) of γ_{eq} can be calculated as

$$\Lambda_{\gamma_{eq}}(x) = \Lambda_{(\gamma_{(TR)})}(x)\Lambda_{(\gamma_{(T-R)})}(x) \quad \text{(C.15)}$$

where $\Lambda_{(\gamma_{(TR)})}(x)$ and $\Lambda_{(\gamma_{(T-R)})}(x)$ is given by (C.14) and (C.5), respectively. The SEP, P_s, can be calculated as follows: For coherent modulation, the exact expression for P_s can be written as

$$P_s(\gamma_s) = \alpha_m Q\left(\sqrt{\beta_m}\gamma_s\right) \quad \text{(C.16)}$$

where α_m and β_m depend on modulation type. Let α and g be the constants that depend on the modulation, then the general expression for P_s in (C.16) for AWGN can be written terms of Gaussian Q function as

$$P_s(\gamma_s) = \alpha Q\left(\sqrt{2g}\gamma_s\right) \quad \text{(C.17)}$$

by setting $\alpha = \alpha_m$ and $g = 0.5\beta_m$. Using the alternate Q function given by $Q(z) = \frac{1}{\pi}\int_0^{\pi/2} exp\left[\frac{-z^2}{2\sin^2\theta}\right] d\theta, \; z > 0$, (C.17) can be written as

$$P_s = \frac{\alpha}{\pi}\int_0^{\pi/2} exp\left[\frac{-g\gamma}{\sin^2\theta}\right] d\theta \quad \text{(C.18)}$$

Thus the average error probability in fading for modulations is given by [90]

$$\bar{P}_s = \frac{\alpha}{\pi}\int_0^{\infty} P_s(\gamma) p_{\gamma_{eq}}(\gamma) d\gamma$$

$$\bar{P}_s = \frac{\alpha}{\pi}\int_0^{\infty}\int_0^{\pi/2} exp\left[\frac{-g\gamma}{\sin^2\theta}\right] d\theta p_{\gamma_{eq}}(\gamma) d\gamma$$

$$= \frac{\alpha}{\pi}\int_0^{\pi/2}\left[\int_0^{\infty} exp\left[\frac{-g\gamma}{\sin^2\theta}\right] p_{\gamma_{eq}}(\gamma) d\gamma\right] d\theta$$

$$\bar{P}_s = \frac{\alpha}{\pi}\int_0^{\pi/2} \Lambda_{\gamma_{eq}}\left(\frac{-g}{\sin^2\theta}\right) d\theta \quad \text{(C.19)}$$

where $\Lambda_{\gamma_{eq}}(s)$ is the MGF associated with pdf $p_{\gamma_{eq}}(\gamma)$ and $g = \sin^2(\pi/M)$. Similar representation can be used to achieve exact $\bar{P}_s$ for MPSK in AWGN as

$$\bar{P}_s = \frac{1}{\pi}\int_0^{\infty}\int_0^{(M-1)\pi/M} exp\left[\frac{-g\gamma}{\sin^2\theta}\right] d\theta p_{\gamma_{eq}}(\gamma) d\gamma$$

$$= \frac{1}{\pi}\int_0^{(M-1)\pi/M}\left[\int_0^{\infty} exp\left[\frac{-g\gamma}{\sin^2\theta}\right] p_{\gamma_{eq}}(\gamma) d\gamma\right] d\theta$$

$$\bar{P}_s = \frac{1}{\pi}\int_0^{(M-1)\pi/M} \Lambda_{\gamma_{eq}}\left(\frac{-g_{psk}}{\sin^2\theta}\right) d\theta \quad \text{(C.20)}$$

where $g_{psk} = \sin^2(\pi/M)$. Substituting (C.15) in (C.20), the average probability of error for MPSK in Nakagami-m fading can be expressed as

$$\bar{P}_s = \frac{1}{\pi}\int_0^{(M-1)\pi/M}\left[\int_0^{\infty} p_{\gamma_{(TR)}}(\gamma) e^{s\gamma_{(TR)}} d\gamma \,.\, \int_0^{\infty} p_{\gamma_{(T-R)}}(\gamma) e^{s\gamma_{(T-R)}} d\gamma\right]\left(\frac{-g_{psk}}{\sin^2\theta}\right) d\theta \quad \text{(C.21)}$$

in terms of PDF by using (C.2) and (C.11), or by

$$\bar{P}_s = \frac{1}{\pi}\int_0^{(M-1)\pi/M} \Lambda_{(\gamma_{(TR)})}\left(\frac{-g}{\sin^2(\theta)}\right) \Lambda_{(\gamma_{(T-R)})}\left(\frac{-g}{\sin^2(\theta)}\right) d\theta \quad \text{(C.22)}$$

in terms of MGF. Substituting (C.14) and (C.4) in (C.22), the SEP can be calculated as

$$\bar{P}_s = \frac{1}{\pi}\int_0^{(M-1)\pi/M} \frac{2}{\Gamma(m_1)\Gamma(m_2)}\left(\frac{m_1}{\bar{\gamma}_{(T-TR)}}\right)^{m_1}\left(\frac{m_2}{\bar{\gamma}_{(TR-R)}}\right)^{m_2} \times \sum_{k=0}^{\mu}\binom{\mu}{k} \times \left(\frac{m_1\bar{\gamma}_{(TR-R)}}{m_2\bar{\gamma}_{(T-TR)}}\right)^{\frac{(m_2-k)}{2}}$$

$$\times \frac{\sqrt{\pi}(2\beta)^{\nu}}{\left(\mu+\frac{1}{2}\right)^{\mu+\nu}} \frac{\Gamma(\mu+\nu)\Gamma(\mu-\nu)}{\Gamma\left(\mu+\frac{1}{2}\right)} \, {}_2F_1\left(\mu+\nu;\nu+\frac{1}{2};\mu+\frac{1}{2};\frac{\alpha-\beta}{\alpha+\beta}\right) \times \left(\left(\frac{m\sin^2(\theta)}{g\bar{\gamma}_{(T-R)}+m\sin^2(\theta)}\right)^{m}\right) d\theta \quad \text{(C.23)}$$

C.2 Error probability of MISO systems

The PDF of $\gamma_{(T-R)}$ for N_t transmit antennas is given by [203]

$$p_{\gamma_{(T-R)}}(\gamma) = \frac{1}{\Gamma(mN_t)}\left(\frac{m}{\bar{\gamma}_{(T-R)}}\right)^{mN_t} \gamma^{mN_t-1} exp\left(\frac{-m}{\bar{\gamma}_{(T-R)}}\gamma_{(T-R)}\right) \quad \text{(C.24)}$$

and the MGF can be expressed as

$$\Lambda_\gamma(s) = \int_0^\infty p_\gamma(\gamma)e^{s\gamma}\,d\gamma = \left(1 - \frac{s\bar{\gamma}}{m}\right)^{-mN_t},\ m \geq 1, \bar{\gamma} = \rho/(N_t R) \quad \text{(C.25)}$$

As given by (C.5), the PDF of $\gamma_{(TR)}$ of the $(T - TR - R)$link is given by

$$p_{\gamma_{(TR)}}(\gamma) = \int_0^\gamma \frac{r^2}{(r-\gamma)^2} \cdot p_{\gamma_{(T-TR)}}\left(\frac{r\gamma}{(r-\gamma)}\right) \cdot p_{\gamma_{(TR-R)}}(r)dr \quad \text{(C.26)}$$

where $p_{\gamma_{(T-TR)}}$ and $p_{\gamma_{(TR-R)}}$ are the PDFs of $\gamma_{(T-TR)}$ and $\gamma_{(TR-R)}$, respectively, given by

$$p_{\gamma_{(T-TR)}}\left(\frac{r\gamma}{r-\gamma}\right) = \frac{1}{\Gamma(N_t m_1)}\left(\frac{m_1}{\bar{\gamma}_{(T-TR)}}\right)^{N_t m_1}\left(\frac{r\gamma}{r-\gamma}\right)^{N_t m_1 - 1} exp\left(\frac{-m_1}{\bar{\gamma}_{(T-TR)}} \cdot \left(\frac{r\gamma}{r-\gamma}\right)\right) \quad \text{(C.27)}$$

$$p_{\gamma_{(TR-R)}}(r) = \frac{1}{\Gamma(m_2)}\left(\frac{m_2}{\bar{\gamma}_{(TR-R)}}\right)^{m_2}(r)^{m_2-1} exp\left(\frac{-m_1}{\bar{\gamma}_{(TR-R)}} \cdot r\right), \quad \text{(C.28)}$$

Substituting (C.27) and (C.28) in (C.26) and solving, $p_{\gamma_{(TR)}}(\gamma)$ can be expressed as

$$p_{\gamma_{(TR)}}(\gamma) = \frac{\gamma^{N_t m_1 - 1}}{\Gamma(m_1 N_t)\Gamma(m_2)}\left(\frac{m_1}{\bar{\gamma}_{(T-TR)}}\right)^{m_1 N_t}\left(\frac{m_2}{\bar{\gamma}_{(TR-R)}}\right)^{m_2} \times exp\left[-\left(\frac{m_1}{\bar{\gamma}_{(T-TR)}} + \frac{m_2}{\bar{\gamma}_{(TR-R)}}\right)\gamma\right]$$

$$\int_0^\infty r^{m_2-1} \times \left(1 + \frac{\gamma}{r}\right)^{N_t m_1 + m_2} exp\left[-\left(\frac{m_1\gamma^2}{\bar{\gamma}_{(T-TR)}r} + \frac{m_2 r}{\bar{\gamma}_{(TR-R)}}\right)\right]dr \quad \text{(C.29)}$$

where m_1 and m_2 are integers. Using (C.9) and (C.10), the PDF of the instantaneous SNR γ in (C.29) can be expressed as

$$p_{\gamma_{(TR)}}(\gamma) = \frac{2\gamma^{N_t m_1 + m_2 - 1}}{\Gamma(N_t m_1)\Gamma(m_2)}\left(\frac{m_1}{\bar{\gamma}_{(T-TR)}}\right)^{N_t m_1}\left(\frac{m_2}{\bar{\gamma}_{(TR-R)}}\right)^{m_2} \times exp\left[-\left(\frac{m_1}{\bar{\gamma}_{(T-TR)}} + \frac{m_2}{\bar{\gamma}_{(TR-R)}}\right)\gamma\right]$$

$$\sum_{k=0}^{N_t m_1 + m_2}\binom{N_t m_1 + m_2}{k} \times \left(\frac{m_1\bar{\gamma}_{(TR-R)}}{m_2\bar{\gamma}_{(T-TR)}}\right)^{\frac{(m_2-k)}{2}} K_{|m_2-k|}\left(2\gamma_{(TR)}\sqrt{\frac{m_1 m_2}{\bar{\gamma}_{(T-TR)}\bar{\gamma}_{(TR-R)}}}\right), \gamma_{(TR)} \geq 0 \quad \text{(C.30)}$$

Using (C.11) the MGF of $\gamma_{(TR)}$ can be calculated by substituting (C.30) in (C.11) and the MGF, $(\Lambda_{\gamma_{eq}})$ of γ_{eq} can be calculated using (C.1) and by substituting the respective terms in (C.12). The SEP, P_s, for MPSK can be calculated by substituting the respective terms in

(C.18). For $(M = 2)$, P_s can be calculated by substituting in (C.21) and for $M = 4$, P_s can be calculated by substituting in (4.110).

C.3 Error probability of SIMO systems

As given by (C.5), the PDF of $\gamma_{(TR)}$ of the $(T - TR - R)$link is given by

$$p_{\gamma_{(TR)}}(\gamma) = \int_0^{\gamma} \frac{r^2}{(r-\gamma)^2} . p_{\gamma_{(T-TR)}}\left(\frac{r\gamma}{(r-\gamma)}\right) . p_{\gamma_{(TR-R)}}(r)dr \qquad (C.31)$$

where $p_{\gamma_{(T-TR)}}$ and $p_{\gamma_{(TR-R)}}$ are the PDFs of $\gamma_{(T-TR)}$ and $\gamma_{(TR-R)}$, respectively. For an uncorrelated Nakagami-m fading, the PDF of $\gamma_{(T-TR)}$ is similar to the one given by (C.6). For convenience we re-write (C.6)

$$p_{\gamma_{(T-TR)}}\left(\frac{r\gamma}{r-\gamma}\right) = \frac{1}{\Gamma(m_1)}\left(\frac{m_1}{\overline{\gamma}_{(T-TR)}}\right)^{m_1}\left(\frac{r\gamma}{r-\gamma}\right)^{m_1-1} exp\left(\frac{-m_1}{\overline{\gamma}_{(T-TR)}} . \left(\frac{r\gamma}{r-\gamma}\right)\right) \qquad (C.32)$$

The PDF of $\gamma_{(TR-R)}$ at the output of L-branch MRC for i.i.d. Nakagami-m fading is given by

$$p_{\gamma_{(TR-R)}}(r) = \frac{1}{\Gamma(m_2 L)}\left(\frac{m_2}{\overline{\gamma}_{(TR-R)}}\right)^{m_2 L} r^{m_2 L-1} exp\left(\frac{-m_2}{\overline{\gamma}_{(TR-R)}} . r\right),\ \gamma \geq 0 \quad (C.33)$$

thus, for $L = N_r = 2$

$$p_{\gamma_{(TR-R)}}(\gamma) = \frac{1}{\Gamma(2m_2)}\left(\frac{m_2}{\overline{\gamma}_{(TR-R)}}\right)^{2m_2} \gamma^{2m_2-1} exp\left(\frac{-m_2}{\overline{\gamma}_{(TR-R)}} . r\right),\ \gamma \geq 0 \quad (C.34)$$

and for $L = N_r = 3$

$$p_{\gamma_{(TR-R)}}(\gamma) = \frac{1}{\Gamma(3m_2)}\left(\frac{m_2}{\overline{\gamma}_{(TR-R)}}\right)^{3m_2} \gamma^{3m_2-1} exp\left(\frac{-m_2}{\overline{\gamma}_{(TR-R)}} . r\right),\ \gamma \geq 0 \quad (C.35)$$

Substituting (C.32) and (C.33) in (C.5) and solving, $p_{\gamma_{(TR)}}(\gamma)$ can be expressed as

$$p_{\gamma_{(TR)}}(\gamma) = \frac{\gamma^{m_1-1}}{\Gamma(m_1)\Gamma(m_2 L)}\left(\frac{m_1}{\overline{\gamma}_{(T-TR)}}\right)^{m_1}\left(\frac{m_2}{\overline{\gamma}_{(TR-R)}}\right)^{m_2 L} \times exp\left[-\left(\frac{m_1}{\overline{\gamma}_{(T-TR)}} + \frac{m_2}{\overline{\gamma}_{(TR-R)}}\right)\gamma\right]$$

$$\int_0^{\infty} r^{m_2 L-1} \times \left(1 + \frac{\gamma}{r}\right)^{m_1+m_2 L} exp\left[-\left(\frac{m_1\gamma^2}{\overline{\gamma}_{(T-TR)}r} + \frac{m_2 r}{\overline{\gamma}_{(TR-R)}}\right)\right] dr \qquad (C.36)$$

Following (C.10), $p_{\gamma_{(TR)}}(\gamma)$ can be further written as

$$p_{\gamma_{(TR)}}(\gamma) = \frac{2\gamma^{m_1+N_r m_2-1}}{\Gamma(m_1)\Gamma(N_r m_2)}\left(\frac{m_1}{\overline{\gamma}_{(T-TR)}}\right)^{m_1}\left(\frac{m_2}{\overline{\gamma}_{(TR-R)}}\right)^{N_r m_2} \times exp\left[-\left(\frac{m_1}{\overline{\gamma}_{(T-TR)}}+\frac{m_2}{\overline{\gamma}_{(TR-R)}}\right)\gamma\right]$$

$$\sum_{k=0}^{m_1+N_r m_2}\binom{m_1+N_r m_2}{k} \times \left(\frac{m_1\overline{\gamma}_{(TR-R)}}{m_2\overline{\gamma}_{(T-TR)}}\right)^{\frac{(m_2-k)}{2}} K_{|m_2-k|}\left(2\gamma_{(TR)}\sqrt{\frac{m_1 m_2}{\overline{\gamma}_{(T-TR)}\overline{\gamma}_{(TR-R)}}}\right), \gamma_{(TR)} \geq 0 \quad \text{(C.37)}$$

The MGF of $\gamma_{(TR)}$ can be calculated by using (C.11) and the MGF $(\Lambda_{\gamma_{eq}})$ of γ_{eq} can be calculated using (C.15). Further, the SEP, P_s, for MPSK can be calculated by substituting the respective terms in (C.21). For $(M = 2)$, P_s can be calculated by substituting in (4.110) and for $M = 4$, P_s can be calculated by substituting in (4.111).

C.4 Error probability of MIMO systems

For an uncorrelated Nakagami-m fading, the pdf of a MIMO system is given by [203]

$$p_{\gamma}(\gamma) = \frac{1}{\Gamma(mN_tN_r)}\left(\frac{m}{\overline{\gamma}}\right)^{mN_tN_r}\gamma^{mN_tN_r-1}e^{-m\gamma/\overline{\gamma}},\ \gamma \geq 0 \quad \text{(C.38)}$$

thus, the PDF of $\gamma_{(T-R)}$ for the direct $(T-R)$ transmission can be written as

$$p_{\gamma_{(T-R)}}(\gamma) = \frac{1}{\Gamma(mN_tN_r)}\left(\frac{m}{\overline{\gamma}_{(T-R)}}\right)^{mN_tN_r}\gamma^{mN_tN_r-1}exp\left(\frac{-m\gamma_{(T-R)}}{\overline{\gamma}_{(T-R)}}\right) \quad \text{(C.39)}$$

and the MGF as

$$\Lambda_{\gamma}(s) = \int_0^{\infty} p_{\gamma_{(T-R)}}(\gamma)e^{s\gamma}d\gamma = \left(1-\frac{s\overline{\gamma}}{m}\right)^{-mN_tN_r},\ m \geq 1, \quad \text{(C.40)}$$

From (C.36), the PDF of the $(T-TR-R)$ transmission for a MIMO system can be expressed as

$$p_{\gamma_{(TR)}}(\gamma) = \frac{\gamma^{N_t m_1-1}}{\Gamma(N_t m_1)\Gamma(N_r m_2)}\left(\frac{m_1}{\overline{\gamma}_{(T-TR)}}\right)^{N_t m_1}\left(\frac{m_2}{\overline{\gamma}_{(TR-R)}}\right)^{N_r m_2} \times exp\left[-\left(\frac{m_1}{\overline{\gamma}_{(T-TR)}}+\frac{m_2}{\overline{\gamma}_{(TR-R)}}\right)\gamma\right]$$

$$\int_0^{\infty} r^{m_2-1} \times \left(1+\frac{\gamma}{r}\right)^{N_t m_1+N_r m_2} exp\left[-\left(\frac{m_1\gamma^2}{\overline{\gamma}_{(T-TR)}r}+\frac{m_2 r}{\overline{\gamma}_{(TR-R)}}\right)\right]dr \quad \text{(C.41)}$$

For $\gamma_{(TR)} \geq 0$, solving (C.41) gives

$$p_{\gamma_{(TR)}}(\gamma) = \frac{2\gamma^{N_t m_1+N_r m_2-1}}{\Gamma(N_t m_1)\Gamma(N_r m_2)}\left(\frac{m_1}{\overline{\gamma}_{(T-TR)}}\right)^{N_t m_1}\left(\frac{m_2}{\overline{\gamma}_{(TR-R)}}\right)^{N_r m_2} \times exp\left[-\left(\frac{m_1}{\overline{\gamma}_{(T-TR)}}+\frac{m_2}{\overline{\gamma}_{(TR-R)}}\right)\gamma\right]$$

$$\sum_{k=0}^{N_t m_1 + N_r m_2} \binom{N_t m_1 + N_r m_2}{k} \times \left(\frac{m_1 \bar{\gamma}_{(TR-R)}}{m_2 \bar{\gamma}_{(T-TR)}}\right)^{\frac{(m_2-k)}{2}} K_{|m_2-k|}\left(2\gamma_{(TR)}\sqrt{\frac{m_1 m_2}{\bar{\gamma}_{(T-TR)}\bar{\gamma}_{(TR-R)}}}\right), \quad \text{(C.42)}$$

The MGF $(\Lambda_{\gamma_{eq}})$ of γ_{eq} can be calculated using (C.15) and the SEP, P_s, of MIMO system for MPSK can be calculated by substituting the respective terms in (C.21).

APPENDIX D

D.1 BER Validation for Nakagami-m fading channels in different fading conditions

Fig. D.1 shows the BER of a Nakagami-m faded system for a SISO system following the baseline approach. Fig. D.1 (i) shows the simulation results for BPSK modulation and Fig. D.1 (ii) shows the simulation results for QPSK modulation with fading parameter $m = 1,2\ and\ 5$. As can be seen, the BER improves as the fading parameter increases. This can be explained on the basis that the Nakagami distribution is often used to model multipath fading as it can model fading conditions that are either more or less severe than Rayleigh fading, the lower the fading parameter the worse the fading, the higher the fading the lesser the effects of fading.

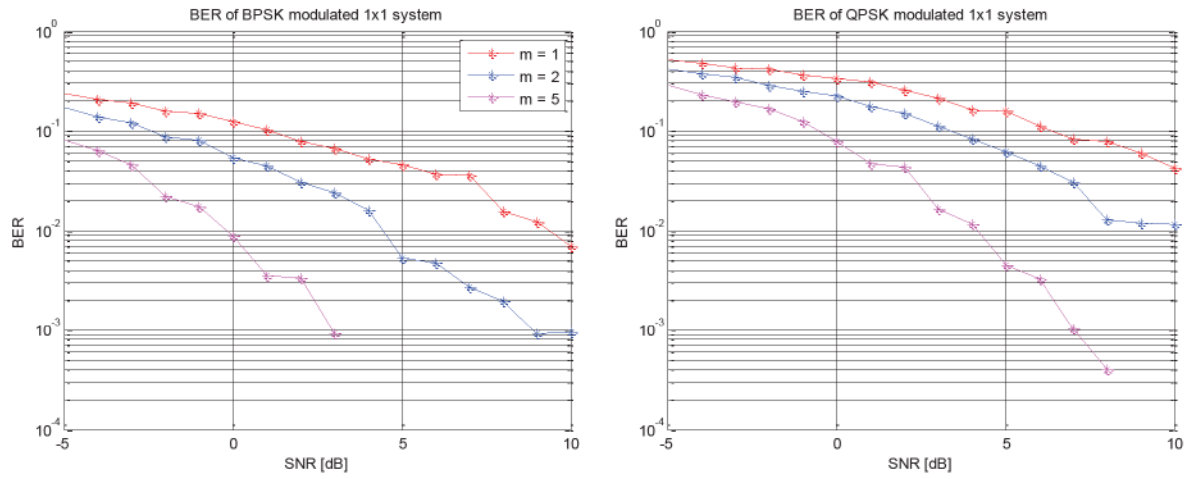

Fig. D.1BER of SISO System with m=1, m=2, and m=5, for BPSK and QPSK modulated Nakagami-m faded channel model

Fig. D.2 shows the simulations results for MISO system following the baseline approach for different fading parameters. The simulations are carried out for the wireless model with two and three transmit antennas with G_2^* with rate $R = 1$ and with G_3^* with rate

$R = 1/2$, respectively. Fig. D.2 (i) and (ii) shows the BER when the transmitted sequence was modulated using BPSK and QPSK, respectively, with $m = 1,2\ and\ 5$ and the figures show that the BER improves as the amount of fading decreases.

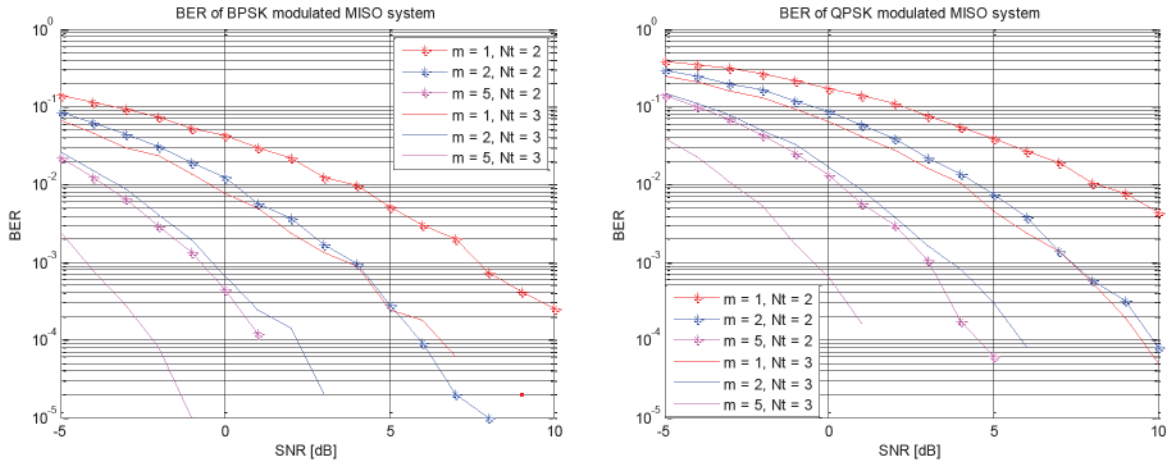

(i) *(ii)*

Fig. D.2 BER of MISO System with m=1, m=2, and m=5, for BPSK and QPSK modulated Nakagami-m faded channel model

Fig. D.3 shows the simulations results for SIMO system following the baseline approach for different fading parameters. The simulations are carried out for the wireless model with two, three, and four receive antennas with MRC performed at the receiver.

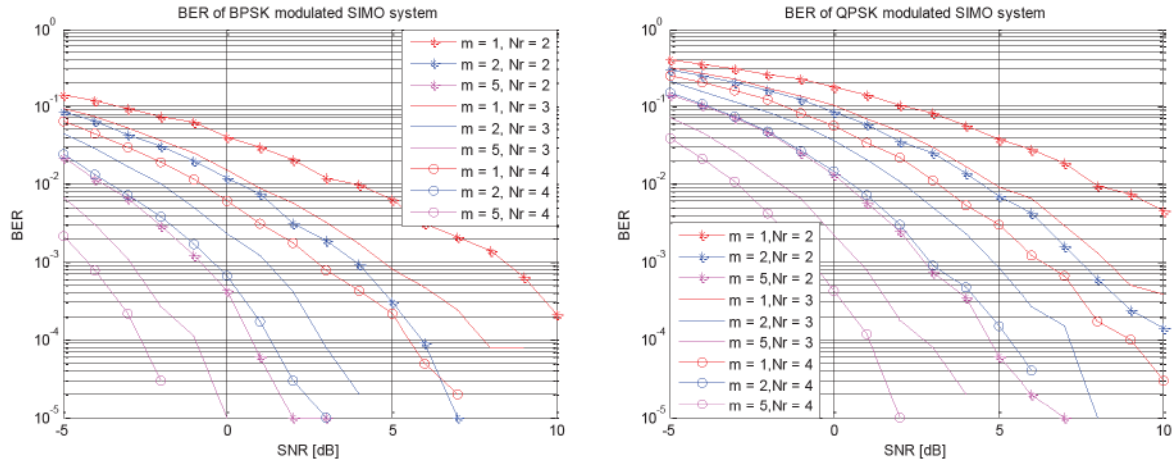

(i) *(ii)*

Fig. D.3 BER of SIMO System with m=1, m=2, and m=5, for BPSK and QPSK modulated Nakagami-m faded channel model

Fig. D.3 (i) and (ii) shows the BER when the transmitted sequence was modulated using BPSK and QPSK, respectively, with $m = 1,2\ and\ 5$ and the figures show that the results are in consistent with the fact that as the effect of fading lowers the BER improves. Fig. D.4 shows the simulations results for the conventional MIMO systems with different fading parameters. The simulations are carried out for two different wireless MIMO models $N_t = 2, N_r = 2$, and $N_t = 2, N_r = 3$. With two transmit antennas the sequence is encoded with G_2^* and three transmit antennas the sequence is encoded using G_3^*. Fig. D.4 (i) and (ii) shows the BER when the transmitted sequence was modulated using BPSK and QPSK, respectively, with $m = 1,2\ and\ 5$ and the figures show that the BER improves as the amount of fading decreases.

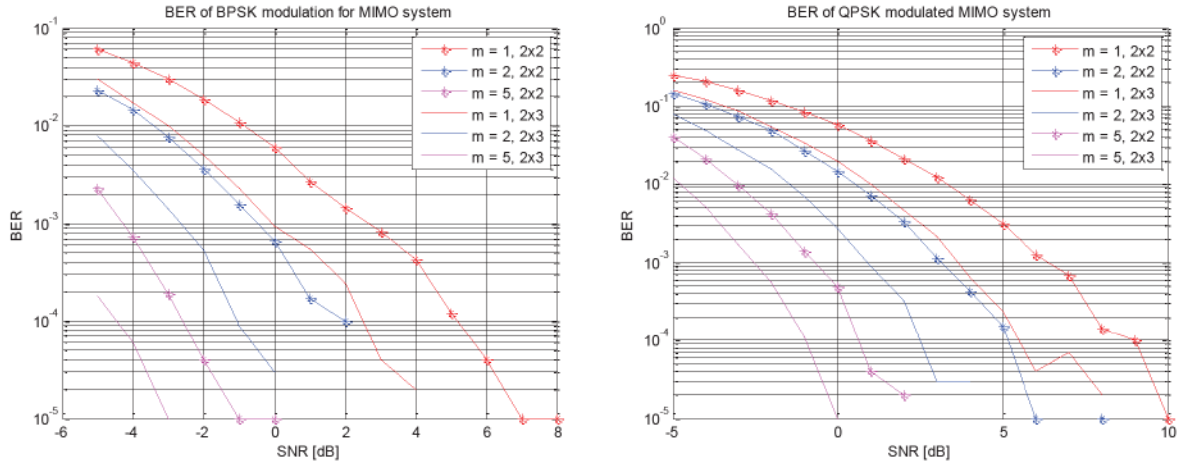

(i) *(ii)*

Fig. D.4 BER of MIMO System with m=1, m=2, and m=5, for BPSK and QPSK modulated Nakagami-m faded channel model